Toll-like Receptor Four and Neutrophil Contributions to Endotoxemia-Enhanced Aminoglycoside Ototoxicity

By

Zachary David Urdang

A Dissertation

Presented to the Program of The Neuroscience Graduate Program and
Oregon Health & Science University
School of Medicine
in partial fulfillment of
the requirements for the degree of

Doctor of Philosophy

March 2018

School of Medicine
Oregon Health & Science University

CERTIFICATE OF APPROVAL

This is to certify that the PhD dissertation of
Zachary David Urdang
has been approved

Mentor/Advisor – Edward Neuwelt

Member – Leslie Muldoon

Member – Peter Barr-Gillespie

Member – Dan Marks

Member – Alfred Nuttall

Member – Xiou Rui Shi

Acknowledgments

I thank Oregon Health and Science University, The Oregon Hearing Research Center for support. All of my mentors at Oregon Health and Science University including Dr.'s Neuwelt, Muldoon, Steyger, Jacoby, Barr-Gillespie, Marks, Nuttall, Shi, Gold, Hullar, Nguyen-Huynh, Clayburgh, and Sullivan.

Additionally, I am thankful for my family for all their loving and caring support. To my close friends who have always been there to help unwind and make it through the tough times and celebrate the good. And to my loving partner, Caroline Blechert, for all her support and understanding of the winding path to PhD.

List of Abbreviations

AABR	automated auditory brainstem response
ABR	auditory brainstem response
ANOVA	analysis of variance
ANSR	auditory neuropathy spectrum disorder
Ag	aminoglycoside
ASC-1	alanine-serine-cysteine transporter
ATP	adenosine triphosphate
AUC	area under the curve
BBB	blood-brain barrier
BC	basal cells
BDNF	brain derived neurotrophic factor
BLB	blood-labyrinth barrier
BMDC	bone marrow derived cell
BSA	bovine serum albumin
CARS	compensatory anti-inflammatory response syndrome
CCL#	chemokine (C-C motif) ligand *number*
CDH23	cadherin 23
CI	cochlear implant
CIN	contrast induced nephropathy
CNS	central nervous system
CNVIII	cranial nerve eight
CoBF	cochlear blood flow
COX	cyclooxygenase
CSF	cerebrospinal fluid
Ct	cycle threshold
Cxcl#	chemokine (c-x-c motif) ligand *number*
DAMP	damage associated molecular pattern

dB	decibel
ddCt	delta-delta cycle threshold
dB-HL	decibel-hearing loss
dB-SPL	decibel-sound pressure level
D-Met	D-methionine
DMSO	dimethylsulfoxide
DPBS	dulbeco's phosphate buffered saline
DPOAE	distortion product of otoacoustic emissions
DSA	digital subtraction angiography
ELISA	enzyme-linked immunosorbent assay
EP	endolymphatic potential
FC	fibrocytes
FITC	fluorescein isothiocyanate
GCSF	granulocyte colony stimulating factor
GFP	green fluorescent protein
GFR	glomerular filtration rate
GSH	glutathione
GST	glutathione
GT	gentamicin
GTTR	gentamicin-texas red
HNC	head and neck cancer
HNCASP	head and neck cancer awareness and screening program
HPV	human papilloma virus
hTR	hydrolyzed texas red
i.a.	intra-arterial
IC	intermediate cells
ICAM	inter-cellular adhesion molecule
IL-#	Interleukin-(*number*)
IVM	intra-vital microscopy
i.v.	intravenous
K	potassium

L-Met	L-methionine
LD50	lethal dose fifty percent
LL37	a.k.a. CAP18 cathelicidin antimicrobial peptide, 18kDa
LPS	lipopolysaccharide
MC	marginal cells
MDR	multi-drug resistant
MET	mechanotransduction
MIC	minimum inhibitory concentration
MIP-#	macrophage inflammatory protein *number*
MMP	matrix metallo-proteinase
MODS	multi-organ dysfunction syndrome
MRI	magnetic resonance imaging
MTD	maximum tolerated dose
MyD88	myeloid differentiation primary response 88
Myo7a	myosin 7 alpha
Na	sodium
NAC	N-acetyl cysteine
NALP3	NACHT, LRR and PYD domains-containing protein 3
NICU	neonatal intensive care unit
NIHL	noise-induced hearing loss
NET	neutrophil extracellular trap
NF	noise floor
NF-κβ	nuclear factor kappa-light-chain-enhancer of activated B cells
NK-cell	natural killer cell
NMDA	N-methyl D-aspartate
NMVI	neutrophil mediated vascular injury
NO	nitric oxide
NSAID	non-steroidal anti-inflammatory drug
NVU	neurovascular unit
OAT	organic anion transporter
OCT	organic cation transporter

OHC	outer hair cell
PAMP	pathogen associated molecular pattern
PBS	phosphate buffered saline
PC	pericyte
PGI	prostoglandin
PCDH15	protocadherin 15
PFA	paraformaldehyde
PRR	pattern recognition receptor
PTS	permanent threshold shift
qRT-PCR	quantitative real-time polymerase chain reaction
RNS	reactive nitrogen species
ROI	region of interest
ROS	reactive oxygen specie
RR	relative risk
Selp	p-selectin
SGLT2	sodium glucose like transporter two
SIRS	systemic inflammatory response syndrome
STAT1	signal transducer and activator of transcription 1
STS	sodium thiosulfate
TEOAE	transiently evoked otoacoustic emission
TLR	toll-like receptor
TMR	tetramethylrhodamine
TNFα	tumor necrosis factor alpha
TRAF	tumor necrosis factor receptor associate factor
TREK1	potassium channel subfamily K member 2
TRIF	TIR-domain-containing adapter-inducing interferon-beta
TRP#	transient receptor potential *alpha-numerical designation*
TXA	thromboxane

Table of Contents

List of Tables

List of Figures

Abstract

Drug-Induced Ototoxicity is a widespread global problem occurring as a side effect of otherwise effective therapies for conditions such as bacterial sepsis (aminoglycosides) and cancers (platinum-based chemotherapy). It is becoming clear that having the conditions requiring these drugs itself puts the patient at increased risk for acquiring life-long hearing loss. This apparent clinical paradox places the provider in difficult position where treating the life-threatening condition will most likely result in poor hearing outcomes. Since these ototoxic therapies are both life-saving and economically viable, understanding the mechanisms of hearing loss and developing effective strategies to preserve hearing during treatment for life-threatening illness has the potential to greatly enhance the quality of life in vulnerable patient populations.

Dedication

I humbly dedicate this work to those who cannot hear: I promise to listen to your deepest concerns. For those who cannot speak: I promise to speak and advocate on your behalf. And for those who are not heard: I promise to always speak up on your behalf. For communication is the only way to achieve peace and prosperity.

1 – Introduction

Significance and Translational Relevance

Aminoglycoside antibiotics are an essential tool for battling serious infections. Cisplatin chemotherapy is an effective therapy for certain cancers. While both of these agents are effective clinical tools, a serious side effect is life-long hearing loss. These drugs first enter the cochlea by crossing the blood-labyrinth barrier (BLB) – a collection of tight-junction coupled endothelial and epithelial barriers that limit trafficking of plasma constituents into the cochlear parenchyma. Inflammation, either systemic or confined to the cochlea, enhances BLB trafficking of both these drugs, potentiating their ototoxicity.

The mechanisms by which inflammation enhances the ototoxic potential of aminoglycoside and chemotherapy is unknown and may include leukocyte-independent or leukocyte-dependent processes. Inflammatory signaling could alter BLB physiology by promoting re-arrangement of tight junctions altering paracellular trafficking routes and/or transcellular routes, such as ion-channel mediated or non-specific pinocytosis. Alternatively, neutrophil-mediated vascular injury is caused when neutrophils adhere to inflamed endothelial cells and degranulate, releasing cytotoxic molecules that injure the endothelium, degrade paracellular tight-junctions, and promote leukocyte diapedesis.

This body of work probes the hypothesis that neutrophil activity is required for inflammation-enhanced BLB trafficking. To test this hypothesis, drug and neutrophil trafficking across the BLB was investigated in mouse models of sepsis and altered responses to inflammation. This translational research has the potential to point the way forward to decreasing the ototoxicity of life-saving therapies in the clinic.

1.1 – Hearing Loss: An Overview

1.1.1 – Epidemiology and Scope of Problem

Hearing loss impacts approximately 5% of the global population and disproportionately impacts underserved populations in developing countries (*1, 2*). Noise exposure is a major cause of hearing loss and prevalence is higher among industrial workers in countries with lax regulations such as Ethiopia (*3*), military combat veterans (*4*), and professional musicians (*5*). In the United States, hearing loss affects around sixty million people (mild unilateral hearing loss or greater) with about 6.6 million individuals over the age of 12 experiencing severe hearing loss (unilateral >60dB-HL shift) (*6*). Adults with hearing loss are more likely to have low educational attainment, lower income (<$20,000/year per family), and un/underemployment (3.21, 1.58, 1.98; odds ratios respectively) (*7*). Conversely, individuals from relatively impoverished communities, such as Peru, are 4-7 times more likely to experience permanent hearing loss during their life (*8*).

Collectively, these socioeconomic and quality of life factors make hearing loss a quintessential challenge facing our global healthcare system. Preventing hearing loss and treating existing hearing loss has the potential to improve social fulfillment, economic potential and overall quality of life. Advocacy for early hearing screening, early intervention, and avoiding ototoxic exposures (such as noise and ototoxic drugs) over a lifetime are three important focus areas.

1.1.2 – Etiologies of Hearing Loss

Two main categories of hearing loss are congenital (*9*) and acquired (*10-12*). Congenital etiologies include genetic molecular defects such as Usher and Alport syndromes, anatomical malformations, and infections. Predominant causes of acquired hearing loss include middle-ear disease, excessive noise, old age (presbycusis),

infections, autoimmune/vascular pathologies, and ototoxic drug exposures such as aminoglycosides and platinum-based chemotherapy.

Many genetic mutations are linked to congenital syndromes involving hearing loss. For example, Usher syndrome is caused by mutations in one of a number of hair cell tip-link (see appendix A for overview of hearing and related anatomy) related genes, such as MYO7a (*13*), PCDH15 (*14*), or CDH23 (*15, 16*). These mutations all disrupt tip-link to tip-link tethering and tension regulation; disruption prevents effective mechanotransduction inducing eventual hair cell degeneration. Another common congenital genetic syndrome is Alport syndrome where a type-4 collagen mutation leads to basement membrane defects and cochlear dysfunction unrelated to hair cells (*17, 18*). Alport syndrome is likely related to vasculopathy due to basement membrane thickening and BLB dysfunction, especially at the capillaries of the stria vascularis.

Congenital, childhood, and adult acquired infections involving the labyrinth also cause hearing loss, with cytomegalovirus as one of the leading etiological agents (*19*). Mechanisms of hearing loss related to viruses such as cytomegalovirus include inflammation; for example, reactive oxygen species (ROS)-producing infiltrating macrophages persist in infected brains and cochleae for weeks (*20*). Even though cytomegalovirus does not seem to directly infect hair cells, nearby infected epithelial and neuronal cells promote cochleotoxic labyrinthine inflammation. Herpes simplex labyrinthitis is another common pathogen that causes acquired hearing loss (*21, 22*). Meningitis is a bacterial cause of hearing loss; interestingly, anti-inflammatory glucocorticoid therapy spares hearing during meningitis, highlighting the inflammatory component bridging infection and hearing loss (*23, 24*).

Middle-ear disease is a major cause of hearing loss, particularly in developing countries and rural areas where pneumococcal vaccination is not routine (*25-27*). Chronic otitis media causes morphological changes in the middle-ear, leading to conductive hearing loss (*28*). Similar to labyrinthitis, immune cells infiltrating the middle-ear produce host tissue damage. Healing of inflamed tissue results in cytologically and morphologically distinct tissue architecture compared to before injury. Chronically, inflammatory damage compounds and eventually compromises middle-ear function due to ossicular ossification and degradation (*29*). Additionally, labyrinthine involvement is

common in middle-ear disease and can involve sensorineural hearing loss (*30*). Furthermore, chronic conductive hearing loss leads to cochlear and CNVIII degeneration (*31*).

Presbycusis is a general term for hearing loss of old age; it can be induced by multiple etiologies such as hair cell or CNVIII degeneration, vascular degeneration, or mechanical disruption of cochlear structures. Interestingly, there is an emerging appreciation that presbycusis is related to long-term low-grade inflammation (*32-34*). Chronic noise exposure over a lifetime can add up producing significant hearing loss (*35*). Vascular pathology from diabetes can cause cochlear BLB dysfunction and hearing loss (*36, 37*). Diabetes related hearing loss correlates with an individual's neutrophil:lymphocyte ratio, demonstrating a link between diabetes, cochlear vasculopathy, and inflammation (*38*). One hypothetical mechanism for the inflammatory component of diabetes related hearing loss is immune cell targeting of glycosylated basement membrane proteins identified as non-endogenous molecules via pattern recognition and/or major histocompatibility receptors.

Drug-induced iatrogenic hearing loss is a substantial worldwide clinical problem. Aminoglycoside antibiotics and platinum-based chemotherapies are two classes of ototoxic drugs that are therapeutically effective but induce life-long hearing loss. The mechanisms by which these drugs induce hearing loss are of central interest in this body of work.

1.2 – Systemic Inflammatory Response Syndrome (SIRS), Sepsis, Shock, Multi-Organ Dysfunction Syndrome (MODS), and Compensatory Anti-inflammatory Response Syndrome (CARS)

1.2.1 – Clinical Definition

Systemic inflammatory response syndrome (SIRS) is a broad diagnosis defined by meeting two out of four clinical criteria (**Table 1.2.1** (*39, 40*)). Conceptually, SIRS is a systemic illness response to a serious bodily insult. SIRS has both infectious and non-infectious etiologies (**Fig 1.2.1**). Potential causative insults include substantial bodily trauma, such a motor vehicle accident, serious burn, or major chemical/drug toxicity. When SIRS criteria are met with documented infection the diagnosis is sepsis. Serious localized infection can disseminate to the blood (bacteremia, viremia, or fungemia) and seed anatomically distant sites worsening the burden of infection. Pathogen-associated molecular patterns (PAMPs) induce expression and systemic release of pro-inflammatory factors. In all cases of SIRS (infection or not), diffuse danger signals trigger body-wide inflammation.

1.2.2 - Pathophysiology of SIRS and significance of neutrophil-mediated vascular injury

SIRS is initiated by generalized immune stimulation by PAMPs and/or damage-associated molecular patterns (DAMPs) (*41, 42*). PAMPs and DAMPs are two broad classifications of molecules that share similar structural motifs. DAMPs derive from cellular damage, and PAMPs derive from pathogenic organisms. Some examples of DAMPs include peroxidized lipids, heat-shock proteins, DNA/RNA, S100 proteins, and saccharides such as hyaluronan/hyaluronic acid. PAMP examples include double stranded RNA, unmethylated CpG motifs, viral membrane proteins, lipoteichoic acid,

peptidoglycan, and formyl peptides. Lipopolysaccharide (LPS), an endotoxin produced by gram-negative bacteria, is a key PAMP used in inflammation research; LPS induces an experimental model of sepsis that is of central importance to this body of work. PAMPs and DAMPs both share structural similarities although differ substantially.

DAMPs and PAMPs act to stimulate non-specific innate immune sensors called pattern recognition receptors (PRRs). Transmembrane toll-like receptors (TLR) (transmembrane receptors) (*43*) and cytoplasmic inflammasomes which include the nod-like receptors (cytoplasmic receptors) (*44*) are the two primary families of PRRs. The array of PAMP and DAMP structures are sensed by the diverse set of pattern recognition receptors which have promiscuous binding pockets capable of binding to multiple structural motifs. PRR signaling converges with expression of pro-inflammatory cytokines and chemokines. The exact profile of cyto/chemokine expression depends on which TLR(s) and/or inflammasome(s) are activated. For example, bacteria will elicit a tumor-necrosis factor response activating granulocytes via the MyD88-dependant pathway and viruses elicit an interferon response via the TRIF-TRAF pathway promoting NK and T-cell activity.

LPS primarily binds TLR4 (*45*). TLR4 activation causes NF-κβ translocation to the nucleus promoting pro-inflammatory cytokine and chemokine transcription (**Fig. 1.2.2.A**). Cyto/chemokinemia ensues precipitating SIRS. Other common experimental models of sepsis include cecal ligation and puncture, which is a surgically controlled bowel perforation and peritonitis paradigm (*46, 47*). Controlled infection with bacterial microbes is another experimental paradigm for sepsis, although it can be difficult to control the morbidity and mortality using live pathogens. For this work we have elected to utilize the LPS endotoxemia model due to the systemic inflammation induced by systemic LPS and for the ability to induce predictable morbidity mortality over a cohort. Furthermore, our experiments did not include treatment with anti-bacterial agents and therefore would not necessarily benefit from using live pathogens (*48*).

A central pathologic feature of SIRS is "capillary leak syndrome (*49, 50*)." Anionic vessel glycocalyx is stripped away from the blood vessels, revealing leukocyte-endothelium adhesion molecules that promote leukocyte diapedesis (*51, 52*). When leukocytes such as neutrophils (the most abundant and first line immune cell in the body)

adhere to cytokine-activated endothelium, they degranulate, releasing cytotoxic molecules such as metalloproteinases (*53*), ROS-producing enzymes such myeloperoxidase (*54, 55*), and cationic pore-forming peptides such as LL-37 (*56*). Collectively these cytotoxic molecules damage endothelial cells and intercellular tight junctions, a process known as neutrophil-mediated vascular injury (**Fig. 1.2.2.B**) (*57*). Another term for this neutrophil activity is NETosis (neutrophil extracellular traps); a specialized form of cell death where NETs are released. NETs consist of anionic nuclear DNA net decorated with the aforementioned cationic cytotoxic neutrophil derived macromolecules and enzymes. Endothelial cells also increase vascular permeability via leukocyte-independent mechanisms, such as cytoplasmic re-localization of cell-cell junction molecules (*58*) or auto-degradation of tight junctions via endogenous protease activity (*59-61*). These pathological processes enhance capillary permeability, allowing plasma and albumin to leak into the extravascular spaces.

Loss of intravascular plasma and albumin exacerbates cardiovascular stresses, further worsening SIRS/sepsis, lowering blood pressure and increasing heart/breath rate (*62-64*). Eventually, systemic hypoperfusion develops (septic shock). After significant hypoperfusion, multi-organ dysfunction syndrome and multi-organ failure syndrome develop (*65*). SIRS-related morbidity and mortality depends on the degree of organ damage and organ failure.

1.2.3 – Compensatory Anti-inflammatory Response Syndrome (CARS)

A pioneer in the field of SIRS, Bone, put it simply by reiterating Newton's mantra, "for every action there is an equal and opposite reaction (*66*)." Thinking about compensatory anti-inflammatory response syndrome (CARS) in this way is useful for a simplistic conceptual framework. SIRS is characterized by intense systemic inflammation orchestrated by pro-inflammatory cyto/chemokines. CARS is the opposite and is characterized by intense immunosuppression. IL-10 is a key regulator of CARS; IL-10 expression is stimulated by pro-inflammatory cues and serves as a negative-feedback regulator to dampen host-tissue damage and restore homeostasis (*67*).

Key features of CARS include IL-10 and prostoglandin E2 production, lymphocyte/leukocyte apoptosis and deactivation, leukopenia, hypothermia, and enhanced susceptibility to infection. This enhanced susceptibility to infection represents a turning point in critically ill patients. In individuals with sepsis this a window for opportunistic infection to completely take over with poor prognosis. In an individual with non-septic SIRS, such as a poly-trauma patient, abstaining from major surgery during CARS can improve patient survival and outcomes as major surgery poses significant infection risk. In patients with sepsis, the IL-6/IL-10 ratio can predict survival with a lower ratio favoring poor prognosis (*68*). Efforts to assess and diagnose CARS are ongoing and a definitive diagnostic for CARS has not yet been identified or developed (*69*).

1.2.4 – Clinical Management of SIRS and Sepsis

Management of patients who meet SIRS criteria largely depends upon etiology and the acute problem(s) (*70*). If the case is non-infectious, such as poly-trauma, management is geared towards acute surgical management, cardiovascular support; adequate fluid resuscitation with addition of crystalloid or albumin, and cardiac pressors (*70*). In cases of sepsis, swift empirical antibiotic therapy improves survival (*71-73*). Notably, time to treatment initiation is correlated with favorable outcome (*73*). Repeat blood cultures and identification of the infectious nidus (or nodes) is essential. Ideally, antibiotic therapy is geared towards specific bacterial species with clinical evidence of infection. However, in many cases and particularly early in hospital admission, antimicrobial therapy is broad and non-specific as to cover many potential pathogens until therapy can be narrowed based on known pathogen(s). Notably, aminoglycosides are often utilized as first-line broad-spectrum antibiotics (*74*).

Immunostimulation and immunosuppression during sepsis is a critical balancing act. Too much immune activation contributes to pathogen-independent SIRS pathology while too little immune activity (CARS) allows infection to run wild. To this end both immunosuppression (*75*) and immunostimulation (*76, 77*) strategies have been developed and tested for therapy during SIRS, sepsis, and CARS. An extreme example of immunosuppression is that of humans with inactivating TLR4 mutations. Even though

TLR4 mutation protects against endotoxemia (*78*), affected individuals experience recurrent infections and typically pass away in their early teens due to sepsis (*79*).

Innate immunity is essential for surviving sepsis. However, over-stimulation of innate immunity enhances mortality. This delicate immune balancing act holds promise for emerging sepsis therapies. The future of sepsis therapy may include methods to gauge a patient's immune status more accurately than is currently possible including white-blood cell assays, quantitative pro-inflammatory biomarker measurements, and other to be determined technologies. Once a clinical determination of what kind of immune response a patient is mounting (or not) a therapeutic immunotherapy intervention could be initiated to tip the scales of the immune system up or down in the patient's favor.

Table 1-2-1: Clinical Criteria for SIRS Diagnosis (*39*).

Clinical diagnosis of SIRS requires meeting two of the four criteria.

Any two of the following meets clinical SIRS criteria	
Pediatric (*40*)	**Adult (*39*)**
Temperature >38.5°C or <36.0°C	Temperature >38.0°C or <36.0°C
Tachypnea: >2SD above normal for age breaths/min	Tachypnea: >20 breaths/min
Tachycardia: >2SD above normal for age beats/min, or <10th percentile if <1-year-old	Tachycardia: >90 beats/min
White blood cell count: Elevated or decreased total count based on normal values for age, or >10% immature neutrophils (band cells)	White blood cell count: >12,000/ml or <4,000/ml

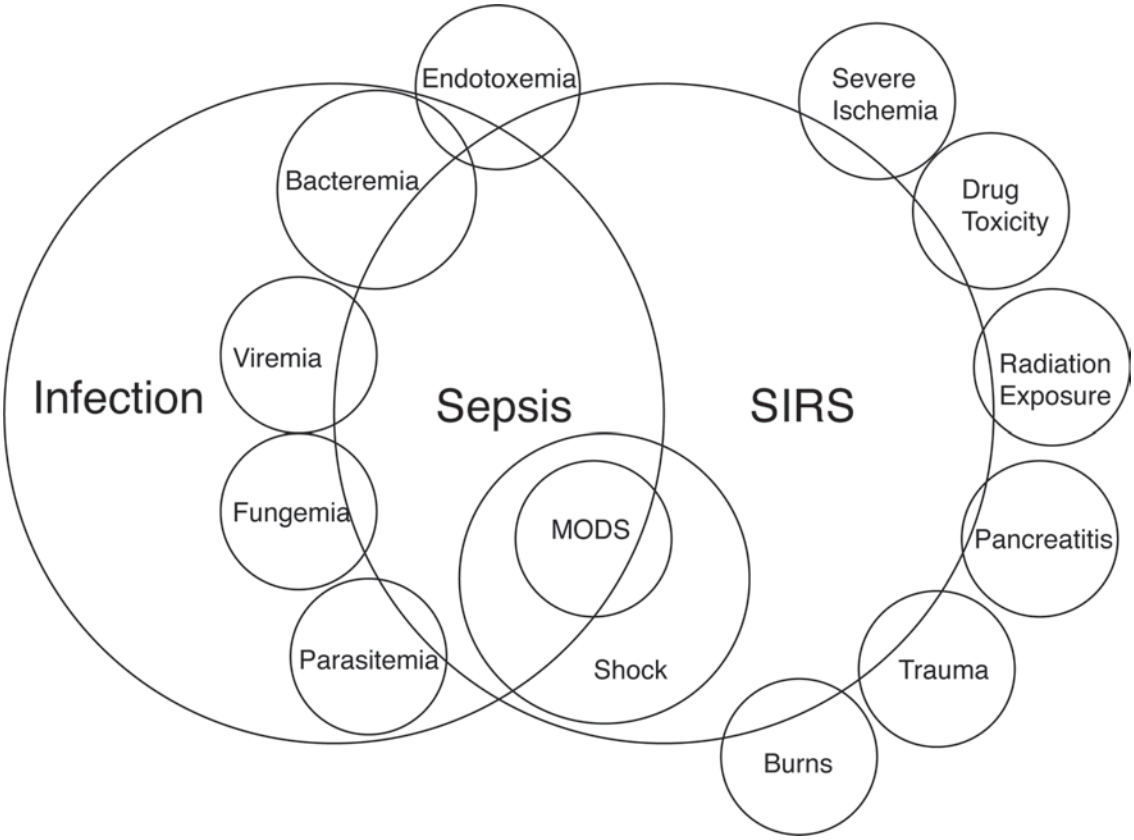

Figure 1.2.1: Overlap and etiologies of infection, sepsis, and SIRS. Modified from (*39*). Overlap of Sepsis and SIRS syndromes along with etiologies. Note that endotoxemia is one way to induce SIRS and is a model for gram-negative bacterial sepsis

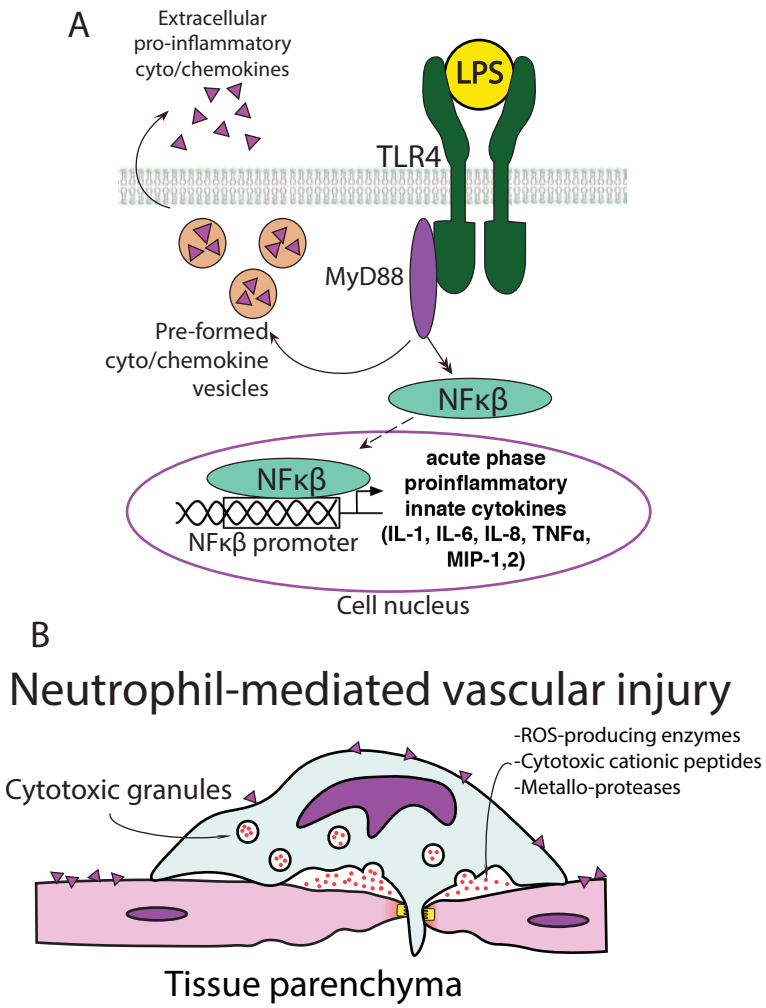

Fig. 1.2.2: TLR4 signaling and downstream neutrophil mediated vascular injury. (A) LPS binds TLR4 and via MyD88 accessory protein activity signals to cause NFκβ transcription factor translocation to the nucleus promoting transcription of pro-inflammatory cyto/chemokines. (B) NMVI occurs when cyto/chemokine activated neutrophils adhere to cytokine-activated endothelium and degranulate releasing cyototoxic molecules which degrade intercellular tight junctions promoting neutrophil diapedesis.

1.3 – Drug-induced Ototoxicity

1.3.1 – Overview of Ototoxic Drugs

Drug induced ototoxicity is a permanent side-effect of clinical aminoglycoside antibiotic and platinum-based chemotherapy treatment. Salicylates, loop-diuretics, erythromycin, and vancomycin are some other ototoxic drugs. Ototoxic drugs also tend to be synergistically ototoxic with one another such as loop-diuretics in combination with aminoglycosides. While molecular targets differ between these ototoxic agents, a key pathophysiological process is ROS generation, which provides insight into shared ototoxic mechanisms (section 1.6).

1.3.2 – Focus on Aminoglycoside Antibiotics

Aminoglycoside antibiotics are polycationic polysaccharides. Streptomycin, derived from *Streptomyces griseus*, was the first aminoglycoside purified by humans *(80)*. Aminoglycosides isolated from other *Streptomyces* species include kanamycin, actinomycin, and tobramycin. Multiple semi-synthetic aminoglycoside analogs have been developed with the goal of outwitting resistant bacterial strains, avoiding toxicities, and for patentability (*81*).

Aminoglycoside bacterial selectivity stems from inhibition of the 30S ribosomal subunit, specifically inhibiting prokaryotic protein synthesis. However, aminoglycosides also bind the eukaryotic mitochondrial ribosomes, causing eukaryotic cross-toxicity (*82*). Certain human mitochondrial rRNA mutations that increase affinity for aminoglycoside binding enhance susceptibility to ototoxicity (*83, 84*).

Another mechanism of action and bacterial selectivity is binding to anionic phospholipids of biological lipid bilayers (*85, 86*) and inhibition of endosomal phospholipase (*87*). Non-specific binding of aminoglycosides to anionic biomolecules induces phospholipidosis and inactivation of transmembrane biomolecules (*88*). Because bacterial cell membranes are anionic and eukaryotic membranes are zwitterionic,

aminoglycosides selectively bind to and disrupt bacterial cellular membrane homeostasis. Some aminoglycosides such as streptomycin enhance Ca^{2+} leak from cell-free liposomes while others such as gentamicin enhance liposome leak to a lesser degree. However, aminoglycoside pore forming activity is less than well characterized pore forming agents such as ionomycin (*89*). This mechanism is reminiscent of endogenous polycationic amphiphilic anti-microbial peptides which share structural similarities to more hydrophilic and less amphipathic aminoglycosides. In fact, a new class of antibiotics based on aminoglycosides has been developed to mimic the action of anti-microbial peptides by adding hydrophobic groups to enhance the amphiphilicity of the drugs (*90, 91*). Amphipathic aminoglycosides bind to phospholipid bilayers and penetrate the hydrophobic surface forming membrane pores and biomolecular flocculation (*92*)

Cellular stress from aminoglycoside exposure results in hair cell apoptosis and necrosis (*93*). While blocking protein synthesis is a prominent feature of cytotoxic activity, ROS production is a hallmark of aminoglycoside ototoxicity and is ameliorated by overexpression of ROS scavenging superoxide dismutase in transgenic mice (*94*). Aminoglycosides are permeant and complete blockers of non-specific cation and Ca^{2+} channels; examples include TRPV4 (*95*), TRPA1 (*96*), and notably the hair cell MET channel (*97-100*). Through this blocking activity, aminoglycosides disrupt Ca^{2+} homeostasis (*101, 102*) and uncouple mitochondrial respiration (*103-105*), which partially explains leukocyte-independent ROS production. Cochlear ROS also derive from ternary interactions between aminoglycosides, ferritin, and polyunsaturated fats (*106*).

Cell death from amionoglycoside induced ROS production and protein synthesis inhibition can cause cellular necrosis and release of innate inflammation promoting DAMPs. Aminoglycosides can also independently activate the NLRP3 inflammasome (*107*). *In vitro*, neutrophil-derived ROS production increases upon aminoglycoside exposure, highlighting the leukocyte contribution to aminoglycoside-induced oxidative stress (*108*). Indeed, NFκβ is activated by aminoglycoside treatment, promoting innate inflammation (*109*). Atorvastatin (*110*) and dexamethasone (*111*) both act to dampen NFκβ activity and are nephro/otoprotective during aminoglycoside therapy.

Overall, DAMP induced inflammation and associated ROS production enhances hair cell death processes by both cell-intrinsic and leukocyte-mediated cytotoxic mechanisms. These mechanisms act together to cause organ damage; the cochlea is both more sensitive to toxicity and also has a lesser affinity for recovery/repair compared to other effected organs such as the kidneys.

1.3.3 – Focus on Platinum-Based Chemotherapy

Cisplatin was first synthesized in 1844 by Italian chemist Michele Peyrone (*112*). However, it was not until 1965 that biophysicist Barnett Rosenberg accidentally discovered cisplatin's cell cycle inhibitory activity while studying electrical field effects on bacterial growth. Rosenberg noticed that electrolysis products from a platinum electrode (cisplatin) inhibited *E. coli* growth (*113*). Follow-up studies in a mouse model of leukemia and sarcoma demonstrated cisplatin's anti-neoplastic activity (*114*). Today, cisplatin and other related platinum adducts are standard of care for germ-line tumors such as medulloblastoma, neuroblastoma, and hepatoblastoma in pediatric patients, and for advanced metastatic cancers (*115*). For other platinum-based chemotherapies that penetrate endothelial barriers to a lesser degree, such as carboplatin, ototoxicity is dependent upon BLB disruption.

When cisplatin is dissolved in water the chloride atoms undergo substitution reactions with water to yield *cis*-$[Pt(NH_3)_2(H_2O)_2]^+$, a potent electrophile. Aquated cisplatin most notably forms coordinate covalent bonds with the purine ring nitrogen atoms of nucleic acids to cross-link and prevent DNA replication (*116*). Blocking the S-phase of cell division explains cisplatin's anti-neoplastic activity by preventing cancer and other highly proliferative cell populations from replicating. Similarly, cells less capable of repairing DNA (such as prokaryotes) are hypersensitive to the cytotoxic activity of cisplatin (*117*). Aquated cisplatin also avidly reacts with proteinaceous cysteine and methionine residues, often resulting in protein inactivation (*118, 119*)

Cisplatin interacts with a number of molecular transporters and ion channels (*120*). Some of these proteins work to keep cisplatin out and others provide pathways for cisplatin to enter cells and organs. For example, the copper transporter is a primary transporter for trafficking cisplatin into cells (*121*). Cisplatin also interacts with the multi-

drug resistance transporters (MDRs), which function to keep toxins out of barrier organs (including the brain, eyes, and ears) and into detoxifying organs (such as the liver). Although expression of the prototypical MDR, MDR1 (also known as p-glycoprotein) increases following cisplatin treatment (*122*), cisplatin does not interact directly with this protein (*123*). One notable transporter is the electrogenic organic cation transporter 2 (OCT2), which some studies suggest is expressed in cochlear hair cells and may be a therapeutic target by blocking with cimetidine (*124-126*). While OCT2 works to transport cisplatin into hair cells, other multi-drug resistant proteins work to pump cisplatin out. Cisplatin is a substrate for the multi-drug resistant protein 2 (MRP2) ATPase which actively pumps cisplatin out of cells; genetic upregulation of MRP2 makes cells more vulnerable to cisplatin, and downregulation protects cells against toxicity (*127, 128*).

Cisplatin interferes with Ca^{2+} homeostasis by direct and permeant block of non-specific cation channels and other Ca^{2+} permeable channels. Some of these channels include L-type and T-type calcium channels, and TRP channels such as TRPV1. Cisplatin interacts with the MET channel of hair cells (*129, 130*) similar to aminoglycosides. Cisplatin also blocks other mechanosensitive channels including TREK-1, and VSORC (*131*). Cisplatin-Texas Red also appears in hair cells of rats two hours after systemic treatment (*132*). These interactions add up to interfere with physiological Ca^{2+} flux, stressing cells and promoting apoptosis/necrosis (*133*). Despite this wealth of literature suggesting that cisplatin directly interacts with Ca^{2+} channels, some still debate whether cisplatin directly interacts with and permeates calcium channels or if cisplatin modulates Ca^{2+} channels indirectly (*120*).

Aquated cisplatin also avidly binds glutathione, quickly depleting endogenous ROS-scavenging capacity. Depletion of glutathione potentiates cellular oxidative stress from both endogenous and cisplatin-induced free radical species (*134-136*). Free-radical mediated cellular stress from ROS and reactive nitrogen species (RNS) damages molecular and cellular components, promoting apoptosis (lower cisplatin concentration) and necrosis (higher cisplatin concentration) (*137*). Oxidative stress is particularly cytotoxic to highly metabolic cells such as cochlear hair cells, renal tubular cells, and neurons. Similar to aminoglycoside ototoxicity, highly metabolic cells are more sensitive

to cisplatin cytotoxicity provides insight to the drug's principal toxicities of ototoxicity, nephrotoxicity, myelotoxicity, and neurotoxicity.

Similar to aminoglycosides, cisplatin's cytotoxic activities act together to generate DAMPs, promoting innate inflammation. STAT1 is induced by cisplatin therapy and contributes to ototoxicity, blocking STAT1 via round window application of siRNA protects hearing in a rat model (*138*). STAT1 is induced by pro-inflammatory NFκβ translocation to the nucleus and is upstream of pro-inflammatory cytokines such as IL-1 and TNFα. Blocking TNFα with the monoclonal antibody etanercept protects hearing in the same cisplatin ototoxicity model (*138*) demonstrating the importance of inflammation in cisplatin ototoxicity and the multiple potentially therapeutic molecular targets along the pro-inflammatory pathway.

Cytotoxic mechanistic overlap between aminoglycosides and platinum chemotherapy is substantial. While the molecular targets of the two drugs do differ, the pathophysiological response to these drugs is quite similar. Specifically, inflammation and ROS production are key common mechanisms underlying ototoxicity.

1.4 –Blood-Labyrinth Barrier – An Introduction

1.4.1 – The Endothelial Barrier Concept

1.4.1.1 – Endothelial Barriers

The concept of a blood-brain-barrier developed when Ehrlich first observed that various azo-based dyes injected systemically into animals were excluded from the brain but not from other organs in the body (*139*). In later experiments, Goldmann (a student of Ehrlich's) injected dye into the CSF and noticed that it remained confined to the CNS (*140*). Dyes are also excluded from other organs such as the retina, gonads, and the cochlear labyrinth. The concept that some substances are selectively excluded from some tissues versus others led to the concept that specialized semi-permeable vascular anatomy regulates molecular trafficking at these organs.

Further experiments demonstrated that different molecules traffic at varying rates into organs with these specialized barrier properties. Molecular properties such as molecular weight, electrostatic charge, hydrophobicity, and conformational three-dimensional structure determine the vascular trafficking rate constant. For example, albumin, a large molecular weight negatively charged and hydrophilic molecule, is excluded from the brain, while the small hydrophobic uncharged molecule propofol rapidly enters brain parenchyma. Mechanisms regulating differential molecular trafficking depends upon individual molecular properties, endothelial cell barriers, as well as pathological, non-physiological, states of the barrier.

1.4.1.2 – Molecular Properties Regulating Trafficking Properties

Molecular weight and radius spatially regulate what spaces a molecule can traffic through (*141*). This is particularly important when the trafficking mechanism is passive diffusion through capillary fenestrae, *e.g.,* paracellular trafficking. For example, in mice deficient in the tight-junctional molecule claudin-5, molecules under 800 Da can traffic into brain parenchyma while larger molecules may not (*142*).

Molecular conformation also contributes to trafficking selectivity. As a general rule, determining the smallest molecular radius based on conformational molecular modeling and analysis can predict radius-selective trafficking. The equilibrium constants molecular conformations and the rate constants for the conformational changes in each direction may also impact trafficking. If the majority of a given molecule exists, in a conformation that excludes it from the barrier, the trafficking rate constant will be low and correlate with the rate constant of conformational change to the barrier-permeable conformation (*143*).

Net ionic charge is also a substantial determinant of barrier permeability (*144*). Vascular barriers tend to exclude anions, while cations are overall more permeable. Trafficking of neutral molecules are not affected by these charge-related trafficking determinants and hydrophilic neutral molecules are ideal for studying passive paracellular trafficking properties. Negatively charged glycocalyx, which lines the vascular endothelium, repulses negatively charged molecules via electrostatic forces; loss of glycocalyx during pathological states such as vascular inflammatory states modulates the barrier ionic selectivity. Another way that ionic charge effects trafficking properties is with regard to ion channels. Ionic charge effects trafficking via ion channels as well due to the impact of electrostatic interactions within the pore and the opening of the pore on charge selectivity. For example, polycationic aminoglycoside antibiotics are permeable to some non-selective cation channels such as the MET channel of hair cells (see section 1.3.2).

Hydrophobicity and hydrophilicity are perhaps the most influential determinants of barrier permeability. Very hydrophobic molecules passively diffuse across vascular barriers by dissolving in cellular lipid-bilayer membranes and re-partitioning into tissue parenchyma. Conversely, very hydrophilic molecules cannot passively diffuse across vascular barriers as they are not lipid soluble and therefore may not integrate into membrane lipid bilayers. The degree of molecular partitioning can be attributed to and predicted by the hydrophobicity index, which is the molecular portioning coefficient between water and octanol (**Fig. 1.4.1**) (*145*).

1.4.1.3 – Endothelial Barrier Properties Regulating Trafficking Properties

Molecules traffic across vascular barriers by five prototypical mechanisms including: passive diffusion, non-specific pinocytosis/transcytosis, ion-channel mediated permeation, specific transporter mediated trafficking, and (pathological) paracellular diffusion (**Fig. 1.4.2**). Other less well described and elusive trafficking mechanisms have also been reported such as passive diffusion through transient transcellular pore structures related to leukocyte transcellular migration (*146*).

As described in section 1.4.1.2, passive diffusion is dependent upon the hydrophobicity of the molecule of interest and can be predicted by the hydrophobicity index.

Endocytotic mechanisms play a significant role in barrier transport. Barrier capillary beds demonstrate fewer caveolae under ultrastructural electron microscopy examination compared to other non-barrier systems (*147, 148*). Pinocytotic activity acts to traffic essential compounds from serum into tissue parenchyma. For example, during infection and inflammatory states, pinocytotic activity increases (*149*). One hypothesis is that enhanced pinocytosis during infection increases tissue parenchymal concentrations of immunoglobulins to promote pathogen neutralization and leukocyte recruitment.

Transport of substances through ion channels and other pore structures, such as aquaporins assist in the maintenance of ionic and osmotic homeostasis. While these proteins have natural ligands which they transport, other non-endogenous molecules also permeate via this mechanism. For example, both cisplatin chemotherapy and aminoglycoside antibiotics are permeable blockers to non-specific cation channels such as TRP channels (*96*) and hair cell mechanotransduction channels in a concentration dependent manner (*97, 130, 150*).

Similar to ion channels, specific carrier-mediated transport selectively traffics substances into and also keeps substances out of tissue parenchyma. For example, sodium-glucose like transporter 2 (SGLT2) co-transports Na^+ and glucose into brain tissues via secondary active co-transport. Organic anion transporters (OATs) are organic anion anti-porters which exchange endogenous dimethyldicarboxylate into cells and exogenous organic anions out of cells (*151*). Other specific transporters such as amino

acid transporters work collectively together to define the molecular selectivity of endothelial barriers.

Lastly, paracellular trafficking between endothelial cells is minimal at baseline in barrier vascular beds. On the other extreme is the fenestrated vascular system of the liver where blood is contiguous with liver parenchyma. After certain pathologies such as auto-immune vasculitis, stroke, trauma, and endotoxemia pathological paracellular trafficking routes not present under homeostatic conditions emerge. A common thread in the mechanism of each of these pathological trafficking routes is an inflammatory component. Overall, alterations in tight-junctional architecture develop by both endothelial independent and leukocyte-dependent interactions with endothelial barrier.

1.4.2 – The Blood-Labyrinth Barrier

1.4.2.1 – Overview of Cochlear Blood Supply

Axelsson published the first unambiguous description of human and guinea pig otological vascular anatomy in 1968 (*152*); still, considerable variation in nomenclature pervades the scientific and medical literature. This section will summarize the findings of Axelsson's work.

Inner-ear tissues are fed by the *labyrinthine artery,* which derives from the *vertebral-basilar-anterior inferior cerebellar – labyrinthine*. Once in the acoustic meatus, the *labyrinthine artery* divides into the *anterior vestibular artery* and *common cochlear artery*. The *common cochlear artery* terminally divides into the *vestibulo-cochlear artery* and the *cochlear artery*.

The *vestibular branches* of the *vestibulo-cochlear branch* supply the basal end of the cochlea, vestibular and semicircular canals. The *cochlear branch* follows the spiral course of the modiolus and is known as the *spiral modiolar artery*.

Arterioles regularly radiate from the *spiral modiolar artery* and are named *radiating arterioles*. *Radiating arterioles* supply either the spiral lamina/ basilar membrane or the lateral wall. In rodents, these circulations are separate; the vasculature of the spiral lamina/ basilar membrane does not anastomose with that of the lateral wall. In humans, communicating vessels of the later wall and basilar membrane exist near the

region of the external spiral sulcus and the insertion of the basilar membrane on the lateral wall; these anastomoses are uncommon.

Circulation of the spiral lamina and basilar membrane originates from radiating arterioles penetrating the spiral lamina in the direction of the organ of Corti. Arcading spiral branches come off of *radiating arterioles* at ninety-degree angles. Depending upon where in the spiral lamina/ basilar membrane these branch points occur determines the name of the branch. The *vessel of the basilar membrane* is the most distal of these vessels and underlies the region under cochlear hair cells. In the middle is the *vessel of the tympanic lip*. Closest to the modiolus are *limbus vessels* which reside within the spiral limbus; *limbus vessels* are unique in that they are the most tortuous of these vessels and are a major source of vascularization of this region. Speculations suggest that *limbus vessels* may contribute to endolymphatic regulation (see *section 1.4.2.4*). At regular intervals, the *vessel of the basilar membrane* and *vessel of the tympanic lip* coalesce into *radiating venules* which feed in to the *spiral modiolar vein* which runs the same course as the *spiral modiolar artery*. After a capillary region, the radius of *limbus vessels* increases and these venules turn course back towards the *spiral modiolar vein*. Often these *spiral limbus venules* never coalesce with the *radiating venules* from the *vessels of the basilar membrane and tympanic lip* but instead insert directly into the *spiral modiolar vein*. Sometimes *limbic vessels* do anastomose with radiating venules from *vessels of the basilar membrane and tympanic lip* close to the *spiral modiolar vein*.

Circulation of the cochlear lateral wall begins with *radiating arterioles* passing through the apical aspect of the scala vestibuli and reaching the superior aspect of the cochlear lateral wall where these arterioles then divide into capillary networks. These capillary networks then converge around the inferior lateral wall in the scala tympani region where venules are formed. *Radiating venules* then traverse the inferior aspect of the scala tympani to reconnect with the *spiral modiolar vein*. Named vessels between the arterial and venous sides of lateral wall circulation project at roughly ninety-degree angles and form spiraling arcades, similar to the spiral lamina/basilar membrane circulation. These vessels include, from apical to basal aspect, the *vessel of the scala tympani, vessel of the vestibular (Reissner's) membrane,* the *stria vascularis* capillary network or the scala media, the *vessel of the spiral prominence*, and *venules of the basilar*

membrane. Well defined and mostly straight-coursing vessels define the apical and basal boundaries of the *stria vascularis* with polygonal capillary arrangements intervening these boundaries. Arterio-venous shunts are common in the cochlear lateral wall circulation with anastomosing vessels connecting structures such as the *vessel of the vestibular membrane* and the *vessel of the spiral prominence*. The function of these arterio-venous shunts is not known although speculation suggests they help regulate cochlear blood pressure, cochlear temperature, and to fine tune cochlear blood flow.

1.4.2.2 – Multiple Barriers Comprise the Blood-Labyrinth Barrier

Endolymph, which fills the scala media, and perilymph, which fills the scala tympani and scala vestibuli, are plasma ultra-filtrates with unique compositions. Similar to CSF, endolymph and perilymph are produced by specialized vascular beds and their compositions are maintained by selective trafficking at the blood-labyrinth barrier (BLB). Similar to the BBB, the BLB concept derives from the observation that changes in plasma composition are selectively reflected in the cochlear lymphatic fluids (*153*).

Specialized vascular and epithelial structures of the inner-ear collectively form the BLB, which is further sub-divided into the blood-perilymph and blood-endolymph barriers. Within these barriers, there are multiple endothelial and epithelial cell barriers, which isolate the blood from the cochlear lymphatic fluids (**Fig 1.4.4**). Collectively, these barriers work to regulate the specialized fluid compositions of the inner-ear. The origins of these specialized lymph fluids is still under active investigation and discussed in detail below.

1.4.2.3 – Blood-Perilymph Barrier

The blood-perilymph barrier is defined by the structures bordering perilymph, specifically, the simple cuboidal epithelium lining the bony portions of the scala tympani and scala vestibuli, the most apical and inferior aspects of the spiral ligament, Reissner's membrane, and the basal aspect of the basilar membrane/ spiral lamina. Further barriers are delineated by the spiral ligament capillaries where the extracellular fluid beyond these capillaries is similar to perilymph. With the exception of the stria vascularis region, the

spiral ligament is considered contiguous with the perilymphatic compartment. Tight-junction coupled basal cells demark the border between the stria vascularis and spiral ligament. Perilymph is similar to CSF in composition with high sodium, low potassium, and low protein. Perilymph is continuous with cerebrospinal fluid via three structures, the cochlear aqueduct, the vestibular aqueduct, and the modiolus via the internal auditory canal housing CNVIII (*154*). The cochlear and vestibular aqueducts are small direct communications filled with loose connective tissue similar to dura mater. Small pores in the modiolus allow CSF communication between the CNVIII sheath and perilymphatic spaces (*155*).

Where perilymph derives is debated. Some suggest that perilymph is a plasma ultrafiltrate and primarily derives from vessels close to the scala vestibuli and in particular, the vessel at the vestibular (Reissner's) membrane (*152*). As circulation in the scala tympani is venous, this region is speculated to reabsorb perilymph. Indeed, differences in perilymphatic composition of the scala vestibuli versus the scala tympani (*156*) support the hypothesis that perilymph is produced in the scala vestibuli and moves towards the scala tympani, slowly changing composition as perilymph bulk flow progresses towards the oval window of the scala tympani. Others have suggested that perilymph may derive from the vascular spring coiled vessels of the modiolus (*152*). Studies where the cochlear aqueduct is obliterated (measures vascular contributions) versus where an animal is exsanguinated (measures CSF contributions) estimate that 22% of perilymph derives from the CSF via the cochlear aqueduct and 78% from cochlear vascular ultrafiltrate (*157*). Studies such as this however have limitations; perilymph production is measured by measuring fluid volume exudation from a small apical cochleostomy. When the perilymphatic space is opened, and the cochlea is no longer a closed system, the positive pressure equilibrates with the surroundings which enhances the outflow of perilymph. This scenario is termed "perilymphatic gusher" (*158*). Another limiting assumption is that when an animal is exsanguinated and the animal expires, the CSF contribution to perilymph production rate remains similar to the *in vivo* situation.

1.4.2.4 – Blood-Endolymph Barrier

Endolymph is a specialized lymphatic fluid found only in the scala media. Unique characteristics include high K^+ and low Na^+ concentrations coupled with an 80-100 mV electric potential, which increases the driving force of ions through the hair cell MET channels, enhancing hearing sensitivity. Endolymph's unique composition is produced by electrochemical pumps on marginal cells and is maintained by the tight-junction coupled epithelium lining the scala media. The blood-endolymph barrier is defined by the epithelial linings of Reissner's membrane superiorly, the basilar membrane and spiral limbus inferiorly, and the marginal cells of the stria vascularis medially. Three cell types predominate in the stria vascularis including the basal cells laterally, interdigitating intermediate cells, and marginal cells which contact endolymph; endothelial cells form the strial capillary network which weave through intermediate cells. Pericytes periodically contact strial blood vessels and regulate strial capillary flow and endothelial-strial barrier integrity (*159*). Perivascular resident macrophage-like melanocytes, also known as strial dark cells, are a monocyte derived cell population and contribute to blood-strial barrier integrity (*160-163*).

Similar to perilymph, the origin of endolymph is also debated. Possible origins include the stria vascularis, the vessels of the spiral limbus (*152*), and perilymphatic communications via aquaporins (*164*). The lymphatic fluid may derive from ultrafiltrate from the stria vascularis, ultrafiltrate from the spiral limbus vessels, aquaporins on Reissner's membrane, or a combination of the three sources. The spiral limbus region is an intriguing prospect in that the vessels in this region are fenestrated and these fenestrations are regulated by cells and cellular structures similar to those of astroglial end-feet of the BBB (*152*). While the contributions of the fluid component of endolymph is debated, good evidence exists that the ion content of endolymph is predominantly regulated by the marginal cells of the stria vascularis (*165*). In particular, Na-K-ATPase expression is significant on the medial surface of marginal cells which contact endolymph (*166*). The endolymphatic compartment does not communicate with perilymph or CSF and thus its generation and reabsorption are a closed system. Endolymph reabsorption likely occurs at the endolymphatic sac, where specialized

phagocytic cells clear any larger molecular weight molecules or cellular debris and features a vascular bed similar to the area postrema. Obliteration of the endolymphatic sac induces endolymphatic hydrops as a result of increased endolymphatic hydrostatic pressure, inducing Meniere's disease (*167*). This observation provides strong evidence that the endolymphatic sac absorbs endolymph.

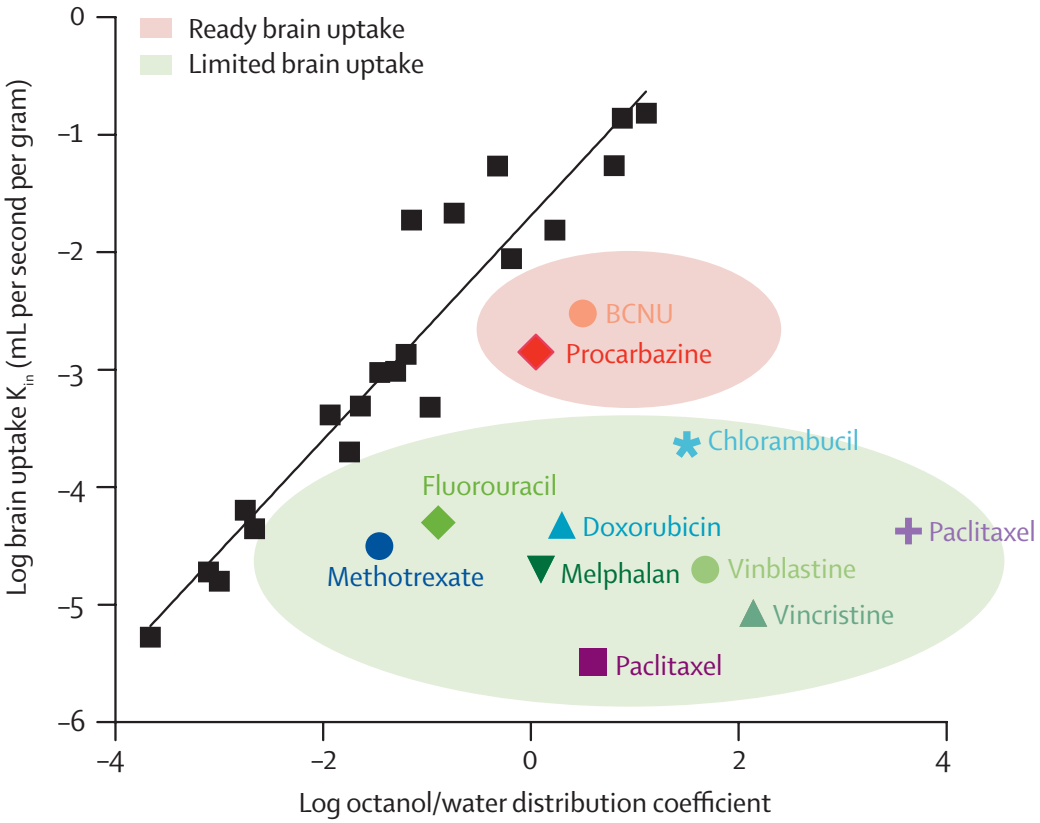

Fig. 1.4.1: Water:octanol partition coefficient of some common cancer chemotherapeutics.

The water:octanol partition coefficient is a measure for how hydrophilic or hydrophobic a molecule is. The lower the ratio the more hydrophobic (octanol soluble). A higher ratio suggests a molecule is more hydrophilic (water soluble). Reproduced with permission from (*145*).

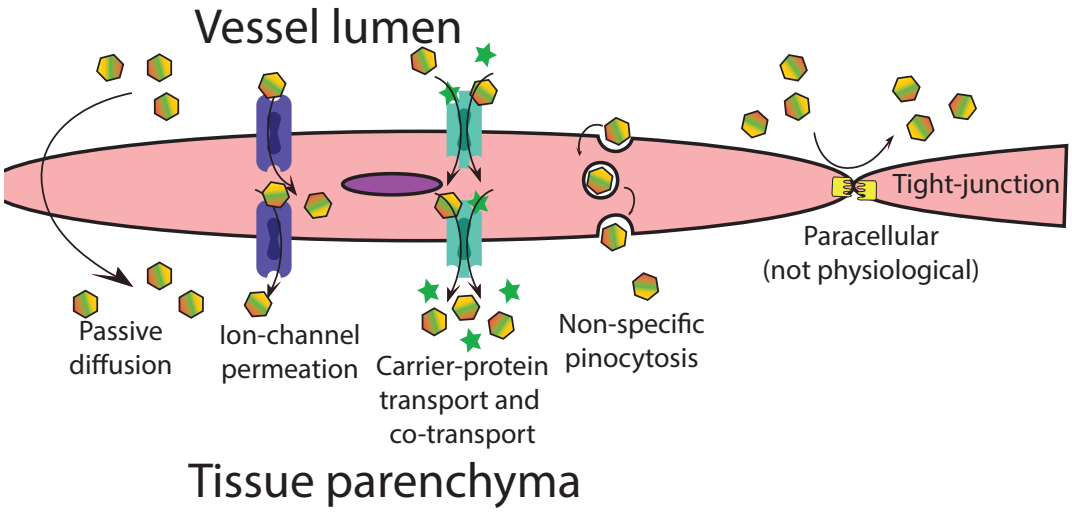

Fig 1.4.2: Five prototypical trafficking mechanisms at endothelial cell barriers such as the BBB and BLB.

The five most commonly discussed endothelial cell barrier trafficking mechanisms in endothelial barrier science. Note that paracellular trafficking at tight-junction coupled endothelial barriers is not significant under physiological conditions. Pathological conditions involving tight-junction disruption can lend to enhanced paracellular trafficking.

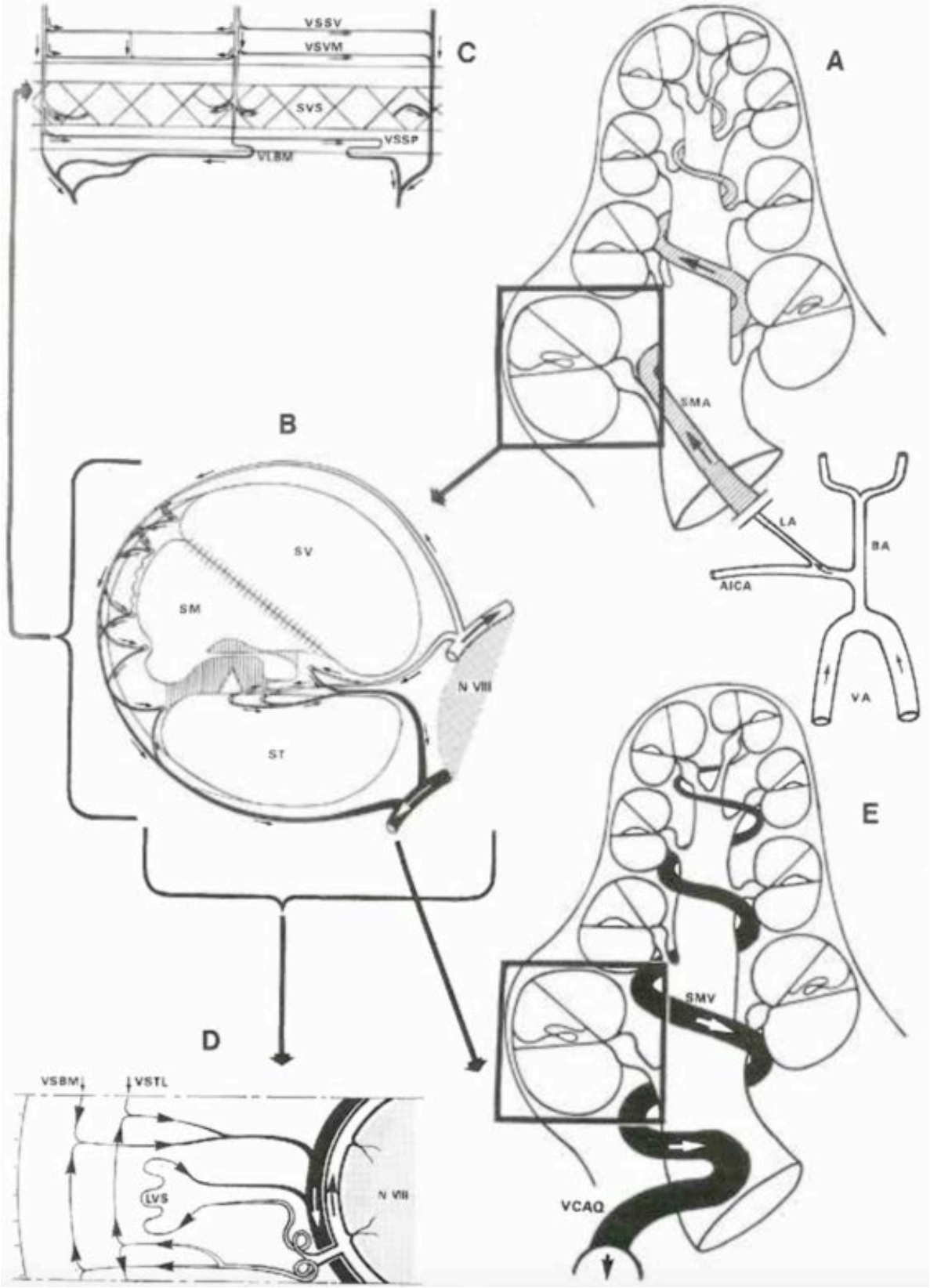
VSSV
VSVM
C
SVS
VSSP
VLBM
A
SMA
B
SV
SM
N VIII
ST
LA
BA
AICA
VA
E
SMV
VCAQ
D
VSBM
VSTL
LVS
N VIII

Fig 1.4.3: Schematic summarizing the cochlear blood supply. Reproduced identically from Axelsson 1968 (*152*).
(A) Major arteries: VA = vertebral artery, BA = basilar artery, AICA = anterior inferior cerebellar artery, LA = labyrinthine artery, SMA = spiral modiolar artery. (B) Radial section of a half turn (framed in A and E): SV = scala vestibuli, SM = scala media, ST = scala tympani, N VIII = acoustic nerve. Cross-hatched areas are avascular. (C) Radial section of the external wall: VSSV = vessel of the scala vestibuli, VSVM = vessel of the vestibular membrane, SVS = stria vascularis, VSSP = vessel of the spiral prominence, VLBM = venules at the basilar membrane. (D) Transverse section of the spiral lamina: VSBM = vessel of teh basilar membrane, VSTL = vessel of teh tympanic lip, LVS = limbus vessels. (E) Major veins: SMV = spiral modiolar vein, VCAQ = vein of the cochlear aqueduct.

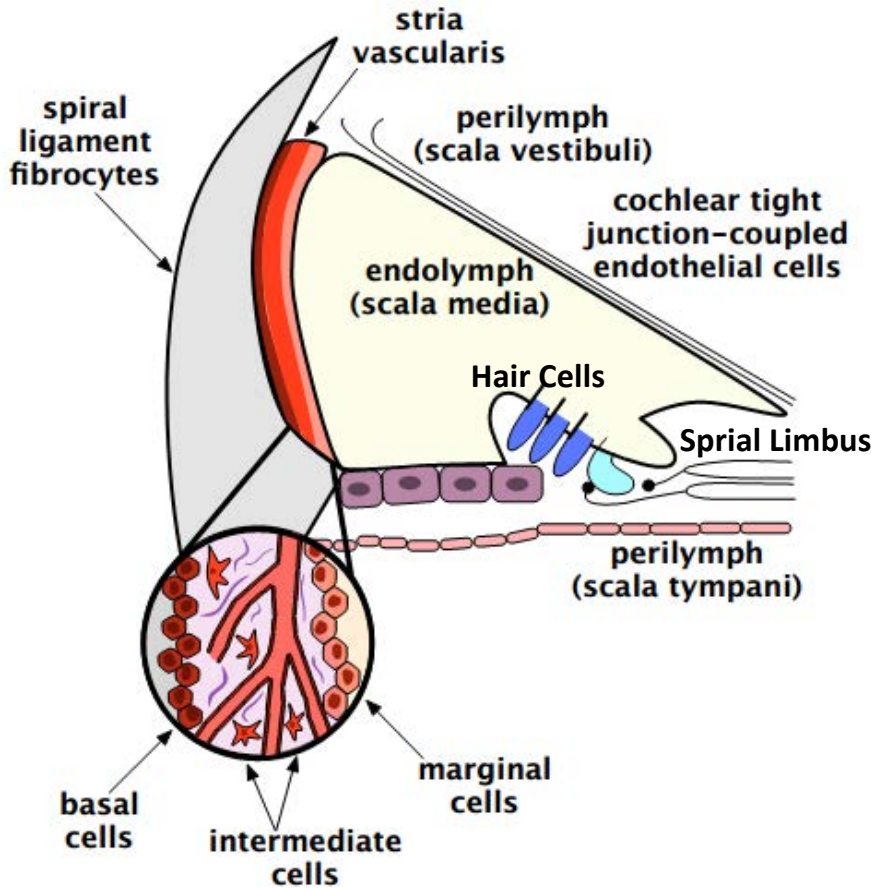

Fig 1.4.4: Schema demonstrating the multiple barriers collectively comprising the BLB. The BLB consists of multiple barriers that collectively form the BLB. The blood-endolymph barrier is defined by the tight-junction couples endothelial cells sealing the scala media and the blood-perilymph barrier that seals the scala tympani and scala vestibuli. There is also the blood strial barrier which forms the barrier between the blood vessels of the stria vascularis and strial parenchymal spaces; see blow up for anatomical detail for the stria vascularis. Other less-defined and less studied vascular regions in the organ of Corti and spiral limbus region may also possess barrier properties.

1.5 – Hearing Restoration and Otoprotective Strategies – Insight to Ototoxic Mechanisms

1.5.1 – Hearing Restoration Strategies and Treatments

Treatment initiatives to restore hearing loss can be divided into three distinct strategies: assistive, restorative, and regenerative. Assistive hearing devices, commonly referred to as hearing aids, amplify acoustic stimuli to bring the stimulus above an impaired hearing threshold. For individuals with light to moderate shifts in hearing threshold (<50dB-HL) these devices do help. One problem with this strategy is that acoustic amplification accelerates noise-induced hearing loss, as loud sound is continuously introduced to the auditory canal (*168*). Another approach is bone-anchored hearing aids which take advantage of bone conduction. These devices are particularly helpful in cases of conductive hearing loss where normal air-conduction and sound wave transduction through the middle-ear is impaired due to sequelae of chronic middle-ear disease. Conduction-based hearing aid devices can also induce sensorineural hearing loss (*169*) highlighting the limitations of acoustic amplification hearing restoration strategies.

Hearing restoration can be achieved with cochlear implants. These unique bio-interfacing machines are the first and most successful functional bionic prosthesis in modern medicine. Cochlear implants consist of a linear electrode array which is inserted through the round window or a small basal cochleostomy. The electrode is then advanced into the scala tympani. These devices work by direct electrical stimulation of spiral ganglion nerve fibers emanating from the cochlear modiolus. Sound is picked up by an externally worn microphone worn close to the ear's pinna and the sound is binned into frequency batches by a speech processor before radio-frequency transmission to the electrode array. Different electrodes along the array are stimulated depending on the frequency distribution of the incoming sound. Because spiral ganglion nerve fibers are tonotopically organized with high-frequency sounds encoded by the basal cochlear fibers and low-frequencies by the apical fibers, cochlear implants can restore frequency

perception. However, electrical stimulation of the organ of Corti stimulates a wider population of neighboring spiral ganglion nerve fibers, resulting in frequency resolution degradation in comparison to the intact cochlea. The result is perception of "vocoded speech," which colloquially speaking sounds like a robot. Coding of sound intensity is achieved by increasing the intensity of electrical stimulation, which increases the spike rate of acoustic nerve fibers. Cochlear implants can miraculously restore hearing to even the most profoundly hard of hearing individuals.

A limitation of cochlear implants is long-term cochlear fibrosis which leads to device failure (*170*). Because cochlear implant materials poorly mimic native tissue and do not express molecules which lend to the body's recognizing the material as "self," a foreign body reaction inevitably ensues leading to long-term fibrous encapsulation of the device. Because the foreign body reaction is mediated by the immune system, steroid-eluting cochlear implant materials have been developed to try to slow down the foreign body reaction. (*171-174*). Additionally, spiral ganglion neurons degenerate at an accelerated rate over the life of an individual experiencing hearing loss and may degenerate even faster with cochlear implantation (*175*). One strategy to try and enhance neuron survival is elution of small molecular mimics of neurotrophic factors BDNF and TrkB (*176, 177*). Another approach utilizes the electronic stimulation of the electrode array for electroporation and localized neurotrophic gene therapy (*178*).

Regenerative strategies aim to replace cells and anatomical features that were once in the hearing apparatus but for a number of reasons have degenerated as a result of some ototoxic insult. A major breakthrough in the area of hair cell regeneration came with the generation of mechanosensitive hair cell-like cells from induced pluripotent and embryonic stem cells (*179*). While hair cell-like cells are an exciting advancement in the field, the challenge remains how to functionally integrate these hair cell-like cells into a damaged cochlea in a functionally meaningful way. For other structures in the auditory pathway such as the tympanic membrane this has not been an issue as the arrangement of tympanic membrane epithelial cells is a homogenous sheet. Seeding of bone marrow derived stem cells onto a perforated tympanic membrane promotes closure of the perforation (*180, 181*). However, the cochlea's highly specialized and particular cyto-architecture is a significant barrier to meaningful bio-integration of stem-cell derived hair

cells. To this extent, bio-scaffolding approaches have been developed for which hair cells could presumptively re-populate in an organized and physiologically meaningful pattern (*182*). Another hair cell regeneration strategy derives from the observation that chickens who lose their hair cells from ototoxic insult regenerate via transdifferentiation from surrounding organ of Corti support cells (*183*). Later it was discovered that this same transdifferentiation route can occur in mammals (*184*) and can be promoted via manipulation of stem cell related signaling pathways such as *Notch* (*185*), *Atoh1* (*186*), and *Math1* (*187*). Advancement of hair cell regeneration to a point of effective clinical application is likely far in the future.

1.5.2 – I.V. Hydration, Peak Drug Level Monitoring, and Other Passive Otoprotective Strategies.

1.5.2.1 – Hydration and Peak-Plasma Concentration Monitoring

Aminoglycoside and cisplatin ototoxicity is dose dependent and related to cumulative area under the curve (AUC) as defined by integrating blood plasma concentration over time (**Equation 1.5.1.1**) (*188-190*). Thus, the risk of ototoxicity (*191*) can be managed by monitoring drug plasma concentration over time (*192, 193*). Constructing a concentration versus time plot allows calculation of the AUC for modeling of customized pharmacokinetic models for individual patients to optimize dosing regimens (*194*).

Favorable clinical outcome is also related to peak plasma concentration (*195*) and therefore achieving both clinical efficacy and avoiding ototoxicity is a fine balancing act. The patient's hydration status is key for two reasons: 1) a dehydrated patient will attain a higher peak plasma concentration after an equivalent mg/kg dose versus a well hydrated patient, and 2) efficient drug metabolism requires adequate hydration for hepatic metabolism and renal excretion of the pharmaceutical. This concept is highlighted in dialysis patients with chronic renal failure and hence impaired aminoglycoside excretion and greatly increased AUC (*196, 197*).

Equation 1.5.1.1: $AUC = \int_0^t C_p dt$, *where* C_p*=Plasma concentration of drug*

1.5.2.2 – Once-Daily Aminoglycoside Dosing

Aminoglycoside toxicity is related to dosing frequency; once-daily dosing exposes patients to a lower risk of nephrotoxicity (*198, 199*), with no increased risk for ototoxicity when compared to continuous *i.v.* infusion or splitting the total daily dose into multiple daily doses (*200-203*). Once-daily dosing has a number of advantages. First, it is simple for the healthcare team as it eliminates the opportunity for inconsistencies in the timing of dosing or slight differences in healthcare worker administration of the drug. Giving a larger dose once a day also means a higher peak-plasma concentration and time where the peak plasma concentration is greater than the minimum inhibitory concentration (MIC), and overall smaller AUC. Together, peak-plasma concentration greater than the MIC and smaller AUC means improved bacterial killing and toxicity risk minimization.

1.5.3 – Acetylsalicylic Acid Otoprotection

1.5.3.1 – Aspirin: History and Pharmacology

Acetylsalicylic acid (aspirin) was first synthesized in 1897 by Hoffman and Eichengrün (*204*) by acetylation of salicylic acid and is the prototypical non-steroidal anti-inflammatory drug (NSAID). Tea brewed with salicylic acid rich willow bark provides relief for arthritis, analgesia during childbirth, and (unsuccessfully) for malaria (*204*). Historical accounts of salicylic acid teas date back as far as the Egyptian Empire, the Roman Empire (*204*), and indigenous civilizations of the Americas (*205, 206*). In 1964 nearly 16-billion aspirin tablets were consumed annually (*207, 208*) and aspirin remains one of the most consumed pharmaceuticals in the world today (*209*). In the United States an estimated 43-million people take aspirin on a regular basis.

Aspirin produces anti-inflammatory effects by permanent inactivation of cyclooxygenase enzymes COX-1 and COX-2 via acetylation of serine residue 530 at the active site (*210*). COX enzymes metabolize arachidonic acid into intermediate cyclic endoperoxidases which are further metabolized to pro-inflammatory molecules including prostacyclins, prostaglandins, thromboxanes (all synthesized by COX1 and 2) and

leukotrienes (synthesized by 5-lipoxygenase). For example, the thromboxane TXA_2 promotes platelet aggregation and increased vascular tone. PGI_2 decreases vascular tone and inhibits platelet aggregation. Although these signaling molecules have opposite effects, the net effect of aspirin is decreased platelet aggregation and increased vascular tone.

Overall, these effects sum to produce anti-inflammatory action. Inflammation relaxes vessels and aspirin hinders this process. Platelet aggregation begins signaling cascades leading to neutrophil NETosis which positively feeds into more inflammation (*211*). Platelet aggregation also positively feeds back to produce more pro-inflammatory cytokine/chemokine to activate local vascular endothelium and leukocytes.

1.5.3.2 – Aspirin is Reversibly Ototoxic

Salicylic acid ototoxicity was first reported in the scientific literature in 1855 by Italian chemist Cesare Bertagnini shortly after humans isolated pure crystalline salicylic acid from willow bark (*212*), although many incorrectly credit Müller (*213*) as the first known author reporting such hearing aberrations (*209*). Large doses of salicylic acid, in the range of 7-15g/day taken for rheumatic arthritis, produce substantial tinnitus, which is alleviated upon therapy cessation. Reversible ototoxicity also occurs with acetylsalicylic acid (aspirin) (*214*).

Early experiments studying aspirin ototoxicity in squirrel monkeys demonstrated increased hearing thresholds with no histological changes by light microscopy and also no ultrastructural changes by electron microscopy (*207*). Other feline, guinea pig, and amphibian studies *in-vivo* and *in-vitro* have demonstrated both decreased compound action potentials measured at the round window and decreased cochlear microphonics, suggesting aberrations in cochlear hair cells. In contrast, other studies have observed only decreased compound action potentials but not cochlear microphonics suggesting no cochlear involvement (*215*). Indeed, aspirin does activate NMDA receptors expressed on the basolateral surface of hair cells (*216*) with a concomitant decrease in primary auditory cortex activity (*217*). There is also a vascular mechanism as aspirin decreases cochlear blood flow through vasoconstrictive properties. Aspirin-induced vasoconstriction and associated decreased blood-flow correlates with elevated hearing thresholds (*218*).

Overall, evidence exists for ototoxic mechanisms at each step of hearing transduction from the cochlea up to the cortex.

1.5.3.3 – Aspirin is Otoprotective During Aminoglycoside and Cisplatin Treatment

Oxymoronically given aspirin's ototoxic properties, aspirin is otoprotective for both aminoglycoside and cisplatin therapy as well as noise-induced hearing loss in both animal models and clinical studies (*93, 219-223*). Doses used in these studies are less than an ototoxic dose. In guinea pigs, sub-cutaneous treatment with sodium salicylate (not aspirin) at 100mg/kg reduced gentamicin-induced hearing loss from 60-70 dB-HL in the gentamicin-alone group to less than 20 dB-HL. This was accompanied by protection of cochlear hair cells (*222*). In a human clinical trial sponsored by the Chinese military, aspirin reduced the incidence of meeting hearing loss criteria from 13% to 3% (*93, 223*).

Aspirin also protects against cisplatin therapy without compromising oncolytic activity of the drug (*219, 220*). Similar to that seen in aminoglycoside therapy, sodium salicylate administered subcutaneously at 100mg/kg to rats reduced a moderate hearing threshold shift of about 30 dB-HL back to baseline levels. Examination of hair cells also demonstrated protection against hair cell loss.

Similar to other phenolic compounds, aspirin is an electron acceptor and rapidly reacts with and neutralizes ROS (*224*). Thus, aspirin acts as an electron sink, mopping up ROS. At higher doses, aspirin can paradoxically increase ROS production, likely via mitochondrial uncoupling (*225*). Aspirin also mops up extrinsically produced ROS from inflammatory cells stimulated by stressed and dying cochlear parenchymal cells. One hypothesis is that aspirin's otoprotective mechanism likely lies between anti-inflammatory COX inhibitory activity and ROS scavenging.

1.5.4 – Sulfur-based Otoprotection

1.5.4.1 – Glutathione is the Prototypical Endogenous ROS Scavenger

Glutathione (GSH, gamma-glutamyl-cysteine-glycine) is the primary endogenous ROS scavenging molecule. GSH reacts with ROS and condenses with another GSH molecule, forming the oxidized S-S bonded dimer GSSG, which is then reductively cleaved by glutathione reductase to replenish the GSH stores. GSH is essential for staving off free radical-mediated cellular and organ parenchymal damage and buffering excess free radical production from overactive and oxidatively uncoupled mitochondria (*226*). Younger mammals are more sensitive to ototoxins and maturation/expression of glutathione-S-transferase correlates with the end of this sensitive period (*227*). Deficiency in glutathione levels predisposes the body to pathologies with inflammatory etiologies such as neurodegeneration including dementia (*228*) and parkinsonism (*229*), idiopathic pulmonary fibrosis (*230*), enhanced ischemia-reperfusion injury (*231*), increased paracetamol hepatotoxicity (*232*), poor outcomes in HIV-positive individuals (*233, 234*), congenital nonspherocytic hemolytic anemia (*235*), as well as many other pathologies.

GSH-like molecules with sulfur-containing functional groups have demonstrated protection against many toxicities including ototoxicity, nephrotoxicity, bone marrow toxicity and others (*236-240*). Like the thiol group on the cysteine residue of GSH, other molecules with thiol and sulfide groups can undergo oxidation reactions, neutralizing free radical species. A common theme in thiol-based protection against drug-induced toxicities and other non-drug related pathology is that free radicals are involved in the pathological mechanism.

1.5.4.2 – Sodium Thiosulfate is Otoprotective

Sodium thiosulfate (STS) is an inorganic reducing agent utilized for gold extraction from mining ore (*241, 242*) and has the classic medical use as an antidote for cyanide poisoning (*243*). Because STS (like all sulfur based chemoprotrectants) can form strong coordinate covalent bonds with cisplatin, thereby inactivating it, STS is useful for

managing the medical complication of cisplatin extravascular extravasation (*244, 245*). Cisplatin inactivation can also neutralize excessive cisplatin levels after supradose exposure to maximize chemo-efficacy (*246*). Another use is for prophylaxis against intravascular calcium salt precipitation (calciphylaxis) in dialysis patients (*247, 248*).

Otto *et al*. first described STS as an otoprotectant in 1988 (*249*). Since then, multiple reports have confirmed this finding demonstrating successful cisplaitn otoprotection in both animal models (*250-252*) and human clinical trials (*253-255*). Importantly, systemic treatment with STS does not diminish antineoplastic effects of cisplatin as long as STS administration is delayed (*256-258*). After systemic administration, STS rapidly enters the cochlear perilymph (*259*). Local intra-tympanic installation of STS into the middle-ear is another efficacious strategy to avoid decreased antineoplastic activity while maintaining otoprotection (*260, 261*).

Although less extensively investigated than other sulfur-based otoprotectants, STS also demonstrates efficacy protecting against aminoglycoside ototoxicity (*262, 263*). However, otoprotection is less appreciable in comparison to D-Met. Interestingly, no reports of STS otoprotection for noise-induced hearing loss exist, which is surprising given the theme of sulfur-based otoprotective efficacy against multiple ototoxic pathologies.

1.5.4.3 – N-Acetyl Cysteine (NAC) is Otoprotective

NAC is acetylated L-cysteine, a net anion and prodrug for L-cysteine *in-vivo*. NAC is rapidly metabolized by cytochrome p450 enzymes in the liver into L-cysteine and subsequently converted into GSH. Thus, NAC replenishes GSH stores, boosting antioxidant activity. Like STS, NAC is also otoprotective and nephroprotective during cisplatin therapy in both human (*264, 265*) and animal models (*252, 266, 267*). NAC also demonstrates otoprotective activity in the contexts of aminoglycoside (*268-271*) and noise-induced hearing loss (*266, 272*). This overlap in protection against multiple pathologies fits with the theme of an overarching ototoxic mechanism.

In the context of cisplatin ototoxicity, NAC demonstrates efficacy in both pre-clinical and clinical studies. Key conclusions from these studies (similar to STS) highlight the importance of route of administration, dose, and timing (*273*). Specifically,

the need for *i.v.* or *i.a.* administration is essential as first pass metabolism in the *i.p. or p.o.* routes likely inactivate NAC making treatment ineffective. Furthermore, *i.a.* administration is more effective in comparison to *i.v.* One small scale clinical study looking at intra-tympanic injection of NAC into the middle ear space demonstrated some protection in two patients although they concluded their study was under-powered and were unable to reach statistical significance between cohorts (*274*). Secondly, a dose around 400mg/kg is also required which is a higher dose of NAC in comparison to other clinical applications such as mucolysis or paracetamol overdose. Lastly, timing is essential to avoid any possible tumor protection. Pro-dosing with NAC decreases cisplatin efficacy while 4 hour delayed administration is chemoprotective without decreasing anti-tumor activity (*275*)

1.5.4.4 – D-Methionine is Otoprotective

L-methionine, an endogenous amino acid, reacts with ROS, yielding L-methionine sulfoxide (MetO), which has two diastereomers, S-MetO and R-MetO. MetO in cysteine-free proteins is a biomarker for oxidative stress *in-vivo* (*276*). Methionine sulfoxide reductase (Msr) can remove the sulfoxide group, regenerating the native thio-ether group. There are two isoforms of sulfoxide reductase: MsrA reduces S-MetO, and MsrB reduces R-MetO. Thioredoxin and thioredoxin reductase can reduce methionine residues incorporated in proteins (*277*).

D-amino acids were classically believed to exist biologically only as components of bacterial cell walls and bacterial derived antibiotics, but not in eukaryotic organisms (*278*). However, discovery of dermorphin isolated from the South American tree frog, *Phyloomedusa sauvagei,* broke this dogma and opened the door for discovery of more endogenously functional polypeptides with D-amino acids in other metazoa (*278, 279*). D-amino acids are actively transported across the rat intestinal epithelium *in-vitro* (*280*) and deaminated to the corresponding α-keto acid where they are either further metabolized in the citric acid cycle or re-aminated to produce the corresponding L-amino acid for incorporation into peptides and proteins (*281*)

D-Met otoprotection was first described in 1996 by Campbell et al. in rats treated with cisplatin (*282*). D-Met protects against noise-induced hearing loss (*283, 284*),

aminoglycoside-induced hearing loss (*285-287*), and platinum chemotherapy-induced hearing loss (*282, 288*). For cisplatin otoprotection, the mechanism of action is partially explained by covalent bonding to and inactivation of cisplatin, opening the possibility that D-Met may protect tumor cells from cisplatin activity (*289*). This possibility is circumvented by local D-Met administration via trans-tympanic injection into the middle-ear space, which provides otoprotection without compromising antineoplastic activity (*290*). Furthermore, the mechanism of ototoxicity cannot be fully explained by covalent inactivation of cytotoxic platinum-adducts since otoprotection affects hair cells (*282*) and the stria vascularis (*291*). Additionally, L-Met also confers otoprotective activity (*292, 293*), suggesting that the non-specific antioxidant activity of methionine protects the cochlea rather than some D-Met specific stereo-interaction (*294*).

1.5.5 – Designer Aminoglycosides

Because the binding pocket between bacterial and mitochondrial ribosomes varies, any particular aminoglycoside will have varying affinities for each ribosome. X-ray crystal structure determination has allowed for rational drug design and development of a synthetic aminoglycoside with enhanced specificity for prokaryotic ribosomes (*295, 296*). This aminoglycoside is less ototoxic compared to traditional aminoglycoside antibiotics (*297, 298*). Presumably, the decreased ototoxicity is due to decreased mitochondrial ribosomal inhibition. This highlights the important link between off-target aminoglycoside activity at the eukaryotic ribosome, ROS production, and the mechanistic link of these to cochlear toxicity.

1.6 – Commonalities in Ototoxic and Otoprotective Mechanisms

A range of otoprotective agents with varying molecular targets protect hearing against diverse ototoxic etiologies, which illuminates the theoretical crossover between ototoxic and otoprotective mechanisms. For example, D-Met protects against NIHL,

cisplatin-induced and aminoglycoside-induced hearing loss. The same is true for NAC, STS, aspirin, and anti-inflammatory steroids.

Despite stark differences in molecular targets of ototoxic insults such as aminoglycosides, platinum chemotherapy, noise, and labyrinthine infection; post-insult and peri-infectious inflammation are common threads in the otopathological processes resulting in permanent hearing loss. ROS are extensively described in each of the afore-mentioned ototoxic pathologies, but where is the source of ROS? We know that ROS derive from both cochlear parenchymal cells and also from infiltrating inflammatory cells. Furthermore, inflammatory cells in the blood can easily interact with vascular endothelium. Otoprotective agents likely work to decrease the ROS burden from all of these sources in a non-specific manner.

Innate inflammation from release of DAMPS, and PAMPs in the setting of infection, may be a common nidus for initiation of the pathophysiology resulting in hearing loss. Antagonizing either class of pattern recognition receptors may be a druggable receptor upstream of ROS that may also work to decrease the ROS burden. Indeed, glucocorticoid therapy blocks leukocyte activities albeit via different receptors and signaling pathways. Exploring the various checkpoints along the inflammatory cascade may provide both insight to basic mechanisms of hearing loss and provide new strategies to ameliorate hearing loss.

2 – Manuscript #1

Endotoxemia-mediated inflammation potentiates aminoglycoside-induced ototoxicity

Authors: J.-W. Koo[1,2*], L. Quintanilla-Dieck[1*], M. Jiang[1*], J. Liu[1,3*], Z. D. Urdang[1*], J. Allensworth[1*], C. Cross[1*], H. Li[1*], P. S. Steyger[1*]

Affiliations:

[1]Oregon Hearing Research Center, Oregon Health & Science University, 3181 SW Sam Jackson Park Road, Portland, Oregon 97239, USA.

[2]Department of Otorhinolaryngology, Seoul National University College of Medicine, Bundang Hospital, 173-82 Kumiro, Bundang-gu, Seongnam 463-707, Republic of Korea.

[3]Department of Otology and Skull Base Surgery, Eye Ear Nose and Throat Hospital, Fudan University, Shanghai 200031, China.

[*]All authors contributed equally to this work

Contributions: Zachary designed and performed all experiments with C3H/HeJ TLR4-mutant mice. Zachary repeated GTTR and cytokine experiments in C57BL/6 mice. Zachary co-wrote and edited the manuscript.

Chapter 2 is modified from the paper published in Science Translational Medicine July, 2015.

2.1 - Abstract

One Sentence Summary: Endotoxemia-mediated inflammation potentiates cochlear uptake of aminoglycosides and subsequent cochleotoxicity.

Abstract: The ototoxic aminoglycoside antibiotics are essential to treat severe bacterial infections, particularly in neonatal intensive care units. Using bacterial lipopolysaccharides (LPS) as an experimental model of sepsis, we tested whether LPS-mediated inflammation potentiates cochlear uptake of aminoglycosides, and permanent deafness. Low dose LPS (endotoxemia) greatly increased cochlear levels of aminoglycosides, vasodilated cochlear capillaries without inducing paracellular flux across the blood-labyrinth barrier (BLB), or elevating serum drug levels. Low dose endotoxemia increased serum, and also cochlear, levels of inflammatory markers. These LPS-induced changes, classically mediated by TLR4, were significantly attenuated in TLR4-hyporesponsive mice. Multiday dosing with aminoglycosides during chronic low dose endotoxemia induced significantly greater hearing threshold shifts compared to non-endotoxemic controls. Thus, endotoxemia-mediated inflammation enhances aminoglycoside trafficking across the BLB, and potentiated aminoglycoside-induced ototoxicity. These data indicate that patients with severe and life-threatening infections are at greater risk of aminoglycoside-induced deafness than previously recognized.

2.2 – Introduction

Severe Gram-negative bacterial infections, including meningitis, bacteremia, and respiratory infections in cystic fibrosis, are treated with aminoglycoside antibiotics like gentamicin (*299-301*). These drugs can induce permanent and debilitating hearing loss, particularly in neonates. About 80% of 600,000 admissions into neonatal intensive care units (NICU) in the United States receive aminoglycosides each year (*302*). The rate of hearing loss in NICU graduates (from all etiologies) is 2 to 4% compared to 0.1 to 0.3% of full-term births from congenital etiologies (*303*). Aminoglycoside-induced ototoxicity could contribute substantially to this increased rate of hearing loss in the NICU population. The irreversibility of hearing loss, particularly in pediatric cases before language development, has extensive quality-of-life implications (*304-307*).

The mechanisms by which circulating aminoglycosides cross the blood-labyrinth barrier (BLB) into the cochlea remain unconfirmed. We previously reported that, in vivo, these drugs predominantly cross the BLB into the stria vascularis and are trafficked via marginal cells into endolymph (*308*). Once in endolymph, these drugs rapidly enter cochlear hair cells via mechanoelectrical transduction (MET) channels located on their apical membranes and induce hair cell death (*97, 308-310*).

Serious infections induce systemic inflammatory response syndrome, elevating serum concentrations of nitric oxide, vasoactive peptides, and inflammatory proteins that can modulate the vascular permeability of the blood-brain barrier (BBB) (*311-313*). Vasoactive peptides also modulate cochlear uptake of gentamicin across the BLB (*314*). However, most studies of ototoxicity involve healthy preclinical models, and the effect of induced systemic inflammation on ototoxicity has only recently been reported (*315*). Here, we used bacterial lipopolysaccharide (LPS) to induce endotoxemia in a classic experimental model of sepsis and inflammation (*316*) in mice to test the hypothesis that systemic inflammation modulates cochlear concentrations of aminoglycosides and inflammatory markers, and exacerbates aminoglycoside-induced ototoxicity.

2.3 – Results

Fluorescently-tagged gentamicin [gentamicin–Texas Red (GTTR)] is an excellent tracer of gentamicin in vivo (*308, 310, 314, 317-320*). By conjugating Texas Red to gentamicin (450 to 477 daltons, three isoforms), the hydrophobicity of the resulting conjugate (1151 to 1179 daltons) is increased, whereas serum pharmacokinetics are slowed, providing greater spatiotemporal imaging and a higher signal-to-noise ratio in heterogeneous cellular structures like the cochlea compared to radiolabeled aminoglycosides or immunohistochemistry (*308, 310, 321-323*). The cytoplasmic intensity of GTTR fluorescence is dose-dependent unlike gentamicin immunofluorescence, where the greater abundance of epitope binding sites can overwhelm the number of available antibodies (*310, 317*). Thus, changes in cochlear uptake of aminoglycosides can be quantitatively assayed using GTTR and confocal microscopy (*310, 314, 317, 320*).

2.3.1 - Strial uptake of GTTR is enhanced by LPS-induced endotoxemia

In Dulbecco's phosphate-buffered saline–treated (DPBS)–treated mice that received an intraperitoneal injection of GTTR 1 hour before fixation, intense fluorescence delineated the strial capillaries of the cochlear lateral wall, with moderate diffuse fluorescence distributed throughout the stria vascularis (marginal cells, intrastrial tissues, and basal cells; **Fig. 2-1A-B**), as previously described (*310*). The spiral ligament fibrocytes exhibited reduced intensities of GTTR fluorescence compared to strial cells (**Fig. 2-1A-B**, and **fig. S1A**), also as seen previously (*310*). Mice intravenously injected with LPS (1 mg/kg) 24 hours before an intraperitoneal injection of GTTR 1 hour before fixation had more intense GTTR fluorescence in all regions of the cochlear lateral wall compared to DPBS-treated mice (**Fig. 2-1A-B**). DPBS- or LPS-treated mice injected with hydrolyzed Texas Red (hTR) 1 hour before fixation displayed negligible fluorescence within the lateral wall, as previously described (*310, 319*).

The mean pixel intensity of GTTR fluorescence was obtained from *xy* optical sections and plotted for specific regions of interest [ROIs; marginal cells, intrastrial tissues (minus capillary structures), basal cells, and spiral ligament fibrocytes] at 1 and 3

hours after GTTR injection (**Fig. 2-1C** and **fig. S1**). In DPBS-treated mice, absolute fluorescence was greatest in marginal cells, with stepwise decreasing fluorescence in intrastrial and basal cells, with a significant drop in spiral ligament fibrocytes (fig. S1A; $P < 0.05$). Strial and spiral ligament fluorescence was significantly greater in basal segments compared to that in apical segments for each ROI (fig. S1A; $P < 0.01$).

GTTR fluorescence was dose-dependently elevated in selected cell types with increasing LPS dose (**Fig. 2-1C** and **fig. S1B**). At 1 hour, significant increases in GTTR fluorescence were observed in every ROI of basal lateral wall segments dosed with LPS (1 mg/kg or higher) (**Fig. 2-1C** and **fig. S1B**; $P < 0.01$ or $P < 0.005$). A similar pattern of increased uptake was observed in the apical coil but with more variable significance (fig. S1B; $P > 0$, $P < 0.05$, $P < 0.01$, or $P < 0.005$). At 3 hours, GTTR fluorescence in lateral wall cells continued to show dose-dependent elevations with increasing LPS dose, reaching significance at LPS of 2.5 and 10 mg/kg (**Fig. 2-1C** and **fig. S1B**; $P < 0.05$ or $P < 0.01$). The rank order of GTTR fluorescence intensity in individual cell types (marginal cells > intrastrial layer > basal cells >> spiral ligament) was generally maintained with increasing LPS dose, with more variable degrees of significance with increasing LPS dose and time (**fig. S1A**). Strial GTTR fluorescence was significantly greater for each ROI in basal segments compared to that in apical segments in DPBS- or LPS-treated mice (fig. S1A; $P < 0.01$). These data indicate that LPS dose-dependently increased GTTR trafficking across the BLB, particularly in the basal coil of the cochlea, the region most associated with the onset of drug-induced hearing loss and sensory cell death (*324, 325*).

In cochlear outer hair cells (OHCs), LPS-induced increases in GTTR fluorescence were consistently observed at 1 hour after GTTR injection compared to DPBS-treated mice, particularly at higher LPS doses (>1 mg/kg), and trended toward significance at higher doses of LPS (≥2.5 mg/kg) at 3 hours after GTTR injection (fig. S2, A and B). In apical coils, LPS did not consistently modulate GTTR fluorescence in OHCs 1 hour after GTTR injection and trended toward significance at 3 hours with higher doses of LPS (≥1 mg/kg). These data suggest that LPS accelerated GTTR entry into basal OHCs and that dynamic increases in GTTR uptake kinetics at later time points, or by apical OHCs, were dissipated by the low doses of GTTR used here.

2.3.2 - Renal function is impaired at higher doses of LPS

Endotoxemia and sepsis affect vascular function in multiple organ systems and can induce decreased glomerular filtration rates and renal dysfunction (*326*). Because GTTR is readily taken up by renal proximal tubules (*318, 320*), decreased glomerular filtration rates and renal dysfunction should reduce proximal tubule uptake of GTTR. As an internal control, we assessed renal GTTR fluorescence intensities during endotoxemia. In DPBS-treated mice, 1 or 3 hours after GTTR injection, GTTR fluorescence was localized as intense puncta close to the lumen and as diffuse fluorescence in the cytoplasm of proximal tubule cells, whereas distal tubule cells had visibly less diffuse fluorescence and no puncta (**fig. S3A**), as seen previously (*318*). In LPS-treated mice, diffuse GTTR fluorescence within proximal tubule cells at 1 hour was significantly reduced only at LPS of 10 mg/kg compared to that in DPBS-treated control tissues (fig. S3C; $P < 0.001$). At 3 hours, cytoplasmic fluorescence in proximal tubule cells of DPBS-treated mice was markedly increased compared to that at 1 hour (fig. S3C) due to longer exposure. However, at 3 hours, only mice treated with LPS (10 mg/kg) had significantly less cytoplasmic GTTR fluorescence compared to DPBS-treated mice (fig. S3; $P < 0.05$), as expected during endotoxemic shock (*326*).

2.3.3 - Low-dose LPS increases cochlear but not serum concentrations of aminoglycosides

Given that LPS (10 mg/kg) can decrease both glomerular filtration rates (*326*) and renal uptake of GTTR (fig. S3), we assessed serum concentrations of GTTR 24 hours after LPS administration using immunoturbidimetry. Serum concentrations of GTTR were significantly higher in mice dosed with LPS (2.5 and 10 mg/kg) than in DPBS-treated mice at 1 or 3 hours after GTTR injection (**Fig. 2-2A** and **tables S1-S2**; $P < 0.01$ and $P < 0.05$, respectively). Serum concentrations of GTTR in mice dosed with LPS (0.1 and 1 mg/kg) were not statistically different from controls at 1 or 3 hours of GTTR exposure (**Fig. 2-2A** and **table S2**). Serum concentrations of GTTR in mice dosed with LPS at 2.5 mg/kg were significantly higher than in mice treated with LPS at 0.1 and 1

mg/kg at both 1- and 3-hour time points (**Fig. 2-2A** and **table S2**; $P < 0.05$ and $P < 0.01$, respectively). To verify that serum concentrations for unconjugated gentamicin were not altered by exposure to LPS (1 mg/kg) for 24 hours, we used enzyme-linked immunosorbent assays (ELISAs). Both GTTR and gentamicin serum concentrations were unchanged in LPS-treated mice compared to those in DPBS-treated mice at 1- and 3-hour time points after drug injection (**Fig. 2-2B-D**). Serum gentamicin was lower at 3 hours after injection, whereas GTTR has a longer serum half-life, as described previously (*310*). In contrast, cochlear concentrations of both GTTR and gentamicin were significantly increased in LPS-treated mice compared to those in DPBS-treated mice at both 1 and 3 hours after injection (**Fig. 2-2C and E**; $P < 0.05$).

Six mice at higher LPS doses died within 24 hours after LPS injection (**table S1**), as predicted (*327*). However, LPS at 1 mg/kg was not fatal, as expected (*327*), yet induced acute weight loss (fig. S4A) associated with endotoxemia and sepsis (*328*). Given that LPS at 1 mg/kg did not increase serum concentrations, yet elevated cochlear concentrations, of GTTR and gentamicin, we used LPS at 1 mg/kg for subsequent experiments.

2.3.4 - Low-dose LPS does not increase paracellular flux across the BLB

Endotoxemia can change the volume of distribution for drugs, including gentamicin (*329*). hTR (also known as sulforhodamine 101; molecular mass, 679) is a membrane-impermeant fluorophore (*330, 331*). We used hTR to test whether exposure to LPS for 24 hours enhanced paracellular flux across the BLB into the interstitial spaces of the stria vascularis and spiral ligament (*332*), using neonatal (P6) mice with an immature BLB as a positive control (*318, 333*). In P6 mice treated with the hTR for 1 hour, fluorescence was distributed throughout strial tissues, with weaker intensities in strial marginal and basal cells (**Fig. 2-3A** and **fig. S5A**). The spiral ligament of P6 mice exhibited less fluorescence compared to strial tissues (**fig. S5A**; $P < 0.01$). In adult DPBS- and LPS-treated mice exposed to hTR for 1 hour, significantly less fluorescence was observed in strial cells and spiral ligament fibrocytes compared to that in P6 mice (**Fig. 2-3A** and **fig. S5A**; $P < 0.05$ or $P < 0.005$). No statistical differences in hTR

fluorescence could be observed between DPBS- and LPS-treated adult mice for any ROI (**Fig. 2-3A** and **fig. S5A**).

Morphometry of cochlear lateral wall tissues revealed that the diameters of strial capillaries in P6 pups were visibly and significantly larger than those in DPBS-treated adult mice (**Fig. 2-3B-C, and E**, and **Table 2-1**; $P < 0.0001$). LPS treatment significantly vasodilated a subset of both apical and basal strial capillaries in adult mice compared to DPBS-treated mice (**Fig. 2-3D-E**, **fig. S5C**, and **Table 2-1**; $P < 0.0001$), resulting in a bimodal distribution of capillary diameters indicative of acute inflammation. Intriguingly, fixed strial capillary diameters may underestimate actual physiological diameters (*334*).

These data indicate that the BLB was relatively impermeable to hTR in adult mice compared to the immature and more permeable BLB of neonatal pups, as has been found for another fluorophore, FM1-43 (*335, 336*). Furthermore, the paucity of hTR flux across the BLB of adult mice was not altered by LPS treatment, suggesting that the physical integrity of the adult BLB was retained despite LPS-induced vasodilation of strial capillaries.

2.3.5 - Low-dose LPS induces robust proinflammatory marker expression

We previously reported that two inflammatory-mediated vasoactive peptides—histamine and serotonin—can modulate cochlear uptake of GTTR (*314*). Twenty-four hours after LPS injection, serum histamine concentrations were not modulated, whereas serum serotonin concentrations were significantly decreased in a dose-dependent manner in LPS-treated mice (**Table 2-2** and **fig. S6**; $P < 0.05$ or $P < 0.001$). This suggested that the loss of vasoconstrictive serotonin is associated with strial vasodilation and potentially increased strial vascular permeability to aminoglycosides.

LPS binds to and activates Toll-like receptor 4 (TLR4) to induce the secretion and transcription of acute-phase inflammatory cytokines and chemokines that orchestrate immune responses (*337, 338*). Given that LPS enhanced cochlear uptake of aminoglycosides, we assessed whether LPS modulated serum and cochlear expression of acute-phase inflammatory markers. Six hours after injection, LPS significantly elevated serum concentrations of all acute-phase proinflammatory proteins tested: TNFα (tumor necrosis factor α), IL-1α (interleukin-1α), IL-1β, IL-6, IL-8 (also known as KC,

CXCL1), MIP-1α (macrophage inflammatory protein–1α), and MIP-2α (**Fig. 2-4A**). In cochlear homogenates, LPS significantly elevated protein concentrations of all early-phase proinflammatory markers, particularly IL-6 and IL-8, but not IL-1β (**Fig. 2-4B**). LPS significantly elevated the anti-inflammatory cytokine IL-10 in serum but not in vascular-perfused cochlear homogenates [**Fig.2- 4A** ($P < 0.05$) and B, respectively]. Exposure to gentamicin for 3 hours did not modulate serum or cochlear inflammatory protein concentrations (**Fig. 2-4A-B**), indicating that gentamicin (at the doses used here) was not a confounding factor. Overall, LPS-induced changes in the serum concentrations of acute-phase proinflammatory proteins were reflected in cochlear homogenates, except for IL-1β and the anti-inflammatory cytokine IL-10 (**Fig. 2-4A-B**).

Twenty-four hours after LPS injection in C57BL/6 mice, plasma concentrations of most tested inflammatory proteins were not elevated (or were below the limit of detection) (**fig. S7A**), consistent with previous findings (*339*). Although IL-6 and MIP-1α concentrations remained significantly elevated compared to those in DPBS-treated controls, they were substantially lower compared to those in the 6-hour time point (**Fig. 2-4A** and **fig. S7A**). In cochlear homogenates of C57BL/6 mice 24 hours after LPS injection, concentrations of all tested inflammatory proteins were significantly elevated, particularly IL-6, IL-8, and MIP-1α (**Fig. 2-5A** and **fig. S7D**). These findings suggested that LPS triggers robust inflammatory responses both systemically and in the cochlea within 6 hours. Furthermore, 24 hours after LPS injection, cochleae continued to exhibit significantly elevated concentrations of tested inflammatory proteins (**Fig. 2-5A**), akin to that induced by middle-ear administration of LPS or bacteria (*340, 341*).

To determine whether increased cochlear inflammatory protein concentrations were due to local (parenchymal) gene transcription, mRNA levels were assayed 6 or 24 hours after LPS injection (with or without gentamicin). At 6 hours, LPS significantly increased mRNA expression (by fivefold or greater) for all eight inflammatory genes tested, particularly *Il-6*, *Il-8*, and Mip-1α (**Fig. 2-4C**). Gentamicin alone did not modulate cochlear mRNA expression of any inflammatory genes tested (**Fig. 2-4C**). Twenty-four hours after LPS injection, cochlear mRNA levels remained significantly elevated for most inflammatory genes tested, except *Tnf*α and *Il-1*β (**fig. S7G**), with greater increases for later-expressing acute-phase cytokines: *Il-6*, *Il-8*, and Mip-2α (**Fig. 2-5B** and **fig.**

S7G). These data show that LPS challenge up-regulated cochlear mRNA transcription for inflammatory proteins within 6 hours, with sustained mRNA transcription for later-expressing acute-phase inflammatory proteins at 24 hours, as in other organs during endotoxemia including the liver, lung (*338*), brain (*342*), and eye (*343*).

2.3.6 - LPS-mediated inflammation is reduced in TLR4-hyporesponsive C3H/HeJ mice

The C3H/HeJ mouse strain is homozygous for an inactivating short-nucleotide polymorphism in TLR4, resulting in greatly attenuated inflammatory responses to LPS exposure (*45*). Twenty-four hours after LPS injection, plasma concentrations of all tested inflammatory proteins in C3H/HeJ mice, and the control C3H/HeOuJ mouse strain, were not different from those in DPBS-treated mice of the same strain (**fig. S7A-C**). Unlike control C3H/HeOuJ mice, C3H/HeJ mice did not experience significant weight loss (fig. S4B; $P < 0.001$).

LPS significantly elevated cochlear homogenate concentrations of all acute-phase proinflammatory proteins 24 hours after injection in control C3H/HeOuJ and C57BL/6 mice compared to those in DPBS-treated mice of the same strains (**Fig. 2-5A** and **fig. S7D-F**; $P < 0.05$). Several inflammatory proteins (TNFα, IL-6, IL-8, MIP-1α, and MIP-2α) were more elevated in C57BL/6 mice compared to those in C3H/HeOuJ mice after LPS treatment (**Fig. 2-5A**). Crucially, several, mostly later-expressing acute-phase inflammatory proteins (IL-1α, IL-6, IL-8, and MIP-1α) were significantly attenuated in cochlear homogenates of LPS-treated C3H/HeJ mice compared to those in LPS-treated C3H/HeOuJ and C57BL/6 mice (**Fig. 2-5A**; $P < 0.05$).

Similar trends were seen with cochlear mRNA levels for tested inflammatory genes for both C3H/HeOuJ and C3H/HeJ mice after LPS treatment. LPS significantly increased cochlear mRNA expression of most inflammatory markers tested (not *Il-1*β) in C3H/HeOuJ mice, particularly later-expressing acute-phase proinflammatory cytokines: *Il-6, Il-8, Mip-1*α, and *Mip-2*α (**fig. S7H**). In contrast, LPS did not modulate cochlear mRNA expression for tested proinflammatory markers in C3H/HeJ mice (fig. S7I). When mRNA expression was compared between strains, there was attenuated

mRNA expression for later-expressing acute-phase proinflammatory cytokines (*Il-8,* *Mip-1*α, and *Mip-2*α) in LPS-treated C3H/HeJ cochleae compared to that in LPS-treated C57/BL6 and C3H/HeOuJ mice, and also for that in *Il-6* compared to that in LPS-treated C57BL/6 mice (**Fig. 2-5B**). mRNA expression of early-phase proinflammatory genes (*Tnf*α, *Il-1*α, and *Il-1*β) was weakly or not significantly elevated in all three mouse strains. mRNA for the anti-inflammatory cytokine *Il-10*was transcribed at significantly higher levels in C3H/HeJ mice compared to that in control C3H/HeOuJ or C57BL/6 mice (**Fig. 2-5** and **fig. S7G-I**; $P < 0.05$). These data demonstrate that cochlear expression of acute-phase inflammatory markers was up-regulated in LPS-treated control C3H/HeOuJ and C57BL/6 mice, and this up-regulation was attenuated for later-expressing inflammatory markers in TLR4-hyporesponsive C3H/HeJ mice 24 hours after LPS injection (**Fig. 2-5**).

2.3.7 - Cochlear lateral wall uptake of GTTR is attenuated in endotoxemic C3H/HeJ mice

Given that LPS-mediated inflammatory responses are attenuated in TLR4-hyporesponsive C3H/HeJ mice, we hypothesized that LPS-enhanced GTTR uptake would also be attenuated in the cochlear lateral wall of TLR4-hyporesponsive C3H/HeJ mice. We injected C3H/HeJ and control C3H/HeOuJ mice with LPS and, 24 hours later, injected GTTR. We found significantly enhanced GTTR fluorescence in strial cells and fibrocytes of LPS-treated C3H/HeOuJ mice compared to that in DPBS-treated C3H/HeOuJ mice (**Fig. 2-6** and **fig. S8A**; $P < 0.05$). LPS also significantly enhanced GTTR fluorescence in strial cells (but not fibrocytes) in LPS-treated C3H/HeJ mice compared to that in DPBS-treated C3H/HeJ mice (**Fig. 2-6** and **fig. S8B**; $P < 0.05$). Crucially, however, LPS-enhanced GTTR uptake was significantly attenuated ($P < 0.05$) in marginal cells, intermediate cells, and fibrocytes, with a downward trend in basal cells, in TLR4-hyporesponsive C3H/HeJ mice compared to that in control C3H/HeOuJ mice (**Fig. 2-6**). The residual expression of inflammatory markers and cochlear uptake of GTTR in C3H/HeJ mice was likely due to the activation of other innate immune system

receptors, such as TLR2 (*344*). These data indicate that TLR4-mediated inflammation mediated (at least in part) LPS-enhanced cochlear uptake of GTTR.

LPS significantly dilated a subset of strial capillaries in C3H/HeOuJ mice compared to DPBS-treated C3H/HeOuJ mice, as we observed for C57BL/6 mice (**Fig. 2-3E-F**, and **Table 2-1**; $P < 0.0001$). Endotoxemia also significantly dilated a smaller subset of strial capillaries in TLR4-hyporesponsive C3H/HeJ mice compared to DPBS-treated C3H/HeJ mice (**Fig. 2-3G** and **Table 2-1**; $P < 0.0001$). However, the degree of capillary dilation in LPS-treated C3H/HeJ mice was significantly attenuated compared to that in LPS-treated C3H/HeOuJ mice (**Fig. 2-3G** and **Table 2-1**; $P < 0.0001$).

2.3.8 - Repeated low-dose LPS exposure exacerbates kanamycin ototoxicity

Because LPS-induced endotoxemia increased the cochlear uptake of aminoglycosides, we hypothesized that chronic exposure to LPS would exacerbate aminoglycoside-induced ototoxicity, as determined by auditory brainstem response (ABR) threshold shifts. Given that chronic dosing with gentamicin is systemically lethal to mice, we used a related aminoglycoside—kanamycin—with a well-established protocol (*324*). One group of C57BL/6 mice received LPS (1 mg/kg) the day before kanamycin treatment and on the 5th and 10th day during a 14-day course of kanamycin treatment (700 mg/kg, twice daily). ABR thresholds were obtained from age-matched mice 1, 10, and 21 days after kanamycin treatment, and shifts from pretreatment thresholds were determined (**Fig. 2-7A-B**, **figs. S9-S11**, and **tables S3-S5**). At all time points, DPBS- and LPS-treated mice had negligible threshold shifts. One day after chronic dosing, kanamycin induced significant threshold shifts at 16, 24, and 32 kHz compared to DPBS- and LPS-treated mice (**fig. S11A** and **table S3**), as expected (*324*). Endotoxemia exacerbated the frequency range of kanamycin-induced threshold shifts (12 to 32 kHz) compared to age-matched control mice not treated with kanamycin (**fig. S11A** and **table S3**).

The 3-week recovery time point is a well-established primary benchmark for many preclinical ototoxicity studies (*324, 345, 346*). At 21 days after treatment, kanamycin-treated mice exhibited a significant permanent threshold shift (PTS) only at 32 kHz compared to DPBS- and LPS-treated mice. Mice that received both LPS and

kanamycin had greater and more significant PTS at 16, 24, and 32 kHz compared to kanamycin-treated mice or mice treated with DPBS or LPS alone (**Fig. 2-7A** and **table S5**). Mice receiving both LPS and kanamycin also had significant PTS at 12 kHz compared to mice treated with DPBS or LPS alone and at 8 kHz compared to mice treated with LPS alone (**Fig. 2-7A** and **table S5**). During the 3-week recovery period, kanamycin-induced threshold shifts did not change significantly at individual frequencies between time points (**fig. S11A-C**). However, there was a loss of significant threshold shifts at 16 and 24 kHz in kanamycin-treated mice at 10 and 21 days after treatment compared to that in DPBS- and LPS-treated mice that were present 1 day after treatment (**fig. S11A-C**, and **tables S3-S5**). This likely reflected the onset of slight, nonsignificant threshold shifts in DPBS- and LPS-treated mice at 10 and 21 days after treatment (**fig. S11A-C**). Endotoxemia, however, increased the degree of kanamycin-induced threshold shifts at 21 days and over a wider frequency range (8 to 32 kHz) compared to 1 day after treatment (**fig. S11A-C**, and **tables S3-S5**). These increased threshold shifts trended toward significance at higher frequencies and reached statistical significance at 32 kHz ($P < 0.05$). Thus, endotoxemia significantly exacerbated kanamycin-induced PTS.

Drug-induced PTS and sensory hair cell death occur in a dose-dependent fashion (*324*). To verify whether endotoxemia exacerbated kanamycin-induced hair cell death, we obtained cytocochleograms of cochlear hair cell survival at 21 days after treatment (**Fig. 2-7B** and **tables S7-S9**). DPBS- and LPS-treated mice had minimal hair cell loss, mostly at the extreme basal (very high frequency) region of the cochlea. Kanamycin induced OHC loss over a wider frequency range in basal cochlear locations, but this was not significant compared to age-matched control mice. LPS-induced endotoxemia significantly enhanced kanamycin-induced OHC loss, and over a much wider frequency range (8 to 64 kHz), compared to non-endotoxemic mice. These data indicate that endotoxemia exacerbated kanamycin-induced OHC death.

We then used hTR to test whether chronic LPS and kanamycin exposure altered the flux of membrane-impermeant hTR across the BLB. Significant threshold shifts were present immediately after chronic treatment with kanamycin, with or without LPS, at 16, 24, and 32 kHz compared to DPBS- and LPS-treated mice (**figs. S11D-S12** and **table S6**). Cytocochleogram data revealed significantly greater OHC loss in the basal (32 to 64

kHz) regions of LPS + kanamycin–treated mice compared to that in all other groups (**fig. S11E** and **table S8**). Nonetheless, no differences in hTR fluorescence intensity were detected in strial cells or spiral ligament fibrocytes between LPS + kanamycin–treated mice and control DPBS– or chronic LPS–treated adult mice (**fig. S11F**). However, all cochlear ROI in adult mice had significantly less fluorescence compared to that in P6 mice (**figs. S5B** and **S11F**). Thus, neither chronic endotoxemia nor chronic kanamycin treatment that induced auditory threshold shifts and OHC loss increased the flux of hTR across the adult BLB.

In endotoxemic mice, there was more kanamycin-induced OHC loss, over a wider frequency range, at 3 weeks compared to that immediately after treatment (**Fig. 2-7B**, **fig. S11E**, and **table S9**). There was also more OHC loss in mice treated with kanamycin only in the 16- to 32-kHz frequency region, corresponding to the PTS in this region 3 weeks after treatment, compared to that immediately after treatment (**Fig. 2-7, fig. S11D-E**, and **table S9**). These increasing losses of OHCs during the recovery period after ototoxic insult have been described previously (*347*). LPS- and DPBS-treated mice also had significant OHC loss in the 32- to 64-kHz region compared to 3 weeks earlier (table S9) that was attributed to the onset of strain-specific age-related hearing loss in these 11-week-old mice (*348*). Nonetheless, kanamycin-induced OHC loss in endotoxemic mice greatly exceeded these age-related losses (**Fig. 2-7B** and **tables S7 and S9**).

2.3.9 - Acute LPS-induced endotoxemia does not alter ABR thresholds

Transtympanic injection of LPS can induce ABR threshold shifts in a dose-dependent manner (*349, 350*). Systemic LPS (0.5 mg/kg per day for 2 days) did not change ABR thresholds or endolymphatic potentials (*315*). Because chronic LPS alone did not induce ABR threshold shifts at 6, 16, or 27 days after the last LPS injection (**Fig. 2-7** and **figs. S9-S11**), we tested whether acute systemic LPS exposure modulated auditory thresholds. Twenty-four hours after injection with LPS (1 mg/kg), no significant threshold shifts were observed within, or between, DPBS- or LPS-treated mice groups (**fig. S13**). The persistence of sensitive auditory function during acute LPS challenge suggests that the physical integrity of the BLB remained intact, because physical disruption of the BLB is thought to impair sensitive cochlear performance (*332*).

2.4 – Discussion

The easy availability and low cost of aminoglycosides contribute to their frequent use worldwide (*325*). Clinical use of aminoglycosides is limited because of the risk of acute nephrotoxicity and, more critically, permanent hearing loss. The risk of ototoxicity is proportional to the dose and duration of aminoglycoside therapy (*325*). Additional factors predisposing patients to aminoglycoside-induced ototoxicity include age, renal dysfunction, mitochondrial mutations, and concurrent exposure to other ototoxic drugs (like loop diuretics) or noise (*351-356*).

We used LPS-induced inflammation as a model for aminoglycoside pharmacotherapy of severe Gram-negative bacterial infections. LPS binds to ubiquitous TLR4 receptors to initiate immune response signaling cascades (*337, 338*). Lysis of bacteria by aminoglycosides and immune cells releases LPS and other bacterial ligands into the interstitial and vascular fluids, potentiating the inflammatory response (the Jarisch-Herxheimer reaction) (*357, 358*).

We found that low doses of LPS (≤1 mg/kg) significantly increased the expression of acute-phase inflammatory markers in serum, plasma, and cochlear tissues, mimicking low-grade sepsis. Furthermore, acute or chronic endotoxemia did not modulate the paracellular flux of membrane-impermeant hTR across the BLB, nor attenuate cochlear function. Nonetheless, LPS-induced endotoxemia increased cochlear concentrations of GTTR and gentamicin, without modulating the serum concentrations of these compounds. Simultaneous exposure to chronic endotoxemia and kanamycin significantly increased PTS and OHC death compared to age-matched mice treated with kanamycin, LPS, or DPBS alone.

2.4.1 - Endotoxemia and cochlear inflammation

Until recently, the cochlea had been considered an immunologically privileged compartment (*359*). Here, we show that endotoxemia can elevate cochlear expression of inflammatory markers. Although vascular inflammatory proteins could potentially be trafficked across the BLB, significantly elevated serum concentrations of IL-1β and IL-10 were not reflected in cochlear tissues, implying that the BLB is not passively

permeable to serum inflammatory proteins. Endotoxemia also significantly increased cochlear mRNA expression of inflammatory proteins. A similar parenchymal response to endotoxemia has been observed in ocular, pulmonary, and cerebral tissues (*339, 342, 343*). The cochlear expression of inflammatory markers was greatly attenuated in LPS-treated mice with hyporesponsive TLR4, as was strial vasodilation and GTTR uptake. Thus, endotoxemia-induced inflammation appears to be associated with changes in BLB physiology that enhanced cochlear loading with gentamicin.

Because cochleae are pooled from several mice to determine cochlear inflammatory marker protein concentrations and mRNA levels, it was not possible to correlate any potential tonotopic gradient in inflammatory protein expression with GTTR uptake, auditory threshold shifts, and OHC loss in the basal regions of the cochlea. To accomplish this correlative analysis will require development of more sensitive biochemical or quantitative immunofluorescence techniques.

Endotoxemia alone did not induce ABR threshold shifts, corroborating a recent study showing that low-dose LPS exposure has little effect on endolymphatic potentials and auditory thresholds (*315*). Disruption of the physical integrity of the strial BLB is thought to elevate ABR thresholds (*332*). This implies that the BLB remained physically intact, even though endotoxemia enhanced aminoglycoside trafficking across the BLB.

2.4.2 - Trafficking across the BLB

Several mechanisms have been proposed for the trafficking of small compounds like aminoglycosides across tight junction–coupled endothelial barrier layers, like the BBB and the BLB (see **fig. S14**). Paracellular flux across the BLB is not thought to occur under normal physiological conditions (*308, 360*) but may arise during inflammation, as has been reported for the BBB (*312*). Pathophysiological opening of paracellular routes can occur by immune cell–dependent and immune cell–independent mechanisms (*361*). In our panel, IL-8 and MIP-2α, strong chemotactic signals for immune cell recruitment and diapedesis into the parenchyma beyond the blood vessels (*362, 363*), were greatly elevated. Immune cells are capable of secreting cytotoxic molecules that disrupt tight junctions between adjacent endothelial cells, opening paracellular trafficking routes (*364*). Alternatively, the tight junction coupling between adjacent endothelial cells could

break down independently of immune cell activity, allowing paracellular flux through disrupted endothelial tight junctions (*365*). Although we did not use markers for immune cell–mediated injury or electron-dense tracers, the lack of hTR flux into the intrastrial tissues of adult mice contraindicated a major contribution by paracellular trafficking during acute endotoxemia. Furthermore, chronic endotoxemia with or without chronic kanamycin treatment did not increase hTR flux across the adult strial BLB, corroborating analogous experiments with mannitol after chronic ototoxic drug treatment (*360*).

Unlike membrane-impermeant hTR, GTTR rapidly traversed the adult BLB into strial tissues and entered cochlear hair cells within 30 min (*308, 310, 318*), suggestive of transcellular trafficking across the BLB. This could occur via several mechanisms characterized in other cell systems. Aminoglycosides and GTTR can permeate through nonselective cation channels, including the MET channel expressed by hair cells (*97, 309*) and TRPV4 channels expressed by endothelial cells (*95, 366*). The sodium-glucose transporter-2 traffics aminoglycosides into cells and facilitates aminoglycoside-induced cytotoxicity (*367*). LPS treatment can up-regulate endothelial cation channel expression (*368*). If endotoxemia increases the expression of aminoglycoside-permeant ion channels or transporters, it will be crucial to determine whether these channels enable LPS-enhanced trafficking of aminoglycosides across the BLB.

Endocytotic and transcytotic trafficking across the BLB has been described previously (*369*) and is increased during endotoxemia in noncochlear capillary beds (*370*). Although aminoglycosides strongly interact with negatively charged phospholipid membranes (*371*), hydrophobic passage (or diffusion) through the membrane is slow (*372*). How endotoxemia potentiates aminoglycoside trafficking routes across the BLB remains to be determined.

2.4.3 - Endotoxemia exacerbates ototoxicity

Chronic kanamycin dosing induced PTS at only 32 kHz. Endotoxemia significantly exacerbated the degree of kanamycin-induced PTS at 32 kHz and at additional lower frequencies. Furthermore, endotoxemia significantly potentiated the degree of kanamycin-induced OHC death, predominantly in the basal region of the cochlea. These data support previous observations that bacteremia and hyperthermia (an

experimental model for sepsis-induced fever) enhanced aminoglycoside-induced ototoxicity in humans and mice, respectively (*373, 374*). Endotoxemia also potentiated aminoglycoside-induced nephrotoxicity (*375*) and heightened the degree of cisplatin-induced PTS (*376*).

Kanamycin-induced OHC loss occurred in a narrower tonotopic range than drug-induced PTS, as reported previously (*324, 377*). This mismatch between the broader frequency ranges of PTS and narrower tonotopic regions of OHC loss has been attributed to functional dysregulation of the stria vascularis, hair cell mechanotransduction, and/or synaptic activity in surviving hair cells (*309, 377, 378*). Although partial recovery of auditory function after kanamycin treatment has been described previously, it only occurred in regions with lower threshold shifts and greater OHC survival (*377*). The basis for this partial recovery is thought to be drug clearance from cochlear tissues, facilitating the repair of hair cell and strial physiology incurred during sublethal toxicity to resume optimal auditory function (*322, 377, 379*). However, once threshold shifts exceed >40 dB (akin to the LPS + kanamycin group), no functional or anatomical recovery of hair cells occurred, resulting in a PTS (*377, 380*).

Endogenous inflammatory responses to Gram-negative bacterial infections are crucial to controlling infection and host survival. However, the clinical use of the life-saving bactericidal aminoglycosides can inadvertently heighten the existing inflammatory response via bacteriolytic release of endotoxins, that is, the Jarisch-Herxheimer reaction (*357, 358, 381*), to potentiate both cochlear uptake of aminoglycosides and ototoxicity. Thus, efforts to ameliorate aminoglycoside-induced ototoxicity (and nephrotoxicity) using pharmacotherapeutic agents, for example, D-METhionine (*381*), should also aim to demonstrate otoprotection in preclinical models with induced inflammation.

The progression of acute-phase inflammation is characterized by changing expression patterns of specific inflammatory proteins over time (*337, 338*), whereas the onset of aminoglycoside-induced ototoxicity in mice requires several days of administration (*324*). We tested inflammation-enhanced cochlear uptake of aminoglycosides only at 24 hours, and this potentiated uptake could be greater at other time points after induction of endotoxemia. We induced endotoxemia using LPS from *Escherichia coli*, yet LPS from other bacteria can also activate TLR4. It will be

important to determine whether other TLR signaling cascades (particularly TLR3 for viremia) also potentiate aminoglycoside-induced ototoxicity. If inner-ear inflammation increases the penetration of non-ototoxic antibiotics (for example, cephalosporins) into the cochlea, then this phenomenon could better preserve auditory and vestibular function during bacterial labyrinthitis (*382*).

We conclude that endotoxemia-induced inflammation potentiated ototoxicity by increasing aminoglycoside trafficking across the BLB into the cochlea. In toto*,* these data suggest that patients receiving aminoglycoside pharmacotherapy for life-threatening bacterial infections are at greater risk of ototoxicity than previously recognized.

2.5 – Materials and Methods

2.5.1 - Study design

The objective was to test the hypothesis that LPS-induced inflammation increased cochlear concentrations of aminoglycosides without renal dysfunction or increased serum aminoglycoside concentrations in C57BL/6 mice. We verified LPS-induced systemic and cochlear inflammation using multiplex ELISAs and quantitative reverse transcription polymerase chain reaction (RT-PCR) (*341*) in C57BL/6 mice and in mice with hypofunctional TLR4 activity (C3H/HeJ) and their strain control (C3H/HeOuJ). We then tested whether LPS-induced inflammation exacerbated aminoglycoside-induced ototoxicity using a well-established protocol for C57BL/6 mice (*324*). All experiments were approved by the Institutional Animal Care and Use Committee of Oregon Health & Science University (OHSU) and followed the ARRIVE (Animals in Research: Reporting In Vivo Experiments) reporting guidelines (*383*).

2.5.2 - Serum and cochlear concentrations of GTTR, gentamicin, serotonin, and histamine

GTTR was prepared as before (*317*). Mice, chosen at random, received a tail vein injection of DPBS or LPS, followed by an intraperitoneal injection of GTTR (2 μg/g), gentamicin (20 μg/g), or hTR (2 μg/g molar equivalent to GTTR) 24 hours later (fig.

S15). LPS-treated mice received one dose (0.1, 1, 2.5, or 10 mg/kg) of LPS (*E. coli* serotype 0111:B4). One or 3 hours after GTTR, gentamicin, or hTR injection, cardiac blood samples were obtained before cardiac perfusion with DPBS followed by 4% paraformaldehyde, and cochleae and kidneys were immersion-fixed. Fixed tissues were counter-labeled with Alexa 488–conjugated phalloidin and examined by confocal microscopy for fluorophore intensity or capillary diameter analyses by operators blinded to treatment groups (*317*). Serum concentrations of the gentamicin epitope of GTTR were obtained by OHSU Diagnostic Services (*310*). Serum and cochlear concentrations of gentamicin or GTTR were also assayed by ELISA according to the manufacturer's instructions (EuroProxima) to determine concentrations. Serum serotonin and histamine concentrations were obtained using ELISA kits (Rocky Mountain Diagnostics).

2.5.3 - Inflammatory protein and mRNA analyses at 6 hours

C57BL/6 mice were randomly grouped and treated as described in fig. S16. For multiplex ELISAs, cochleae were homogenized before performing multiplex ELISAs in duplicate (*341*). For quantitative RT-PCR, excised cochleae were placed in RNAlater (Ambion) and stored at 80°C.

Tissue RNA was extracted, reverse-transcribed using an RT^2 first-strand kit, prepared for RT-PCR using custom PCR arrays optimized for reaction conditions, primers, and probes (SABiosciences), and analyzed using the SABiosciences PCR Array Data Analysis Web Portal (*341*).

2.5.4 - Inflammatory protein and mRNA analyses at 24 hours

Twenty-four mice for each strain (C57BL/6, C3H/HeOuJ, and C3H/HeJ) were randomly grouped and treated as shown in fig. S16. For ELISAs, six cochleae from three mice per sample were pooled in protein extraction buffer before multiplex ELISA, in triplicate. Absolute protein concentrations from DPBS-treated mice were subtracted from LPS-treated mice, and the 95% CIs derived from Student's *t* test were propagated. For mRNA levels, RNAs from each pair of cochleae were obtained and complementary DNA samples analyzed in triplicate using RT^2 qPCR Primer Assays read on an Applied

Biosystems Step One Plus qRT-PCR. Relative expression levels were calculated using the $\Delta\Delta C_t$ method normalized to glyceraldehyde-3-phosphate dehydrogenase (GAPDH).

2.5.5 - Ototoxicity studies

ABRs to pure tones were used to obtain measures of cochlear function before and after treatments to determine threshold shifts (*317, 367*). For toxicity studies, mice were randomly divided into four groups: (i) DPBS only, (ii) LPS only, (iii) kanamycin only, and (iv) LPS plus kanamycin (**fig. S17**). Mice received kanamycin (700 mg/kg) (or DPBS) twice daily for 14 consecutive days (*324*). Mice received a tail vein injection of LPS (1 mg/kg) (or DPBS) the day before kanamycin treatment and on the 5th and 10th day during kanamycin treatment. ABRs were obtained before kanamycin treatment and 1, 10, and 21 days after kanamycin treatment before fixation and cytocochleogram analyses by operators blinded to treatment groups (*324*). Additional mice in each group received hTR for 1 hour after ABR testing on day 14 of chronic LPS and/or kanamycin treatment, before fixation and processing for hTR fluorescence intensity and cytocochleogram analyses as described above. Neonatal pups (P6) were used as positive controls.

2.5.6 - Statistical analyses

Statistical analyses were chosen on the basis of data under analysis. In brief, Wilcoxon signed-rank test was used for GTTR intensity analyses, the Mann-Whitney U test for ordinal variables (for example, **Fig. 2-2A**), and Student's unpaired t test for single-variable analyses (for example, **Fig. 2-2B-E**). For vasodilation analyses, we used one-way ANOVA with Tukey post hoc tests. For ELISA studies in C57BL/6 mice, we used a one-way ANOVA with Bonferroni multiple comparison correction with family-wise 95% confidence levels, whereas comparisons of mRNA levels in C57BL/6 mice were determined as significant if the 95% CI did not overlap with 1 (control-treated baseline). To compare ELISA and mRNA data between strains, a one-way ANOVA with either Bonferroni or Dunnett's post hoc tests and a family-wise 95% confidence level was used. For ABR and cytocochleogram analyses, we used two-way ANOVA with Bonferroni or Tukey post hoc tests. The statistical analyses used, number of replicate

measurements, and number of mice are stated in each figure legend or in the Supplementary Materials. *P* values <0.05 were considered significant.

2.6 – Figures and Tables

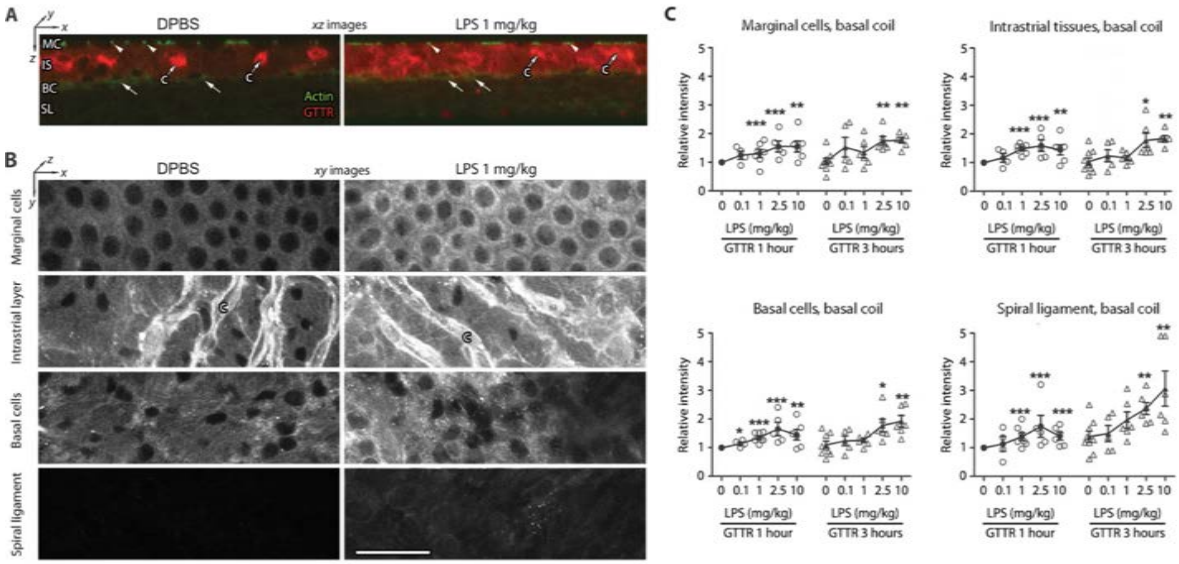

Fig. 2-1. Cochlear lateral wall uptake of GTTR is enhanced by LPS.
(**A**) In *xz* planes of the cochlear lateral wall 1 hour after GTTR injection, F-actin labeling (green) revealed tight junctions (arrowheads) between marginal cells (MC), with amorphous labeling in basal cells (BC; arrows). In DPBS-treated mice, intense GTTR fluorescence (red) distinguished strial capillaries (c), with less intense fluorescence in marginal cells, intrastrial layer (IS), and basal cells of the stria vascularis. The spiral ligament (SL) fibrocytes presented substantially less intense GTTR fluorescence compared to strial cells. LPS-treated mice displayed more intense GTTR fluorescence in the lateral wall (right panel) compared to DPBS-treated mice (left panel). (**B**) A focal series of *xy* planes through marginal cells, intrastrial tissues, basal cells, and fibrocytes at successively lower *xy* planes in the *z* axis, 1 hour after GTTR injection. LPS-treated mice exhibited more intense GTTR fluorescence in grayscale (right panels) compared to DPBS-treated mice (left panels). Scale bar, 50 μm. (**C**) Mean pixel intensities of GTTR fluorescence in lateral wall ROIs (excluding capillary structures) are dose-dependently increased with increasing doses of LPS at 1 and 3 hours after GTTR injection (relative to DPBS-treated mice at 1 hour), with statistical significance in every cell type at 1 hour of LPS (1 mg/kg or higher dose) (*$P < 0.05$, **$P < 0.01$, ***$P < 0.001$, Wilcoxon signed-rank test; error bars, SEM; *n* as in table S1).

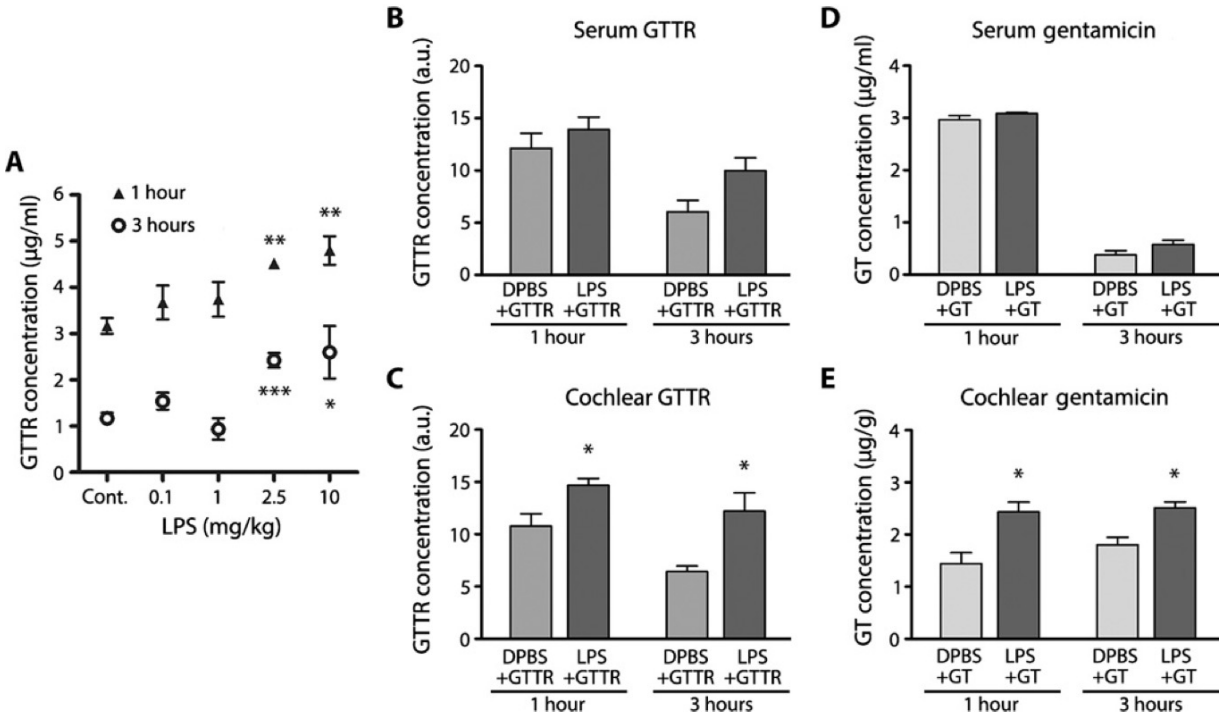

Fig. 2-2 Low-dose LPS does not alter serum concentrations but does alter cochlear concentrations of aminoglycosides.

(**A**) Using immunoturbidimetry, GTTR serum concentrations were significantly higher in LPS (2.5 and 10 mg/kg)–treated mice than in controls at 1 or 3 hours. There was no difference between DPBS-treated mice and those dosed with LPS at 0.1 and 1 mg/kg, nor between mice dosed with LPS at 2.5 and 10 mg/kg. Serum concentrations of GTTR in mice treated with LPS at 2.5 mg/kg were significantly higher than in those treated with LPS at 0.1 and 1 mg/kg at both time points ($P < 0.05$). Elevated serum GTTR concentrations in mice treated with LPS at 10 mg/kg showed borderline significance at 1 hour compared to those treated with LPS at 0.1 and 1 mg/kg ($P = 0.087$ and $P = 0.053$, respectively) and variable significance at 3 hours ($P = 0.27$ and $P = 0.028$, respectively; see also table S2; $*P < 0.05$, $**P < 0.01$, ***P < 0.005, Mann-Whitney U test; n as in table S1). (**B** and **D**) Using ELISA, serum concentrations of GTTR or gentamicin were not statistically different between DPBS-treated and LPS (1 mg/kg)–treated mice at 1 or 3 hours after injection. (**C** and **E**) Cochlear concentrations of GTTR or gentamicin (GT) were significantly increased in LPS (1 mg/kg)–treated mice compared to those in controls at 1 or 3 hours after injection ($*P < 0.05$, Student's unpaired t test; $n = 4$ per group). Error bars, SEM; a.u., arbitrary units.

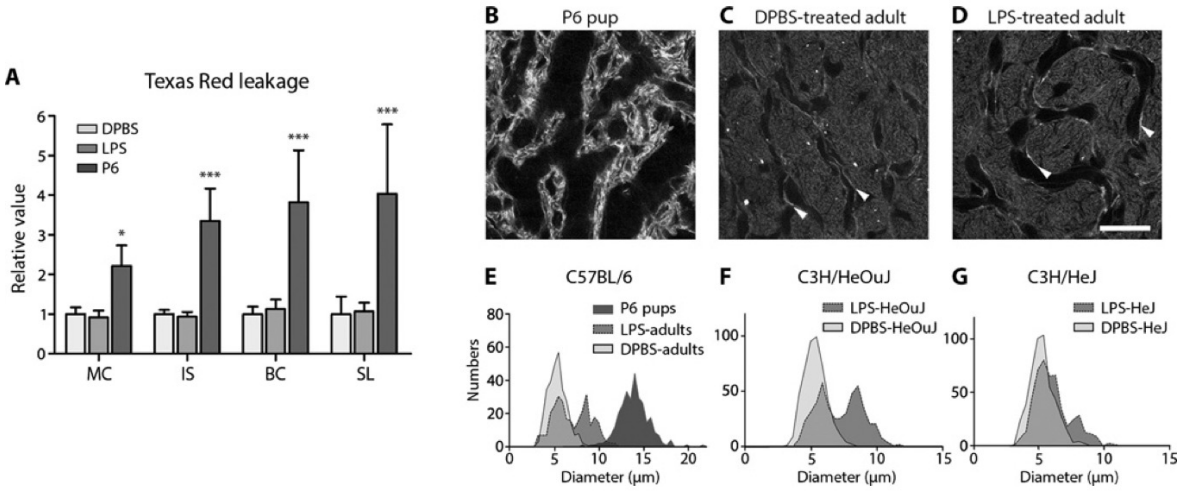

Fig. 2-3.LPS does not alter BLB permeability but vasodilates basal strial capillaries. (**A**) The relative mean intensities of hTR fluorescence in marginal cell (MC), intrastrial tissue (IS), basal cell (BC), and spiral ligament (SL) layers from P6 pups were significantly elevated compared to the same ROIs in adult mice. There was no difference in hTR fluorescence of lateral wall ROIs between DPBS- and LPS-treated adult mice [$*P < 0.05$, $***P < 0.001$, two-way analysis of variance (ANOVA) with Bonferroni post hoc tests; $n = 6$ cochleae per group; error bars, SD]. Absolute fluorescence intensities are shown in fig. S5A. (**B** and **C**) In P6 mice, the lumen of strial capillaries, revealed by phalloidin labeling, was larger than in adult DPBS-treated mice (endothelial cells indicated by white arrowheads). (**D**) Twenty-five hours after LPS treatment, a subpopulation of strial capillaries were dilated compared to DPBS-treated mice (C). Scale bar, 20 μm. (**E**) Strial capillary diameters in P6 mice were wider than those in DPBS-treated adults (see also **Table 2-1**). LPS-treated adult mice had a subset of dilated strial capillaries, resulting in a bimodal distribution. (**F**) LPS also dilated a subset of strial capillaries in C3H/HeOuJ mice compared to DPBS-treated C3H/HeOuJ mice. (**G**) In TLR4-hyporesponsive C3H/HeJ mice, LPS dilated fewer strial capillaries compared to LPS-treated control C3H/HeOuJ mice (F), resulting in an asymmetrical bimodal distribution. A Gaussian regression curve fit was applied to obtain the bimodal peak means in **Table 2-1**.

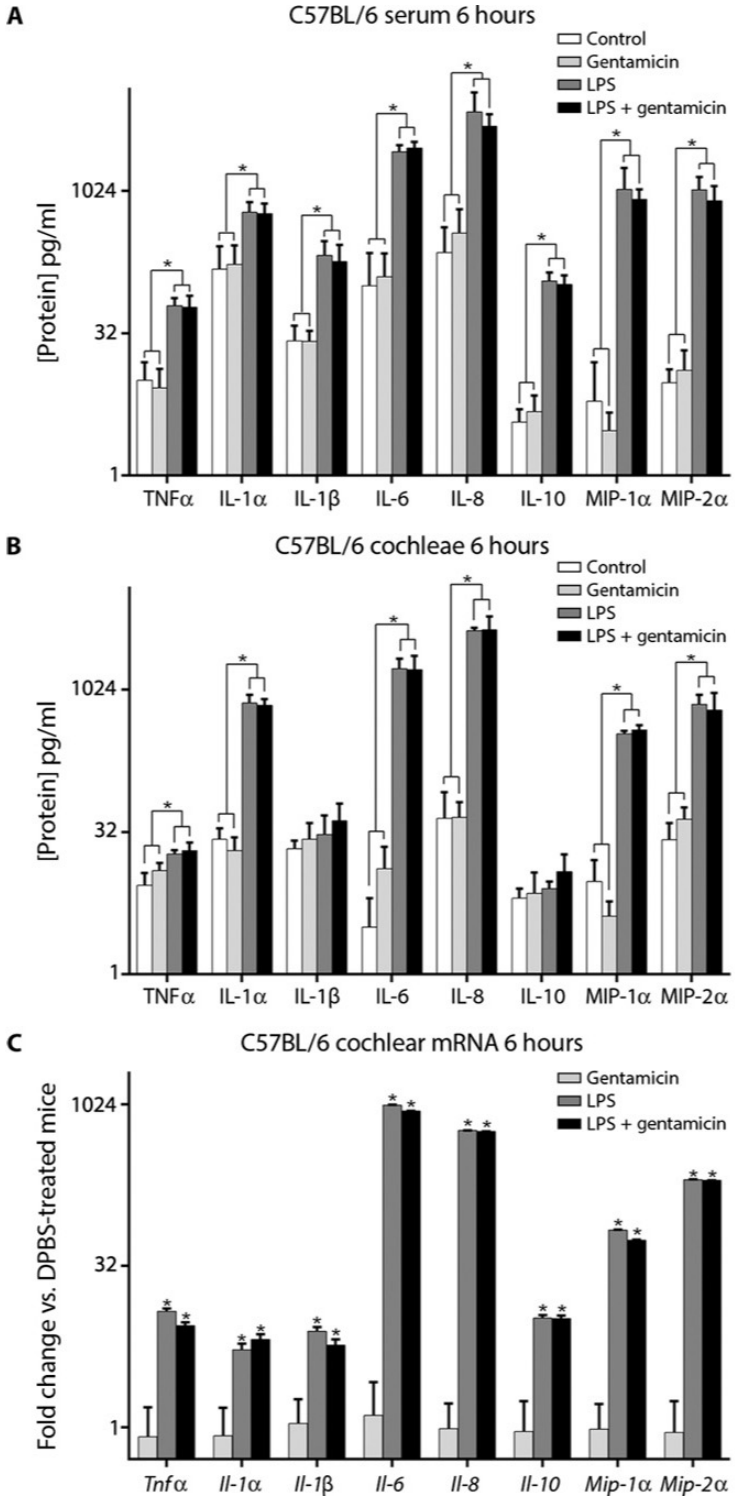

Fig. 2-4. Low-dose LPS induced major inflammatory responses in serum and cochleae within 6 hours.

(**A**) Significant increases in selected serum inflammatory proteins were observed 6 hours after LPS (±gentamicin) injection compared to DPBS-treated mice (±gentamicin; *n*= 10 per cohort). (**B**) Significant increases in cochlear inflammatory proteins were observed 6 hours after LPS (±gentamicin) injection for TNFα, IL-1α, IL-6, IL-8, MIP-1α, and MIP-2α (but not IL-1β and IL-10) compared to DPBS-treated mice [±gentamicin; *n* = 5 per cohort; 4 cochleae per sample; measured in duplicate; *, significant difference after one-way ANOVA with Bonferroni multiple comparison correction and a family-wise 95% confidence level; error bars, 95% confidence intervals (CIs) derived from Student's *t* test]. (**C**) Significant increases in cochlear mRNA for selected inflammatory markers were observed 6 hours after LPS (±gentamicin) injection when normalized to DPBS-treated mice [*n* = 6 per cohort; 2 cochleae per sample; *, significant difference if the 95% CI does not overlap with 1 (that is, DPBS-treated mice baseline)]. Gentamicin did not modulate serum or cochlear expression of inflammatory proteins or mRNA for inflammatory markers.

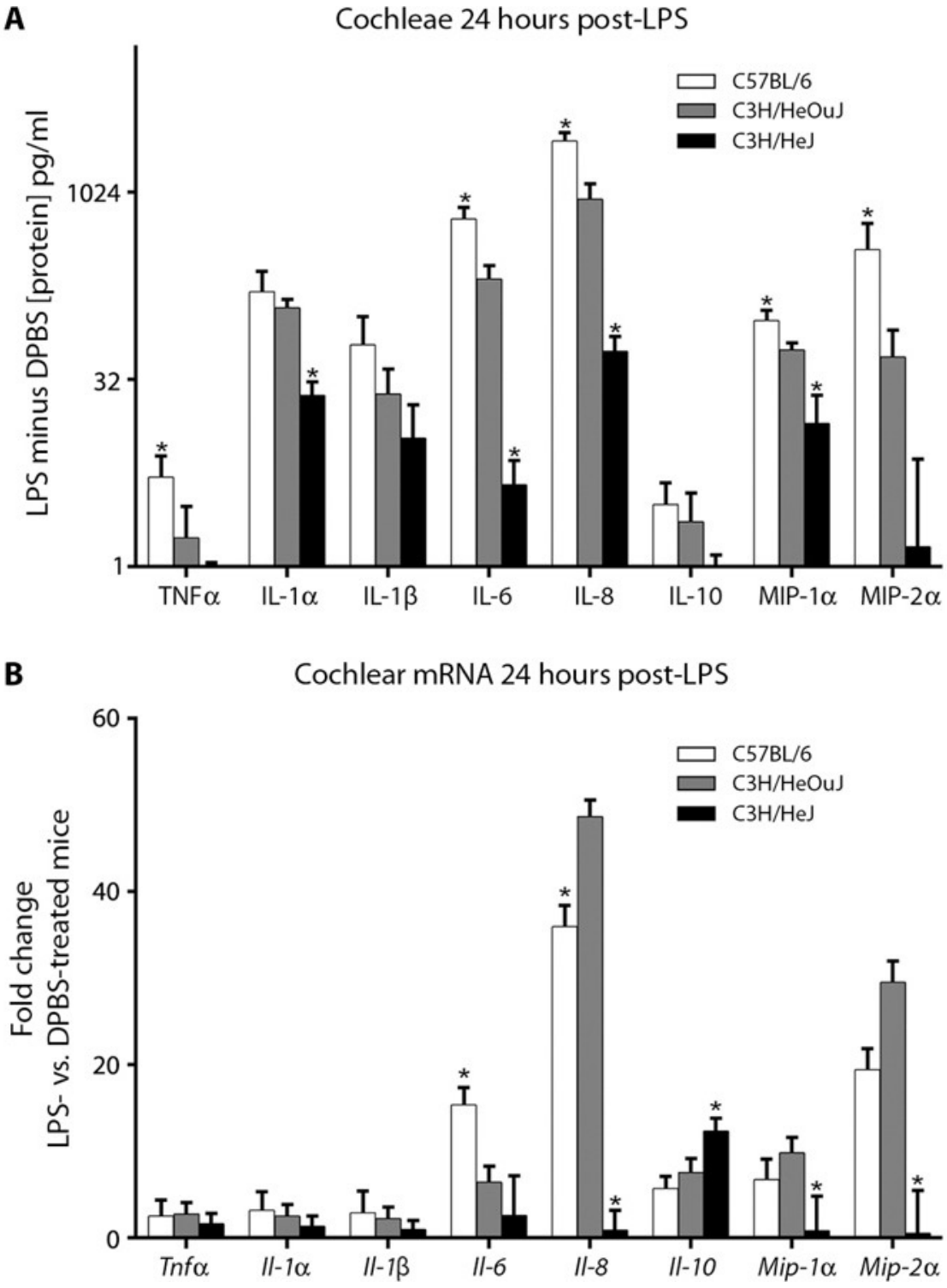

Fig. 2-5. TLR4-mediated cochlear inflammatory markers are attenuated in C3H/HeJ mice.

(**A**) All selected acute-phase inflammatory proteins (except for IL-10) were significantly elevated in cochleae from LPS-treated C57BL/6 and C3H/HeOuJ mice compared to those from DPBS-treated mice of the same strain. Several inflammatory proteins (TNFα, IL-6, IL-8, MIP-1α, and MIP-2α) were more elevated in C57BL/6 compared to those in C3H/HeOuJ mice after LPS. In TLR4-hyporesponsive cochleae from C3H/HeJ mice, only a subset of inflammatory proteins (IL-1α, IL-6, IL-8, and MIP-1α) were elevated after LPS, with small differences between the means for TNFα and IL-10. Expression of predominantly later-expressing inflammatory markers (IL-1α, IL-6, IL-8, and MIP-1α) was significantly attenuated in LPS-treated C3H/HeJ mice compared to that in LPS-treated C3H/HeOuJ and C57BL/6 mice ($n = 4$ per cohort; 6 cochleae from 3 mice per sample). (**B**) In C57BL/6 and C3H/HeOuJ mice, significant increases were observed in cochlear expression of *Il-1β*, *Il-6*, *Il-8*, *Il-10*, *Mip-1α*, and *Mip-2α* mRNA after LPS treatment when normalized to DPBS-treated mice. These increases were attenuated for *Il-8*, *Mip-1α*, and *Mip-2α* in LPS-treated C3H/HeJ mice compared to those in LPS-treated C3H/HeOuJ mice. *Il-10* mRNA expression was significantly higher in C3H/HeJ mice compared to that in C3H/HeOuJ and C57BL/6 mice ($n = 4$ per cohort; 2 cochleae from 1 mouse per sample). Error bars, 95% CI derived from Student's *t* test; *, significant difference compared to C3H/HeOuJ mice after one-way ANOVA with Dunnett's post hoc tests and a family-wise 95% confidence level. See also fig. S6.

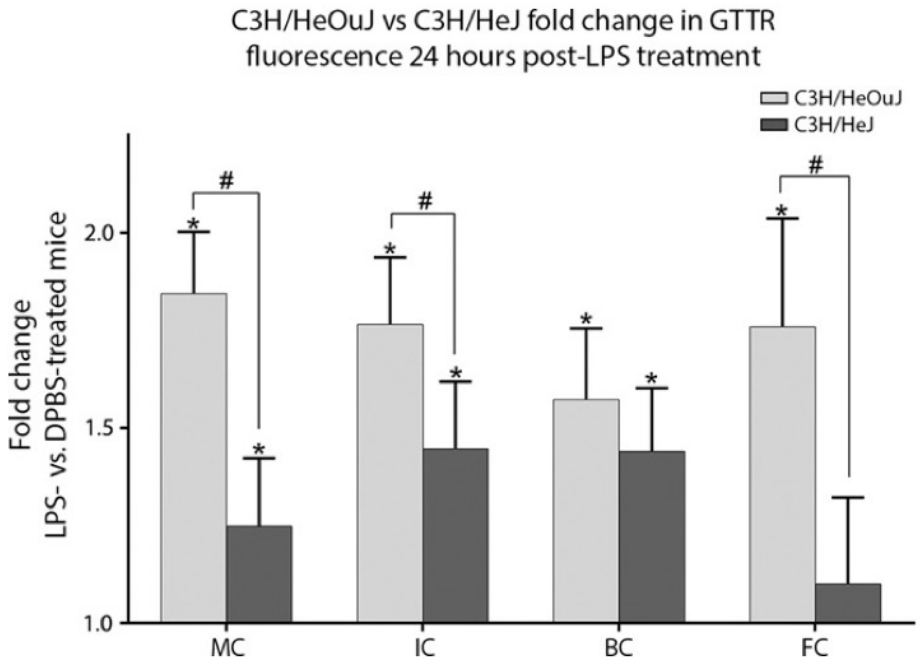

Fig. 2-6.LPS-induced GTTR uptake by lateral wall cells is attenuated in TLR4-hyporesponsive C3H/HeJ mice.

The fold change in GTTR intensity in LPS-treated mice over DPBS-treated mice is shown. GTTR fluorescence was significantly enhanced in strial marginal (MC), intermediate (IC), and basal (BC) cells, as well as fibrocytes (FC) of LPS-treated C3H/HeOuJ mice compared to that in DPBS-treated C3H/HeOuJ mice. LPS also significantly enhanced GTTR fluorescence intensities in strial cells (but not fibrocytes) in LPS-treated C3H/HeJ mice compared to that in DPBS-treated C3H/HeJ mice. Note that LPS-induced GTTR uptake was significantly attenuated ($P < 0.05$) in marginal cells, intermediate cells, and fibrocytes in C3H/HeJ mice compared to that in C3H/HeOuJ mice (*$P < 0.05$; $n = 8$ per bar; error bars, 95% CI derived from Student's t test; significance was determined if 95% CI did not overlap with 1; $P < 0.05$, unpaired one-way t test between strains; see fig. S8 for raw data).

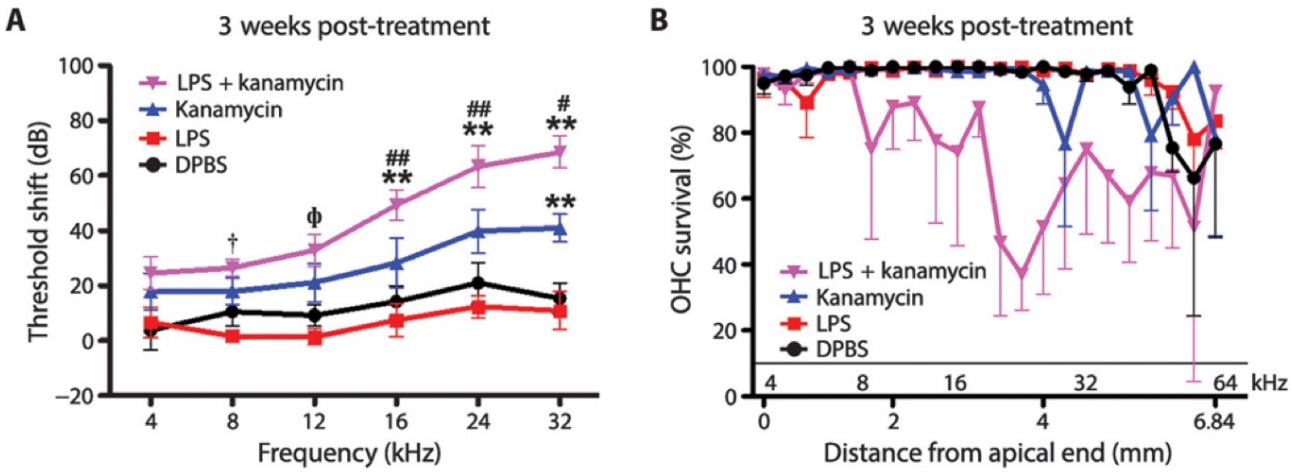

Fig. 2-7. Chronic endotoxemia potentiates kanamycin ototoxicity.

(**A**) Three weeks after chronic LPS (or DPBS) exposure ± kanamycin (see fig. S13), ABR threshold shifts for LPS-only mice ($n = 5$) were not different from DPBS-treated mice ($n = 4$). Kanamycin alone ($n = 5$) induced a small but significant PTS at only 32 kHz (**$P < 0.01$) compared to DPBS-treated mice. Mice that received LPS + kanamycin ($n = 6$) had significant PTS at 16, 24 (*$P < 0.01$), and 32 kHz ($P < 0.05$) compared to those treated with kanamycin, DPBS, or LPS only (**$P < 0.01$). Mice receiving LPS + kanamycin also had significant PTS at 12 kHz compared to those treated with DPBS or LPS only ($P < 0.05$ and $P < 0.01$, respectively), or LPS-only mice at 8 kHz ($P < 0.05$). Error bars, SD. All statistical results were produced using two-way ANOVA with Bonferroni post hoc correction with 95% family-wise confidence intervals. (**B**) Cytocochleogram for mice in (A) revealed that OHC loss in the basal cochlear regions was greater and over a wider frequency range in LPS + kanamycin–treated mice compared to that in mice treated with LPS, DPBS, or kanamycin alone. Mean cochlear length = 6.84 (±0.79, SD) mm. Error bars, 95% CI derived from Student's *t* test. See also figs. S9 to S11 and tables S5 and S7 for statistical comparisons using two-way ANOVA Bonferroni post hoc correction with 95% family-wise confidence intervals.

Table 2-1. Vasodilation of strial capillaries by LPS.

In basal coils, strial capillary diameters in P6 pups were significantly larger than those in DPBS-treated C57BL/6 adult mice (****$P < 0.0001$). LPS dilated a subset (45%) of strial capillaries in adult mice. The population of capillary diameters in LPS-treated C57BL/6 mice was significantly greater compared to that in DPBS-treated C57BL/6 mice ($P < 0.0001$). LPS also dilated a subset (50%) of strial capillaries in C3H/HeOuJ mice. In TLR4-hyporesponsive C3H/HeJ mice, LPS dilated a smaller subset (22%) of strial capillaries. The population of capillary diameters in LPS-treated C3H/HeJ mice was significantly greater compared to that in DPBS-treated C3H/HeJ mice ($P < 0.0001$). The population of capillary diameters in LPS-treated C3H/HeJ mice was significantly smaller compared to that in LPS-treated C3H/HeOuJ mice ($P < 0.0001$, one-way ANOVA with Tukey post hoc tests). In apical coils, LPS dilated a subset (45%) of strial capillaries in C57BL/6 mice. The population of apical strial capillary diameters in LPS-treated C57BL/6 mice was significantly greater compared to that in DPBS-treated C57BL/6 adult mice ($P < 0.0001$). A Gaussian regression curve fit was applied to obtain the peak means of the bimodal distributions in **Fig. 2-3**.

Mouse	LPS	Diameter (±s.d.) in μm	Bimodal diameter (±s.d.) in μm [% of N]	N (number of mice)	Significance (vs in-strain- DPBS-treated mice)
Basal coils C57BL/6 P6 pups	**–**	**13.8 (±1.5)**		**300 (3)**	***
C57BL/6 adults	**–**	**5.1 (±1.0)**		**300 (3)**	
C57BL/6 adults	**+**	**5.3 (±0.9)**	**8.6 (±1.1) [45.3%]**	**300 (3)**	***
C3H/HeOuJ adults	**–**	**5.3 (±0.8)**		**480 (4)**	
C3H/HeOuJ adults	**+**	**5.7 (±0.8)**	**8.6 (±0.9) [49.7%]**	**480 (4)**	***
C3H/HeJ adults	**–**	**5.3 (±0.9)**		**480 (4)**	
C3H/HeJ adults	**+**	**5.4 (±0.8)**	**8.1 (±0.9) [22.1%]**	**480 (4)**	***
Apical coils C57BL/6 adults	**–**	**5.0 (±0.7)**		**480 (4)**	

C57BL/6 adults	**+**	**5.6 (±0.6)**	**8.1 (±1.0) [59.8%]**	**480 (4)**	*******

Table 2-2. Effect of LPS on serum concentrations of histamine and serotonin.
Serum histamine concentrations were not affected by increasing doses of LPS. Serum serotonin concentrations were significantly decreased at all LPS doses compared to DPBS-treated mice (*$P < 0.05$, **$P < 0.001$, Mann-Whitney U test; *n* in table S1 at 3 hours after GTTR injection).

LPS dose (mg/kg)	Histamine (ng/ml, ±s.e.m.)	Serotonin (ng/ml, ±s.e.m.)
0	33 (±2)	2770 (±100)
0.1	25 (±3)	2135 (±285) *
1.0	24 (±4)	579 (±157) **
2.5	28 (±3)	830 (±246) **
10	36 (±6)	837 (±329) **

2.7 – Supplementary Materials

Supplementary Materials and Methods

Preparation of GTTR.

Gentamicin sulfate (200 mg/ml in 0.1 M potassium bicarbonate, pH 10) and succinimidyl esters of Texas Red (Invitrogen, CA; 10 mg/ml in dimethyl formamide) were agitated together for 1 week at room temperature to produce an approximately 100:1 molar ratio of gentamicin:Texas Red. A high ratio of free gentamicin to Texas Red esters ensures that only one Texas Red molecule is conjugated to any individual gentamicin molecule. We used reversed phase chromatography using C-18 columns (Grace Discovery Sciences, IL) to purify the conjugates from unconjugated gentamicin, and contamination by unreacted Texas Red.

Serum and cochlear levels of GTTR, gentamicin, serotonin, and histamines.

The care and use of all animals reported in this study were approved by the Animal Care and Use Committee of Oregon Health & Science University in keeping with the National Institutes of Health's Guid for the Care and Use of Laboratory AnimalsC57BL/6 mice (15-25 g; 4-7 weeks old) with normal Preyer's reflex were divided into control and LPS-treated groups. The control group mice received a tail vein injection of DPBS (50 µl/10g) at 0 hours, then an intraperitoneal (i.p.) injection of gentamicin (20 mg/kg) or GTTR (2 mg/kg) 24 hours later (see fig. S11). The LPS group received an intravenous (i.v.) injection of LPS followed by an i.p. injection of GTTR or gentamicin 24 hours later. The LPS group received one of several dosages of LPS (E. Coli) serotype 0111:B4, Sigma-Aldrich Co., St Louis, MO, USA; 0.1, 1, 2.5, or 10 mg/kg in DPBS, 50 µl/10 g). Six mice (5 out of 19 in 10 mg/kg group, 1 out of 13 in 2.5 mg/kg group) died within 24 hours after LPS injection, as expected.

One or 3 hours after gentamicin or GTTR injections, mice were sacrificed, blood samples obtained prior to cardiac perfusion with DPBS followed by 4% paraformaldehyde in DPBS. Cochleae were then excised and immersion fixed in 4% paraformaldehyde. The level of the gentamicin epitope of GTTR in serum samples was obtained by particle-enhanced turbidimetric inhibition immunoassay by OHSU

Diagnostic Services. The Mann-Whitney U test was used to test for differences between groups. Serum serotonin and histamine levels were obtained from samples collected 3 hours after GTTR (27 hours after LPS or DPBS) injection using ELISA fast track kits for serotonin or histamine (Rocky Mountain Diagnostics, Colorado Springs, CO, USA) by the Oregon Clinical and Translational Research Institute. The Mann-Whitney U test was used to test for differences between groups.

Cochlear imaging.

At 1 or 3 hours after GTTR injection, anesthetized mice were transcardially perfused with DPBS, then 4% paraformaldehyde; the cochleae and kidneys excised and post-fixed. The lateral wall and cochlear coils containing the organ of Corti were isolated, and kidneys vibrotome-sectioned ~70 μm thick. Prepared tissues were permeabilized with 0.5 % Triton X-100 for 45 min, rinsed, labeled with Alexa-488-conjugated phalloidin, post-fixed for 15 minutes and rinsed. Tissues from the quarter turn of the basal coil adjacent to the hook region were mounted on slides and examined using a Bio-Rad MRC 1024 ES laser scanning confocal system attached to a Nikon Eclipse TE300 inverted microscope. All GTTR fluorescence images were acquired at the same laser intensity and gain settings, including control tissues. Images of each ROI from the red channel were manually segmented for pixel intensity determination (ImageJ). To normalize data between experimental sets, the mean intensity was ratioed against the control specimen (intensity at 1 hour time point of control animal, at each ROI area) and plotted. The Mann-Whitney U test was used to test for the difference in the relative fluorescence intensity of GTTR between control and experimental groups at each time point and each ROI. Absolute GTTR fluorescence intensity between cell layers of the cochlear lateral wall was compared using Wilcoxon signed rank test after background intensity was subtracted.

In addition, mice in each group received 2 μg/g hTR (equimolar to 2 μg/g GTTR) for 1 hour, 24 hours after LPS injection, then fixed and processed for intensity analysis as described above by blinded operators. Neonatal pups (P6) were used as a positive control. Differences between groups were determined using 1-way Analysis of Variance (ANOVA) with Tukey post-hoc tests. In addition, strial capillary calibers in apical and basal cochlear lateral wall segments were determined as described previously.

Gentamicin ELISAs.

Paraformaldehyde-perfused cochleae from 4 mice in each DPBS or LPS group at each time point (1 or 3 hours) were excised and stored at -80° _C. Thawed cochleae were weighed and then homogenized using BioMasher III kits (DiagnoCine, NJ), with 100 µl homogenizing buffer (SDB, 1.15g Na2HPO4; 0.2g KH2PO4; 0.2g KCl; 30g NaCl; 0.5 ml Tween 80 in 1 liter distilled water, pH 7.4; EuroProxima, Arnhem, The Netherlands). After removal of bone fragments, the protein extract was centrifuged at 4°C, and the supernatant used for gentamicin ELISA according to the manufacturer's instructions (EuroProxima, Arnhem, The Netherlands) to determine gentamicin or GTTR levels in serum and cochleae (normalized to cochlear mass). Student's unpaired t-test was used to compare gentamicin levels between groups.

Inflammatory protein and mRNA analyses 6 hours.

As shown in fig. S12, the vehicle control group was anesthetized prior to a tail vein injection of DPBS i.v. at 0 hours, followed by an i.p. injection of DPBS at 3 hours. Using the same time points, a second group received DPBS i.v. followed by gentamicin i.p. ; the third group received 1 mg/kg LPS i.v., followed by DPBS i.p.; and the last group received 1 mg/kg LPS, followed by gentamicin i.p.. At the 6 hour time point, all mice were anesthetized and cardiac blood collected, the vasculature perfused with ice-chilled DPBS prior to excision of both cochleae and stored at -80° C. Each group contained 16 mice. Gentamicin was administered at a dose of 300 mg/kg, a non-lethal dose to determine any effect of gentamicin on inflammatory protein serum levels.

Recent advances allow multiplex ELISAs to measure multiple cochlear inflammatory proteins simultaneously within a single sample. Thawed cochleae from 10 mice were homogenized as above with 100 µl T-PER (extraction buffer, source). Bone fragments were removed by centrifugation at 4°C, and protein concentration of the supernatant determined using the Bradford assay and normalized prior to performing multiplex ELISA using Q-Plex Array (Quansys Biosciences, USA) in duplicate, as described previously.

Recent advances enable quantitative RT-PCR analyses on primer arrays of multiple genes for inflammatory protein genes to quantify cochlear gene expression. Six pairs of excised cochleae from each group were placed in RNAlater (Ambion, Inc,

Austin, TX, USA) and stored at -80° C. Tissue RNA was extracted with the Qiagen RNeasy Mini Kit, and sample concentrations of RNA equalized. RNA was reverse-transcribed using an RT2 first-strand kit (SABiosciences Corp, Frederick, MD, USA), and prepared for real-time polymerase chain reaction (RT-PCR), using custom PCR arrays optimized for reaction conditions, primers, and probes (from SABiosciences Corp). The data was analyzed using the SABiosciences PCR Array Data Analysis Web Portal. The housekeeping gene used was glyceraldehyde-3-phosphate dehydrogenase (GAPDH) has been verified to standardize samples routinely. One-way ANOVA with Bonferroni multiple comparison correction was used to compare gene expression and protein levels.

Inflammatory protein and mRNA analyses: 24 hours.

Twenty-four mice of each strain (C57BL/6, C3H/HeOuJ, C3H/HeJ; 5-6 weeks old) were anesthetized prior to a tail vein injection of LPS (1mg/kg), or DPBS (5µl/g; see fig. S12). Twenty-four hours later, mice were anesthetized, cardiac blood collected in Na2EDTA in pyrogen-free sterile epitubes, the vasculature perfused with ice-cold DPBS, cochleae excised and stored at -80˚C. For ELISAs of cochlear inflammatory proteins, 8 cochleae from 4 mice were pooled in protein extraction buffer prior to multiplex ELISA using a Quansys® platform, as described above, and measured in triplicate (2.5, 1.5, and 1mg/ml protein concentration) for each sample. Absolute protein concentrations from DPBS-treated mice were subtracted from LPS-treated mice, and the 95% Student's confidence intervals propagated. One-way ANOVA using Dunnett's post-hoc multiple comparison test was used to compare protein levels.

For mRNA levels of cochlear inflammatory proteins, cochleae from 8 mice of each strain (N=4 LPS, N=4 DPBS) were excised and processed as described above. RNA from each pair of cochleae was extracted using an RNeasy kit, and 400ng of RNA from each sample reverse-transcribed using an RT2 first strand kit. cDNA samples were analyzed in triplicate using RT2 qPCR Primer Assays read on an Applied Biosystems Step One Plus qRT-PCR. Relative expression levels were calculated using the ΔΔCt method normalized to GAPDH. One-way ANOVA using Dunnett's post-hoc multiple comparison tests was used to compare mRNA levels.

ABRs and drug-induced ototoxicity studies.

ABRs to pure tones were used to ensure normal cochlear function prior to toxicity studies and determine threshold shifts following kanamycin treatment. Briefly, needle electrodes were placed subcutaneously below the test ear, at the vertex, with a ground electrode near the paw. Each ear of each anesthetized mouse was stimulated individually with a closed tube sound delivery system sealed into the ear canal. The ABR to 1 ms rise-time tone burst stimuli at 4, 8, 12, 16, 24 and 32 kHz was recorded and thresholds obtained for each ear. Only mice with normal bilateral, baseline ABR thresholds were used. For toxicity studies, mice were divided into 4 groups, (i) DPBS only; (ii) LPS only; (iii) kanamycin only and (iv) LPS plus kanamycin (fig. S13). Mice received 700 mg/kg kanamycin (or DPBS) twice daily for consecutive 14 days. Mice received a tail vein injection of 1 mg/kg LPS (or vehicle) the day before the first day on kanamycin treatment, and every 5th day thereafter during kanamycin treatment (2 additional injections). ABRs were obtained before kanamycin treatment, and 1, 10 and 21 days after kanamycin treatment. Mice were subsequently euthanized, fixed, labeled with Alexa 488-conjugated phalloidin and Hoechst nuclear dyes, prior to imaging with an Olympus FV1000 confocal microscope for hair cell apices and nuclei. Blinded operators constructed cytocochleograms by counting the presence or absence of hair cells along the length of the cochlea in ImageJ software. The frequency map and the length of each cochlea were obtained using the Measure Line and Mosaic J plugins in the ImageJ software. A 2-way ANOVA using Bonferroni post-hoc multiple comparison test correction was used to test for differences between groups.

For BLB permeability studies following chronic LPS and/or kanamycin treatment (as described above), except, on day 14 mice in each of the 4 groups underwent ABR testing, then received 2 μg/g hTR (equimolar to 2 μg/g GTTR) for 1 hour prior to fixation and processing for confocal imaging, pixel intensity and cytocochleogram analyses by blinded operators as described above. Differences between groups were determined using 1-way ANOVA with Tukey post-hoc tests.

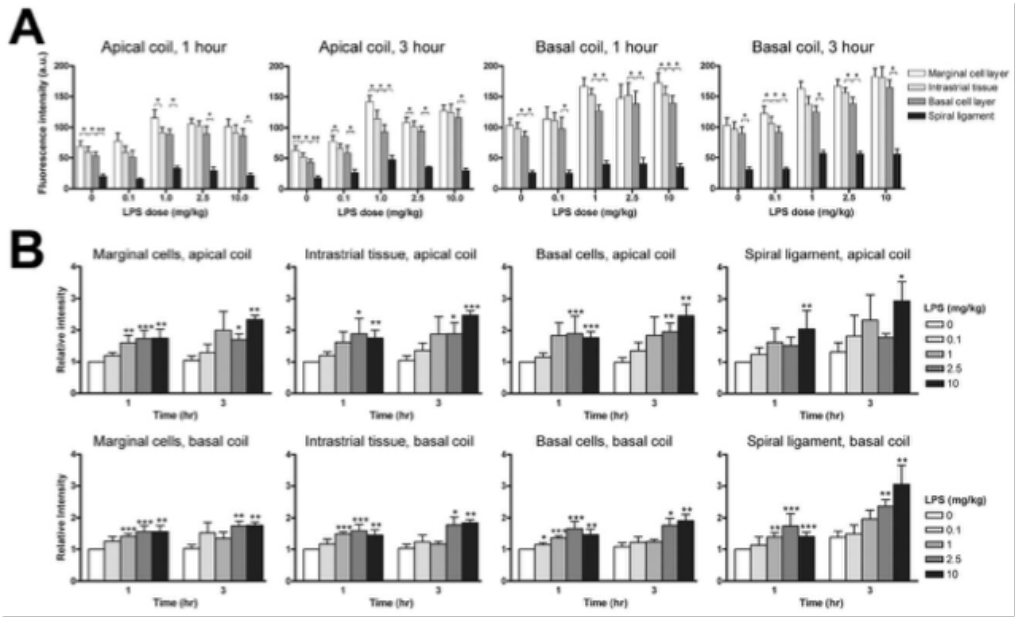

Fig. 2-S1: LPS treatment enhances cochlear lateral wall uptake of GTTR.
(A) In DPBS- treated mice treated with GTTR for 1 hour prior to fixation, absolute GTTR fluorescence is greater in marginal cells, with decreasing levels of fluorescence in intra-strial layers and basal cells, with a substantial drop in spiral ligament fibrocytes. Strial levels of fluorescence were significantly greater for each ROI in basal segments compared to apical segments ($P<0.01$; parametric paired t-test). In LPS-treated mice, GTTR uptake in strial cells and the spiral ligament was dose-dependently increased with LPS doses greater than 1 mg/kg. The rank order of fluorescence intensity in individual cell types (marginal cells > intra-strial layer > basal cells >> spiral ligament) was generally maintained with increasing LPS dose, although more variable degrees of statistical significance were observed with increasing LPS dose and time of GTTR exposure (Wilcoxon signed rank test; *$P<0.05$; **$P<0.01$; ***$P<0.005$; error bars = s.e.m.; N in Table S1). (B) Intensity analysis of GTTR fluorescence in lateral wall cells after treatment with different doses of LPS (relative to DPBS-treated mice). GTTR fluorescence is increasingly elevated in marginal cells, intra-strial tissues (excluding capillary structures), basal cells and spiral ligament fibrocytes with increasing LPS dose at 1 and 3 hours after GTTR injection. In the basal coil, every cell type examined at 1 hour after GTTR injection showed significantly increased fluorescence at 1 mg/kg LPS or higher (Wilcoxon signed rank test; *$P<0.05$; **$P<0.01$; ***$P<0.005$; error bars = s.e.m.; N in Table S1). Strial and spiral ligament fluorescence was significantly greater in basal segments compared to apical segments for each ROI ($P<0.01$; parametric paired t-test).

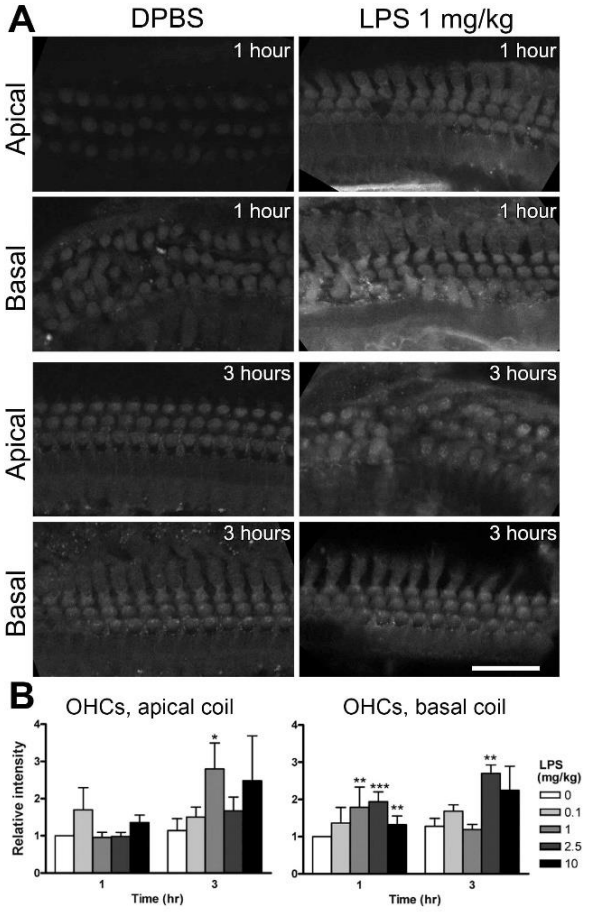

Fig. 2-S2. OHC uptake of GTTR is accelerated by LPS exposure.
(A) In cochlear OHCs, 24 hours after treatment with 1 mg/kg LPS and 1 hour after exposure to GTTR, confocal images of OHCs in basal coils show increased GTTR uptake compared to OHCs from DPBS-treated mice. Increases in GTTR fluorescence were not as apparent at 3 hours post-GTTR injection. Scale bar = 50 μm. (B) Intensity analysis of GTTR fluorescence in cochlear OHCs after treatment with different doses of LPS (relative to the fluorescence in OHCs at 1 hour) for apical or basal coils. In apical coils, LPS did not consistently modulate GTTR uptake 1 hour after GTTR injection, but trended to significance 3 hours after GTTR injection at higher doses of LPS (> 1 mg/kg). In basal coils, GTTR fluorescence was most consistently and significantly elevated 1 hour after GTTR injection, and trended to significance only at higher doses of LPS (>2.5 mg/kg LPS) 3 hours after GTTR injection (*P<0.05, **P<0.01, ***P<0.001).

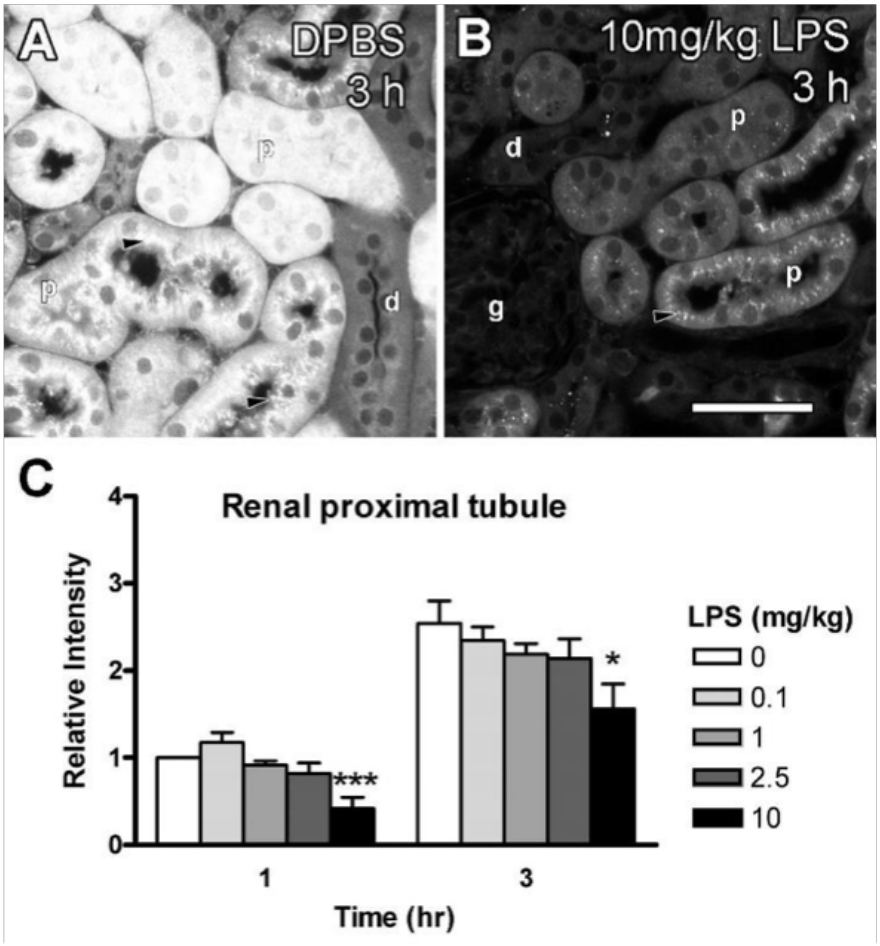

Fig. 2-S3. Renal uptake of GTTR is reduced only at high doses of LPS.
(A) In DPBS-treated mice at 3 hours after injection with GTTR, intensely-labeled puncta of GTTR fluorescence is localized near brush border microvilli (arrowheads) and diffusely distributed throughout the cytoplasm of proximal tubule cells (p). Note the weaker intensity of GTTR fluorescence in distal tubule cells (d). (B) In LPS-treated mice at 3 hours after injection with GTTR, the intensity of diffuse cytoplasmic GTTR fluorescence in proximal tubule cells is visibly decreased compared to DPBS-treated mice (A). Note also the visible reduction in GTTR-labeled puncta in proximal tubule cells, and negligible fluorescence in the glomerulus (g). Scale bar = 50 μm. (C) The intensity of GTTR fluorescence in proximal tubule cells in mice treated with different doses of LPS. Only in mice treated with 10 mg/kg LPS is a significant reduction in GTTR fluorescence observed, at either 1 or 3 hours after GTTR injection (Student's t-test; *P<0.05; ***P<0.001).

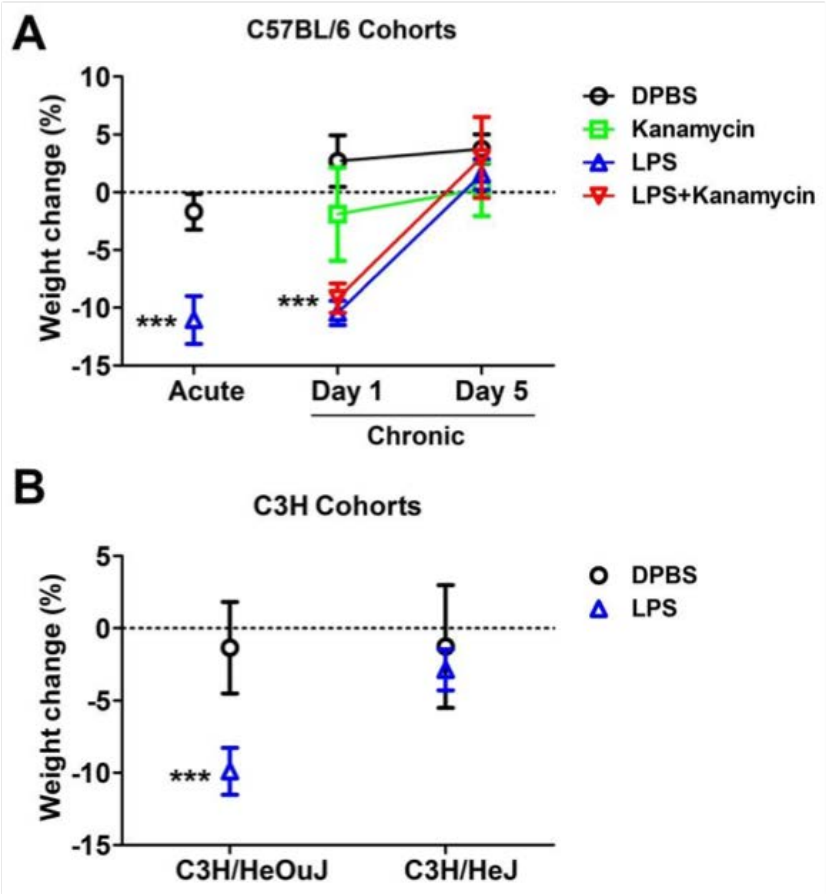

Fig. 2-S4. LPS induces acute anorexia.

(A) After 24 hours, LPS-treated C57BL/6 mice exhibited significant weight loss (~10%) compared to DPBS-treated C57BL/6 mice (Acute; N=32/cohort). LPS-treated C57BL/6 mice (±kanamycin) used in chronic toxicity experiments (Chronic, N as in Fig. 7) also displayed significant weight loss at 24 hours compared to DPBS-treated mice (±kanamycin). Over time, LPS-treated mice (±kanamycin) regained weight, with weights comparable to DPBS-treated mice (±kanamycin) by day 5. (B) LPS-treated C3H/HeOuJ mice also displayed significant weight loss 24 hours after LPS injection compared to DPBS-treated C3H/HeOuJ mice (N = 12 for DPBS, 13 for LPS). LPS-treated C3H/HeJ mice displayed attenuated weight loss 24 hours after LPS injection compared to LPS-treated C3H/HeOuJ mice (unpaired, two-tailed t-test; error bars=s.d.; ***P<0.001).

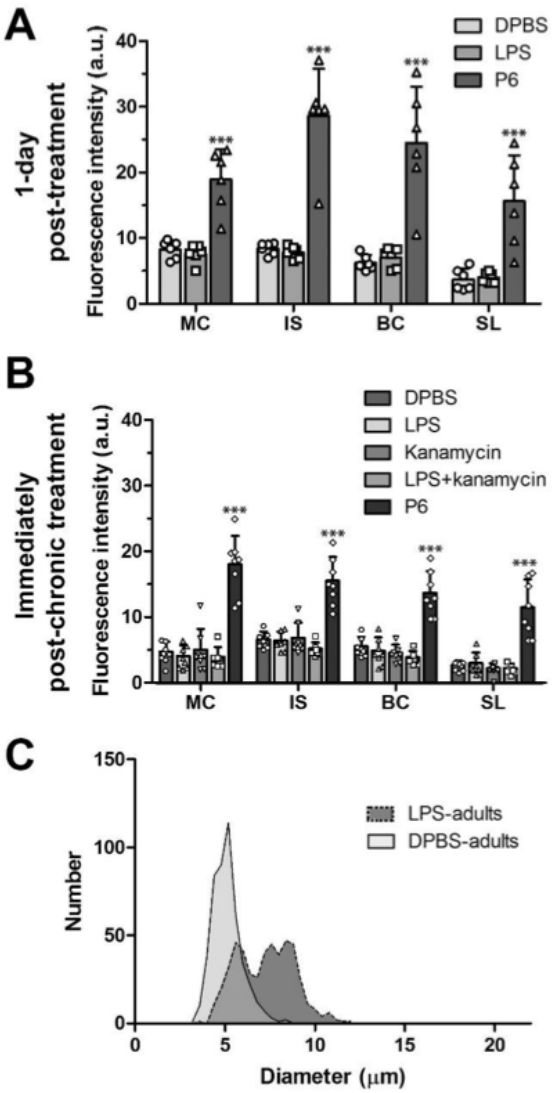

Fig. 2-S5. LPS does not alter BLB permeability yet vasodilates apical strial capillaries.

(A) Twenty-five hours after LPS, and 1 hour after hTR injection, the absolute mean intensities of hTR fluorescence in marginal cell (MC), intra-strial tissue (IS), basal cell (BC) and spiral ligament (SL) fibrocytes layers from P6 pups are significantly elevated compared to lateral wall ROIs in adult mice. There was no difference in fluorescence of lateral wall ROIs from DPBS- or LPS-treated adult mice (***P< 0.001, 2-way ANOVA with Bonferroni post-hoc tests). (B) After chronic treatment with kanamycin (±LPS), the absolute mean intensities of hTR fluorescence in lateral wall ROIs from P6 pups were significantly elevated compared to those in adult mice. There was no difference in hTR fluorescence of lateral wall ROIs from DPBS-, LPS-, kanamycin- or LPS+kanamycin-treated adult mice (***P<0.001; N=6 cochleae/group; error bars=s.d.; 2-way ANOVA with Bonferroni post-hoc tests). (C) Twenty-five hours after LPS, a subpopulation of apical strial capillaries were dilated compared to DPBS-treated mice (see also Table 1), resulting in a bimodal distribution. A Gaussian regression curve fit was applied to obtain the bimodal peak means in Table 1.

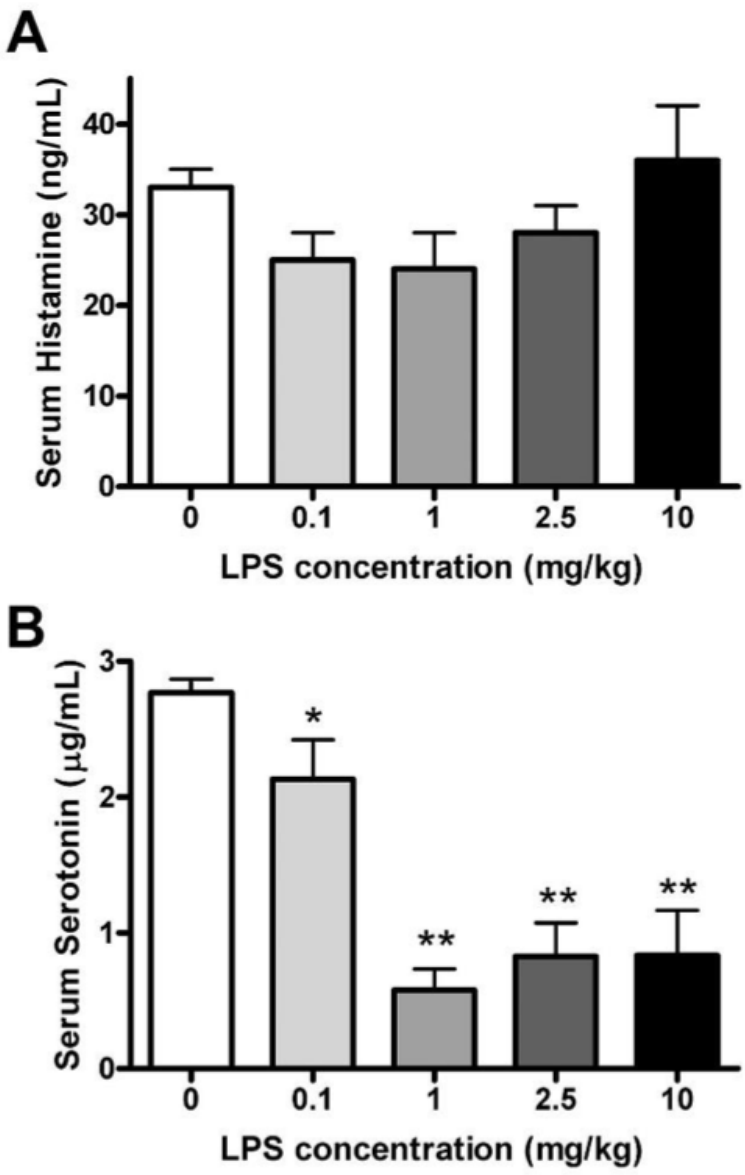

Fig. 2-S6. Serum serotonin, but not histamine, concentrations were decreased with increasing doses of LPS.

(A) Serum histamine levels were not statistically affected by increasing doses of LPS, nor show a trend. (B) Serum serotonin levels were significantly decreased at all LPS doses compared to DPBS-treated mice (0 LPS; *P<0.05, **P<0.001). The Mann-Whitney U test was used to test for differences between groups.

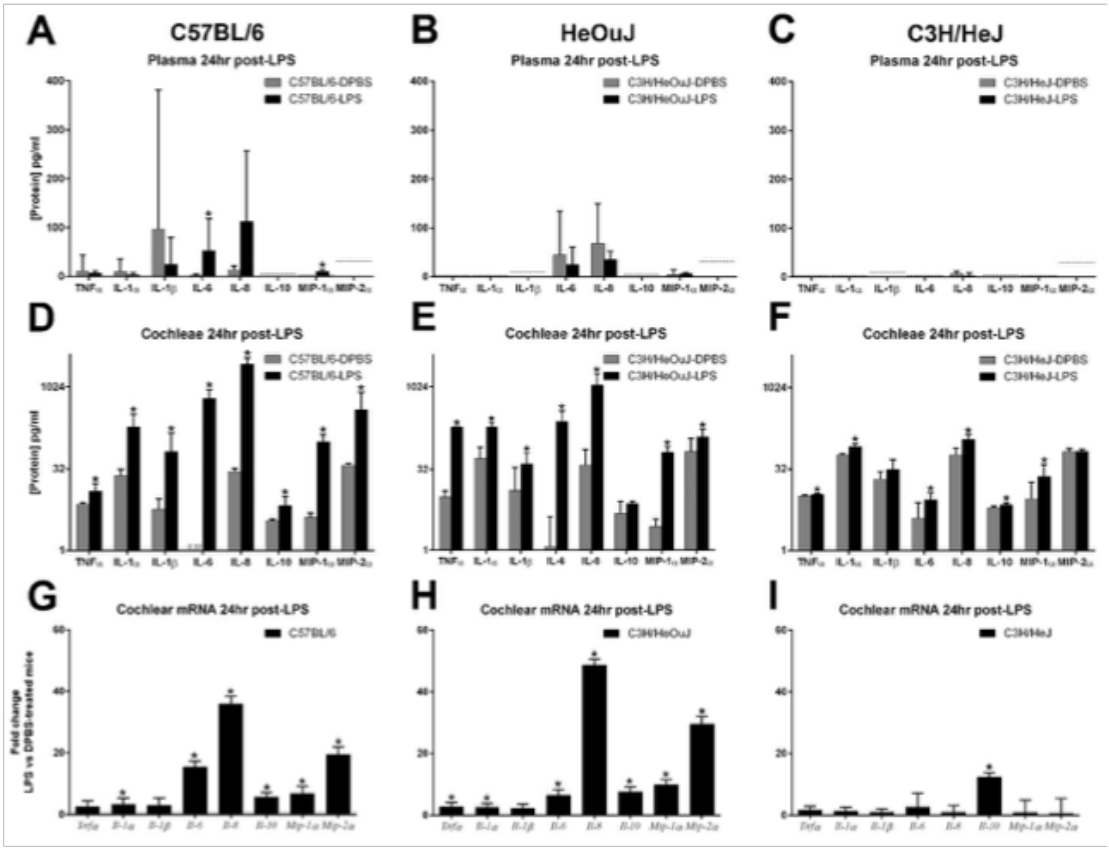

Fig. 2-S7. TLR4-mediated inflammatory markers are modulated by LPS.

(A) Twenty-four hours after 1 mg/kg LPS injection, plasma levels of most acute phase inflammatory proteins in C57BL/6 mice were not significantly different (or below the limit of detection indicated by the dashed line) compared to DPBS-treated C57BL/6 mice, except for IL-6 and MIP-1α. (B) Twenty-four hours after LPS injection, plasma levels of all tested acute phase inflammatory proteins in C3H/HeOuJ mice were not significantly different (or below the limit of detection) compared to DPBS-treated C3H/HeOuJ mice. (C) Twenty- four hours after 1 mg/kg LPS injection, plasma levels of all tested acute phase inflammatory proteins in C3H/HeJ mice were not significantly different (or below the limit of detection) compared to DPBS-treated C3H/HeJ mice. (For A-C: N=4/cohort, measured in duplicate; error bars = 95% CI derived from Student's t test; *significant difference compared to DPBS-treated mice of the same strain after a 1-way unpaired Student's t-test at the 95% CI.) (D) Twenty-four hours after 1 mg/kg LPS injection, cochlear concentrations of tested inflammatory proteins from C57BL/6 mice were all significantly elevated above baseline levels in DPBS-treated C57BL/6 mice, with the greatest changes observed for IL-6, IL-8, MIP-1α and MIP-2α. (E) In cochleae from C3H/HeOuJ mice, all acute phase pro-inflammatory proteins were significantly elevated 24 hours after LPS injection compared to DPBS-treated C3H/HeOuJ mice, except for IL- 10. (F) In TLR4-hyporesponsive cochleae from C3H/HeJ mice 24 hours after LPS injection, only a subset of acute phase inflammatory markers (TNFα, IL-1α, IL-6, IL-8, IL-10, and MIP-1α) were significantly elevated compared to DPBS-treated C3H/HeJ mice. (For D-F: N=4/cohort; 6 cochleae pooled from 3 mice/sample, measured in triplicate; error bars = 95% CI derived from Student's t test; *significant difference compared to DPBS-treated mice of the same strain after a one-way unpaired Student's t test at the 95% CI.) (G, H) When cochlear mRNA levels in C57BL/6 (G) and C3H/HeOuJ (H) mice were assayed, significant increases were observed in Il-1α, Il-6, Il-8, Il-10, Mip-1α and Mip-2α mRNA 24 hours after LPS injection compared to DPBS-treated mice of the same strain, and for Tnfα in C3H/HeOuJ mice. (I) In C3H/HeJ mice, LPS significantly increased anti-inflammatory Il-10 mRNA levels 24 hours after LPS injection, but not for any pro-inflammatory markers. (For G-I: N=4/cohort; 2 cochleae from 1 mouse/sample, measured in triplicate; error bars = 95% CI derived from Student's t test; *significant difference is noted if the 95% CI does not overlap with 1).

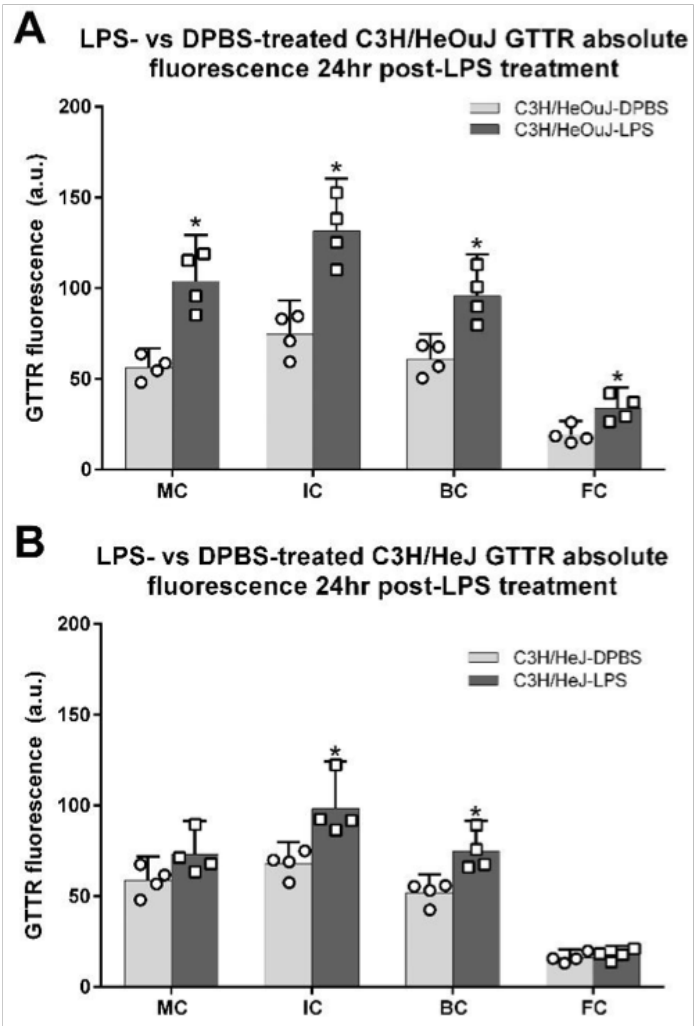

Fig. 2-S8. LPS-induced GTTR uptake by cochlear lateral wall cells in control C3H/HeOuJ and TLR4-hyporesponsive C3H/HeJ mice.

(A) The fluorescence intensity of GTTR in marginal cells (MC), intermediate cells (IC), and basal cells (BC) of the stria vascularis, as well as spiral ligament fibrocytes (FC), were significantly greater in LPS-treated C3H/HeOuJ mice over DPBS-treated C3H/HeOuJ mice. (B) The fluorescence intensity of GTTR in strial marginal, intermediate and basal cells, as well as spiral ligament fibrocytes were increased in LPS-treated C3H/HeJ mice over DPBS-treated C3H/HeJ mice. However, the LPS-induced increase in GTTR fluorescence was only significant for intermediate and basal cells (unpaired t-test 1-way; *$P<0.05$; N=4; error bars = 95% CI derived from Student's t test).

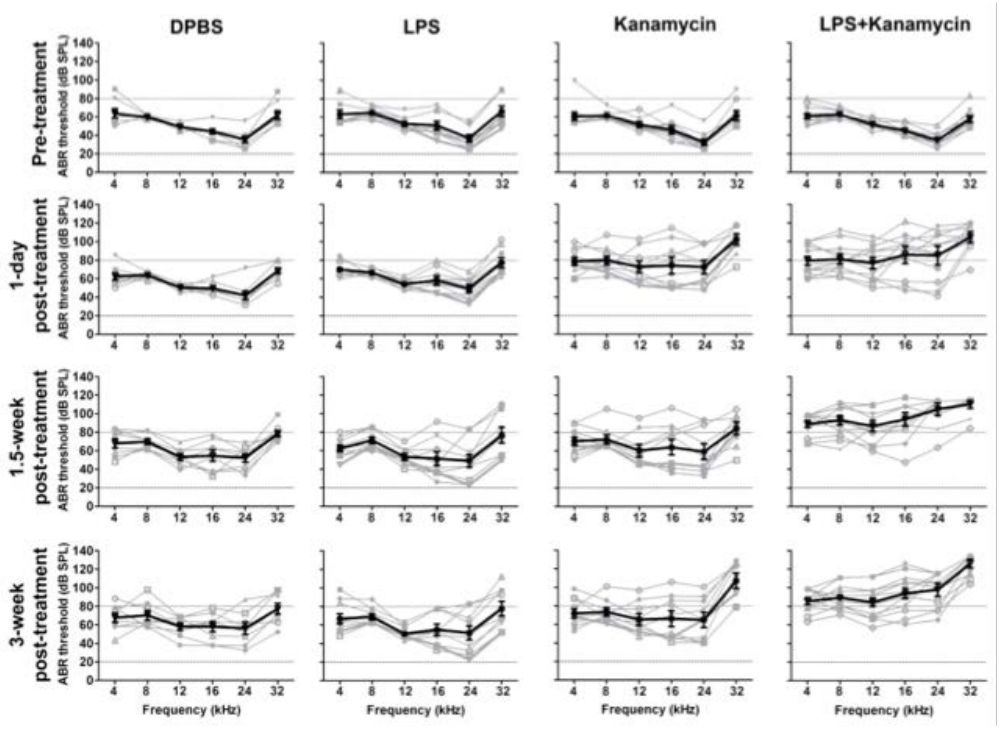

Fig. 2-S9. Absolute ABR thresholds are elevated by chronic kanamycin, or kanamycin plus LPS, dosing.

Absolute ABR thresholds for each ear of C57BL/6 mice (in gray) in each group, at stated time points before or after LPS and/or kanamycin treatment, with age- matched controls (DPBS-treated). Black line indicates the group mean (±s.d.). Note the general elevation in thresholds at 1.5 and 3 weeks post-treatment for mice treated with both LPS and kanamycin (bottom right panel) compared to age-matched DPBS-only or LPS-only treated mice (bottom row, two left panels).

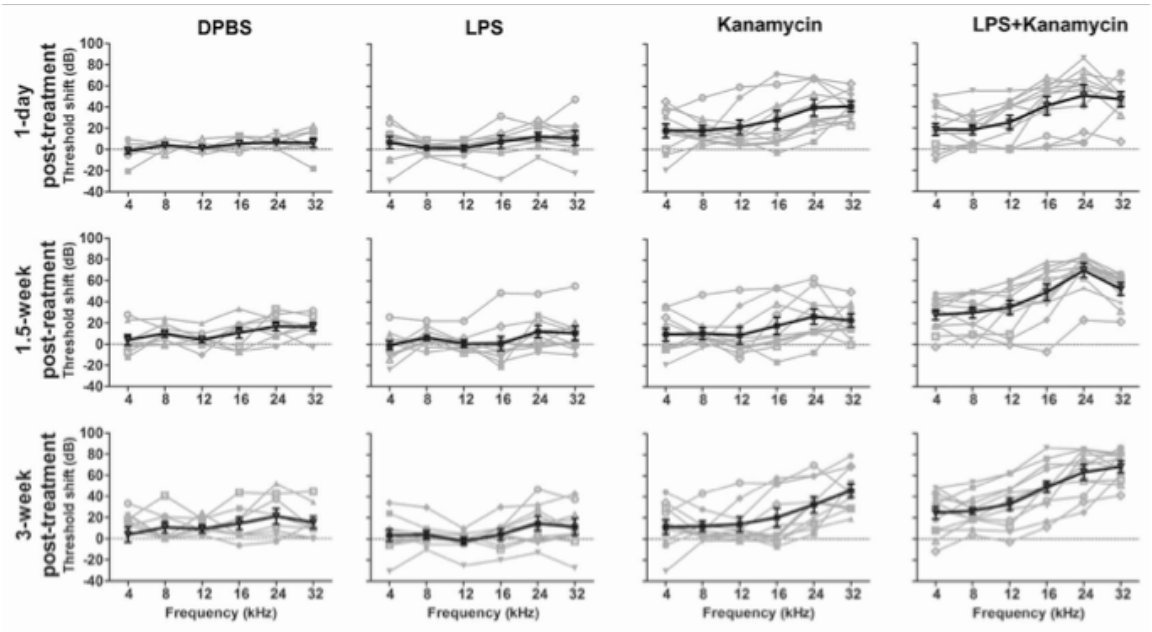

Fig. 2-S10. Threshold shifts induced by chronic kanamycin, or kanamycin plus LPS, dosing.

ABR threshold shifts for each ear of C57BL/6 mice (in gray) in each group, at stated time points after LPS and/or kanamycin treatment, with age-matched controls (DPBS). Black line indicates the group mean (±s.d.). Note the general elevation in individual and mean threshold shifts at 1.5 and 3 weeks post-treatment for mice treated with both LPS and kanamycin (lower two extreme right panels) compared to age-matched mice in other groups (bottom two rows, leftmost panels).

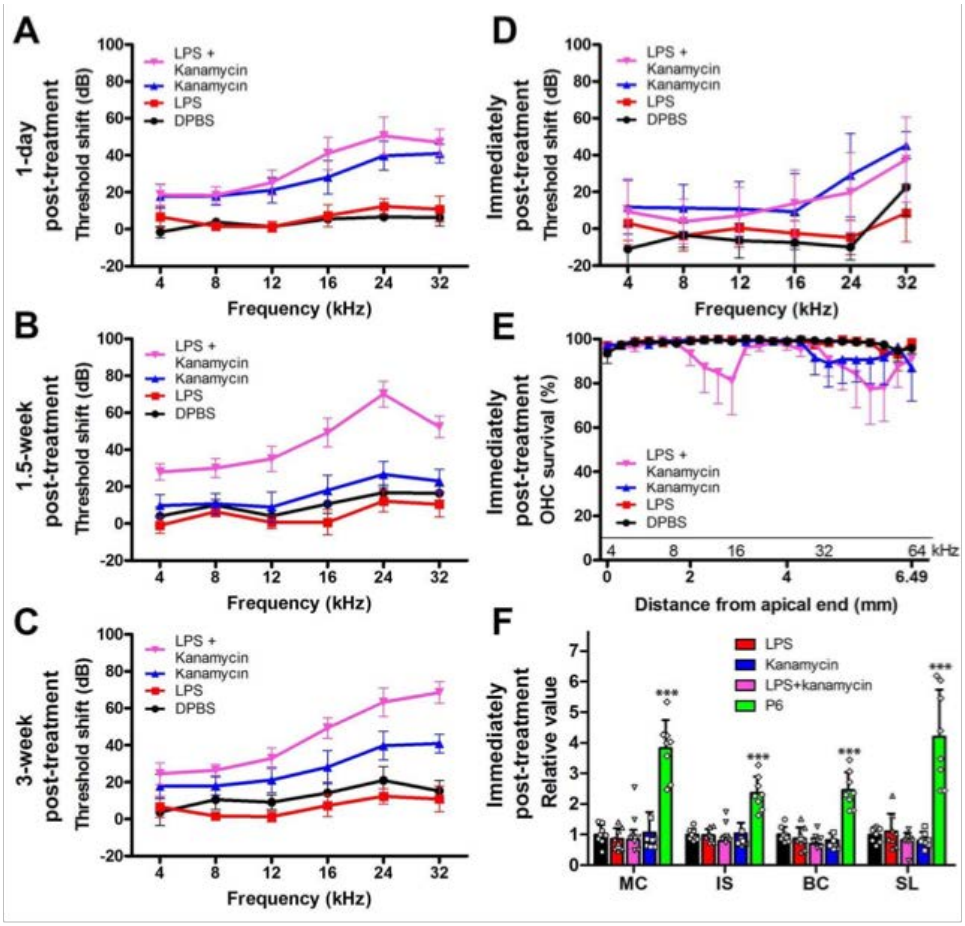

Fig. 2-S11. Effect of chronic kanamycin treatment, with or without LPS, on ABRs, OHC survival and BLB permeability.

C57BL/6J mice were treated as described in the text (see fig. S17). One day post-treatment (A), kanamycin (N=5) and LPS+kanamycin (N=6) induced significant threshold shifts at 16, 24 and 32 kHz compared to DPBS- (N=4) and LPS-treated (N=5) control mice. LPS+kanamycin also induced significant threshold shifts at 12 kHz compared to controls (table S3). Ten days post-treatment (B), threshold shifts for kanamycin-treated mice were no longer significantly different from DPBS- and LPS-treated mice (table S4). LPS+kanamycin induced significant threshold shifts at 4, 12, 16, 24 and 32 kHz compared to DPBS-treated mice, and at all frequencies compared to LPS-treated mice (table S4). LPS+kanamycin also induced significant threshold shifts at 16, 24 and 32 kHz compared to kanamycin-treated mice (table S4). Three weeks post-treatment (C), kanamycin induced a significant PTS only at 32 kHz compared to DPBS-treated mice (table S5). LPS+kanamycin induced significant PTS at 16, 24 and 32 kHz frequencies compared to kanamycin-, DPBS- and LPS-treated mice;

and also at 12 kHz compared to DPBS- and LPS-treated mice, as well as LPS-only mice at 8 kHz (table S5). Error bars=s.d. Data in A-C are from the same mice and correspond to Fig. 7A,B and P values in tables S3-S5. (D) Immediately after chronic treatment, kanamycin (N=5) induced significant threshold shifts at 4, 24 and 32 kHz compared to DPBS-treated (N=5) mice, and at 24 and 32 kHz compared to LPS-treated (N=6) mice. LPS+kanamycin (N=7) induced significant threshold shifts at 16, 24 and 32 kHz compared to DPBS-only mice; and at 24 and 32 kHz compared to LPS-only mice (table S6). LPS+kanamycin did not induce significantly different threshold shifts at any frequency compared to kanamycin-treated mice (table S6). Error bars=s.d. Data in D correspond to fig S11E,F and P values in table S6. (E) Immediately after chronic treatment, kanamycin-treated mice exhibited greater OHC loss in the basal 32-64 kHz region of the cochlea compared to DPBS- and LPS-treated mice, but this was not significant (table S8). LPS+kanamycin-treated mice had substantially greater OHC loss over a wider frequency range compared to the kanamycin-only group, as well as DPBS- and LPS-only mice that was statistically significant in the 23-64 kHz region (see also fig. S12; table S8). In the more apical 8-16 kHz region, 2 mice in the LPS+kanamycin-treated group exhibited almost total OHC loss, while the remaining 4 mice had negligible OHC loss, contributing to increased error and lack of significance (table S8). Mean cochlear length = 6.49 (±2.6, s.d.) mm. Error bars=95% CI derived from Student's t test. (F) The relative mean intensities of hTR fluorescence in marginal cell (MC), intra-strial tissue (IS), basal cell (BC) and spiral ligament (SL) fibrocyte layers from P6 pups are significantly elevated compared to adult mice. There was no difference in hTR fluorescence of lateral wall ROIs from DPBS-, LPS-, kanamycin or LPS+kanamycin-treated adult mice (***P<0.005; N=6 cochleae/group; error bars=s.d.; 2-way ANOVA with Bonferroni post-hoc tests).

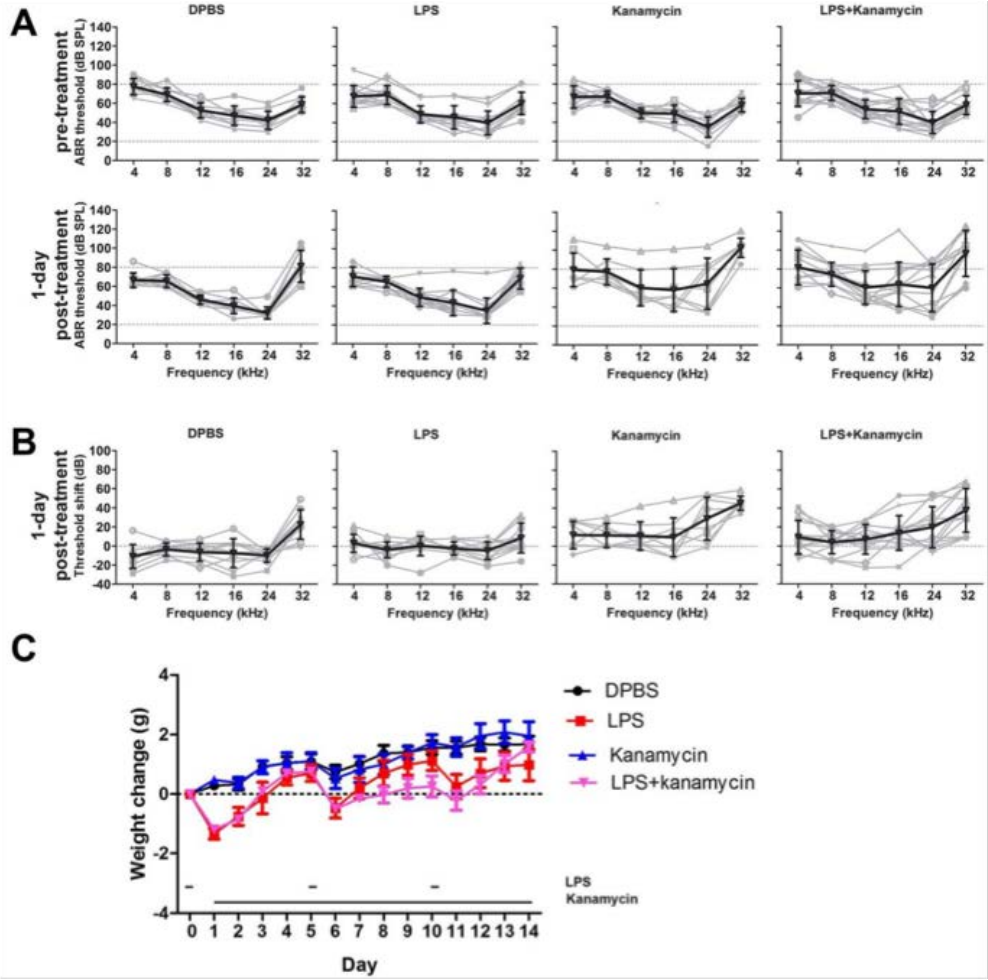

Fig. 2-S12. Absolute ABRs, threshold shifts and weight changes induced by chronic LPS, kanamycin, or LPS+kanamycin in C57BL/6 mice.

(A) Absolute ABR thresholds for individual ears (in gray) by group prior to treatment, and one day post-treatment with chronic exposure to LPS and/or kanamycin, with age-matched controls (DPBS-treated). Black line indicates the group mean (±s.d.). (B) ABR threshold shifts for individual ears (in gray) by group, one day post-treatment with chronic exposure to LPS and/or kanamycin, with age-matched controls (DPBS-treated). (C) Twenty-four hours after each LPS treatment on day 0, day 5 or day 10, LPS-treated mice exhibited substantial weight loss (~10%) compared to DPBS-treated C57BL/6 mice). Over time, mice generally regained weight after LPS treatment (±kanamycin) with weights comparable to DPBS-treated mice (±kanamycin) after 5 days.

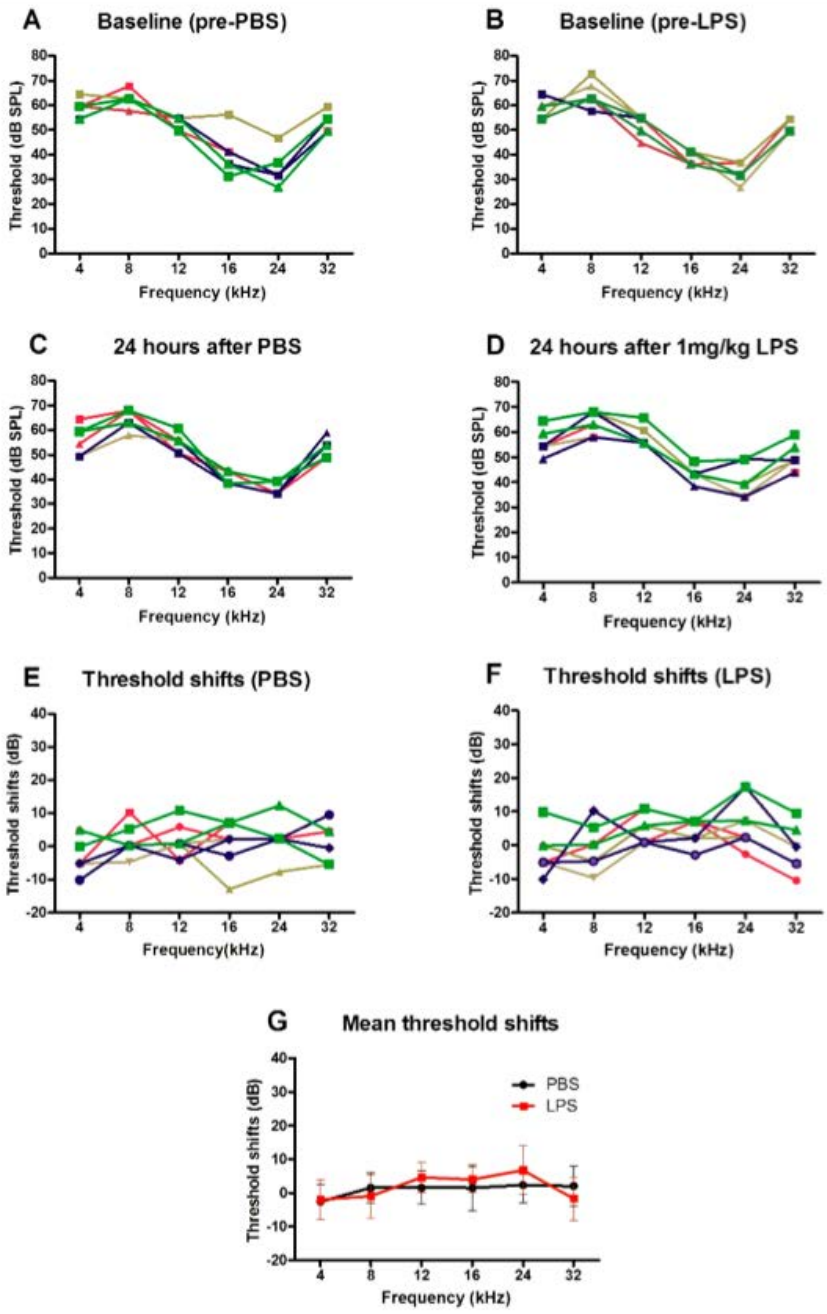

Fig. 2-S13. Acute LPS-induced endotoxemia does not alter ABR thresholds.

(A, B) Baseline ABR thresholds prior to i.v. injection with DPBS or 1 mg/kg LPS (4 C57BL/6 mice/group; 2 ears/mouse; each mouse identified by individual color; left ears ■; right ears ▲). (C, D) ABR thresholds 24 hours after injection with DPBS or 1 mg/kg LPS; no obvious changes were observed. (E, F) Threshold shifts from baseline for each ear 24 hours after injection with DPBS or 1 mg/kg LPS. (G) Group mean threshold shifts (±s.d.) of mice pre-treated 24 hours earlier with either DPBS or 1 mg/kg LPS. No statistically significant threshold shifts were observed within each group or between groups (N=4 mice per group).

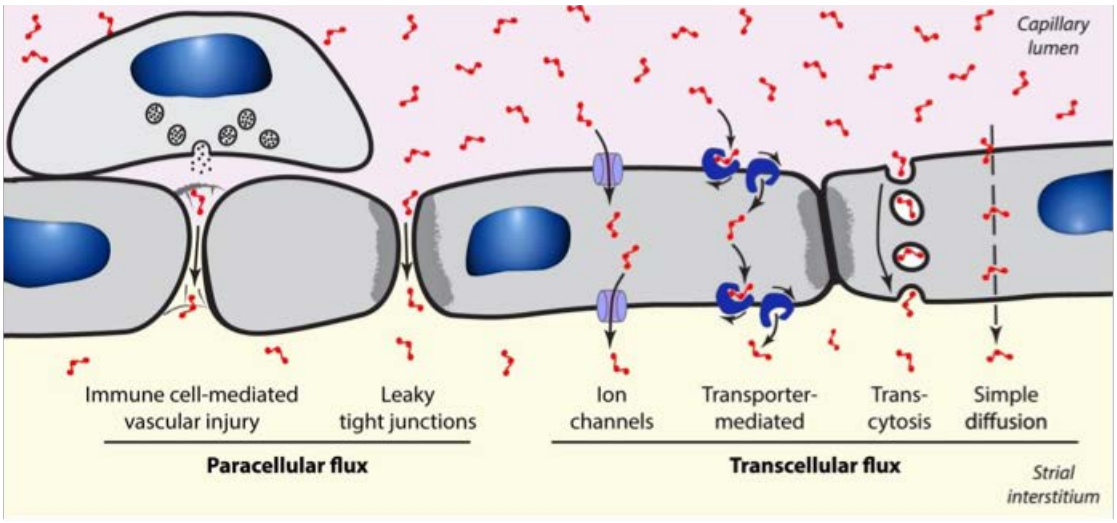

Fig. 2-S14. Schematic displaying potential mechanisms for aminoglycoside trafficking across the BLB.

Two possible mechanisms of paracellular flux include immune cell-mediated, or immune cell-independent, breakdown of tight junction-coupling between endothelial cells. Transcellular flux of hydrophilic, cationic aminoglycosides include permeation of non-selective cation channels, translocation via substrate transporters, transcytosis through the cell, and/or diffusion across the hydrophobic plasma membrane.

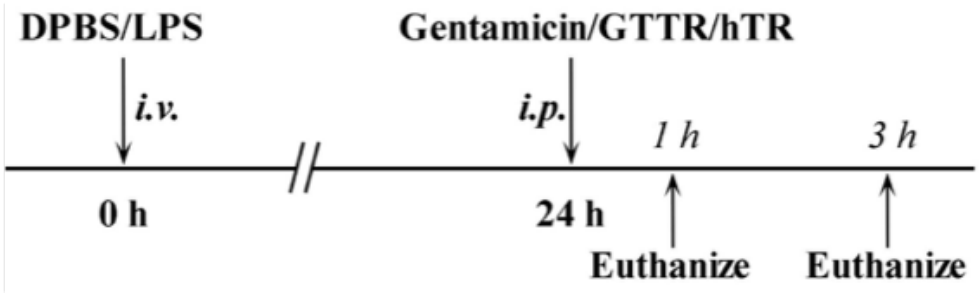

Fig. 2-S15. Acute LPS and aminoglycoside dosing paradigm.
Different doses of LPS were injected i.v., and 24 hours later, GTTR, gentamicin or hTR was injected i.p. Control C57BL/6 mice received an i.v. injection of DPBS. Mice were sacrificed 1 or 3 hours after aminoglycoside injection.

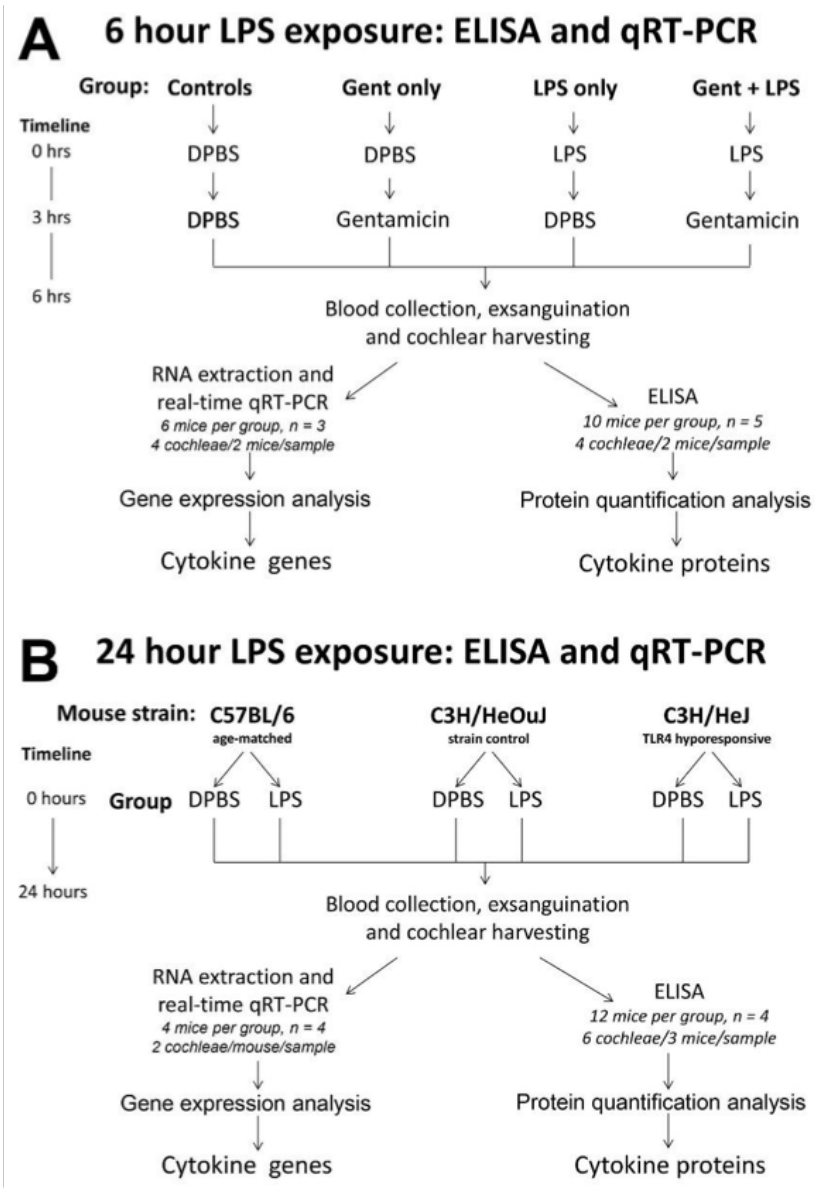

Fig. 2-S16. ELISA and qRT-PCR experimental designs for 6- and 24-hour LPS exposures.

(A) 6 hour. Sixteen C57BL/6 mice per group. Control mice received an i.v. tail vein injection of DPBS at 0 hours, then an i.p. injection of DPBS at 3 hours. At the same time points, a second group received DPBS i.v. followed by gentamicin i.p.; a third group received 1 mg/kg LPS i.v., followed by DPBS i.p.; the fourth group received LPS i.v. and, 3 hours later, gentamicin i.p. Gentamicin was administered at a dose of 300 mg/kg. At 6 hours, all mice were sacrificed, and both cochleae plus a blood sample collected. Cochleae from 10 mice were used for ELISA protein quantification (4 cochleae/sample; N=5); while cochleae from 6 mice were used for mRNA extraction and real-time quantitative RT-PCR (qRT-PCR; 4 cochleae/sample; N=3). (B) 24 hour. Sixteen mice per group, with two groups (1 mg/kg LPS, or vehicle control DPBS) per mouse strain C57B/l6, C3H/HeOuJ (strain control) and C3H/HeJ (TLR4-hyporesponsive). All mice received an i.v. tail vein injection of DPBS or LPS at 0 hours. At the 24 hour time point, all mice were sacrificed, and both cochleae plus a blood sample collected. Cochleae from 12 mice per group (6 cochleae/sample; N=4) were used for ELISA protein quantification; while cochleae from 4 mice per group (2 cochleae/sample; N=4) were used for RNA extraction and real-time qRT-PCR.

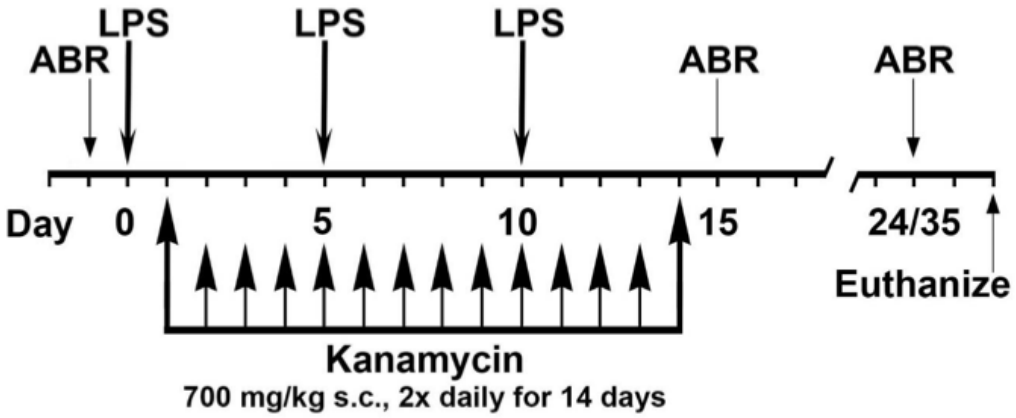

Fig. 2-S17. Chronic LPS–induced endotoxemia and kanamycin ototoxicity protocol. For toxicity studies, mice were divided into 4 groups, (i) DPBS only; (ii) LPS only; (iii) kanamycin only and (iv) LPS+kanamycin. Mice received 700 mg/kg kanamycin (or DPBS) subcutaneously twice daily for consecutive 14 days. Auditory brainstem responses (ABRs) to pure tones were obtained prior to LPS and kanamycin dosing, and also 1, 10 and 21 days after cessation of kanamycin dosing to determine any threshold shifts following LPS and/or kanamycin administration compared to age-matched controls (i.e., DPBS- or LPS-only groups). Mice received 1 mg/kg LPS (or DPBS) 1 day prior to kanamycin treatment, and on the fifth and tenth day during kanamycin treatment (2 additional injections).

Table 2-S1. Number of mice in each condition for Figs. 1 and 2A and fig. S1.

* GTTR was i.p. injected 24 hours after i.v. injection of LPS or DPBS.

LPS dose (mg/kg)	*GTTR *i.p.*		Died	Total
	1 hour	3 hour		
0	12	9	-	21
0.1	4	5	-	9
1.0	6	6	-	12
2.5	5	6	1	12
10	6	6	5	17
Total	33	32	6	71

Table 2-S2. Probability of significant difference in GTTR serum concentrations for Fig. 2A.

Serum levels of GTTR were significantly elevated in 2.5 and 10 mg/kg LPS-treated mice compared to DPBS-treated controls (0 mg/ml LPS). Serum levels of GTTR in the 2.5 mg/kg LPS group were significantly higher than 0.1 and 1 mg/kg groups both at 1 hour and 3 hour time points (Mann-Whitney U test).

LPS	1 hour				3 hour			
(mg/kg)	0.1	1	2.5	10	0.1	1	2.5	10
0	0.19	0.24	0.006	0.002	0.104	0.261	<0.001	0.013
0.1		0.7	0.046	0.087		0.073	0.006	0.268
1			0.042	0.053			0.006	0.028
2.5				0.58				0.81

Table 2-S3. Probability of a significant difference in threshold shifts 1 day after chronic LPS–induced endotoxemia with or without kanamycin treatment.

One day following chronic exposure to LPS±kanamycin (see fig. S17), ABR threshold shifts from baseline were obtained (fig. S10A). Threshold shifts for DPBS-only mice (N=4) were not different from LPS-treated mice (N=5). Kanamycin alone (N=5) induced significant threshold shifts at 16, 24 and 32 kHz compared to DPBS- and LPS-treated mice. Mice that received LPS+kanamycin (N=6) had significant threshold shifts at 12, 16, 24 and 32 kHz frequencies compared to DPBS- and LPS-treated mice. Mice receiving LPS+kanamycin did not have significant threshold shifts at any frequency compared to kanamycin-treated mice. *P<0.05, **P<0.01; ***P<0.001; 2-way ANOVA with Bonferroni post-hoc tests. Statistical analyses correspond to data in figs. S9, S10 and S11A.

	DPBS	LPS	Kanamycin
4 kHz			
LPS	-		
Kanamycin	-	-	
LPS+kanamycin	-	-	-
8 kHz			
LPS	-		
Kanamycin	-	-	
LPS+kanamycin	-	-	-
12 kHz			
LPS	-		
Kanamycin	-	-	
LPS+kanamycin	*	**	-
16 kHz			
LPS	-		
Kanamycin	*	*	
LPS+kanamycin	***	***	-
24 kHz			
LPS	-		
Kanamycin	***	**	
LPS+kanamycin	***	***	-
32 kHz			
LPS	-		
Kanamycin	***	***	
LPS+kanamycin	***	***	-

Table 2-S4. Probability of a significant difference in threshold shifts 1.5 weeks after chronic LPS–induced endotoxemia with or without kanamycin treatment.

One and a half weeks following chronic exposure to LPS±kanamycin (see fig. S13), ABR threshold shifts from baseline were obtained (fig. S10B). Threshold shifts for DPBS-only mice (N=4) were not different from LPS-treated mice (N=5). Kanamycin alone (N=5) induced negligible threshold shifts compared to DPBS- and LPS-treated mice. Mice that received LPS+kanamycin (N=6) had significant threshold shifts at 4, 12, 16, 24 and 32 kHz frequencies compared to DPBS-treated mice, and at 4, 8, 12, 16, 24 and 32 kHz compared to LPS-treated mice. Mice receiving LPS+kanamycin also had significant threshold shifts at 16, 24 and 32 kHz compared to kanamycin-treated mice. *P<0.05, **P<0.01; ***P<0.001; 2-way ANOVA with Bonferroni post-hoc tests. Statistical analyses correspond to data in figs. S9, S10 and S11B.

	DPBS	LPS	Kanamycin
4 kHz			
LPS	-		
Kanamycin	-	-	
LPS+kanamycin	*	***	-
8 kHz			
LPS	-		
Kanamycin	-	-	
LPS+kanamycin	-	**	-
12 kHz			
LPS	-		
Kanamycin	-	-	
LPS+kanamycin	***	***	**
16 kHz			
LPS	-		
Kanamycin	-	-	
LPS+kanamycin	***	***	***
24 kHz			
LPS	-		
Kanamycin	-	-	
LPS+kanamycin	***	***	***
32 kHz			
LPS	-		
Kanamycin	-	-	
LPS+kanamycin	***	***	***

Table 2-S5. Probability of significant difference in threshold shifts 3 weeks after chronic LPS–induced endotoxemia with or without kanamycin treatment.

Three weeks after chronic LPS exposure (3x 1 mg/kg LPS i.v., 5 days apart) ±kanamycin (700 mg/kg, 2x daily for 14 days, see fig. S17), ABR threshold shifts from baseline were determined (Fig. 7C, and fig. S11C). Threshold shifts for DPBS-only mice (N=4) were not different from LPS-treated mice (N=5). Kanamycin alone (N=5) induced a significant PTS at only 32 kHz compared to LPS- and DPBS-treated mice. Mice that received LPS+kanamycin (N=6) had significant PTS at 16, 24 and 32 kHz compared to kanamycin-only, as well as DPBS-only and LPS-only mice. Mice receiving LPS+kanamycin also significant PTS at 12 kHz compared to DPBS- and LPS-only mice, as well as LPS-only mice at 8 kHz. *P<0.05, **P<0.01; 2-way ANOVA with Bonferroni post-hoc tests. Statistical analyses correspond to data presented in Fig. 7A,B, and figs. S9, S10 and. S11C.

	DPBS	LPS	Kanamycin
4 kHz			
LPS	-		
Kanamycin	-	-	
LPS+kanamycin	-	-	-
8 kHz			
LPS	-		
Kanamycin	-	-	
LPS+kanamycin	-	*	-
12 kHz			
LPS	-		
Kanamycin	-	-	
LPS+kanamycin	*	**	-
16 kHz			
LPS	-		
Kanamycin	-	-	
LPS+kanamycin	**	**	**
24 kHz			
LPS	-		
Kanamycin	-	-	
LPS+kanamycin	**	**	**
32 kHz			
LPS	-		
Kanamycin	**	**	
LPS+kanamycin	**	**	*

Table 2-S6. Probability of a significant difference in threshold shifts immediately after chronic LPS–induced endotoxemia with or without kanamycin treatment.
Immediately following chronic exposure to LPS±kanamycin (see fig. S17), ABR threshold shifts from baseline were obtained (fig. S10D). ABR threshold shifts for the DPBS-only mice (N=5) were not different from LPS-treated mice (N=6). Kanamycin alone (N=5) induced significant threshold shifts at 4, 24 and 32 kHz compared to DPBS-treated mice, and at 24 and 32 kHz compared to LPS-treated mice. Mice that received LPS+kanamycin (N=7) had significant threshold shifts at 16, 24 and 32 kHz frequencies compared to DPBS-only mice; with significant threshold shifts at 24 and 32 kHz compared to LPS-only mice. Mice receiving LPS+kanamycin did not have significant threshold shifts at any frequency compared to kanamycin-treated mice. *P<0.05, **P<0.01; ***P<0.001; 2-way ANOVA with Bonferroni post-hoc tests. Statistical analyses correspond to data presented in fig. S11D-F and S12.

	DPBS	LPS	Kanamycin
4 kHz			
LPS	-		
Kanamycin	**	-	
LPS+kanamycin	**	-	-
8 kHz			
LPS	-		
Kanamycin	-	-	
LPS+kanamycin	-	-	-
12 kHz			
LPS	-		
Kanamycin	-	-	
LPS+kanamycin	-	-	-
16 kHz			
LPS	-		
Kanamycin	-	-	
LPS+kanamycin	**	-	-
24 kHz			
LPS	-		
Kanamycin	***	***	
LPS+kanamycin	***	***	-
32 kHz			
LPS	-		
Kanamycin	**	***	
LPS+kanamycin	-	***	-

Table 2-S7. Probability of a significant difference in OHC survival 3 weeks after chronic LPS–induced endotoxemia with or without kanamycin treatment.

Three weeks following chronic exposure to LPS (±kanamycin), cytocochleograms of OHCs were obtained (Fig. 7B). No significant differences in OHC survival occurred between DPBS- , LPS-, kanamycin- and LPS+kanamycin-treated groups in the more apical, lower frequency (4-8 kHz) regions of the mouse cochlea. Substantial losses of OHCs occurred in higher frequency (8-64 kHz) regions of LPS+kanamycin-treated cochleae that were significantly different from DPBS-, LPS- and kanamycin-treated groups. LPS+kanamycin also induced significant IHC loss only in the 16-32 kHz region compared to DPBS-, LPS-, and kanamycin-treated mice ($P<0.05$, $P<0.05$ and $P<0.01$, respectively). 2-way ANOVA using Tukey post-hoc tests; **$P<0.01$, ****$P<0.0001$. Statistical analyses correspond to cytocochleogram data presented in Fig. 7B.

	DPBS	LPS	Kanamycin
4-8 kHz			
LPS	-		
Kanamycin	-	-	
LPS+kanamycin	-	-	-
8-16 kHz			
LPS	-		
Kanamycin	-	-	
LPS+kanamycin	**	**	**
16-32 kHz			
LPS	-		
Kanamycin	-	-	
LPS+kanamycin	****	****	****
32-64 kHz			
LPS	-		
Kanamycin	-	-	
LPS+kanamycin	****	****	****

Table 2-S8. Probability of a significant difference in OHC survival immediately after chronic LPS–induced endotoxemia with or without kanamycin treatment.
Immediately following chronic exposure to LPS (±kanamycin), cytocochleograms of OHCs were obtained (fig. S11E). No significant differences in OHC survival occurred between DPBS-, LPS-, kanamycin- and LPS+kanamycin-treated groups in apical, lower frequency (4-16 kHz) regions of the cochlea. Substantial loss of OHCs occurred in basal high frequency regions of LPS+kanamycin-treated cochleae that were significantly different from DPBS-, LPS- and kanamycin-treated groups. LPS+kanamycin also induced significant IHC loss only in at 32 kHz compared to DPBS- and LPS-treated mice, but not at any other frequency or with kanamycin treated mice ($P<0.01$ and $P<0.05$, respectively). 2-way ANOVA with Tukey post-hoc tests; ***$P<0.001$, ****$P<0.0001$. Statistical analyses correspond to cytocochleogram data in fig. S11E.

	DPBS	LPS	Kanamycin
4-8 kHz			
LPS	-		
Kanamycin	-	-	
LPS+kanamycin	-	-	-
8-16 kHz			
LPS	-		
Kanamycin	-	-	
LPS+kanamycin	-	-	-
16-32 kHz			
LPS	-		
Kanamycin	-	-	
LPS+kanamycin	***	****	***
32-64 kHz			
LPS	-		
Kanamycin	-	-	
LPS+kanamycin	***	****	***

Table 2-S9. Probability of decreasing OHC survival 3 weeks after chronic LPS–induced endotoxemia with or without kanamycin treatment compared to immediately after treatment.

The mean OHC survival (±s.d.) per frequency region immediately after, and 3 weeks following, chronic exposure to LPS±kanamycin (see cytocochleograms in Fig. 7B, and fig. S11E) are shown. Three weeks after treatment, significantly greater OHC loss was observed in LPS+kanamycin treated mice in 8-64 kHz regions of the cochlea compared to immediately after chronic treatment. Three weeks after kanamycin treatment, significantly greater hair cell loss was only observed in the 16-32 kHz region. LPS- and DPBS-treated mice also had significant OHC loss in the 32-64 kHz region compared to 3 weeks earlier. LPS also induced significant IHC loss only in the 32-64 kHz region ($P<0.05$) compared to all other groups. All analyses done using Student's t- test; *$P<0.05$, **$P<0.01$; ****$P<0.0001$. Statistical analyses correspond to cytocochleogram data in Fig. 7B and fig. S11E.

Percent OHC survival/region	Recovery period		T-test between groups
	0 days	3 weeks	
4-8 kHz			
DPBS	97.0 (±5.2)	97.6 (±3.2)	n.s.
LPS	98.1 (±2.7)	94.8 (±9.5)	**
Kanamycin	97.9 (±2.8)	98.1 (±2.7)	n.s.
LPS+kanamycin	96.7 (±4.5)	96.7 (±4.4)	n.s.
8-16 kHz			
DPBS	98.8 (±1.9)	99.7 (±1.2)	*
LPS	99.2 (±1.6)	99.1 (±2.2)	n.s.
Kanamycin	99.5 (±1.4)	99.6 (±1.4)	n.s.
LPS+kanamycin	94.6 (±14.5)	87.1 (±26.7)	*
16-32 kHz			
DPBS	99.5 (±1.6)	96.2 (±12.9)	*
LPS	99.5 (±1.3)	99.4 (±1.8)	n.s.
Kanamycin	99.3 (±1.73)	96.0 (±13.0)	*
LPS+kanamycin	93.0 (±18.7)	63.6 (35.8)	****
32-64 kHz			
DPBS	98.0 (±3.7)	89.2 (±19.6)	****
LPS	97.3 (±6.6)	92.7 (±12.4)	****
Kanamycin	90.9 (±16.4)	92.6 (±14.7)	n.s.
LPS+kanamycin	86.8 (±25.9)	66.4 (31.7)	****

3 – Manuscript #2

Toll-like Receptor 4 Signaling and Downstream Neutrophil Activity Mediate Endotoxemia-Enhanced Blood-Labyrinth Barrier Trafficking

Authors: Zachary D. Urdang[1,2], Jessica L. Bills[1]†, David Y. Cahana[1]†, Leslie M. Muldoon[1], Edward A. Neuwelt[1]

Affiliations:

[1]Oregon Health and Science University, Blood-brain barrier research program.

[2]Oregon Health and Science University, MD/PhD program and Neuroscience Graduate Program.

†Equal contributors

Chapter 3 is modified from the paper submitted to Otology & Neurotology.

Contributions: Zachary conceptualized designed and performed all experiments and analyses. Zachary wrote the manuscript.

Abstract

Hypothesis: Both toll-like receptor 4 (TLR4) and downstream neutrophil activity are required for endotoxemia-enhanced blood-labyrinth barrier (BLB) trafficking.

Background: Aminoglycoside and cisplatin are valuable clinical therapies; however, these drugs often cause life-long hearing loss. Endotoxemia enhances the ototoxicity of aminoglycosides and cisplatin in a TLR4 dependent mechanism for which downstream pro-inflammatory signaling orchestrates effector immune cells including neutrophils. Neutrophil-mediated vascular injury can enhance molecular trafficking across endothelial barriers and may contribute to endotoxemia-enhanced drug-induced ototoxicity.

Methods: Lipopolysaccharide (LPS) hypo-responsive *Tlr4*-KO mice and congenitally neutropenic granulocyte colony stimulating factor (G-CSF) *G-csf*-KO mice were studied to investigate the relative contributions of TLR4 signaling and downstream neutrophil activity to endotoxemia-enhanced BLB trafficking. C57BL/6 wild-type mice were used as a positive control. Mice were treated with LPS and 24 hours later cochleas were analyzed for gene transcription of innate inflammatory cytokine/chemokine signaling molecules, neutrophil recruitment, and vascular trafficking of the paracellular tracer biocytin-TMR.

Results: Endotoxemia enhances cochlear transcription of innate pro-inflammatory cytokines/chemokines in endotoxemic C57BL/6 and *G-csf*-KO, but not in *Tlr4*-KO mice. More neutrophils were recruited to endotoxemic C57BL/6 cochleas compared to both *Tlr4*-KO and *G-csf*-KO cochleas. Endotoxemia enhances BLB trafficking of biocytin-TMR in endotoxemic C57BL/6 cochleas and this was attenuated in both *Tlr4*-KO and *G-csf*-KO mice.

Conclusion: Together these results suggest that *Tlr4*-KO mediated innate immunity cytokine/chemokine signaling alone is not sufficient for endotoxemia-enhanced trafficking of biocytin-TMR and that downstream neutrophil activity is required to enhance BLB trafficking. Clinically, targeting neutrophilic inflammation could protect hearing during aminoglycoside, cisplatin, or other ototoxic drug therapies.

3.1 – Introduction

Drug-induced ototoxicity imposes significant functional and socioeconomic challenges for individuals who experience lifelong hearing loss as sequelae of treatment for conditions such as sepsis, especially as neonates (*384, 385*); multi-drug resistant tuberculosis, particularly in developing countries (*386, 387*); lung infections in the setting of cystic fibrosis (*388, 389*); and cancers treated with platinum-based chemotherapies (*390, 391*). Indeed, the very conditions these drugs are used to treat may actually enhance the risk of sustaining life-long hearing loss as a side effect of treatment. This clinical paradox poses a difficult situation for the treating physician. While these therapies are effective treatments, life-long hearing loss can significantly adversely affect long-term quality of life. These adverse effects can be of particular challenge in neonatal/pediatric patients, for whom early hearing loss can delay language acquisition and subsequent acquisition of education and social attainment (*392*).

Endotoxemia, as a model for gram-negative sepsis, enhances the risk and severity of drug-induced hearing loss in mice after treatment with ototoxic drugs such as cisplatin (*393*), aminoglycosides such as kanamycin (*394*), and synergistic combination of kanamycin/furosemide (*395*). In neonatal intensive care unit patients, meeting criteria for systemic inflammatory response syndrome (SIRS) (*39, 40*) (**Table S1**) in the setting of suspected bacterial sepsis increases the risk-ratio of sustaining life-long hearing loss after empirical gentamicin therapy (*396*). A previous study demonstrated that endotoxemia-enhanced aminoglycoside ototoxicity is tied to increased aminoglycoside trafficking at the BLB. Furthermore, endotoxemia-enhanced BLB trafficking is mechanistically tied to TLR4 activity as C3H/HeJ mice, with a hypomorphic *Tlr4* gene variant, did not exhibit enhanced BLB trafficking during endotoxemia (*394*). TLR4 is a potent immune sensor, promoting innate inflammation in response to pathogen and damage associated molecular patterns (PAMPs and DAMPS) such as LPS, which is a commonly used experimental TLR4 agonist. Binding of LPS to TLR4 induces release and production of innate pro-inflammatory signals, which orchestrate downstream inflammatory effector cell activity (*78, 397*). Thus, immune cells may mechanistically contribute to endotoxemia-enhanced BLB trafficking.

Neutrophils are the most abundant white blood cell and are first responders to innate inflammatory cues, including SIRS and LPS-endotoxemia. Neutrophil-mediated vascular injury is a long appreciated pathological vascular change that occurs during sepsis and is a result of intravascular neutrophil release of neutrophil extracellular traps (NETs or NETosis) (*57, 398, 399*). Because neutrophil-mediated vascular injury is elicited by neutrophil activity downstream of TLR4, we tested the hypothesis that knockdown of neutrophil numbers would rescue endotoxemia-enhanced BLB trafficking, similar to that observed in *Tlr4*-KO hypomorphic C3H/HeJ mice (*394*). To test this hypothesis, we investigated BLB pathophysiology and the relative contributions of TLR4 signaling and downstream neutrophil activity during endotoxemia in *Tlr4*-KO mice (reduced *Tlr4* signaling) and *G-csf*-KO neutropenic mice (model for severe congenital neutropenia). Our results demonstrate that both TLR4 mediated cytokine/chemokine signaling and downstream neutrophil activity are both required for endotoxemia-enhanced BLB trafficking.

3.2 – Materials and Methods

3.2.1 - Experimental animals

All protocols and procedures were approved by Oregon Health and Science University's (OHSU) intuitional animal care and use committee (IACUC IP00000843). Animals were bred in-house by OHSU staff. C57BL/6 and *Tlr4*-KO founder mice were procured from Jackson Lab. The *G-csf*-KO founder mice were generously provided by Dr. Jason Shohet of Baylor Medical School. Both male and female mice were used at ages 16-20 weeks with weights ranging from 18-30 g. Animals were housed in gender-separated boxes in groups of between 3-6 mice. Animals were allowed free access to food and water and kept under a twelve-hour light/dark cycle.

3.2.2 - Lipopolysaccharide solution preparation

LPS (Millipore-Sigma, Cat# L3012) was dissolved in 0.05% endotoxin-free bovine serum albumin (BSA) (Equitech Bio, Cat# BAH70-0050) in phosphate-buffered saline (PBS) at a concentration of 2.0 mg/ml. LPS and vehicle solutions were filter-sterilized into sterile vacuum tubes using a 0.05 μm polypropylene filter and kept on ice during use on the same day.

3.2.3 - Endotoxemia induction and tissue collections

Mice were lightly anesthetized using ketamine/xylazine "half-strength mouse cocktail" (100 mg/kg ketamine, 5 mg/kg xylazine in saline; 5 μl/g *i.p.*). Once adequate sedation was achieved, animals were treated with sterile LPS (2 mg/ml; 5 μl/g *i.v.*) or vehicle 0.5% endotoxin-free BSA in PBS (5 μl/g *i.v.)* solutions. Animals were allowed to recover on a heat pad before being returned to the housing facility. Twenty-four hours later mice were re-anesthetized with "full-strength mouse cocktail" (100 mg/kg ketamine, 10 mg/kg xylazine in saline; 5 μl/g *i.p.*) and once adequate sedation had been reached, mice were perfused with 10 ml room-temperature PBS via the left ventricle.

3.2.4 - qRT-PCR analysis

Temporal bones from PBS-perfused mice were placed in RNA preservative (RNAlater, Millipore-Sigma, Cat# R0901) and their cochleas dissected. Excess RNAlater was removed and tissues were pooled into samples of four cochleas from two mice, flash frozen in liquid nitrogen, and stored at -80 °C. RNA was isolated from samples of pooled cochleas (four cochleas from two mice) using an RNeasy kit and concentrated via Speed Vac on low heat. RNA concentration and quality was determined using a NanoDrop 2000 series spectrophotometer (ThermoFischer Scientific, ND2000). RNA from each sample (150 ng) was utilized for reverse-transcription cDNA synthesis via TaqMan RT-reagents (Applied Biosystems, Cat# N8080234). 5ng of cDNA was used for each TaqMan primer/probe qRT-PCR reaction in a 96-well format using TaqMan Gene Expression Master Mix (Applied Biosystems, Cat# 4369016). Samples were run in duplicate on a AB7300 (Applied Biosystems) plate reader over 60 PCR cycles. Cycle threshold (Ct) values were exported to Excel and delta-delta Ct (ddCt) analysis was hand-calculated using *18S* as the housekeeping gene for calculation of delta Ct (dCt). Duplicate wells that did not agree within 2 Ct were excluded from analysis.

3.2.5 - Biocytin-TMR vascular tracer treatment

Biocytin-TMR (Setareh Biotech, Cat# 6662) in PBS (1% (m/m), 5 ul/g, *i.v.*) was administered to mice 23.25 hours after LPS treatment and allowed to circulate for 45 minutes prior to euthanasia.

3.2.6 - Cochlear immunohistochemistry and Biocytin-TMR counter labeling

Following intracardiac perfusion of 10 ml room-temperature PBS, mice were perfused with 10 ml of room-temperature 4% paraformaldehyde (PFA) in PBS. Cochleas were dissected and fixed for 24 hours in 4% PFA. Cochleas were decalcified in 10% EDTA in Tris-buffered saline pH 7.4 for 7 days, then sectioned at 50 μm with a vibratome (*400*). Tissues were washed in PBS, then blocked with 0.5% Triton X-100 and 5% donkey serum in PBS for 1 hour, followed by incubation with primary antibody in

blocking solution overnight at 4 °C (Ly6G, 1A8 clone BioLegend cat# ab154885; 2.5 μg/ml). Sections were washed 3x in PBS, then incubated with secondary antibody in blocking solution overnight (Donkey Anti-Rat IgG H&L (Alexa Fluor 647) preadsorbed; abcam cat# ab150155, 0.5 μg/ml). Sections were washed 3x1 hour in PBS followed by treatment with Streptavidin Alexa Fluor 568 (ThermoFisher, Cat# S11226) at 10 μg/ml in PBS with 0.5% Triton X-100, 0.1 mM $CaCl_2$, and 10% donkey serum for 1 hour. Tissues were washed 2x1 hour in PBS with 0.2% Triton X-100 and incubated overnight with Hoescht (1 ug/ml) and Lycopersicon Esculentum lectin-488 (Vector cat# DL-1174; 200 μg/ml) in PBS. Next, sections were washed 2x1 hour with 0.2% Triton X-100 in PBS, washed 1x1 hour with PBS, post-fixed in 4% PFA for 15 minutes then washed 3x20 minutes in PBS, then mounted on slides with Vectashield mounting medium.

3.2.7 - Confocal microscopy

Four-color z-stacks of cochlear sections were collected at 20x magnification on a Zeiss LSM 880 laser-scanning confocal microscope with an inverted microscope base and Airyscan capabilities for faster image acquisition. Three cochlear sections were imaged for each individual mouse. The microscope laser power and detector settings were calibrated to the brightest slide

3.2.8 - Biocytin-TMR vascular tracer quantification

Confocal image stacks were analyzed using Fiji. Red channel z-stacks of cochlear sections were combined into maximum intensity projections and regions of interest were hand drawn (Fig. 4a). Mean pixel intensities for each region of interest were averaged over the three cochlear sections for each animal; this value was used for cohort-level statistical analysis.

3.2.9 - Statistics

Graphpad Prism v7.0a was used to calculate statistical tests as indicated in each figure legend. For ratiometric analyses (**Fig. 3-4** and **Fig 3-S1**) 95% confidence intervals were hand-calculated in Excel and graphs plotted using Prism.

3.3 – Results

3.3.1 -Tlr4-KO but not G-csf-KO dampens cochlear innate immune marker transcription

Tlr4 mutant C3H/HeJ mice demonstrate reduction in endotoxemia-enhanced aminoglycoside uptake and concomitant reduced innate immune marker expression (*394*). Because neutrophil activity is downstream of *Tlr4* activity, we assessed cochlear transcription of innate immune cytokines and chemokines in *Tlr4-KO* and *G-csf*-KO mice. Mice were treated with high dose LPS (10 mg/kg *i.v.)* to model a high-morbidity/mortality gram-negative sepsis situation indicating aminoglycoside therapy. The LD50 of LPS in mice is somewhere between 12.5-60 mg/kg depending on dosing, LPS-type/purity, and route of administration (*47, 401-403*). Additionally, high dose LPS was chosen to model clinical situations where a patient is most at risk for experiencing long term aminoglycoside side effects, such as lifelong hearing loss.

After twenty-four hours of endotoxemia, cochleas were collected for qRT-PCR analysis of innate immune system pro-inflammatory cytokine and chemokine transcripts (**Fig. 3-1**, **Table 3-S2**). Wild-type C57BL/6 mice served as the positive control, as endotoxemia induces cochlear transcription of innate immune markers (*394, 404*). Indeed, endotoxemia upregulated the transcription of a majority of these innate immunity markers, as demonstrated by decreased dCt values for most genes analyzed with the exception of *Il-10* and *Ccl3* (**Fig. 3-2A**).

Neutropenic *G-csf*-KO mice, which have wild-type *Tlr4*, demonstrated a qualitatively similar transcript profile as compared to wild-type mice. All genes analyzed were upregulated, with the exceptions of *Il-10, Selp, and Ccl5* (**Fig. 3-2B**). By contrast, transcription of pro-inflammatory markers in *Tlr4*-KO mice were not upregulated with the exception of a very small, yet statistically significant, dCt difference in *Icam1* (Fig 3-2C).

Fold changes in transcript level were calculated using the ddCt method (Fig. 3-S1A). These fold change values are artificially inflated because cochlear homogenates from vehicle-treated animals had baseline transcription levels below the lower limit of

detection (Ct > 60). Baseline gene transcription was similar between strains. Two exceptions were *Cxcl2* upregulation in *G-csf*-KO mice and *Selp* upregulation in both *Tlr4*-KO and *G-csf*-KO strains.

3.3.2 - Endotoxemia recruits neutrophils to the BLB of wild-type but not Tlr4-KO or G-csf-KO mice

TLR4-induced pro-inflammatory cytokine/chemokine activity promotes innate immune cell activity and associated neutrophil-mediated vascular injury. Because of this we used an antibody against the neutrophil-specific marker Ly6G to investigate the presence of neutrophils in cochlear sections of C57BL/6, *Tlr4*-KO, and *G-csf*-KO mice treated with 10 mg/kg LPS or vehicle. Because *Tlr4*-KO mice do not express LPS-induced pro-inflammatory genes (**Fig. 3-1C**), we hypothesized that few neutrophils would be recruited to carry out LPS-mediated cochlear inflammation. *G-csf*-KO mice are neutropenic and the sparse neutrophils in these animals are anergic and underdeveloped (*405*); we therefore hypothesized that few neutrophils would be recruited to the cochleas of these mice.

More neutrophils appeared in endotoxemic C57BL/6 wild-type mice (**Fig. 3-3A-B**, **3H**) compared to vehicle treated mice (**Fig. 3-3C**). This observation of more neutrophils in wild-type cochleas was in contrast to the small number of neutrophils in cochlear sections of both endotoxemic and vehicle-treated *Tlr4*-KO mice (**Fig. 3-3D-E**), which exhibit diminished pro-inflammatory signaling, and *G-csf*-KO mice (**Fig. 3-3F-G**) which have greatly reduced numbers of neutrophils. Given the attenuated pro-inflammatory gene expression profile in *Tlr4*-KO and chronic neutropenia in *G-csf*-KO mice this result makes sense.

3.3.3 - Endotoxemia enhances BLB biocytin-TMR trafficking in C57BL/6 mice and is rescued in Tlr4-KO and G-csf-KO mice

Endotoxemia and local LPS treatment, as well as other innate immune reaction provoking stimuli, compromise endothelial barriers, including the blood-brain barrier, the blood-retinal barrier, and the BLB (*406, 407*) which could be due to neutrophil-mediated

vascular injury. Analogously, neutropenia decreases drug uptake in the lungs of pneumonitic mice (*408*). Since *Tlr4*-KO and *G-csf*-KO mice express differential patterns of innate immune pro-inflammatory markers (**Fig.3-2**) and neutrophil recruitment (**Fig. 3-3**), we tested the hypothesis that both *Tlr4* and neutrophil activity are required to enhance vascular trafficking at the BLB. To test this hypothesis, we treated endotoxemic and vehicle-treated C57BL/6, *Tlr4-KO*, and *G-csf*-KO mice with the paracellular vascular tracer biocytin-TMR (*148*) and quantified parenchymal uptake via confocal microscopy (**Fig. 3-4**, **Fig. 3-S2**).

Endotoxemia increased the normalized biocytin-TMR fluorescence intensity ratios in all ROIs (**Fig. 3-4A**) in C57BL/6 mice, but not in *Tlr4*-KO or *G-csf*-KO mice with the exception of the spiral ligament regions in the *Tlr4*-KO strain (**Fig. 3-4B**). Analysis of the absolute fluorescence levels also demonstrated that biocytin-TMR uptake was increased in cochleas of C57BL/6 mice (**Fig. 3-4C-D**, **Fig. 3-S2A**) but not in *Tlr4*-KO mice (**Fig. 3-4E-F**, **Fig. 3-S2B**) or *G-csf*-KO mice (**Fig. 3-4G-H**, **Fig. 3-S2C**), again with the exception of the spiral limbus region in *G-csf*-KO mice (**Fig. 3-S2C**). The baseline fluorescence intensity was also compared between strains. C57BL/6 and *Tlr4*-KO strains had comparable baseline biocytin-TMR uptake, while G-CSF-KO mice demonstrated significantly more baseline uptake of biocytin-TMR in all anatomical ROIs (**Fig. 3-S2D**).

3.4 – Discussion

We set out to determine if *Tlr4*-KO mediated cytokine/chemokine signaling is sufficient or whether downstream neutrophil activity is also required for endotoxemia-enhanced BLB trafficking. Endotoxemic neutropenic *G-csf*-KO mice exhibit robust enhancement of cochlear pro-inflammatory innate immune gene transcription similar to wild-type C57BL/6 mice (*393, 404*). This response was greatly attenuated in LPS-hyporesponsive *Tlr4*-KO mice, similar to observations with the *Tlr4* hypomorphic C3H/HeJ mouse strain (*394*). C57BL/6 and *G-csf*-KO mice both harbor wild-type *Tlr4* genes whereas *Tlr4*-KO mice do not. Therefore, attenuated cyto/chemokine signaling in *Tlr4*-KO mice was not surprising. Still, the cochlear pro-inflammatory marker response to endotoxemia was not completely null in *Tlr4*-KO mice. Although TLR4 is the canonical and most potent LPS sensor, there is evidence for other LPS sensors. For example, the non-canonical inflammasome is activated by intracellular LPS-mediated dimerization of caspase-11 (*403*); in addition, there is controversial evidence that LPS activates TLR2 (*409-411*).

Innate immune pro-inflammatory markers selected for the qRT-PCR panel are endothelial-leukocyte adhesion molecules, cytokines, and chemokines, which orchestrate downstream immune effector cells such as neutrophils and monocytes/macrophages (**Table S2**) causing neutrophil-mediated vascular injury. Therefore, we wanted to assess the numbers of Ly6G+ neutrophils in cochlear sections of endotoxemic vs vehicle-treated mice in C57BL/6, *Tlr4*-KO, and *G-csf*-KO mice. Endotoxemic wild-type C57BL/6 mouse cochlear sections demonstrated the most Ly6G+ neutrophils. In both *Tlr4*-KO and *G-csf*-KO strains, neutrophils were rarely observed in cochlear sections of endotoxemic mice. In vehicle-treated mice, neutrophils were also very rarely observed in all three mouse strains. C57BL/6 mice with a wild-type immune system and robust transcription of innate immune chemokines/cytokines neutrophils would be expected to show an increase in neutrophil numbers and activity after LPS challenge. In *Tlr4*-KO mice with greatly dampened innate immune cytokine/chemokine signaling, neutrophils have fewer cues directing them to carry out immune functions and incur neutrophil mediated vascular injury. *G-csf*-KO mice are congenitally neutropenic and their greatly reduced

neutrophil numbers, with an immature phenotype diminishes endotoxemia-mediated neutrophil recruitment.

To assess the relative contributions of inflammatory signaling and downstream neutrophil activity endotoxemia-enhanced BLB trafficking, we quantified cochlear biocytin-TMR distribution in endotoxemic relative to vehicle-treated C57BL/6, *Tlr4*-KO, and *G-csf*-KO mice. This demonstrated enhanced biocytin-TMR trafficking in the stria vascularis, spiral ligament, and interestingly in the spiral limbus region of C57BL/6 wild-type mice. In *Tlr4*-KO mice, enhanced BLB trafficking was not significantly enhanced in either the stria vascularis or the spiral limbus region although there was very small statistically significant increase in biocytin-TMR trafficking in the spiral ligament region. In *G-csf*-KO mice, endotoxemia-enhanced trafficking of biocytin-TMR returned to baseline levels in all cochlear regions examined. *G-csf*-KO mice demonstrated significantly increased baseline cochlear uptake of biocytin-TMR. Increased baseline biocytin-TMR uptake in G-csf-KO mice could be due to the difference in genetic background of this strain compared to the other two which are C57 background thus we concentrated on normalized fold-change vascular tracer uptake. Another possible explanation for the difference in baseline biocytin-TMR uptake is the difference in baseline transcription levels of inflammatory markers (**Fig. 3-S1B**), and in particular *Cxcl2*. Presumably, other related pro-inflammatory markers not measured in the current study are also upregulated; enhanced baseline expression of these cytokines and chemokines could be sufficient to cause endothelial cell-independent enhanced baseline trafficking activities at the BLB in *G-csf*-KO mice.

This study was limited by the use of only one vascular tracer. Endothelial transport mechanisms other than paracellular trafficking are almost certainly involved. Our gene panel is also limited to a subset of genes that we felt are good indicators of the innate inflammatory response; however, they do not examine other aspects of an inflammatory reaction such as macrophage or adaptive immune activity. Other leukocyte markers besides Ly6G could also expand the scope of this study on cochlear leukocyte activity including macrophage and adaptive immune system cell markers

A pathophysiological hallmark of SIRS and sepsis is perturbed endothelial barrier properties causing capillary leak syndrome (*412*), for which endotoxemia is a classic

model system (*413*); neutrophil-mediated vascular injury is a significant contributor to capillary leak (*414-418*). At baseline, the primary endothelial transport mechanisms are passive diffusion, ion-channel permeation, carrier-mediated transport, and pinocytosis; paracellular BLB trafficking is not a major mechanism under physiological conditions (**Fig. 3-5A**). Within minutes to hours LPS-mediated activation of TLR4 induces cytokine/chemokine transcription (**Fig. 3-5B**) enhancing transcellular BLB trafficking in an endothelial-cell independent manner (*148*). These transcellular mechanisms include increased ion-channel permeation through channels such as TRP-channels (*97, 309*), enhanced carrier-mediated transport via molecules such as SGLT2 (*419*), and non-specific pinocytosis/transcytosis. Initial enhanced transcellular trafficking activities are believed to enhance immune globulin uptake into tissue parenchyma where they can mount an immune response (*370, 420, 421*). Concurrently, endothelial barriers increase the expression of leukocyte adhesion molecules such as P-SELECTIN (*422*) and ICAM1 (*423, 424*) promoting leukocyte adhesion, neutrophil-mediated vascular injury, and diapedesis leading to paracellular trafficking (*407, 425*) routes (hours later) not present under healthy physiological states (**Fig. 3-5C**) (*148, 422, 426*). Enhanced BLB trafficking at early time points is likely most reliant on increased transcellular trafficking mechanisms (pino/transcytosis, ion-channel, and specific transporters) with paracellular theoretically becoming more apparent at later time points after neutrophil-mediated vascular injury accumulation (**Fig. 3-5D**).

Endotoxemia diminishes the endolymphatic potential (EP) (*395*) and enhances perilymph uptake of the vascular tracer fluorescein (*425*). Less is known about endolymph uptake of vascular tracers as sampling rodent endolymph is difficult although some indirect methods suggest endolymph as an important aminoglycoside trafficking route (*427, 428*). Diminished EP suggests diminished cell-cell coupling both at BLB vessels, and the epithelial cells lining the scala-media immediately adjacent to cochlear vasculature. Furthermore, decreased EP means reduced electrogenic potential energy barrier for trafficking of polycations such as aminoglycosides into endolymph. Neutrophil granule-derived NETs contain proteases such as matrix-metalloproteinases which directly degrade tight-junction proteins (*364, 429*), and reactive oxygen species (ROS) generating enzymes non-specifically damage host-tissues (*430*). Rescue of

endotoxemia-enhanced biocytin-TMR trafficking by genetic deletion of neutrophils (*G-csf*-KO) suggests directly that knocking down neutrophil activity, and associated NET release (*431*), diminishes paracellular trafficking into cochlear parenchyma.

Pharmacologic strategies to prevent drug-induced hearing loss could require efforts to block both transcellular uptake as well as neutrophil-mediated vascular injury, blocking subsequent paracellular disruption. Transcellular strategies could include non-specific cation channel blockers expressed at the BLB if such a druggable candidate is identified, or local cochlear administration of agents that reduce pinocytosis. Interestingly, anti-inflammatory treatments (such as aspirin (*93, 432-434*)) and anti-ROS thiol-based therapies such as D-Methionine (*268, 285, 435, 436*) have demonstrated efficacy in both pre-clinical and clinical studies of sepsis (*437*), aminoglycoside and cisplatin ototoxicity (*438-442*). Because ROS-dampening thiol-based therapies work in the isolated contexts of sepsis, and ototoxic drugs, there is likely overlap in the mechanisms of each pathology. Indeed, sepsis, and aminoglycoside/cisplatin ototoxicity involve ROS. Where exactly cochlear ROS are generated is unknown. ROS could derive from leukocytes recruited by DAMPs released by necrotic cochlear cells, and/or directly from stressed cochlear cells. This study suggests that neutrophil-mediated vascular injury, which involves ROS-mediated cell damage, is an important contributor to endotoxemia-enhanced BLB trafficking.

3.5 – Conclusions

Understanding the mechanisms leading to drug-induced hearing loss may lead to either patient management strategies and/or pharmacological strategies to protect hearing during ototoxic therapies. This study suggests neutropenia may protect patients' hearing functionality. Furthermore, targeting neutrophil activity such as ROS-generating neutrophil-derived NET-associated enzymes could be a promising pharmacological strategy to ameliorate drug-induced hearing loss.

3.6 – Figures and Tables

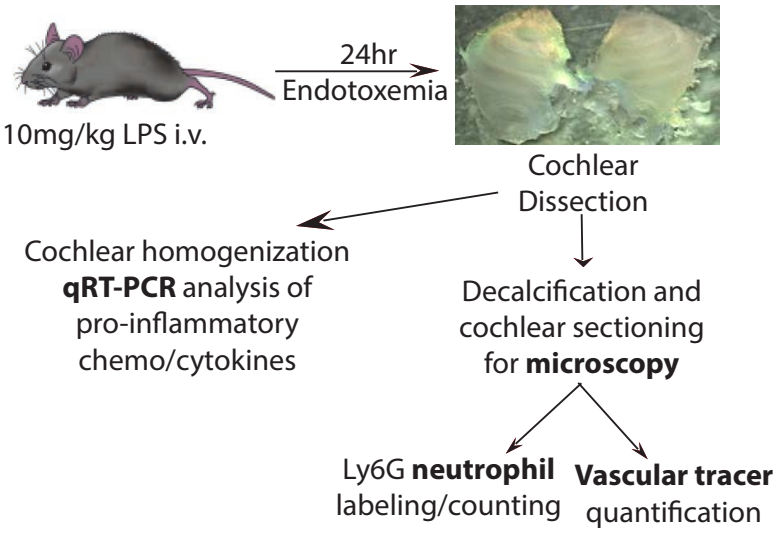

Figure 3-1. Study Design.

Mice were treated with 10mg/kg LPS *i.v.* and cochleas collected 24 hours later for qRT-PCR analysis, neutrophil counts, and vascular tracer quantification.

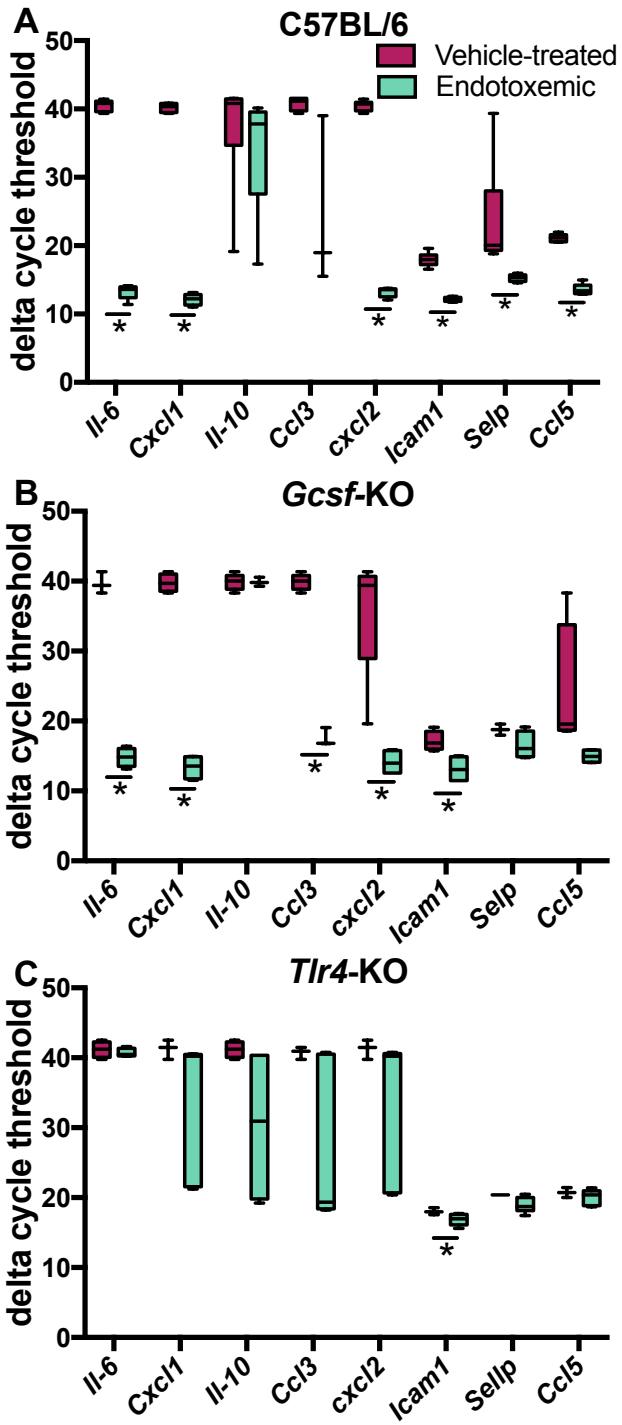

Figure 3-2. Cochlear innate immunity gene transcription in endotoxemic vs vehicle-treated C57BL/6, *Tlr4*-KO, and *Gcsf*-KO mice.

Mice were treated with 10 mg/kg LPS *i.v*. and cochleas collected 24 hours later for qRT-PCR analysis. delta cycle threshold values normalized to *18S* are presented. (**A**) dCt values for endotoxemic vs vehicle-treated wild-type C57BL/6, (**B**) LPS-hyporesponsive *Tlr4*-KO, (**C**), and neutropenic *Gcsf*-KO mice. (n=3-7 per cohort). Box and whisker plots. * indicates $p<0.05$ after student's t-test.

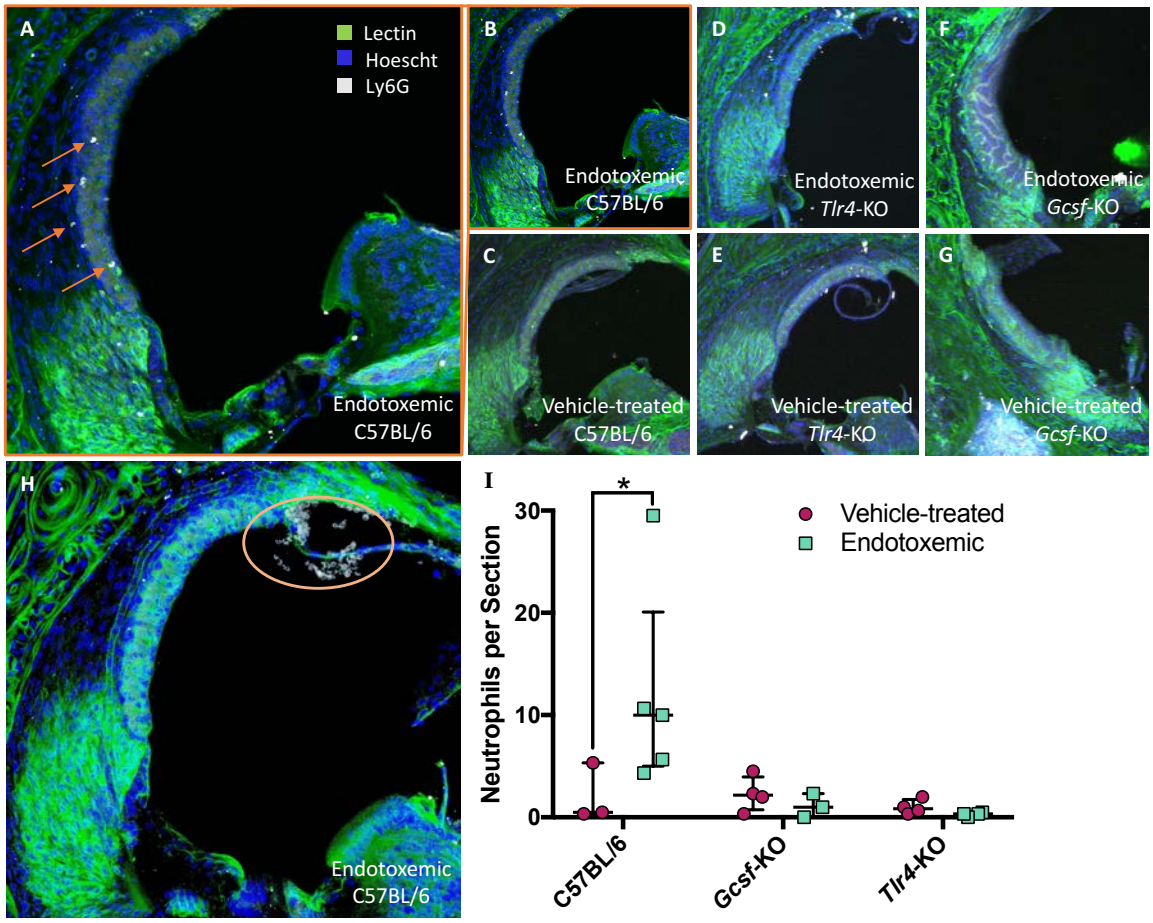

Figure 3-3. Endotoxemia recruits' neutrophils to wild-type but not *Tlr4*-KO or *Gcsf*-KO mice.

(**A-H**) Representative cochlear sections of mice treated with either 10 mg/kg LPS or vehicle and labeled with Ly6G neutrophil marker (white), a lectin to label blood vessels (green), and Hoescht for nuclei (blue); mouse strain and treatment indicated on panel. (**A**) Larger representation of panel **B**. (**H**) A severe case of cochlear neutrophilic infiltration marked with orange circle. (**I**) Quantification of cochlear neutrophils. Each data point is one individual averaged over three cochlear sections. Error bars are median with interquartile range. * indicates $p<0.05$ for one-tailed Mann-Whitney U test.

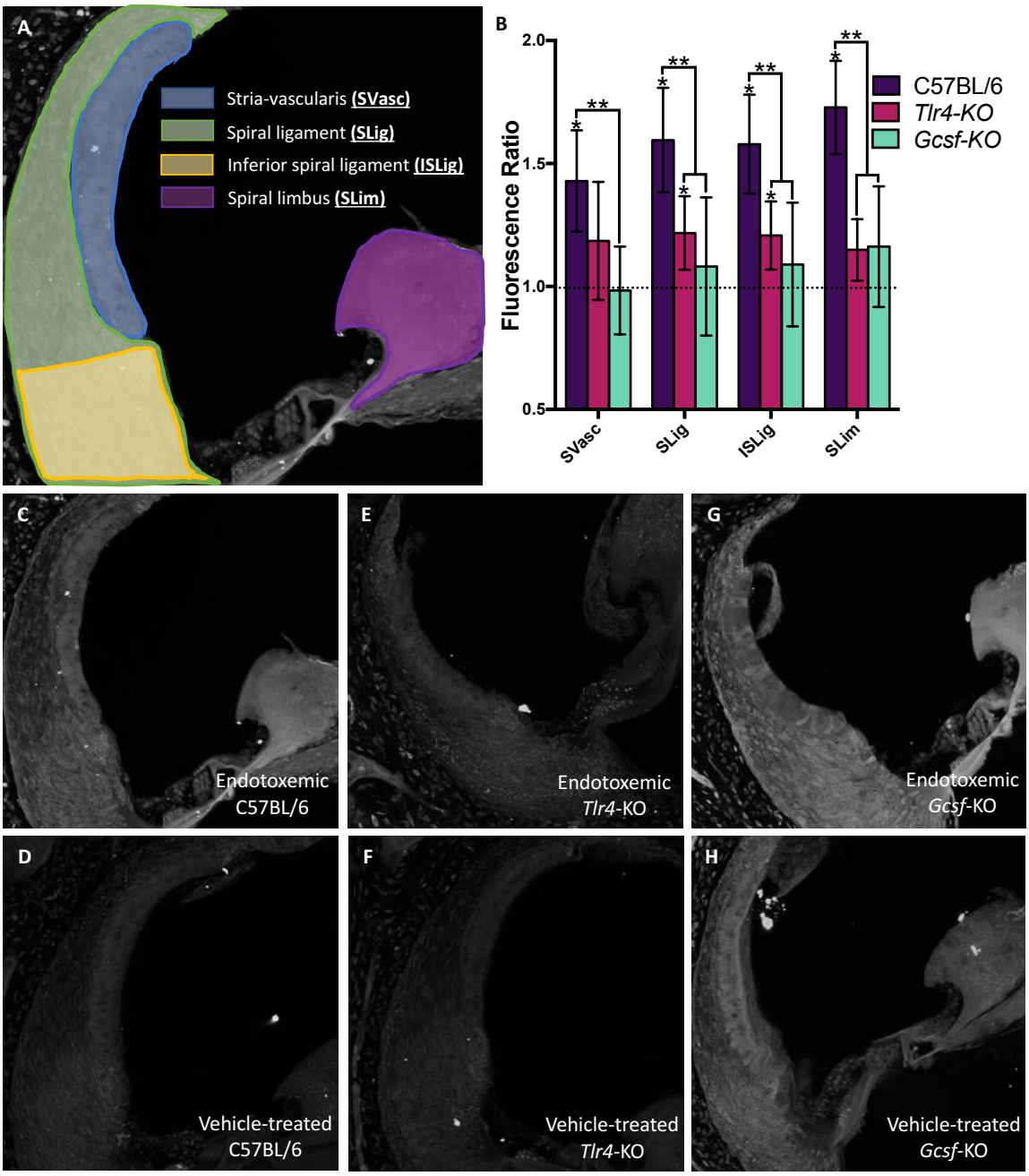

Figure 3-4. Biocytin-TMR vascular tracer quantification during endotoxemia.

Mice were treated with either 10 mg/kg LPS *i.v*. or vehicle and 24 hours later with 1% biocytin-TMR. Cochleas were imaged via quantitative confocal microscopy. (**A**) Regions of interest were hand-drawn in Fiji and each anatomical region quantified (**B**) for C57BL/6, *Tlr4*-KO and *Gcsf*-KO mice (n=3-5 per cohort). 95% student's-t confidence intervals. * $p<0.05$ for LPS treatment normalized to vehicle treatment within a mouse strain. ** $p<0.05$ between indicated mouse strains. SVasc = stria vascularis, SLig = spiral ligament, ISLig = inferior spiral ligament, SLim = spiral limbus (**C-H**) Representative cochlear sections of mice treated with biocytin-TMR and counter-labeled with Streptavidin Alexa Fluor 568. Strain and treatment are indicated in each panel.

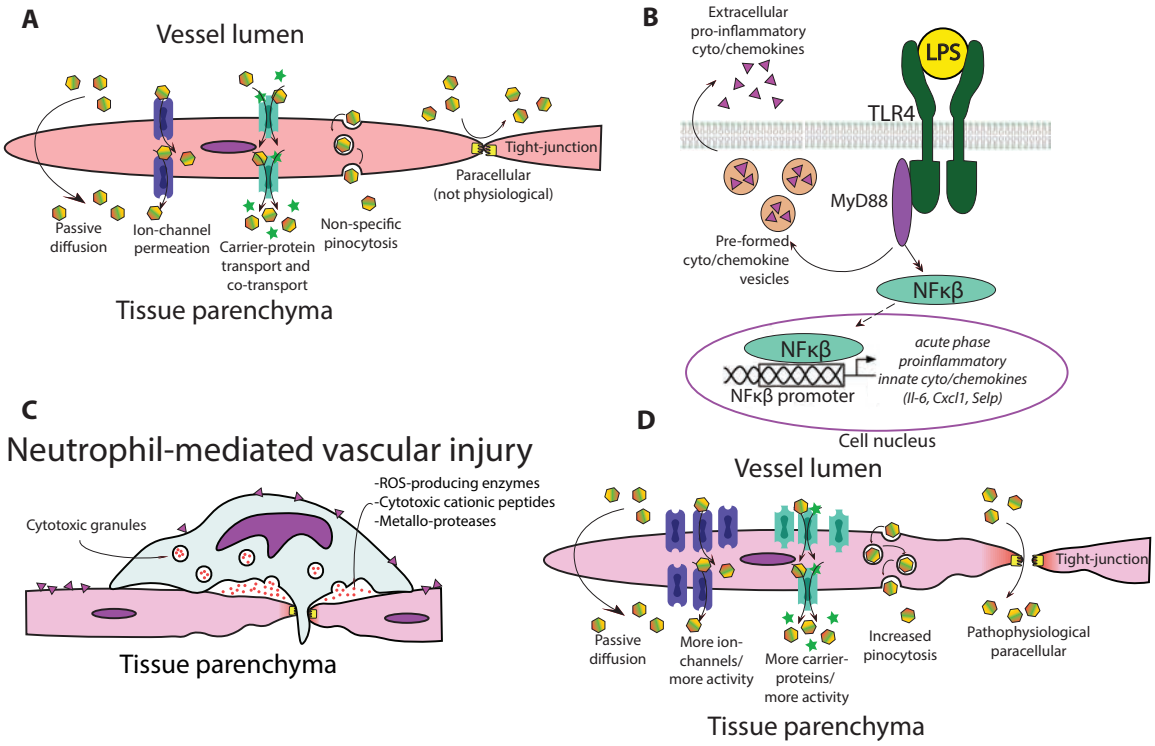

Figure 3-5. Model for endotoxemia-enhanced BLB trafficking.

.(**A**) Baseline BLB trafficking mechanisms. Paracellular trafficking is largely absent during healthy physiological states. (**B**) Endotoxemia stimulates TLR4 signaling inducing cytokine/chemokine expression (**C**) Chemokine/cytokine activated neutrophils and other white blood cells adhere to activated endothelium and degranulate causing neutrophil-mediated vascular injury. (**D**) Possible endotoxemia-induced pathophysiological trafficking routes emerge in injured vasculature allowing enhanced cochlear ototoxic drug uptake.

3.7 – Supplementary Materials

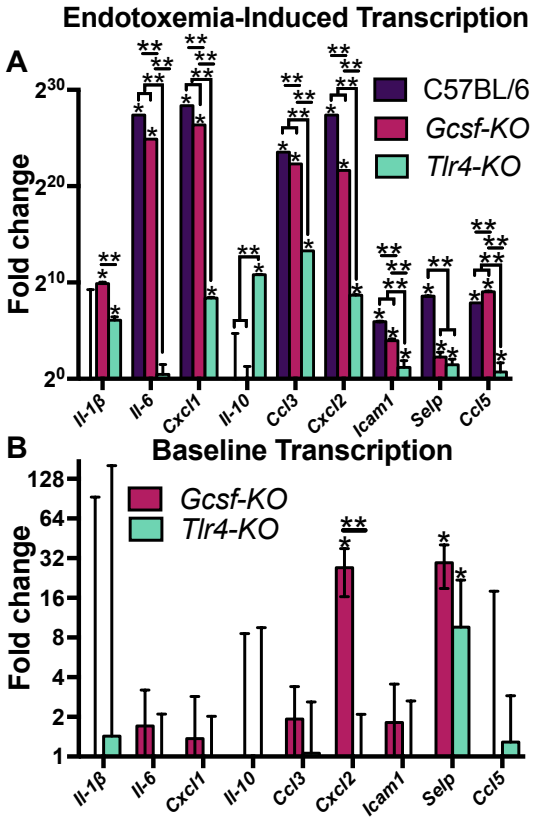

Figure 3-S1. Gene transcript fold change during endotoxemia and at baseline.
(**A**) Fold change in gene transcription was calculated for LPS-treated vs vehicle-treated mice. (**B**) Baseline dCt values for vehicle-treated KO animals were compared to baseline dCt values of vehicle-treated C57BL/6 mice to determine fold-change differences of baseline gene transcription. Data is expressed as fold change of LPS-treated versus vehicle-treated cohorts or KO versus wild-type (n=3-7 per cohort). 95% student's t CI. * indicates $p<0.05$ for LPS treatment normalized to vehicle treatment within a mouse strain. ** indicates $p<0.05$ between indicated mouse strains.

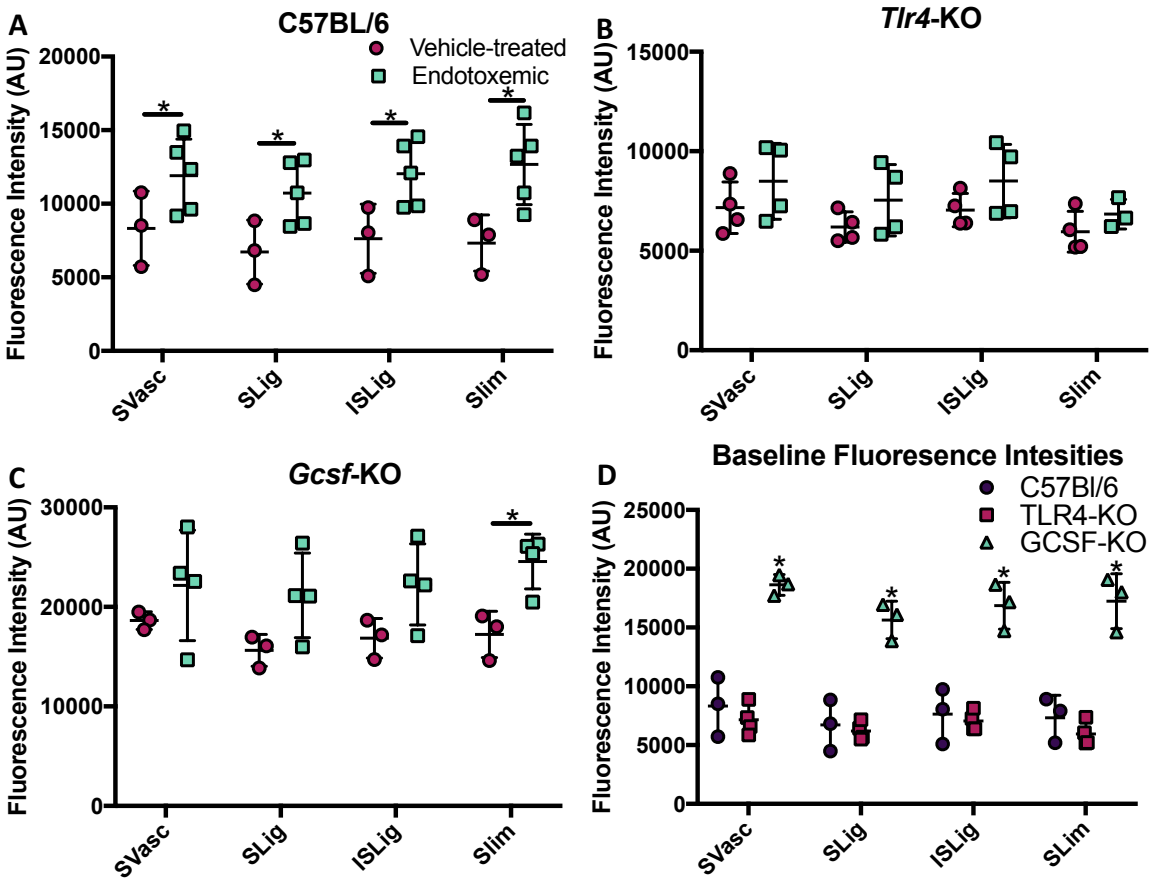

Figure 3-S2. Raw fluorescence intensities for biocytin-TMR tracer experiment. SVasc = stria-vascularis, SLig = spiral ligament, ISLig = inferior spiral ligament, SLim = spiral limbus. (**A-C**) Raw mean pixel intensity AU values for each cochlear ROI for C57BL/6 wild-type, *Tlr4*-KO, and *Gcsf*-KO mice. Error bars are SD; * indicates $p<0.05$ after student's t test. (**D**) Baseline biocytin-TMR trafficking after vehicle-vehicle treatment* indicates $p<0.05$ after one-way ANOVA.

Table 3-S1. Pediatric and adult SIRS criteria.

Any two of the following meets clinical SIRS criteria	
Pediatric (*40*)	**Adult (*39*)**
Temperature >38.5°C or <36.0°C	Temperature >38.0°C or <36.0°C
Tachypnea: >2SD above normal for age breaths/min	Tachypnea: >20 beats/min
Tachycardia: >2SD above normal for age beats/min, or <10th percentile if <1-year-old	Tachycardia: >90 beats/min
White blood cell count: Elevated or decreased total count based on normal values for age, or >10% immature neutrophils (band cells)	White blood cell count: >12,000/ml or <4,000/ml

Table 3-S2. Innate immunity marker gene panel and gene functions.

Gene name	**Function (*443*)**
Interleukin one beta – IL-1β	Pyrogen, induces endothelium to express adhesion molecules, induces chemokine secretion.
Interleukin six – IL-6	Pyrogen, stimulates acute-phase protein production: *e.g.* C-reactive protein, ferritin, fibrinogen, serum amyloid A. Pro-inflammatory endothelial cell activation.
Chemokine C-X-C motif ligand one – CXCL1 (aka KC in mice)	Chemotactic for neutrophils.
Interleukin ten – IL-10	Anti-inflammatory mediator. Major regulator for compensatory anti-inflammatory response syndrome (CARS(*67*))
Chemokine C-C motif ligand three – CCL3	Chemotactic for myeloid lineage immune cells, primarily neutrophils.
Chemokine C-X-C motif ligand two – CXCL2	Expressed primarily by activated monocytes/macrophages. Chemotactic for neutrophils.
Intercellular adhesion molecule one – ICAM1	Endothelium-leukocyte inflammatory adhesion molecule.
P-selectin –SELP	Promotes NETosis(*444*), endothelium-leukocyte adhesion.
Chemokine C-C motif ligand five – CCL5	Chemotactic for monocyte/macrophage and NK cells. T cell-dendritic cell interactions.

4 – Discussion and Key Findings

4.1 – Endotoxemia Enhances Drug-Induced Ototoxicity

Platinum-based chemotherapy and aminoglycoside antibiotics persist as essential clinical tools despite severe side effects such as ototoxicity, nephrotoxicity, and myelotoxicity. Primary reasons for this include clinical efficacy and economic accessibility. This body of work strengthens the growing consensus (*314, 315, 376, 394, 425*) that inflammation enhances the risk and severity of these life-changing side effects. Furthermore, this body of work accentuates the role of neutrophils as driving mediators of capillary injury. Future work to understand the mechanisms involved in inflammation-mediated capillary injury might focus on endothelial cell-independent and leukocyte-mediated vascular injury from neutrophils and other immune cells including the cytotoxic molecules which mediate this injury.

Endotoxemia enhances aminoglycoside ototoxicity as demonstrated by higher ABR thresholds in endotoxemic mice treated with equivalent kanamycin regimens (*394*) (**Fig 2.7**). In this body of work, mice were treated with 1mg/kg LPS *i.v.* 24 hours prior to twice-daily kanamycin administration at 700 mg/kg *i.p.* for fifteen-days. LPS was re-administered at the same dose and route for a second and third time on days five and ten of the fifteen-day kanamycin regimen (*394*). A similar study by Hirose *et al.* utilized a single-dose furosemide plus kanamycin ototoxicity model and came to equivalent conclusions that endotoxemia enhances the ototoxic potential of kanamycin plus furosemide. Hiroseet al. administered LPS at 0.5 mg/kg *i.p.* 48-hours and again 24-hours before a single combined dose of kanamycin (1000 mg/kg *i.p.*) plus furosemide (180 mg/kg *i.p.*) 45-minutes after kanamycin (*315*). A separate study investigating cisplatin ototoxicity first treated mice with 5mg/kg cisplatin *i.p.* followed by two doses of LPS *i.p.* at 1.25, 2.5, and 5.0 mg/kg *i.p.* 6-hours after and again 24-hours after cisplatin treatment. Because endotoxemia enhances the ototoxic potential of multiple ototoxic drug regimens with different LPS doses and routes of administration it is clear that systemic inflammation enhances ototoxicity.

Local (*407*), systemic (*445, 446*), and even intrauterine (*447*) LPS exposure can also cause permanent hearing loss. Other forms of cochlear inflammation can also induce hearing loss including auto-immune disorders and cochlear infection (*448*). Host-tissue damage from leukocytes and lymphocytes mediate inflammation-related hearing loss (*449*).

Ototoxic drug exposure plus labyrinthitis enhances the ototoxicity of both of these ototoxic stimuli. Low dose endotoxemia (≤ 1 mg/kg *i.v.*) itself does not cause hearing loss (*394, 395*) yet enhances kanamycin and cisplatin ototoxicity. How and why this enhanced ototoxicity occurs is likely linked both to enhanced drug activity, enhanced inflammation-mediated damage, and perturbed BLB physiology.

Aminoglycoside-induced mitochondrial respiratory uncoupling and interactions with iron produce excessive ROS, which demands increased utilization of cellular ROS-scavenging capacity. Platinum derivatives directly bind to and deplete endogenous ROS-scavenging molecules such as glutathione. In both cases, these drugs act to increase the cellular ROS burden and demand increased ROS-scavenging. Because cellular ROS scavenging directs towards drug-induced stresses, diminished ROS-scavenging capacity is available to stave off inflammatory host-tissue damage. In summary, not only do drugs in of these classes cause cellular damage, but the precipitous DAMP-induced inflammation is more toxic to cochlear tissues due to decreased ROS-buffering capacity.

Conversely, a major pathological process of inflammation is ROS generation, which demands cellular ROS scavenging. Inflammation-mediated ROS production and the precipitous enhanced demand for ROS-scavenging capacity worsens the cellular damage induced by cisplatin–mediated and aminoglycoside-mediated ROS production and subsequent ROS-mediated cellular damage. In this sense, both drug-induced and inflammation-related ROS positively feed back on each other to worsen the cytotoxic effects of each process.

Inflammation also acts upon endothelial barriers, which comprise barrier organs such as the BLB. Enhanced trafficking of ototoxic drugs into the cochlear parenchymal compartment due to impaired BLB selectivity properties enhances the ototoxic potential of these drugs. These processes, such as neutrophil-mediated vascular injury, pose as additional synergistic mechanisms for inflammation plus ototoxic drugs.

4.2 – Endotoxemia Involves Labyrinthitis and Enhanced BLB Trafficking

We demonstrated that endotoxemia induces cochlear expression of innate pro-inflammatory cytokines and chemokines in wild-type and *Gcsf*-KO mice, which have wild-type *Tlr4* (**Figs. 2.4, 2.5, and 3.2**). Endotoxemia is a systemic condition and TLR4 is ubiquitously expressed in mammals; it is therefore not necessarily a surprise that endotoxemia involves labyrinthitis. Dogmatically, this work contributes to the paradigm shift that inflammation occurs in organs classically described as immuno-privileged, namely the barrier organs (*450*). Indeed, these organs, such as the brain, cochlea, and eye, do mount immune reactions consisting of fewer immune cell infiltrates. In comparison, in non-barrier organs with fenestrated endothelia, such as the liver, endotoxemia recruits substantial immune cell infiltrate (*451*). In this sense, the dogma that barrier organs are immuno-privileged organs is correct. However, the notion that barrier organs are not affected by inflammatory states is falling out of favor. Instead, how barrier organs respond to inflammation is unique. A primary pathophysiological inflammation-related derangement is barrier dysfunction and capillary leak.

Endotoxemia, even low dose, enhances BLB trafficking. Interestingly, some molecular selectivity still remains at lower doses (**Fig. 2.3**). Texas Red more easily traffics across the BLB of post-natal day 3 mouse pups with an underdeveloped BLB. However, Texas Red does not traffic across the BLB in healthy nor endotoxemic wild-type mice treated with 1 mg/kg LPS. Despite this selective exclusion of anionic Texas red, polycationic fluorescent gentamicin-Texas red, and native gentamicin trafficking are both enhanced by low dose endotoxemia (**Figs. 2.1 and 2.2**). Trafficking of anionic fluorescein into perilymph is also enhanced by low dose endotoxemia (*425*). High-dose endotoxemia (10 mg/kg) also enhances BLB trafficking of biocytin-TMR (**Fig. 3.4**) demonstrating endotoxemia-enhanced BLB trafficking for multiple vascular tracers and at multiple LPS doses.

Baseline Texas red trafficking during endotoxemia and increased Texas red trafficking in neonatal mice could be due to a number of factors including

pharmacokinetic, cochlear development, and active transport out of the cochlear parenchyma. Texas red (a.k.a. sulforhodamine 101) is a well characterized anionic ligand for MDR1 which is highly expressed in both the liver (*452, 453*) and BLB (*454*). Neonatal mice only begin to express MDR1 in the cochlear lateral wall around the third week of life; MDR1 reach adult levels by the sixth week (*455*). Thus, the observed trafficking in neonatal mice could be due to the dearth of MDR1 expression in the neonatal versus adult cochlear lateral wall. Furthermore, the tight junctions in the neonatal mouse BLB are underdeveloped, which allows paracellular molecular trafficking (*456, 457*). In the liver MDR1 acts to move organic anions out of circulation and thus the lack of MDR1 expression in the neonatal liver would greatly prolong the serum half-life of sulforhodamine 101 and therefore increase the total cochlear exposure to Texas red. In adult mice, the half-life of sulforhodamine 101 is only fifteen minutes. Thus, with the 45-minute circulation time utilized in the experiment presented in **Fig 2.2**, only 12.5% of the initial serum concentration would remain. In neonatal mice, one would predict a longer half-life and thus a greater serum AUC. These two factors could be sufficient to generate the observed enhanced BLB uptake of sulforhodamine 101 in neonatal versus adult mice. However, endotoxemia downregulates MDR1 activity at the BBB (*458*) and therefore enhanced sulforhodamine 101 BLB trafficking would be predicted due to decreased efflux pumping by MDR1.

Prolonged pharmacokinetics and the developmental pattern of MDR1 expression are two possible mechanistic contributors explaining the observation that sulforhodamine 101 traffics across the neonatal mouse BLB but not the adult endotoxemic or vehicle-treated control. Another possible mechanistic contributor is enhanced paracellular trafficking during the neonatal period which theoretically persists until development of the EP which requires fully developed tight junctional complexes (*457*).

Higher dose (10 mg/kg, *i.v.*) endotoxemia enhances biocytin-TMR trafficking across the BLB (**Fig. 3-4**). The enhanced BLB trafficking is likely due to a combination of molecular transport mechanisms (**Fig. 3-5**). Biocytin-TMR's molecular weight is 869 g/mol and has a net +1 charge at physiological pH due to a free primary amine on the linker moiety. Biocytin-TMR is extensively described in the literature as a tracer for paracellular trafficking (*148, 459-462*); however, other modes of transport may contribute

but have not been thoroughly explored. Because of the literature precedent for biocytin-TMR, we conclude that higher dose endotoxemia promotes paracellular trafficking route development, allowing for enhanced biocytin-TMR trafficking. Other routes of transport and BLB compromise very likely also emerge during endotoxemia. Future studies should concentrate on non-paracellular routes and may include utilization of mice deficient in transcytosis, such as the caveolin1-KO, or the MDR1-KO mouse line deficient in active transport BLB exclusion to parse out the relative contributions of the principal barrier transport mechanisms.

4.3 – TLR4 Activity Promotes Endotoxemia-Mediated Labyrinthitis and Enhances BLB Trafficking

As described earlier, TLR4 is the canonical innate immune sensor for gram-negative LPS and hence a primary signaling molecule during experimental endotoxemia. We demonstrated in two separate mouse models the dependence of endotoxemia-enhanced BLB trafficking on TLR4 activity. First, we demonstrated in the TLR4 hypomorphic C3H/HeJ mouse line that an inactivating mutation in TLR4 is sufficient to ameliorate low dose (1 mg/kg *i.v.*) endotoxemia-mediated labyrinthitis as measured by labyrinthine innate proinflammatory cytokine and chemokine expression (**Fig. 2-5**). In a separate experiment utilizing high dose (10 mg/kg *i.v.*) endotoxemia, TLR4-KO mice demonstrated a qualitatively similar innate immune cytokine/chemokine response to endotoxemia as in C3H/HeJ mice (**Fig. 3-2**). This decrease in endotoxemia-induced cytokine/chemokine expression was accompanied by amelioration of endotoxemia enhanced gentamicin-Texas red BLB trafficking in C3H/HeJ mice (**Fig. 2-6**) as well as amelioration of endotoxemia enhanced biocytin-TMR BLB trafficking in TLR4-KO mice (**Fig. 3-4**).

TLR4's most prominent biological role is promotion of innate inflammation. Two divergent but related signaling pathways immediately downstream of TLR4 activity are governed by the expression of adaptor proteins MyD88 and the TRIF/TRAF duo (*463*) MyD88-dependant TLR4 signaling promotes NF-κβ translocation to the nucleus which

turns on acute phase response related proteins. TRIF/TRAM work to promote interferon response factor (IRF) translocation to the nucleus, turning on interferon related genes. Both of these divergent pathways act to orchestrate the innate inflammatory response. Depending upon the cell type and which TLR4 adaptor molecule(s) predominates determines each cell's role in the inflammatory response.

In vascular smooth muscle cells TLR4 activation may result in vasodilation. However, it is unlikely the direct TLR4 signaling that cues the vascular smooth muscle to relax but instead molecules downstream of TLR4 such as NO (*464*). However, TLR4 activity can directly modulate non-leukocyte cellular activity. One example is in leukocyte-independent systems of BBB derived endothelial cell cultures. In these systems, LPS can down-regulate tight-junction expression and electrical resistance across cellular monolayers. Therefore, LPS acts by both intrinsic cellular responses and by the action of leukocyte-mediated host-tissue damage.

4.4 – Neutrophil Activity Downstream of TLR4 Enhances BLB Trafficking

Endotoxemia recruits neutrophils to the cochlea in wild-type but not TLR4-KO nor neutropenic GCSF-KO mice (**Fig. 3-3**). This observation coincides with the observed proinflammatory cochlear cytokine and chemokine profile. The cytokines and chemokines on the gene panel were selected because these genes act to mediate the neutrophilic phase of acute inflammation (**Table 3-S2**). As neutrophils are the first responders in acute innate inflammation body-wide during endotoxemia, cochlear neutrophilic inflammation is not a surprise. These experiments link neutrophil activity, cytokine/chemokine expression patterns, and molecular trafficking at the BLB. We demonstrate that enhanced biocytin-TMR trafficking requires neutrophil activity and that neutrophil activity depends on an adequate TLR4-dependant cytokine/chemokine response. Knocking down either TLR4 activity of neutrophil numbers is sufficient to ameliorate endotoxemia-enhanced BLB trafficking. Thus, proinflammatory signaling alone is not sufficient to perturb BLB physiology but requires neutrophil activity.

Neutrophil activity correlates to vascular barrier pathophysiology and organ damage in multiple disease contexts. Indeed, neutropenia can protect against inflammation-mediated tissue damage in the setting of stroke (*465*), multiple sclerosis (*466*), meningitis (*55, 467, 468*), traumatic brain injury (*469-471*), endotoxemia acute lung injury (*472*), as well as other non-neuronal pathologies. Because parenchymal neutrophil activity elicits host tissue damage neutrophil activity may also contribute to hearing loss in ways beyond effecting BLB related physiology. Neutropenia decreases lung parenchymal uptake in inflamed lungs in comparison to animals with normal neutrophil counts (*408*) similar to these findings where neutropenia decreases molecular trafficking in inflamed cochleas. Targeting neutrophil activity directly or the cytokines and chemokines that direct them can protect against neutrophil-mediated pathology. For example, inhibiting neutrophil-derived lytic enzymes such as neutrophil elastase can protect against mortality in a cecal ligation and puncture model of sepsis in rats (*473*), TLR4-KO protects against noise-induced hearing loss (*474*), MMP inhibitors attenuate cochlear lateral wall damage during locally applied LPS-mediated otitis media (*429*), and sudden sensorineural hearing loss correlates with systemic inflammatory biomarker elevations (*475*). Because neutrophils are the most numerous immune cell and the first responders to innate inflammatory cues (*476*), targeting neutrophil activity is a logical junction to intervene in pathophysiological inflammatory processes.

5 – Summary, Conclusions, and Translational Implications

5.1 – Summary and Conclusions

Ironically, the very disease aminoglycoside therapy treats enhances the risk of hearing loss. For the clinician, enhanced toxicity makes treating sepsis with aminoglycoside antibiotics a difficult decision, particularly when the pathogen has a known sensitivity to the drug. Attempts to cure a patient must be balanced by the morbidity and potential complications of the treatment. Careful dosing, and adequate

hydration are the mainstays in preventing aminoglycoside toxicity. Understanding the mechanisms of aminoglycoside ototoxicity and how inflammation enhances this side effect helps further complication-free treatment for conditions such as sepsis. We show here that both TLR4 activity and downstream neutrophil activity is required for endotoxemia-enhanced BLB trafficking.

Because a common complication of cisplatin treatment is neutropenia, and neutropenia is a strong risk factor for developing sepsis, often neutropenic cancer patients treated with cisplatin are later treated with aminoglycoside antibiotics for sepsis. Because neutropenia protects against endotoxemia-enhanced BLB trafficking, it spurs the notion that possibly neutropenia is an indication for ototoxicity-free aminoglycoside therapy. Further observational and prospective clinical studies could be carried out to determine the risk of aminoglycoside ototoxicity as it relates to the septic neutropenic cancer patient. Perhaps these individuals will largely be protected from ototoxicity compared to septic patients with neutrophil counts within the standard range. However, studying the effect of neutropenia and aminoglycoside ototoxicity in cisplatin-treated patients may confound any conclusions, or diminish the power of a study to detect any otoprotective effect of neutropenia because cisplatin is also ototoxic.

Protecting a patient with adjunct otoprotective therapy is another approach to help stave off aminoglycoside and platinum induced ototoxicity. Aspirin and thiol-based pharmaceuticals are two well studied classes otoprotectants with excellent promise to preserve the clinical utility of aminoglycosides and platinum chemotherapy. Steroids such as dexamethasone are also otoprotective in the settings of drug-induced and inflammation-induced hearing loss. A common thread between NSAIDs such as aspirin, thiol-based agents, and steroids is the anti-inflammatory activity of all these compounds. Aspirin acts to directly neutralize ROS and to dampen inflammation through classic COX inhibition. Thiols exert anti-inflammatory activity by mopping up inflammation-related ROS as well as inflammation-independent ROS. Dexamethasone acts to directly dampen any inflammatory response. This mechanistic convergence provides insight to the basic science of ototoxicity and how inflammation overlaps with ototoxic drug exposure. Ototoxic drugs are in part ototoxic due to the inflammatory reaction they provoke. Thus, it makes sense that inflammation enhances the ototoxicity potential of ototoxic drugs.

Future studies examining the effects of immune modulation in relation to drug-induced otopathology and hearing loss may provide insight for therapeutic strategies to protect hearing.

5.2 – Study Limitations

One major consideration in the interpretation of this body of work is the selection of endotoxemia as a model for sepsis/SIRS. Other model systems considered during the conception of these experiments included cecal ligation and puncture, and *i.v.* injection of either lysed or living bacteria. Other models of sepsis/SIRS considered included viremia or *i.v.* poly-I:C (as a model for viremia).

An advantage of utilizing cecal ligation and puncture is that it is a good model for endogenous bacterial peritonitis with a SIRS response; a disadvantage of this approach is that cecal ligation and puncture is uniformly lethal without surgical intervention and repair. Furthermore, the invasive surgery itself is a major traumatic event and requires ample surgical time in the lab in comparison to other models. *i.v.* injection of live pathogens is advantageous in that treatment modalities may be administered to try and cure the animals of the experimentally induced bacteremia. For example, aminoglycoside antibiotics could be administered after induction of bacteremia and adjunctive otoprotective compounds could be administered along with or after antibiotics to try and protect hearing. This integrated clinical animal model is advantageous in that many variables could be tested at once including hearing loss, survival, and otoprotective compounds. Disadvantages of this approach include inconsistent animal mortality, and protocol complexity which could further add to inconsistencies in the results. Models for viremia could be particularly translatable as most cases of suspected sepsis in the neonatal intensive care unit are cases of viremia (*477*). We decided upon LPS-induced endotoxemia due to consistency in dosing/lethality, because our experimental questions did not require the use of live pathogens, because aminoglycosides are used to treat gram-negative infection, and due to convenience and ease of *i.v.* tail injections.

Another limitation in the initial finding that endotoxemia enhances aminoglycoside ototoxicity is the sole use of ABR to measure hearing thresholds in the

animals. However, cytocochleograms did confirm outer hair cell loss and bolstered the ABR data. Other modalities with greater sensitivity could have bolstered this set of data. Other methods include measuring distortion products of otoacoustic emissions which measures outer hair cell function, and measurement of compound action potentials in the round-window niche.

A limitation in experiments looking at neutrophil numbers was the use of Ly6G as the sole neutrophil marker. Co-labeling with antibodies against CD45, CD11B, and other markers not specific for neutrophils, but instead, other immune cells (such as CD11) would bolster confidence that the Ly6G+ cells are in fact neutrophils.

In terms of vascular tracers utilized to investigate vascular permeability only four tracers were used: gentamicin, gentamicin Texas Red, Texas Red, and biocytin-TMR. Gentamicin and gentamicin Texas Red are unique in that trafficking mechanisms are still a hot topic of debate. As mentioned in section 5.1, Texas Red (sulforhodamine 101) is a substrate for organic anion transporters and is therefore not a strict tracer for paracellular trafficking. Biocytin-TMR is generally described in the literature as a paracellular tracer, however this tracer is likely a substrate for the biotin receptor.

For gene expression the primary limitation was bias in selection of our gene panel. Utilizing combined MS-MS proteomics and RNAseq technologies would provide a comprehensive unbiased characterization of the cochlear transcriptional and translational response to endotoxemia. Personnel, access to experimental apparatuses, and time restraints are all reasons why this route was not pursued.

Two other general limitation of this study include only one experiment looking into functional hearing outcomes, and the fact that most data was collected from *ex vivo* tissue samples. Functional hearing assays in both TLR4-KO and GCSF-KO mice could have provided interesting results either bolstering or disagreeing with the genetic, inflammatory, and genetic analyses. More studies utilizing *in vivo* methods could improve the confidence of conclusions drawn from these *ex vivo* tissue samples.

5.3 – Future Directions

As mentioned in section 5.2, additional *in vivo* studies would bolster the confidence of the findings in these studies. Utilization of animal models with fluorescent leukocytes in combination with the cochlear thin window technique (appendix C) would provide an opportunity to observe cochlear leukocyte dynamics *in vivo* during endotoxemia.

Studies triple-labeling for neutrophils would increase the confidence that the Ly6G+ cells observed in these studies are in fact neutrophils. Performing flow cytometry to look at a pan-leukocyte panel would remove the bias of this work towards neutrophils and expand possible white blood cell actors to other cells types such as T-cells and macrophages for which other groups such as Hirose *et al*. have focused on over the past two decades. This work, however, is novel in that the neutrophil is the focus and has been rarely described in cochlear pathology in comparison to the macrophage.

Utilization of magnetic resonance imaging (MRI) in combination with iron nanoparticle and/or gadolinium-based contrast is one way to observe BLB permeability in real-time using a paired statistical analysis scheme. Indeed, pilot studies utilizing this study have been initiated in the Long Evan's rat model (**Fig. 5.3.1**). An n of one has demonstrated that gadolinium and Ferumoxytol imaging agents trafficking into the lymphatic spaces of the rat cochlea 24 hours after induction of endotoxemia (Ferumoxytol data not shown). This project is at a stage of translating the LPS-endotoxemia model to the rat which is more sensitive to equivalent LPS doses in comparison to the mouse.

Clinically, a logical research question stemming from this study is: are patients with neutropenic fever and sepsis who are treated with aminoglycoside antibiotics at greater risk for hearing loss. A clinical study looking at suspected cases of neonatal sepsis treated with aminoglycoside antibiotics are more at risk of incurring hearing loss has already been conducted (appendix B). It would be interesting to see if this trend holds in neutropenic patients or if neutropenia protects hearing in a human cohort.

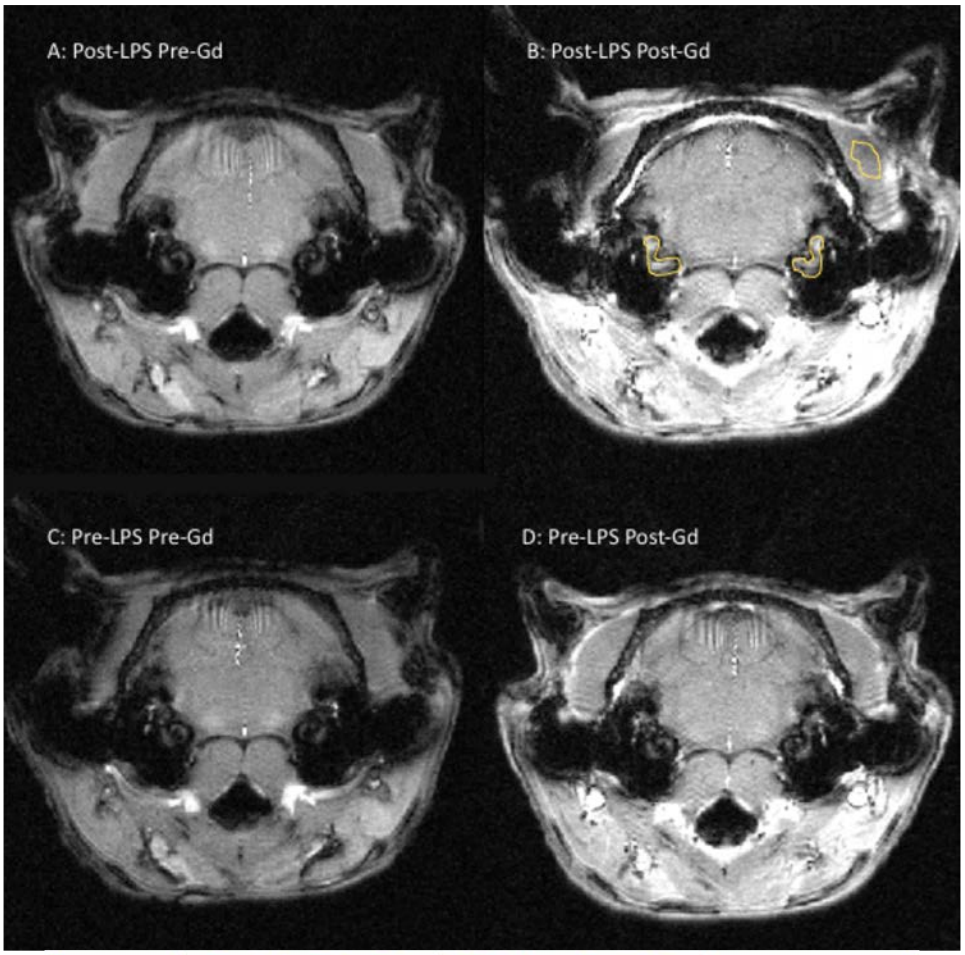

E	Cochlea Pre Gd Average	Cochlea Post Gd Average	Post-Pre
Pre-LPS	35136	465399	113863
Post-LPS	378503	759776	381272

Fig. 5.3.1: Pilot BLB trafficking MRI study in endotoxemic rats.
(A) Briefly, an adult Long Evan's rat was treated scanned in a 12T MRI instrument and then injected with gadolinium-based contrast prior to (B) dynamic imaging post-injection. The rat was then treated with 10 mg/kg LPS. 48 hours later the animal was re-imaged both prior to (C) and after an additional gadolinium injection (D). Regions of interest were defined as in panel (B) (yellow lines) and the average pixel intensity was determined and normalized to temporalis muscle signal intensity. The gadolinium induced change in signal intensity was then calculated before and after LPS (E) demonstrating that LPS enhances the trafficking of gadolinium-based contrast across the BLB.

Appendix A: Basics of Hearing

A.1 – Basics of Hearing

A.1.1 – Sound

Sound is defined by sinusoidal waves in air (or other matter) pressure produced by vibrations. Compressions and rarefaction are the terms for regions in space and time where the pressure in the material medium is increased or decreased respectively compared to the surroundings. Sound waves can travel through any kind of matter and cannot exist in a vacuum where there is no medium to transduce the waves. The speed at which sound waves travel through a material is related to the materials, density, elasticity, and compressibility. Sound waves are described by six dimensions; frequency, amplitude, time, and space (3 dimensions of space).

Frequency relates to the perception of pitch. Higher frequency sound is perceived as higher pitch and lower frequencies as lower, deep pitched sounds. Amplitude relates to the volume of a sound heard and is quantified by the arbitrarily defined decibel scale where 0 dB is the amplitude threshold where an "average" human can hear a sound. This unit is specifically called dB-HL or "decibel hearing level." dB-HL can be physically defined by the physical pressure exerted by the wave by a unit called dB-SPL where 0 dB-SPL translates to 20 μPa.

A.1.2 – Outer Ear

The external ear, or pinna, is the portion of the ear visible with the unaided eye. Sound is collected and funneled via the pinna's spiral structure before transmission through the external auditory canal. Sound of higher frequencies (2000-4000 Hz) is further amplified via the external auditory canal which terminates on the tympanic membrane. Which sounds are amplified by the external auditory canal depends upon the resonant frequency of the canal. Shorter and narrower canals will amplify higher

frequency sounds while longer wider canals amplify lower frequency sounds. As individuals develop, the resonant frequency shifts to progressively lower frequencies.

A.1.3 – Middle-ear

The middle-ear is defined as the air-filled space where the three auditory bones reside referred to as ossicles. The tympanic membrane is attached to the first and largest ossicle, the malleus, next in line is the incus, and finally the stapes. Ossicles are named after their shape and refer to the hammer, anvil, and stirrup respectively. Sound vibrations reach the tympanic membrane via the external auditory canal and transduce these sound waves to the tympanic membrane. Tympanic membrane vibration is then transduced to the malleus, through the incus, and to the stapes which inserts on to the oval window. The surface area of the tymapanic membrane is larger than the surface area of the oval window. because of the change in surface area, pressure exerted on the tympanic membrane is transduced to a greater pressure on the oval window; the same force distributed over the tympanic membrane is concentrated on to the smaller oval window.

Because the middle-ear is a closed air-filled space changes in environmental pressure alter the pressure within the middle-ear. The eustacian tube is a tubular structure connecting the middle-ear with the pharynx and is normally closed. The closed state of the eustacian tube prevents breathings sounds from reaching the middle-ear. When pressure differences exist between the middle-ear and the environment the eustacian tube temporarily opens generating an open space between the middle-ear and the pharynx which is continuous with environmental air pressure. Colloquially this physiological process as known as "ear popping."

A.1.4 – Inner-Ear

Sound pressure waves transduced via the ossicles are propagated on to the oval window which is in contact with the perilymph of the scala tympani. Concentration of physical force via increased pressure on the round window serves to impedance match the sound wave as the physical medium changes from air to perilymph. Sound waves then travel along the scala tympani to the apical helicotrema where the scala tympani is

renamed the scala vestibuli. Sound waves then travel back down the cochlea where they run into the round window. These waves vibrate the basilar membrane while they travel. The tectorial membrane is relatively stationary compared to the organ of Corti of the basilar membrane. Via this action, sound waves are converted to sheer forces exerted upon the stereocilia of hair cells.

Displacement of hair cell stereocilia opens (still unidentified) mechanically gated non-specific cation channels on the apical tip of the stereocilia causing hair cell depolarization via K^+ and Ca^{2+} currents. Hair cell depolarization enhances glutamate release at the basal side of hair cells via ultra-fast ribbon synapses. Glutamate then traverses the synaptic cleft and stimulates CNVIII fibers radiating from the modiolus.

A.1.5 – Pitch and Volume Decoding

Pitch is coded by the tonotopic distribution of frequency specific regions of the organ of Corti. Higher pitch sounds are transduced by hair cells near the base of the cochlea and lower pitch sounds by apical hair cells. The geometrical shape of the cochlea is such that basal portions of the basilar membrane resonate with higher frequency sounds and lower frequency sounds resonate with the apical basilar membrane regions. Basilar membrane vibrations are further amplified via the "acoustic amplifier" wherein outer hair cells expand and contract in phase with the sound waves via the protein activity of harmonin. Thus, frequency discrimination of sound based on stimulation of tonotopically distributed hair cells and paired cochlear nerve fibers allows for pitch perception.

Perception of sound volume is the ability to sense and discriminate sound waves of variable amplitude. Sound waves with larger amplitudes displace hair cell stereocilia to a greater degree. Greater stereocilia displacement depolarizes hair cells to a larger degree versus smaller displacements. The cellular potential of hair cells determines the rate at which glutamate is released by the glutamatergic ribbon synapses; greater depolarization correlates with faster glutamate release. When a cochlear nerve fiber receives more glutamate, the action potential spike rate increases. Increased spike rate corresponds to perception of a louder sound.

A.1.6 – Cranial Nerve VIII to the Auditory Cortex

Auditory pathways beyond the cochlea are not a focus of this work and only a simplified version of the ascending auditory pathway is summarized here. *Cranial nerve VIII* (a.k.a. acoustic nerve, or auditory nerve, or cochlear nerve) nerve fibers are tonotopically arranged as described in section *A.1.5*. This tonotopic distribution is preserved as these nerve fibers travel up the brainstem and eventually to the primary auditory cortex *A1* which also preserves this tonotopic organization. *Cranial nerve VIII* travels from the cochlea to through the internal auditory canal of the skull and synapses with the ipsilateral *cochlear nucleus*. From there, projections are sent to both the ipsilateral and contralateral *superior olivary nuclei*, followed by the ipsilateral *inferior colliculus*, the *medial geniculate body*, and then to *A1*.

Once acoustic frequency information reaches *A1* neural circuits continue to merge onto higher order neurons in *A2, A3* etc. eventually reaching broca's area which is responsible for language. It is the merging of information that allows for efficient perception of more complicated acoustic parameters. For example, a neuron on *A2* may receive inputs from all *A1* fibers encoding the individual frequencies of the C-major chord. Thus, a specific neuron (mini neural circuit) in *A2* can encode a more complex auditory feature. This idea is translatable for neurons in Broca's area where specific neurons or circuits may encode specific words, phrase, or sounds.

Spatial coding of sound requires bi-aural hearing and is based upon interaural time and intensity differences. This is that slight differences in timing and intensity for which sound reaches both ears allows spatial localization of sounds. Interaural time and intensity differences are then decoded by the cross-over of nerve fibers projected from the *cochlear nuclei* to the ipsilateral and contralateral *superior olivary nuclei*.

Appendix B: SIRS and Aminoglycoside Induced Hearing Loss Risk in Neonatal Intensive Care Unit Patients

Effect of sepsis and systemic inflammatory response syndrome on neonatal hearing screening outcomes following gentamicin exposure

Authors: Campbell P. Cross[a], Selena Liao[b], Zachary D. Urdang[a,c], Priya Srikanth[e], Angela C. Garinis[a,d], Peter S. Steyger[a,b,d]

a Oregon Hearing Research Center, Oregon Health & Science University, 3181 SW Sam Jackson Park Road, Portland, OR 97239, USA
b Otolaryngology, Oregon Health & Science University, 3181 SW Sam Jackson Park Road, Portland, OR 97239, USA
c Oregon Health & Science University, MD/PhD Program, 3181 SW Sam Jackson Park Road, Portland, OR 97239, USA d Portland Veterans Administration, National Center for Rehabilitative Auditory Research (NCRAR), 3710 SW US Veterans Hospital Road, Portland, OR 97239,USA
e Department of Public Health & Preventive Medicine, Oregon Health & Science University, 3181 SW Sam Jackson Park Road, Mail Code CB 669, Portland, OR 97239, USA

Appendix B is modified from the paper published in The International Journal of Pediatric Otorhinolaryngology September 1st, 2015.

Contributions: Zachary conceptualized and assisted in some of the data analysis and interpretation. Zachary co-wrote and edited the manuscript.

B.1 – Abstract

Objectives: Hearing loss in neonatal intensive care unit (NICU) graduates range from 2% to 15% compared to 0.3% in full-term births, and the etiology of this discrepancy remains unknown. The majority of NICU admissions receive potentially ototoxic aminoglycoside therapy, such as gentamicin, for presumed sepsis. Endotoxemia and inflammation are associated with increased cochlear uptake of aminoglycosides and potentiated ototoxicity in mice. We tested the hypothesis that sepsis or systemic inflammatory response syndrome (SIRS) and intravenous gentamicin exposure increases the risk of hearing loss in NICU admissions.

Methods: The Institutional Review Board at Oregon Health & Science University (OHSU) approved this study design. Two hundred and eight infants met initial criteria, and written, informed consent were obtained from parents or guardians of 103 subjects ultimately enrolled in this study. Prospective data from 91 of the enrolled subjects at OHSU Doernbecher Children's Hospital Neonatal Care Center were processed. Distortion product otoacoustic emissions (DPOAEs; *f*2 frequency range: 2063–10,031 Hz) were obtained prior to discharge to assess auditory performance. To pass the DPOAE screen, normal responses in >6 of 10 frequencies in both ears were required; otherwise the subject was considered a "referral" for a diagnostic hearing evaluation after discharge. Cumulative dosing data and diagnosis of neonatal sepsis or SIRS were obtained from OHSU's electronic health record system, and the data processed to obtain risk ratios.

Results: Using these DPOAE screening criteria, 36 (39.5%) subjects would be referred. Seventy-four (81%) subjects had intravenous gentamicin exposure. Twenty (22%) had ≥4 days of gentamicin, and 71 (78%) had <4 days. The risk ratio (RR) of referral with ≥4 days of gentamicin was 1.92

($p = 0.01$). Eighteen subjects had sepsis or met neonatal SIRS criteria, 9 of whom had ≥5 days of gentamicin and a DPOAE referral risk ratio of 2.12 ($p = 0.02$) compared to all other subjects. Combining subjects with either vancomycin or furosemide overlap with gentamicin treatment yielded an almost significant risk ratio (RR = 1.77, $p = 0.05$) compared to the rest of the cohort.

Conclusions: We report an increased risk of referral with DPOAE screening for those receiving ≥4 days of intravenous gentamicin administration that may contribute to the greater prevalence of hearing loss in NICU graduates. We propose an expanded prospective study to gather a larger cohort of subjects, identifying those with sepsis or neonatal SIRS, to increase the statistical power of this study design. Subsequent studies also need to obtain follow-up diagnostic audiological data to verify whether the outcomes of DPOAE screening, in addition to the standard AABR screen, is a reliable predictor of permanent hearing loss following gentamicin exposure in the NICU.

B.2 – Introduction

Hearing loss in patients discharged from neonatal intensive care units (NICUs) range between 2% and 15% of admissions, compared to a 0.2–0.3% rate of congenital hearing loss in full-term births (*478*). Risk factors for hearing loss in the NICU include illnesses or conditions requiring more than 48 h of NICU admission, genetic predisposition, family history of childhood sensorineural hearing loss, hyperbilirubinemia exceeding 30 mg/dl (requiring exchange transfusion), persistent pulmonary hypertension requiring mechanical ventilation, meningitis, seizures, in-utero infections (cytomegalovirus, herpes simplex, toxoplasmosis, rubella, syphilis) and TSH abnormalities, among others (*479-481*). Bacteremia (sepsis), prolonged duration of therapy, and other drug administration factors have also been proposed as risk factors for ototoxicity in adult populations (*480, 482*). Exposure to intravenous aminoglycoside antibiotics like gentamicin in the NICU may contribute up to 25% of this unexplained rate of hearing loss (*482*). Experimental models of systemic inflammation show increased cochlear uptake of gentamicin into the cochlea and exacerbation of ototoxicity (*314, 394*). This ototoxic synergy between gentamicin exposure and systemic inflammation may also contribute to the higher rates of hearing loss observed in NICU subjects.

This investigation is part of a larger study to measure noise exposure levels in the NICU and to determine the relationship between noise exposure, intravenous gentamicin exposure, and hearing screening outcomes (*483*). Here, we describe a sub-analysis performed to identify the inflammation status of enrolled NICU subjects in relation to their prospectively acquired DPOAE outcomes, and total days of gentamicin exposure. A retrospective chart review was conducted to identify the number of NICU graduates diagnosed with sepsis or systemic inflammatory response syndrome (SIRS) who also received intravenous gentamicin treatments (*40, 484*).

Objective screening methods used to identify subjects with increased risk for hearing loss included a distortion product otoacoustic emissions (iDPOAE) test in addition to the standard automated auditory brainstem response (AABR) hearing screen shortly before discharge. The AABR is currently the primary screening tool for infants in the NICU, whereas healthy infants are screened either with AABR or with DPOAEs

(*485*). The AABR reflects neural activity from the infant's auditory pathway has adequate neural integrity from the inner-ear (cochlea) to upper brainstem (medial geniculate body) in response to transient sounds or clicks (*481, 483, 486*), and can detect infants at risk for auditory neuropathy spectrum disorder (ANSD). ANSD is characterized by normal outer hair cell function and abnormal, absent, or non-synchronous auditory nerve function (*485*). Computerized AABR testing reduces human error, and manpower costs, in hearing screening (*481*). Infants who 'refer' on this test are often re-screened before a diagnostic hearing evaluation is recommended.

DPOAEs, on the other hand, are frequency-specific byproducts of normal cochlear function when stimulated with two simultaneous tones close in frequency and level. DPOAEs are measured using an ear-level microphone and provide information about cochlear outer hair cell function, which is the primary site of cochlear damage for initial noise-induced hearing loss and aminoglycoside-induced ototoxicity in adult populations (*484, 487*). DPOAE responses are influenced by hearing loss at the eliciting stimulus frequencies, ($f1$ and $f2$, where $f1 < f2$), emission frequency ($2f1 - f2$) and higher frequencies coded by more basal cochlear regions (*488*). This makes DPOAE responses a valuable screening tool for detecting the onset of ototoxicity that first appears at higher frequency (basal) cochlear locations. The current study used clinical DPOAE tests in addition to the standard AABR to screen for potential hearing loss in a cohort of NICU subjects, most of whom were dosed with intravenous gentamicin at least once during admission.

B.3 – Materials and Methods

B.3.1 - Enrollment and inclusion criteria

The Institutional Review Board at Oregon Health & Science University (OHSU) approved this study design (eIRB protocol #8434). The admission notes of 252 premature (gestational age <37 weeks) infants to the NICU between August 2012 and October 2013 were screened. Two hundred and eight infants met initial criteria, and written, informed consent were obtained from parents or guardians of 103 subjects ultimately enrolled in

this study. Forty-four patients were excluded prior to enrollment. Exclusion criteria included diagnosis of congenital hearing loss, or other known causes of hearing loss, including infections such as herpes simplex, rubella, syphilis, cytomegalovirus, or meningitis. Patients with known craniofacial or otologic abnormalities such as midfacial hypoplasia, microtia or aural atresia, were also excluded. For this study, prospective DPOAE and gentamicin dosing data were successfully collected on 93 infants. Two subjects were excluded due to preexisting conditions associated with hearing loss (one with intraventricular hemorrhage, and another with congenital hydrocephalus), leaving a total subject cohort of 91.

Subject demographics and characteristics are shown in **Table B.1**. Intravenous gentamicin medication exposure was obtained from OHSUs electronic health record system (EPIC). To identify subjects with sepsis or meeting criteria for neonatal SIRS (i.e., signs of systemic inflammation), a chart review of subject vital signs, blood culture results and progress notes was performed in EPIC (**Table B.2**). Only subjects that met sepsis or SIRS criteria on the same day as receiving a dose of gentamicin were included in the inflammation group. Since gentamicin also binds to albumin and other serum proteins (17–27% protein-bound), and elevated serum calcium levels can weaken this association increasing free gentamicin levels, standard laboratory measures (including white blood cell count, albumin levels and calcium levels) for each subject were also obtained and examined (*489*).

B.3.2. - Audiologic outcome measurements

Ninety-one NICU subjects who met the inclusion criteria were tested with DPOAE equipment at discharge between August 2012 and October 2013. DPOAE testing was performed with the Bio-logic Scout Sport (Natus Medical Incorporated, Mundelein, IL), with decibel levels of 65 dB/55 dB, and an $f2/f1$ ratio of 1.22. Ten $f2$ frequencies were used per ear: 2063, 2531, 2953, 3563, 4172, 4969, 5953, 7031, 8391, and 10,031 Hz. A normal DPOAE value was defined as a distortion product (DP) >0 with a difference between DP and noise floor (NF) >6. Reduced and absent OAEs for any given frequency were defined as "abnormal." A reduced value was defined as a DP <0 with a DP-NF >6. An absent value was defined as a DP-NF <6. To pass the DPOAE screen,

normal responses in more than 6 out of 10 frequencies in both ears were required; otherwise the subject was considered a "referral" for potential hearing loss evaluation after discharge.

Subjects admitted to the NICU were also screened with AABR tests prior to discharge from the hospital by OHSU Audiology staff using already-established institutional hearing screening protocols. The Natus ALGO 5 AABR hearing screener was used to complete a physiologic screen of the auditory pathway. Screening involved placing 3 sensors (forehead, nape of neck, and shoulder) and a set of earphones over the ears. Soft click stimuli (35 dB nHL) were presented through the earphones at a rate of 37 clicks/second. During the test, sound traveled through the outer ear and middle-ear and into the cochlea, where it was converted into an electrical signal that travels along the auditory nerve and generates identifiable brainwaves that were processed and analyzed by the ALGO screener. Each ear was analyzed separately. A statistical detection algorithm was used to determine if brainwave responses matched normative data. Subjects were categorized as a 'pass' if responses were within the normative data, otherwise they were categorized as a 'refer'. The subjects screened with AABR were of at least 34 weeks corrected gestational age, and close to discharge from the hospital. If a subject did not pass the initial screening, a second screening was completed at a later time and prior to discharge. If a subject received a second 'refer', the subject was referred for diagnostic audiologic testing. Diagnostic audiologic evaluations post-discharge from the NICU were assessed by chart review in EPIC. Statistical analysis was performed using Stata version 13.1, using the "cs" command for cohort risk-ratio calculations.

B.4 – Results

Thirty-six (39.5%) of the 91 subjects in this cohort would have been referred for follow-up diagnostic audiology testing based on our DPOAE screening criteria, including 23 (25%) with combined low frequency (2063–3563 Hz) and high frequency (4172–10,031 Hz) referrals. Thirteen (14%) subjects would be referred only on the high frequency range and not the low frequency range. This is compared with 6 subjects (6.32%) that were referred based on standard clinical AABR screening criteria. Five of these 6 (83%) referred both on AABR and on DPOAE screening, while one referred on

AABR, but passed the DPOAE screen. Therefore, the DPOAE screen identified an additional 7 subjects with potential high frequency hearing loss, frequently associated with initial onset of ototoxicity, that were not identified with the standard AABR screen (*490, 491*). Among the 91 subjects, 74 (81%) had intravenous gentamicin exposure at least once during their NICU admission. Twenty (22%) had ≥4 days of gentamicin, and 71 (78%) had <4 days, including 17 (18.7%) with zero gentamicin dosing. The risk ratio (RR) of a DPOAE referral with ≥4 days of gentamicin, regardless of inflammation status, was 1.92 ($p = 0.01$, 95% CI: 1.22, 3.03).

Eighteen (20%) out of 91 subjects showed clinical evidence of systemic inflammation (7 with sepsis; 11 with neonatal SIRS). Nine of these 18 received ≥5 days of gentamicin, with a DPOAE referral risk ratio of 2.12 compared to all subjects receiving <5 days of gentamicin ($p = 0.02$, 95% CI: 1.35, 3.34). The risk ratio of a DPOAE referral in sepsis/SIRS subjects at the lower threshold of ≥4 days of gentamicin (11/18) compared to the rest of the subject cohort trended toward statistical significance (RR = 1.70, $p = 0.09$, 95% CI: 1.00, 2.88). Twenty (22%) subjects had gentamicin treatment overlapping with other known synergistic ototoxic agents – vancomycin or furosemide – the risk ratio, when comparing this group to the rest of the cohort, also trended toward significance (RR = 1.77, $p = 0.050$, 95% CI: 1.08, 2.88; **Table B.3**).

At 18 months after discharge of the last enrolled subject, less than one-third of subjects had retrievable follow-up diagnostic audiometric data available for review. This insufficient follow-up data could not be used to draw any analytical conclusions on the relationship between gentamicin exposure and subsequent performance on DPOAE testing by providing corroborative diagnostic audiometric analysis.

Blood panel measures including white blood cell count, albumin levels and calcium levels were reviewed to categorize states of inflammation as well as characterize the pharmacokinetics of gentamicin dosing. The average white blood cell count per day per patient was a largely incomplete data set, and did not yield usable data for analysis. The average albumin value on the days subjects with sepsis/SIRS received gentamicin was 2.17, whereas the remaining subjects had an average of 2.43. The average calcium for subjects with sepsis/SIRS on days gentamicin was administered was 8.91, whereas the other 73 subjects had an average of 8.11. However, there was no significant relationship

between these lab values, gentamicin exposure and referral on DPOAE or AABR screening.

B.5 – Discussion

Previous studies have reported that ototoxicity from aminoglycoside antibiotics ranges between 2% and 25%, and that the rate of hearing loss in the NICU setting ranges between 2% and 15%, compared to 0.3% in full-term births (*478, 482*). A substantial part of this differential prevalence of hearing loss between NICU graduates and full-term births may be associated with intravenous gentamicin administration due to clinical observation of sepsis and/or SIRS, as well as potential ototoxic synergy of aminoglycoside treatment with concomitant vancomycin, and/or loop diuretics (*315, 394, 492-495*). Some of the risk for this increased prevalence of hearing loss may also be due to systemic inflammation secondary to bacterial infection (sepsis, necrotizing enterocolitis, gastroschisis, among other etiologies), and subsequent lysis of bacteria, over and above the ototoxic properties of aminoglycoside antibiotics.

Lipopolysaccharide (LPS), an endotoxin in the outer membrane of gram-negative bacteria, is released into the serum following bacterial cell lysis, leading to a robust immune response, activation of macrophages and subsequent release of pro-inflammatory cytokines (*314, 394*). Prior studies have shown that LPS potentiates the ototoxicity of aminoglycosides and loop diuretics, leading to extensive high frequency hearing loss (*315, 394*). Markers of inflammation and LPS increase cochlear uptake of aminoglycosides, particularly into the highly vascularized stria vascularis, potentially due to dysregulation of the integrity of the blood–labyrinth barrier (*394, 407, 425*). Increased aminoglycoside trafficking across the stria vascularis will lead to greater clearance into endolymph and uptake by cochlear hair cells across their apical membrane and greater ototoxicity and sensory hair cell loss (*310, 394, 427, 428*).

Our data show that subjects who receive 4 or more days of gentamicin treatment, i.e. longer than the standard broad-spectrum rule-out sepsis treatment of gentamicin plus ampicillin of 2–3 days (while blood culture results are pending for narrowing of antibiotic therapy) are at an increased risk for hearing loss. Subjects with identified sepsis, as well as those with SIRS, are at even higher risk for hearing loss following

gentamicin exposure compared to those without signs of inflammation. Subjects with inflammation tend to receive longer treatments of gentamicin as they are sicker, and receive more gentamicin treatment to eradicate the infection. Thus, NICU patients, especially those with sepsis/SIRS, are at higher risk for ototoxicity after receiving intravenous gentamicin treatment. It is crucial for NICU providers to carefully consider the duration of exposure to gentamicin and the consequent risk of hearing loss in their patients. A swift change to non-ototoxic antibiotic therapy should be a priority once the causative organism has been identified via positive blood culture or other means of bacterial species identification. There was also a trend toward significance when gentamicin treatment overlapped with other ototoxic medications such as furosemide and/or vancomycin in the NICU population, despite their low percentage within this small cohort, making this population very vulnerable for potential hearing loss.

Another study of young adults showed that DPOAEs in the 4–8 kHz range are affected by UHF (ultra-high frequency) hearing loss in the 11.2–20 kHz range, and concluded that this may be due either to outer hair cell damage not yet detected by pure-tone thresholds, or to damaged basal cochlear (high frequency) outer hair cells that then dysregulate more apical (lower frequency) cochlear functions (*496*). Further, DPOAEs have been shown to successfully detect high-frequency ototoxicity (at 8, 9, and 10 kHz) following streptomycin administration in adult human subjects (*497*). Other studies have investigated DPOAEs combined with AABR as a method for detecting potential hearing loss in the neonatal population, with mixed results (*498, 499*). In spite of these mixed results, it has been shown that DPOAE is a more sensitive test than AABR for early detection of gentamicin ototoxicity, and that two-stage screening protocols using both DPOAE and AABR yield lower false-positive rates with specificity >94% (*481, 500*).

Prior studies have examined the factors that can lead to a "false referral" using DPOAE equipment (*501, 502*). Some of these factors include middle-ear fluid collection/infection, probes too thick to fit the size of the subject's external meatus, and improper seal of the probe with the external meatus. Several studies have found that DPOAE false-positive rates are higher in the lower frequency ranges compared to high frequency ranges (*485, 501, 503*). Another study examining a cohort of 350 randomly selected NICU babies and non-hospitalized healthy babies found a 0.003% false negative

rate and a 0.028% false positive rate of DPOAE referrals, when comparing TEOAEs (transient evoked otoacoustic emissions) to DPOAEs (*502*). Based on this study, it is unlikely that our referral criteria resulted from false-positive DPOAE referrals.

The major limitation of this study is the lack of follow-up diagnostic audiology, with data only available from less than one-third of subjects. This lack of follow-up data is partly a consequence of study design. Funding for parents to attend follow-up appointments, and other necessary preparations were not incorporated into this pilot study design. The lack of data may also be due to parent inability to access care, lack of need for follow-up due to normal initial AABR screen, subjects living or moving out of state and follow-up audiology data not incorporated in this state's Early Hearing Detection and Intervention database, or other unknown factors. This issue has so far prevented the longitudinal study of these subjects to better determine the long-term hearing outcomes of subjects exposed to gentamicin after discharge from the NICU. However, our data suggest that DPOAE screening in the NICU setting, in addition to the already-performed AABR, is useful to screen patients for high-frequency hearing loss due to ototoxicity that might otherwise be missed by the standard AABR hearing screen alone.

B.6 – Conclusions

This study reports an association between neonates receiving ≥4 days of intravenous gentamicin and an increased referral rate on DPOAE screening. This could contribute to the increased hearing loss rates observed in the NICU setting. Subjects with sepsis or SIRS (i.e., inflammation) are at higher risk of hearing loss. We propose an expanded study to gather a larger cohort of subjects, including those with sepsis and neonatal SIRS, to increase the statistical power of these observations. In addition, subsequent studies need to obtain reliable follow-up diagnostic audiological data to further verify whether the DPOAE screening data, in addition to the use of the standard AABR screen, is a reliable predictor of permanent hearing loss due to cumulative gentamicin dosing in the NICU.

Table B.1. Subject demographics and other pertinent characteristics.
Ninety-one subjects were enrolled; 7 subjects were septic, and 11 met SIRS criteria. No subjects had hyperbilirubinemia ≥30 mg/dl, though 73% received phototherapy. No subjects had meningitis or seizures. Only 3% had any kind of TSH abnormality. Only gentamicin exposure and sepsis/SIRS status were used for analysis with DPOAE referral.

	Range [lower limit, upper limit]	**Mean (SD)**	**Number (%)**
Gestational age (weeks)	[24.14, 36.9]	33 (2.96)	
Gender: male/female			54 (59%)/37 (41%)
Length of stay in NICU (days)	[3, 215]	34.7 (36.7)	
Race			
White/Caucasian			70 (77%)
Hispanic/Latino/Pacific Islander			21 (23%)
Birth weight (kg)	[0.61, 3.255]	1.87 (0.61)	
Birth weight < 1.5 kg			25 (27%)
APGAR Score (1 min)			
≤6			40 (44%)
≥7			51 (56%)
APGAR Score (5 min)			
≤6			21 (23%)
≥7			70 (77%)
Hyperbilirubinemia			73 (80%)
>30 mg/dl			0 (0%)
Required phototherapy			67 (73%)
Required exchange transfusion			0 (0%)
Subjects with signs of inflammation			18 (20%)
Sepsis			7 (8%)
Meet SIRS criteria			11 (12%)
Gentamicin exposure			74 (81%)
<4days			71 (78%)
≥4 days			20 (22%)
Vancomycin exposure			16 (18%)
Loop diuretic exposure (furosemide)			13 (14%)

	Range [lower limit, upper limit]	Mean (SD)	Number (%)
Meningitis			0 (0%)
Seizures			0 (0%)
TSH abnormality			3 (3%)

Table B.2. Pediatric SIRS criteria used to identify subjects with SIRS by electronic health record review.

Only subjects meeting SIRS criteria on the same day as receiving intravenous gentamicin were considered for this analysis. If a subject met SIRS criteria, but did not receive gentamicin on that day, the subject was not categorized as a SIRS plus gentamicin subject in this analysis.

Age group	**Tachycardia**	**Bradycardia**	**Respiratory rate (breaths/min)**	**Leukocyte count leukocytes × 10^3 mm^{-3}**	**Systolic blood pressure (mm Hg)**
0 days to 1 week	>180	<100	>50	>34	<65
1 week to 1 month	>180	<100	>40	>19.5 or <5	<75
1 month to 1 year	>180	<90	>34	>17.5 or <5	<100
2–5 years	>140	N/A	>22	>15.5 or <6	<94
6–12 years	>130	N/A	>18	>13.5 or <4.5	<105
13 to <18 years	>110	N/A	>14	>11 or <4.5	<117

Source: Adapted from Goldstein et al. (*40*).

Table B.3. Overlapping administration of ototoxic medications.
Medication overlap was widespread in this cohort. Overlap was defined as at least one day of receiving either vancomycin or furosemide on the same day as gentamicin treatment. Fourteen (15%) of 91 subjects had overlap between gentamicin and vancomycin. Six (6.6%) of 91 subjects had overlapping gentamicin and furosemide treatment. There were three sepsis subjects who overlapped all three medications, and two subjects with SIRS who overlapped all three medications. Medication overlap was found to almost be a significant factor associated with referral on the DPOAE screen ($p = 0.05$).

	91 total subjects in cohort	**Subjects with gentamicin overlap**	**Subjects with gentamicin overlap and ≥4 days of gentamicin**	**7 subjects with sepsis**	**11 subjects with SIRS**
Vancomycin exposure	16 (18%)	14 (15%)	11 (79%) 4 of whom were septic 4 of whom met SIRS criteria 3 without sepsis or SIRS	4 subjects with sepsis, who had overlapping vancomycin and gentamicin exposure	4 subjects with SIRS, who had overlapping vancomycin and gentamicin exposure
Furosemide exposure	13 (14%)	6 (6.6%)	5 (83%) 3 of whom were septic 2 of whom met SIRS criteria	3 subjects with sepsis, who had overlapping furosemide, vancomycin, and gentamicin exposure	2 subjects with SIRS, who had overlapping furosemide, vancomycin, and gentamicin exposure

Appendix C: Development of A Thin Cochlear Window to Observe Cochlear Blood Flow

Thin and open vessel windows for intra-vital fluorescence imaging of murine cochlear blood flow

Authors: Xiaorui Shi, Fei Zhang, Zachary Urdang, Min Dai, Lingling Neng, Jinhui Zhang, Songlin Chen, Sripriya Ramamoorthy, Alfred L. Nuttall

Oregon Hearing Research Center, Department of Otolaryngology/Head & Neck Surgery, Oregon Health & Science University, Portland, OR, USA

Appendix C is modified from the paper published in Hearing Research April 15th, 2014.

Contributions: Zachary was the first to achieve a thin-window for observation of cochlear blood flow. Zachary performed some of these experiments and analyzed the data. Zachary co-wrote and edited the manuscript and presented at ARO 2012.

C.1 – Abstract

Normal microvessel structure and function in the cochlea is essential for maintaining the ionic and metabolic homeostasis required for hearing function. Abnormal cochlear microcirculation has long been considered an etiologic factor in hearing disorders. A better understanding of cochlear blood flow (CoBF) will enable more effective amelioration of hearing disorders that result from aberrant blood flow. However, establishing the direct relationship between CoBF and other cellular events in the lateral wall and response to physio-pathological stress remains a challenge due to the lack of feasible interrogation methods and difficulty in accessing the inner-ear. Here we report on new methods for studying the CoBF in a mouse model using a thin or open vessel-window in combination with fluorescence intra-vital microscopy (IVM). An open vessel-window enables investigation of vascular cell biology and blood flow permeability, including pericyte (PC) contractility, bone marrow cell migration, and endothelial barrier leakage, in wild type and fluorescent protein-labeled transgenic mouse models with high spatial and temporal resolution. Alternatively, the thin vessel-window method minimizes disruption of the homeostatic balance in the lateral wall and enables study CoBF under relatively intact physiological conditions. A thin vessel-window method can also be used for time-based studies of physiological and pathological processes. Although the small size of the mouse cochlea makes surgery difficult, the methods are sufficiently developed for studying the structural and functional changes in CoBF under normal and pathological conditions.

C.2 – Introduction

Normal function of the microcirculation in the cochlear lateral wall is critically important for maintaining ion and fluid balance in the inner-ear. Sensory hair cells are strikingly vulnerable to ischemia, and disruption of cochlear blood flow (CoBF) is implicated in many inner-ear pathologies (*165, 504-512*). Surgical access to the cochlea, however, is challenging. Direct measurement of CoBF is difficult and techniques for assessing blood flow are still under development. Various methods are used for assessment of CoBF, including laser-doppler flowmetry (LDF), magnetic resonance imaging (MRI), fluorescence intra-vital microscopy (FIVM), fluorescence microendoscopy (FME), as well as approaches based on injection of dye labeled or radioactive microspheres into the blood stream (*513-520*). Approaches such as LDF, MRI, and injection of microspheres into the blood plasma are limited in providing information on relative change in blood flow rather than absolute flow rate in individual vessels. FME, a powerful tool for studying CoBF which consists of a flexible imaging fiber coupled to a system for detecting fluorescence, enables investigation of CoBF in single vessels. While FME is limited to certain cochlear areas, including the round window membrane, spiral ligament, and osseous spiral lamina, the endoscope is versatile and small enough for relatively non-invasive imaging of regional (near the round window) blood flow. It is not suitable, however, for imaging blood flow in the stria vascularis. Recently developed optical microangiography (OMAG) enables visualization of CoBF in the apical area of the intact cochlea, however, the method provides less sufficient resolution to resolve individual capillaries of the stria vascularis in a mouse model (*520*).Fluorescent IVM in combination with a vessel-window in the cochlear otic wall enables sufficient optical resolution for investigation of capillary diameter and blood flow velocity under experimental conditions. It is an established and well validated method for research of lateral wall pathophysiology in larger rodents such as the guinea pig (*521-523*). IVM provides excellent temporal resolution for real-time tracking of changes in cochlear hemodynamics *in vivo*. However, IVM has not heretofore been developed for the murine model. In this report we demonstrate the feasibility of open and thin vessel-window preparations in an adult mouse model using an FIVM system. Both

thin and open otic windows provide quantitative images useful in studies of lateral wall CoBF. A thin vessel-window minimizes damage and experimental artifacts in *in vivo* imaging of cochlear events and opens opportunities for longer time series imaging of the cochlear microcirculation in mouse models. By contrast, an open vessel-window preparation provides for better resolution and easier application of pharmacological agents to the cochlear lateral wall (e.g, therapeutic or totoxic agents), but at the cost of possibly disturbing cochlear homeostasis. Nevertheless, the two methods do provide complimentary means for studying structural and functional changes in the cochlear microcirculation under normal and pathological conditions. Application of these techniques with recently developed transgenic mice models has the potential for significantly advancing research on CoBF, particularly for unraveling the links between hearing function and pathology related to CoBF and the blood-labyrinth barrier.

C.3 – Materials and Methods

C.3.1 - Animals

Mice used in this study were purchased from the Jackson Laboratory, including the strains C57BL/6J (stock number: 000664, ages: 6–8 weeks); C57Bl/6-Tg mice (UBC-GFP, stock number: 004353, ages: 4 weeks); CBA/CaJ mice (stock number: 000654, ages: 6 ~ 8 weeks); NG2DsRedBAC transgenic mice (stock number: 008241000664, ages: 8 ~ 12weeks). CBA/CaJ mice were used in the sound stimulation experiments. C57BL/6J and 57Bl/6-Tg mice were used in bone marrow transplantation experiments [C57Bl/6-Tg mice served as donor mice, C57BL/6J mice the recipients, reconstituted green fluorescence protein (GFP) labeled-bone marrow derived cells (GFP-BMDCs) were assessed at age 18 months]. Neural/Glial antigen 2 (NG2) DsRedBAC transgenic mice were used in experiments to study pericytes (PCs). All animal experiments reported here were approved by the Oregon Health & Science University Institutional Animal Care and Use Committee (IACUC). The approval number is MU7_IS00001157. Euthanasia was carried out using methods approved by the American Veterinary Medical Association Panel on Euthanasia.

C.3.2 - Surgical preparation

C.3.2.1 - Surgery to create an open window

The mice were anesthetized with an i.p. injection of a mixture of ketamine (100 mg/ml; 0.067 mg/gm) and xylazine (20 mg/ml; 0.013 mg/gm) wrapped in a heating pad, and maintained with rectal temperature approximately 37 °C. Anesthetic depth was ascertained by monitoring the paw reflex and the general muscle tone. The left bulla was opened via a lateral and ventral approach, leaving the tympanic membrane and ossicles intact (*522*). Two different methods can be employed to create an open vessel-window: (1) The open vessel-windows can be created using a small knife blade (a custom milled #16 scalpel) to make a rectangular fenestrate (approximately 0.1 × 0.1 mm) over the spiral ligament. The area is by gently scored and then elevated with the knife (*522*).

(2) The open vessel-window can be created by scraping the lateral wall bone until a thin spot is cracked. The bone chips are removed with small wire hooks, and a window opened over the spiral ligament. The latter method is generally found more convenient. In both procedures the vessel-window is covered with a cut microscope coverslip (Cat# 12–542A, Fisher Scientific) to preserve normal physiological conditions and provide the best optical view for recording vessel images.

C.3.2.2 - Surgery to create a thin vessel-window

In preparation for a thin vessel-window, the mucosa on the bone of the basal turn was first removed and then the bone dried using sterile cotton swabs. Using the same custom milled #16 scalpel (as above), the bone was thinned with extremely slow and gentle cutting. No direct downward pressure was applied to the bone. The thickness of the cochlear lateral wall was occasionally checked by adding saline to the thinned area and viewing it in the operating microscope. The bone cutting was accomplished by light sweeping motions nearly parallel to the cochlear lateral wall were used (when thinning the cochlear wall fails, the speed and volume of perilymph leakage indicates the fistula). In preparation for a 'chronic' thin vessel-window, the opened bulla was cleaned with sterile gauze and sealed with a piece of $3 \times 2 \times 1$ mm^3 subcutaneous adipose tissue. The surgical wound was closed under sterile conditions. Immediately after the procedure was completed, the animal received a subcutaneous injection of meloxicam at 1 mg/kg. To re-assess the thinned window, the bulla was re-opened and adipose tissue gently removed. If necessary, the area of the thin otic capsule was recreated by removing any fibrous tissue using the custom made scalpel blade. The thickness of the fibrous tissue in the 'chronic' preparation is dependent on the intervening time between the two consecutive experiments. If the two experiments are done within one week, the fibrous tissue over the tinned vessel-window is relatively thin. Thicker fibrous tissue occurred when more than one week intervened between experiments. This procedure can be repeated to allow further experiments. Meloxicam was administered at the same dose as described previously for recovery surgery).

C.3.3 - Recording CoBF with fluorescein isothiocyanate dextran (FITC-dextran) labeling of blood plasma

CoBF was visualized using FITC-dextran dye as a contrast medium for the blood stream (*522*). FITC-dextran (see **Table C.1** Sigma) was slowly administrated intravenously to the mouse at a concentration of 40 mg/ml in 0.1 ml physiological solution over a 5 min interval. The blood vessels were imaged using an Olympus BXFM fluorescence microscope equipped with a long working distance objective (20 × , 0.42 NA or 50 × , 0.55 NA). The instrument lamp housing includes a multiple band excitation filter (390/482/563/640 nm BrightLine® quad-band pass) and a compatible emission filter (446/523/600/677 nm BrightLine® quad-band band pass). The video was recorded with a Hamamatsu Orca-ER high resolution digital B/W CCD Camera (model C4742-80-12AG) at a rate of 30 frames/sec and digitally saved to a computer disk. By adjusting the optical focus, blood vessels of either the spiral ligament or the stria vascularis can be 'imaged'.

C.3.4 - Blood vessel diameter, blood flow velocity and vascular permeability measurements

The internal (luminal) diameter of the capillaries was determined from acquired images. Image J was used to determine the distance between two fixed points across the capillary (*510*). Capillary diameter was measured at locations of maximum response. Dilation was assessed as a percentage of the baseline diameter. Blood velocity was determined from captured video frames and analyzed off-line, calculated by a cross-correlation method using custom-made image analysis software (*510*). In brief, the luminal intensity spatial structure is captured in image sequences which are cross-related using the custom software. For two locations along a vessel the time difference of maximum correlation was determined. Blood flow velocity was calculated by dividing the spatial distance between the image locations (D) by the time difference.

Vascular permeability *in vivo* was assessed by recording tracer movement observed through the prepared open vessel-window. Vascular permeability in control and noise-exposed animals (immediately at the cessation of the loud sound stimulation

regime) was assessed using a FITC conjugated bovine albumin tracer (see **Table C.1** FITC–albumin, 66 kDa, A-9771, Sigma). FITC-albumin (40 mg/ml in 100 μl saline) was i.v. administered into the femoral vein of the anaesthetized mouse 10 min prior to recording. Albumin leakage was quantified by comparing the mean fluorescence intensity (I) of two 10 × 5 μm windows: one window within the vessel (I_v) and the other in the perivessel interstitium (I_i), 10 μm away from the vessel wall. $I_{background}$ was measured as the mean intensity over the observed area just prior to intravenous infusion of FITC–albumin (with video analysis software). The albumin leakage index (Alindex) was calculated as $[(I_i - I_{background\ away\ from\ vessel\ area})/(I_v - I_{background\ away\ from\ vessel\ area})] \times 100\%$ (*524*).

C.3.5 - Imaging and assessment of PC contractility

To better visualize fluorescently labeled PCs in NG2DsRedBAC transgenic mice, blood vessels were labeled with FITC-dextran. PCs were recognized by the red fluorescence signal of the NG2DsRedBAC excited at 563 nm wavelength, the emission fluorescence acquired through a 600 nm filter. Blood vessels were visualized by exciting at 482 nm and collecting the emission through a 533 nm filter. The created open vessel-window was monitored by video-microscopy using a long working-distance objective lens (20 × , NA 0.42).

To determine PC contractility, extracellular $CaCl_2$ at 10 mM was topically perfused to the open vessel-window. Blood vessel diameter was measured before and after $CaCl_2$ application, and the effect of $CaCl_2$ on PC contractility analyzed. Image J software was used to measure the luminal diameters at both PC and non-PC locations (more than 10 μm distant from the PC soma). Luminal diameter near PC and non-PC locations, as well as the size of PCs, was measured at the beginning of the perfusion of the agent and at the time when the change in diameter was a maximum.

C.3.6 - Bone marrow cell transplantation

The method of bone marrow cell transplantation was previous published (*525*). Briefly, recipients (C57BL/6J mice) were irradiated (at 9 Gy) with γ-emitting source and reconstituted with a single periorbital sinus injection of 2×10^7 GFP$^+$-BMDCs in 200 μl of

modified HBSS from donor transgenic C57Bl/6-Tg mice. Two transplanted mice (age 18 months from a group of mice used in different study) were used to visualize fluorescent labeled bone marrow cells in the opened window. To visualize the capillary boundary, endothelial cells were pre-labeled with the fluorescent dye 1,1-Dioctadecyl-3,3,3,3-tetramethylindocarbocyanine Perchlorate Dil (*510*), dissolved in dimethyl sulfoxide (DMSO, 6 mg/ml, 472301, Sigma). Immediately prior to i.v. infusion, the stock solution was diluted with PBS to a final concentration of 3 mg/ml, filtered, and injected into the mouse's femoral vein. 0.1 ml of the dye solution was slowly administrated over a 5 min interval. Since DMSO has an effect on vessel diameter (*526*), the final concentration of DMSO in Dil was less than 0.01% by volume.

To visualize GFP-BMDC migration in the cochlear lateral wall, the vessels were labeled with fluorescence dye Dil. The GFP-BMDCs were observed through the vessel-window at 482 nm excitation and 523 nm emission. Vessels were visualized at 563 nm excitation and 600 nm emission. The images were recorded with a CCD camera at 30 frames/sec and digitally saved.

C.3.7 - Measurement of the endocochlear potential (EP)

The method used to measure EP was previously reported (*162*). Briefly, the endocochlear potential was recorded under anesthesia as described above, with a silver–silver chloride reference electrode placed under the skin of the dorsal head. An incision was made in the inferior portion of the left post-auricular area and the bulla perforated, exposing the basal turn of the cochlea. A micropipette electrode (~2 μm) filled with 150 mM KCl was advanced through the surgical field into the spiral ligament in control and in experiment mice (immediately after creating an open vessel-window). Potentials were recorded with entry of the electrode tip into endolymph, and the electrode advanced until a stable potential was observed. The signal was amplified (model 3000 AC/DC differential amplifier; A-M Systems, Inc.) and displayed in real-time to guide the procedure. DC potentials were digitalized by an A/D converter and recorded on a computer. The calibrated computer recording was used to measure the EP potential in a post-procedure analysis.

C.3.8 - Measurement of thickness of the thinned otic bone

Cochleae from mice subjected to otic bone thinning and controls were perfused with 4% paraormaldehyde (PFA), with the cochlea subsequently harvested, post-fixed in 4% PFA at 4 °C, and decalcified overnight in Decal® bone decalcifier. The decalcified cochlea was rinsed with two changes of PBS, and dehydrated in graded ethanol baths from 70% to 100%. Baths were repeated two times for 30 min at each ethanol concentration. The cochlea was then cleared with at least two changes of citrisolve or until the tissue was fully translucent. Next the cochlea was bathed 2X for 45 min in paraffin wax embedding medium under vacuum at 56 °C. The cochlea was then oriented in a tissue mold and embedded in paraffin wax. The tissue was cut into 5 μm thick sections, collected on Superfrost Plus glass slides, and incubated for 2 h at 60 °C for adhesion. The specimens were viewed under DIC microscopy on an inverted FV1000 Olympus laser-scanning confocal microscope and thin section micrographs were recorded. Using a calibrated reticle, thickness of the otic bone was assessed ex-vivo for 10 mid-sections, 5 thin otic windows and 5 controls.

C.3.9 - Sound stimulation

For ‘medium-level’ sound stimulation, a 40 kHz pure tone (a frequency localized for stimulation of the basal turn) was applied in the external ear canal. Sound was administered closed field at an intensity of 85 dB SPL. CoBF was recorded for 3 min prior to sound stimulation, the last 3 min of the 10 min stimulation session, and for an additional 3 min with the sound stimulation turned off.

For exposure to noise (‘high-level’ sound), the animals were placed in wire mesh cages and exposed to broadband noise at 120 dB SPL in a sound exposure booth for 3 h and for an additional 3 h the following day. The noise exposure regime, routinely used in our laboratory, produces permanent loss of cochlear sensitivity (*527*).

C.3.10 - Isolation of the cochlear stria vascularis

After the thin window was created, the whole cochlea was isolated and the thin vessel-window was opened. The whole cochlea was immersed in 4% PFA fixative overnight. The entirety of the stria vascularis was isolated under a dissecting microscope and the isolated tissue imaged under a light microscope. The location of thin-vessel-window was identified by the 'left-over bone chips' on the edges of surgical vessel-window. Location of the vessel-window was determined using a calibrated reticle.

C.3.11 - Statistics

All experiments were performed multiple times to validate the observations, with the data expressed as means ± SD. Statistical analysis was conducted using a Student's *t* test. A 95% confidence level was considered statistically significant.

C.4 – Results

C.4.1 - Visualization of blood vessels in the cochlear lateral through thin and open vessel-windows

The location of the thin and open vessel-windows made at the basal turn of the mouse cochlea is shown in **Fig. C.1A** (indicated by the dotted rectangle area). **Fig. C.1B-C** compare the optical quality of *in vivo* lateral wall blood vessels through thin and open vessel-windows. Blood vessels can be visualized with an intravenous injection of FITC-dextran to the blood plasma in both window preparations. However, the image quality of blood vessels viewed through an open vessel-window is discernibly better than through the thin vessel-window.

In the thin vessel-window preparation, a thickness of otic bone approximately half the value of the thickness of an intact otic bone enables imaging useful for identifying vasculature. **Fig. C.1D–F** are paraffin cross sections, showing that non-thinned otic bone thickness in a normal adult, 4–6 week old CBA/CAJ mouse is approximately 72.2 ± 10.6 μm (n = 5, **D**), where the thinned otic bone was in the range of 31.0 ± 11.9 μm, n = 5, **E**). An opened otic bone is shown in **(F)**.

C.4.2 - Effect of an open vessel-window on EP

The thin window preparation leaves an intact lateral wall and minimizes disruption of the delicate homeostatic balance in the inner-ear. An open window approach can cause the loss of perilymphatic fluid or a micro-injury to the cochlear spiral ligament, altering cochlear homeostasis. To evaluate the quality of the open vessel-window, we measured the EP in individual animals when the open vessel-window was made. **Fig. C.2A – E** show representative EP recordings. The EP's of the five mice with an open vessel-window showed positive values ranging from +84 mV to +100 mV with a mean of +96.8 mV ± 8.7 (**Fig. C.2F**). Our results show the open vessel-window preparation does not substantially effect EP when surgery is conducted with extreme gentleness and care (**Fig. C.2F**, n = 5, $P > 0.05$).

C.4.3 - Research applications of the two window preparations

C.4.3.1 - An open vessel-window used to assess vascular leakage

An open vessel-window approach provides better spatial and temporal resolution of blood vessels compared to a thin vessel-window approach. For example, an open vessel-window preparation, combined with administration of a fluorescent tracer such as FITC-albumin, enables study of the vascular permeability in the cochlear lateral wall. **Fig. C.3** demonstrates vascular permeability in control (**A**) and noise-exposed mice (**B**). When animals were exposed to wide-band noise at 120 dB SPL for 3 h/day for two consecutive days, the barrier becomes more permeable to large substances such as FITC-albumin, consistent with our previous report (*527, 528*). The difference in FITC-albumin leakage in control and noise-exposed animals can be compared by measuring background fluorescent signal, as demonstrated in **Fig. C.3C** ($n = 5$, $^*P < 0.001$).

C.4.3.2 - An open vessel-window used to study PC contractility

An open vessel-window approach in combination with a transgenic mouse model can be used to study PC contractility. (NG_2) is specifically expressed in cochlear PCs (*529*). PCs can be clearly visualized using a transgenic NG2DsRedBAC mouse model combined with an open vessel-window and fluorescence IVM system. **Fig. C.4A** demonstrates that fluorescent labeled PCs are clearly visible on FITC–dextran labeled blood vessels through an open vessel-window.

Using the NG_2DsRedBAC transgenic mouse, in conjunction with an open vessel-window and time-lapse photography, the role of PC contractility in regulating capillary diameter in the mouse model can be analyzed by comparing changes in lumen diameter at PC and non-PC locations. **Fig. C.4B-C**, captured images before and 3 min after topical application of 10 mM $CaCl_2$ to show effect of the vasoactive agent on PC contractility. No obvious change in capillary diameter at both PC and non-PC locations before and after application of $CaCl_2$ was found. The method also permits *in vivo* study of the effect of other vasoactive agents such as adenosine triphosphate (ATP) and nitric oxide (NO) on

PC physiology, all important for understanding CoBF regulation at a microvasculature level.

C.4.3.3 - An open vessel-window used to track GFP⁺-BMDC migration

An open vessel-window preparation can be used to directly demonstrate that circulating bone marrow cells infiltrate to the cochlear lateral wall. Bone marrow derived stem cells have been shown to migrate to injured tissue such as the noise damaged cochlear lateral wall (*525, 530, 531*). With this preparation, GFP⁺-BMDC migration in an older (18 month) GFP⁻-BMDC transplanted normal mouse can be directly visualized and recorded *in vivo*. The GFP⁺-BMDCs are better observed when the vasculature is labeled with a red fluorescence dye such as DiI. **Fig. C.5A–F** show GFP⁺-BMDCs in the blood circulation and outside blood vessel under both low (20x lens, **Fig. C.5A–C**) and high magnification (50x lens, **Figs. C.5D–5F**).

C.4.3.4 - A thin vessel-window used to study the effect of sound on CoBF

The thinned otic bone preparation minimizes disturbance of underlying cochlear lateral wall tissue. A thin vessel-window approach can be utilized to study CoBF under physiological conditions. **Fig. C.6** demonstrates the effect of 'medium-level' sound on CoBF in a thin vessel-window preparation made in the region of the basal turn situated 80% from the apex (indicated by the red square in **Fig. C.6A**). This location maps to 40 kHz sound stimulation (based on the sound frequency-map of (*532*). With a thin vessel-window, we are able to measure the change in CoBF following 40 kHz sound stimulation at 85 dB SPL without surgically disturbing cochlear lateral wall tissues. **Fig. C.6**, a representative image, shows the optical quality of microvessels in the thin vessel-window. Panels C and D in **Fig. C.6** respectively show measurements of the change in vessel diameter (Δ diameter = 7.49%, $n = 15$, $^*P < 0.05$) and blood flow velocity (Δ velocity = 24.8%, $n = 15$, $^*P < 0.05$) in mice after 10 min of sound exposure.

C.4.3.5 - A thin vessel-window preparation can be used in longer time studies

A thin vessel-window can also potentially be used for some prolonged studies. For example, it can be used to assess the effect of drug treatment or multiple sound exposures on the same microvasculature. The bulla after each imaging session can be surgically closed and the blood vessels within the thin vessel-window can be imaged over the course of days. In **Fig. C.7**, we demonstrate the optical clarity of microvessels imaged through the thin vessel-window on days one, three, and seven after the window was created. The same microvasculature were clearly visualized after FITC-dextran was intravenously injected to the blood plasma. In this preparation, no evidence of perilymph leakage (i.e. accidental creation of a cochleostomy) was seen during multiple imaging sessions (though surgical skill is required to obtain these results).

C.5 – Discussion

Normal hearing requires tight control over cochlear microcirculation. Reduced CoBF and disruption of the BLB are closely associated with a number of hearing disorders (*504, 505, 507, 508, 510, 533-536*). However, techniques for assessing blood flow in the cochlear lateral wall are still under development. Here we report on new thin and open vessel-window approaches which, used in combination with fluorescence IVM, facilitate the study of CoBF and physiopathology of various lateral wall cell types in mouse models. Further progress in understanding cochlear microcirculation in mouse models, especially in transgenic models, will lead to a better understanding of CoBF associated cochlear homeostasis.

Two distinct networks, including the capillaries of the spiral ligament and capillaries of the stria vascularis, are arranged in parallel in the cochlear lateral wall (*152*). Spiral ligament capillaries are usually smaller in diameter than strial capillaries (*537*). The strial capillaries are tightly packed with red blood cells. The velocity of blood flow in the strial network is much slower than in vessels of the spiral ligament (*522*). Both capillary systems are essential for maintaining cochlea hemostasis, ion balance, and nutrient supply. The specific functions of the two vessel systems have not fully characterized. Smooth muscle cells in arteriole vessel walls and PCs on capillaries are thought to regulate lateral wall blood flow in the spiral ligament (*538*). In contrast, capillaries of the stria vascularis are highly specialized vascular epithelia which form into polygonal loops (*152*). These capillaries comprise the blood-labyrinth-barrier, similar to the BBB (blood-brain-barrier) and BRB (blood-retina-barrier). Strial capillaries have a minor role in blood flow regulation, but a crucial one in maintaining the EP, ion transport, and endolymphatic fluid balance essential for the ear's sensitivity (*512, 528, 539*).

In this study of the mouse cochlea, we demonstrate that both capillaries of the spiral ligament and capillaries of the stria vascularis can be visualized with fluorophore labeling in open or thin window preparations under a fluorescence IVM system. The setup of the IVM system permits convenient placement of the animal preparation and manipulation of microscope position in the x-y plane. The vessels of the spiral ligament

and vessels of the stria vascularis are distinguished by location and can be used to assess blood flow with adjustment of the optical focus. Most of the capillaries in the middle part of the spiral ligament passing in (optically) front of the stria vascularis run a more or less straight course from scala vestibule to scala tympani in the spiral ligament (*522*). These features enable the capillaries of the spiral ligament and stria vascularis to be distinguished.

In general, the choice of the thin or open window approach is determined by experimental goals. A thin vessel-window with intact lateral wall minimizes disruption of the delicate homeostatic balance in the inner-ear, but an open window approach provides better imaging resolution as well as better access to the tissue for stimulation with various drugs and chemicals. For example, the open vessel-window approach provides sufficient resolution for determination of vascular permeability and cell migration using different fluorescent tracers. Open vessel-windows are useful for examining changes in cell morphology, as well as pathophysiological parameters, in mouse models. PCs are of particular interest in cochlear physiology due to their role in modulating CoBF (*538*). In this study, using NG2DsRedBAC transgenic mice, the NG2 labeled PCs were readily observed in an open window preparation (**Fig. C.4**). Investigation of the contractility of PCs on the strial capillaries was facilitated by applying $CaCl_2$ to the open vessel-window. Change in vessel diameter at PC and non-PC locations was measured, with the level of change in capillary diameter taken as an indicator of PC contractility. An open vessel-window also proved extremely useful for tracing GFP+-cells in a second transgenic mouse model. In this study, we demonstrated the utility of the open window method in transgenic strains by observing GFP+-BMDCs in a post GFP+ bone marrow transplanted normal mouse (**Fig. C.5**). In the experiment, the microvasculature was labeled with the red fluorescent dye, Dil, and GFP+ transplanted cells observed as green fluorescence. Locations of the green fluorescence labeled cells were easily identified within and outside the vessel. GFP+ transplanted cells outside the vessel indicate bone marrow cell migration to the stria vascularis in the aged mice. The drawback of an open vessel-window approach is the high degree of surgical skill required. A vessel-window which does not unduly disturb the underlying tissue is essential for maintaining a constant EP. In most of our studies we were able to maintain a constant and normal EP (as shown in **Fig. C.2**).

The thin otic capsule window approach reported here is adopted from the thin cranial window, a technique widely used in brain studies (*540*). IVM is ideally suited to a thin cochlear vessel-window preparation for two reasons: 1) The original thickness of otic bone (approximately 70 μm) is thinned by half, reducing the optical scattering to levels sufficient for adequate visualization of vessels without the need to resort to 2-photon imaging and lower temporal resolution. 2) Imaging through a thin window leaves the lateral wall substantially intact, minimizing disruption of the delicate homeostatic balance in the inner-ear. The main drawback of the thin window preparation is the increased optical scattering (relative to the open window preparation) and the introduction of bone auto- fluorescence to increase the background signal of the image. However, these disadvantages are offset by the advantage of observing physiologically intact functional changes in CoBF and lateral wall biology. With intravenous injection of fluorescent dye, improvement to the signal-to-noise ratio enables observation of vessel diameter and blood flow velocity (**Fig. C.6**). The approach is preferred if time-series imaging is required to assess an effect on cochlear lateral wall physiology at multiple time points without disturbing the perilymphatic compartment. For example, a thin vessel-window approach can be used to determine the dynamic changes in blood flow velocity and vessel diameter immediately following and at different time points after certain applications. These methods can also be exploited to investigate the acute healing response to cochlear insults such as trauma, infection, noise, foreign bodies, ototoxic drugs, or potentially any agent affecting the lateral wall. Although many other imaging modalities exist for tracking cells of various phenotypes in the inner-ear, thin and open window methods have an advantage in unlocking a library of readily available transgenic mouse models for studying inner-ear pathophysiology. For example, two-photon microscopy bypasses the problem of otic capsule induced optical scattering. Two-photon imaging, using a long working distance air objective and thin-window preparation, in our experiments resulted in increased spatial resolution at the expense of temporal resolution (data not shown). The decrease in temporal resolution limits real time *in vivo* analysis to single vessels and introduces movement artifacts.

Overall, this study demonstrates that fluorescence contrast video imaging of the microcirculation, viewed through either thin or open windows on the cochlea, provides sufficient resolution for CoBF studies.

Table C.1. Fluorescence tracers applied in the study.

Name	Type	Company	Catalog number	Molecular weight
Fluorescein isothiocyanate dextran (FITC-dextran)	Reagent	Sigma–Aldrich	46945	70 kDa
1,1-dioctadecyl-3,3,3,3-tetramethylindocarbocyanine perchlorate (DiI)	Reagent	Sigma–Aldrich	46895	933.87 g/mol
Fluorescein isothiocyanate dextran (FITC-albumin)	Reagent	Sigma–Aldrich	A-9771	66 kDa

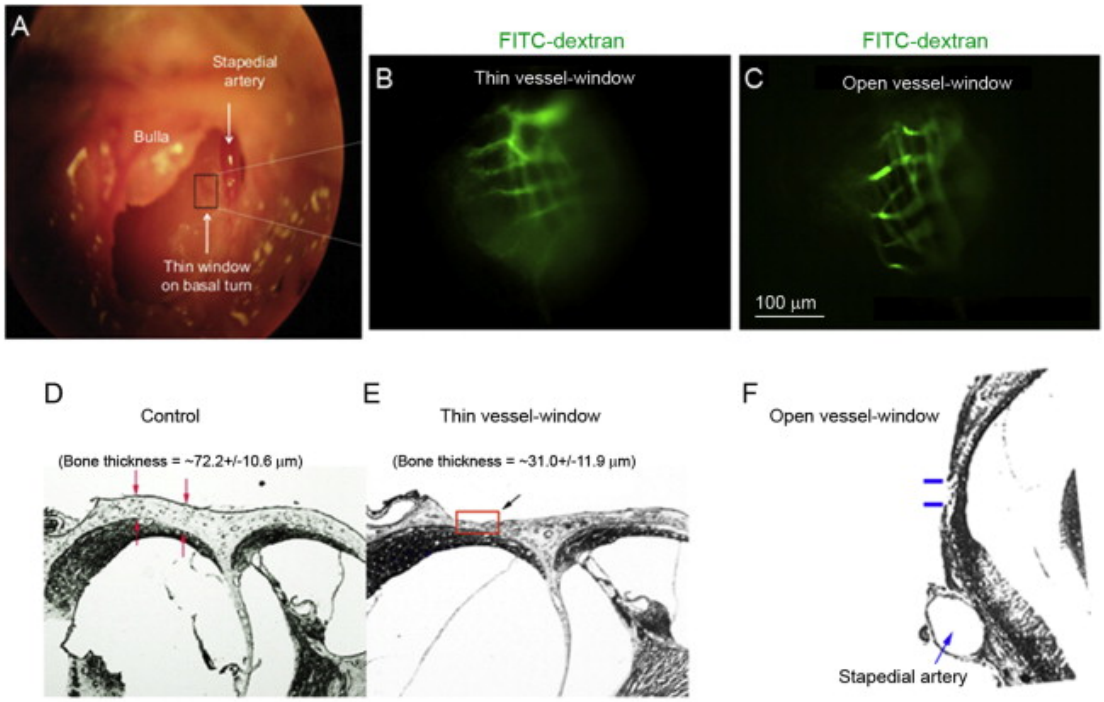

Fig. C.1. Thin and open cochlear vessel windows.

(A) The surgical view shows an opened bulla and location of the vessel-window (indicated by a black color rectangle in panel A) on the basal turn of a murine cochlea. Cochlear blood vessels are visualized with intravenously administrated FITC-dextran to the blood plasma. (B) and (C) show respectively *in vivo*captured images of strial blood vessels from a video monitor though a thin vessel-window and an open vessel-window. (D, E and F) Paraffin cross sections show the thickness of the otic bone in control (D), thinned otic bone (E, indicated by a red color rectangle), and open otic bone (F, indicated by blue color lines) preparations. (For interpretation of the references to colour in this figure legend, the reader is referred to the web version of this article.)

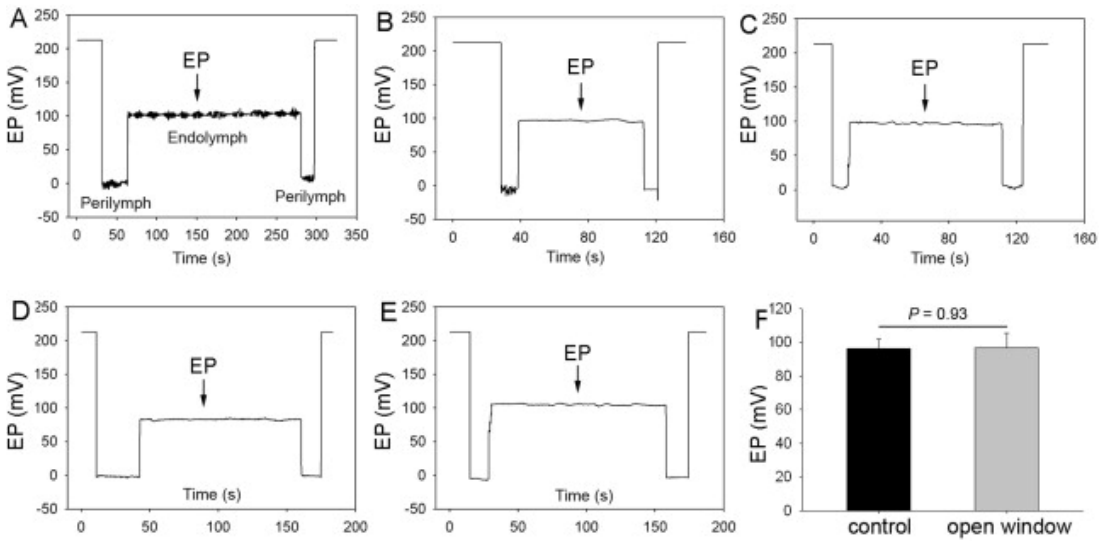

Fig. C.2. EP During window vessel observations.

Representative EP waveforms (A)–(E) and average EP (F) values in an open vessel-window cochlea. There is no statistical difference in EP between the control and an open vessel-window preparation ($n = 5$, $^*P > 0.05$).

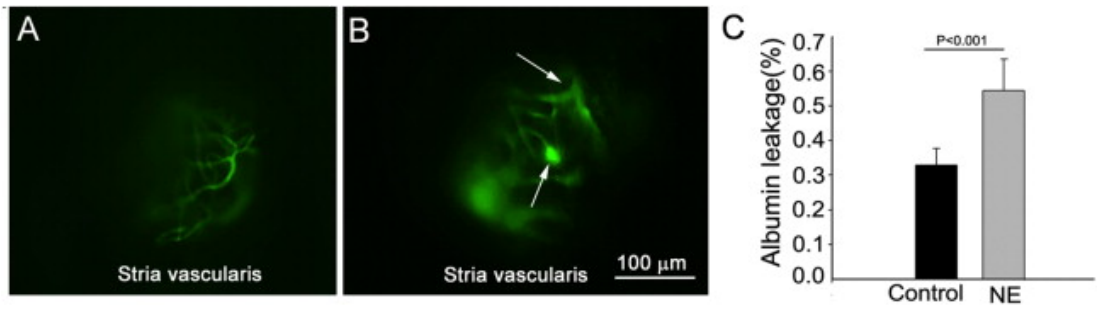

Fig. C.3. Vessel window vascular permeability studies.

An open vessel-window preparation was used to study vascular permeability in control and noise-exposed mice. (A) shows FITC-albumin labeled blood vessel from the stria vascularis in a control animal. (B) shows FITC-albumin extravasation from leaked capillaries in a noise-exposed animal. The arrows point out the leakage sites. (C) The difference in albumin leakage in control and noise-exposed animals, seen as a general increase in the background signal, was statistically significant ($n = 5$, $^*P < 0.001$).

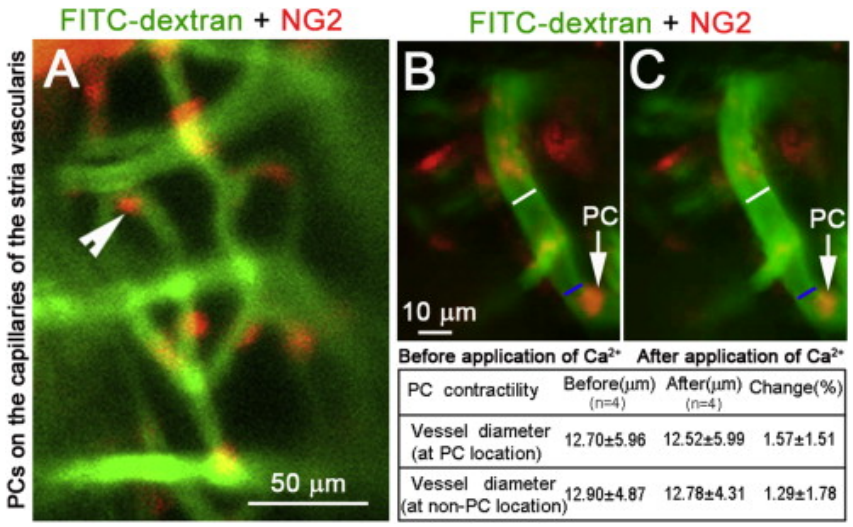

PC contractility	Before(μm) (n=4)	After(μm) (n=4)	Change(%)
Vessel diameter (at PC location)	12.70±5.96	12.52±5.99	1.57±1.51
Vessel diameter (at non-PC location)	12.90±4.87	12.78±4.31	1.29±1.78

Fig. C.4. Vessel window in transgenic fluorescent NG2 mouse strain.
An open vessel-window preparation was used to visualize PCs and determine PC contractility using a NG.DsRed labeled-PC transgenetic cell mouse model. (A) shows fluorescent labeled-PCs (red) distributed on the strial blood vessels labeled by intravenous injection of FITC-dextran. (B) and (C) show PCs contractility before and after application of 10 mM $CaCl_2$. White lines on images B and C indicate the measured site of blood vessel diameter at the non-PC location (~10 μm away from the PC site). Blue lines on images B and C indicate measured blood vessel diameter at PC location. There is no obvious change of vessel diameter at both PC- and non-PC locations (see data in the table).

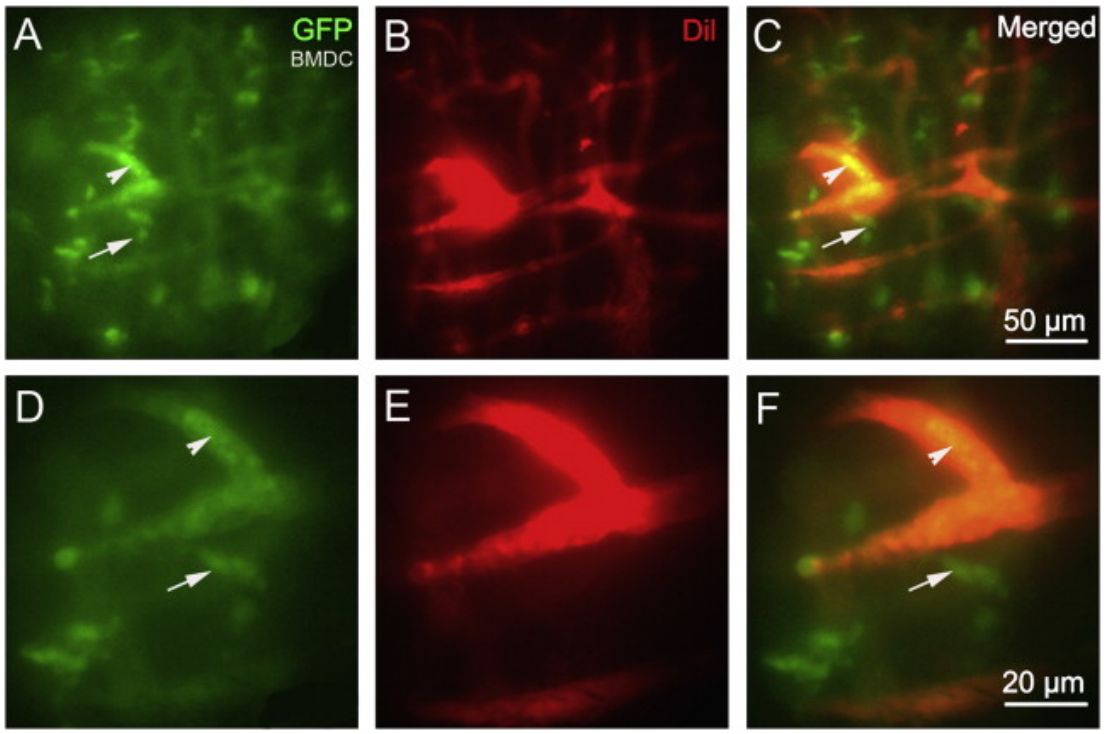

Fig. C.5. Thin window preparation in GFP-labeled bone marrow transplant mouse. An open vessel-window preparation was used to visualize GFP-BMDCs migration from cochlear lateral wall blood vessels in the lateral wall of a living mouse 18 months after bone marrow transplantation from a GFP donor mouse. (A)–(F) GFP-BMDCs are shown migrated outside the blood vessel (red, labeled by DiI) under both low magnification (A)–(C) and high magnification (D)–(F). (Arrowheads point out GFP bone marrow cells that are inside of the blood vessels. Arrows point out GFP positive bone marrow cells that are outside of the blood vessels). (For interpretation of the references to colour in this figure legend, the reader is referred to the web version of this article.)

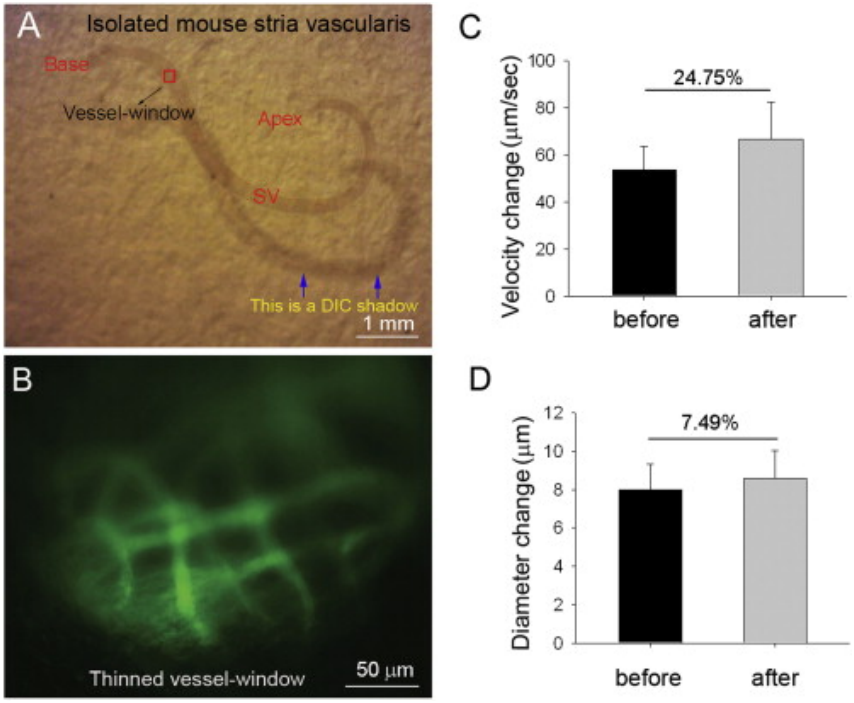

Fig. C.6. Cochlear thin window preparation blood flow velocity during sound exposure. A thin vessel-window preparation was used to study sound-induced changes in blood-flow velocity and blood vessel diameter. (A) Isolated tissue of the cochlear lateral wall, where the red square indicates the location of the thin vessel-window. (B) FITC-dextran labeled blood vessel are visualized with IVM imaging through the thinned vessel-window. (C)–(D) Changes in CoBF velocity (C) and blood vessel diameter under control and sound stimulated conditions (D, $n = 5$, $^*P < 0.05$).

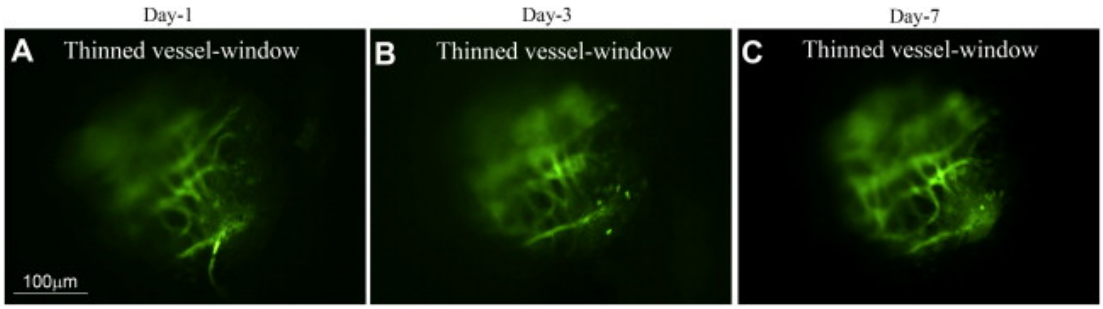

Fig. C.7. Chronic thin window vessel preparation for long-term cochlear vessel studies. A thin vessel-window preparation can be used for time-based studies. (A), (B), and (C) respectively show captured images of FITC-dextran labeled blood vessel from a video monitor though a thin vessel-window at days 1, 3, and 7 after the thin vessel-window was created. At all time-points the FITC-dextran labeled blood vessel can be clearly seen through the same thin vessel-window.

Appendix D: NAC Manuscript

Dose escalation study of intravenous and intra-arterial *N-a*cetylcysteine for the prevention of oto- and nephrotoxicity of cisplatin with a contrast-induced nephropathy model in patients with renal insufficiency

Author: Edit Dósa, Krisztina Heltai, Tamás Radovits, Gabriella Molnár, Judit Kapocsi,Béla Merkely, Rongwei Fu, Nancy D. Doolittle, Gerda B. Tóth, Zachary Urdang, and Edward A. Neuwelt

[1]Heart and Vascular Center, Semmelweis University, 68 Városmajor Street, Budapest, 1122 Hungary

[2]1st Department of Internal Medicine, Semmelweis University, 26 Üllői Street, Budapest, 1085 Hungary

[3]Public Health & Preventive Medicine, Oregon Health & Science University, 3184 S.W. Sam Jackson Park Rd, CB669, Portland, OR 97329 USA

[4]Department of Neurology, Oregon Health & Science University, 3184 S.W. Sam Jackson Park Rd, L603, Portland, OR 97329 USA

[5]Department of Neurosurgery, Oregon Health & Science University, 3184 S.W. Sam Jackson Park Rd, L603, Portland, OR 97329 USA

[6]Portland Veterans Affairs Medical Center, 3710 S.W. US Veterans Hospital Rd, Portland, OR 97239 USA

[7]Blood–Brain Barrier and Neuro-Oncology Program, Oregon Health & Science University, 3181 S.W. Sam Jackson Park Road, L603, Portland, OR 97239 USA

Appendix D is modified from the paper published in Fluids and Barriers of the CNS October 3rd, 2017.

Contributions: Zachary edited and contributed to authorship of this manuscript.

D.1 – Abstract

Background: Cisplatin neuro-, oto-, and nephrotoxicity are major problems in children with malignant tumors, including medulloblastoma, negatively impacting educational achievement, socioemotional development, and overall quality of life. The blood-labyrinth barrier is somewhat permeable to cisplatin, and sensory hair cells and cochlear supporting cells are highly sensitive to this toxic drug. Several chemoprotective agents such as *N*-acetylcysteine (NAC) were utilized experimentally to avoid these potentially serious and life-long side effects, although no clinical phase I trial was performed before. The purpose of this study was to establish the maximum tolerated dose (MTD) and pharmacokinetics of both intravenous (IV) and intra-arterial (IA) NAC in adults with chronic kidney disease to be used in further trials on oto- and nephroprotection in pediatric patients receiving platinum therapy.

Methods: Due to ethical considerations in pediatric tumor patients, we used a clinical population of adults with non-neoplastic disease. Subjects with stage three or worse renal failure who had any endovascular procedure were enrolled in a prospective, non-randomized, single center trial to determine the MTD for NAC. We initially aimed to evaluate three patients each at 150, 300, 600, 900, and 1200 mg/kg NAC. The MTD was defined as one dose level below the dose producing grade 3 or 4 toxicity. Serum NAC levels were assessed before, 5 and 15 min post NAC. Twenty-eight subjects (15 men; mean age 72.2 ± 6.8 years) received NAC IV (N = 13) or IA (N = 15).

Results: The first participant to experience grade 4 toxicity was at the 600 mg/kg IV dose, at which time the protocol was modified to add an additional dose level of 450 mg/kg NAC. Subsequently, no severe NAC-related toxicity arose and 450 mg/kg NAC was found to be the MTD in both IV and IA groups. Blood levels of NAC showed a linear dose response ($p < 0.01$). Five min after either IV or IA NAC MTD dose administration, serum NAC levels reached the 2–3 mM concentration which seemed to be nephroprotective in previous preclinical studies.

Conclusions: In adults with kidney impairment, NAC can be safely given both IV and IA at a dose of 450 mg/kg. Additional studies are needed to confirm oto- and nephroprotective properties in the setting of cisplatin treatment.

Clinical Trial Registration URL: https://eudract.ema.europa.eu. Unique identifier: 2011-000887-92

D.2 – Background

Cisplatin is a common chemotherapeutic agent used to treat various types of malignant tumors. However, side effects such as neuro-, oto-, and nephrotoxicity limit the application of cisplatin. Cisplatin ototoxicity is of particular concern in children with malignant tumors where life-long hearing impairment can cause serious psychosocial deficits including social isolation, limited employment opportunities and associated earning potential, and an overall decrease in quality of life measures (*541, 542*). The pathogenesis is not completely understood, but it is likely to be caused by depletion of intracellular glutathione (GSH) and generation of immune cell- and organ parenchymal-derived reactive oxygen species (ROS) and other free radicals (*543*). Cisplatin is able to cross the blood-labyrinth barrier and enter the cochlea and sensory hair cells where it causes degeneration of the cochlear supporting cells, outer and inner hair cells and results in a progressive, irreversible hearing loss (*544, 545*). For example, in medulloblastoma where the standard of care treatment includes cisplatin, ototoxicity occurs in approximately 80–90% of children treated with standard therapy (*545*). Nephrotoxicity occurs in one-third of patients and can be potentially severe or life-threatening. Moreover, these toxicities utilize substantial healthcare resources and thus an inexpensive, effective, prophylactic protective strategy is of clear interest. Several oto- and nephroprotective approaches were developed (such as hydrating the patients during treatment, using less toxic cisplatin analogues) to avoid these reactions, including various chemoprotective agents used in experimental models (dimethylthiourea, melatonin, selenium, vitamin E, *N*-acetylcysteine [NAC], sodium thiosulfate) (*252, 545-551*).

N-Acetylcysteine is a sulfur-containing cysteine analog. It has been applied for decades as a mucolytic drug and as an antidote for acetaminophen overdose, as well as to prevent contrast-induced nephropathy (CIN) (*552*). More recently, interest has been raised for the use of NAC in the prevention of cisplatin induced oto- and nephrotoxicity. Interestingly, CIN from iodine-based contrast agents and cisplatin share common mechanistic features including both intrinsic cellular- and inflammation-related ROS mediated cellular and stromal peroxidation damage (*553-558*). The following properties of NAC are hypothesized to be paramount for the prevention of oto- and nephrotoxicity:

(1) NAC is thought to act as a vasodilator through nitric oxide effects, thus improving blood flow, (2) NAC is a precursor to GSH, the body's endogenous ROS scavenger, (3) the antioxidant properties of NAC dampen inflammation caused by damage-associated molecular patterns that arise from biological macromolecule peroxidation by ROS and cellular necrosis, and (4) NAC prohibits apoptosis and promotes cell survival by the activation of an extracellular signal-regulated kinase pathway (*552*). When NAC enters the systemic circulation it can only leave the blood vessels after N-deacetylation and subsequent carrier mediated active transport of L-cysteine by the alanine–serine–cysteine transporter (ASC-1) (*559*). Once in the brain, L-cysteine may act as an antioxidant or can be converted to GSH. Our group and others have shown a low level delivery of radiolabeled NAC across the BBB (*560-562*). We demonstrated that even at very high NAC concentration (1200 mg/kg) delivery was less than 0.5% of the administered dose per gram tissue after intravenous (IV) administration in rats, but was significantly enhanced by intra-arterial (IA) administration (*562*). It is possible that NAC is a ligand for ASC-1 prior to deacetylation or that NAC is rapidly deacetylated in the blood and the observed radioactivity in the brain was due to radioactive cysteine. In the setting of inflammation, oxidative stress could impair the BBB to increase NAC leak (*560, 561*). In case of a brain tumor, vessels supplying the tumor possess impaired barrier properties so both NAC and cisplatin can enter the tumor tissue to some degree.

A literature review revealed 38 trials evaluating NAC in the prevention of CIN, 15 with positive and 23 with negative outcomes, and 17 meta-analyses with conflicting conclusions (*563*). There has been significant heterogeneity between studies due to various routes of administration and different dosages (*563, 564*). Most trials followed Tepel's regimen of 600 mg of NAC orally twice a day for 48 h and 0.45% saline intravenously, before and after injection of the contrast agent, or placebo and saline as control (*564*).

Similar to CIN, NAC has demonstrated mixed results in the literature as an otoprotectant in the context of cisplatin therapy (*252, 552, 565-568*). Still, a handful of reports with positive results suggest otoprotective properties during cochlear insults through ROS mediated mechanisms. Dosing, route, and timing of NAC administration seem to be important variables in NAC medicated otoprotection. Whether or not NAC

trafficking into the extravascular cochlear compartment occurs is an understudied question, and hence extravascular trafficking may not be required for otoprotective activity. NAC could potentially act by intravascular activity on ROS producing immune cells which can compromise blood-labyrinth barrier integrity and thus prevent enhanced cochlear uptake of cisplatin.

Preclinical ototoxicity studies demonstrated that IV or IA administration of NAC is required to achieve high blood concentration necessary for otoprotection (*252, 267, 546, 566*). As Stenstrom observed, oral NAC is cleared via the portal vein on the first pass through the liver, however 31 of 38 reviewed trials ignored this first pass clearance and gave very small doses (*552, 569*). We assume that either the oral route or the applied low IV doses were likely a large factor in the negative results seen in previous clinical trials. We hypothesized that NAC at high IV and IA (via the descending aorta) doses can be injected with an acceptable toxicity profile in children with malignant tumors. Our primary goal was to perform a dose escalation study in pediatric patients. Due to rejection of our pediatric toxicity trial by the Institutional Review Board this phase I study used an adult population of subjects with stage 3 or worse kidney failure undergoing a radiologic procedure requiring iodine-based contrast media. Patients with renal failure were chosen with the thought that this population would be particularly sensitive to adverse events and thus the observed maximum tolerated dose (MTD) would include a large margin of safety when translated to the pediatric population. Using this study design we were also able to not only examine the chemoprotective properties of NAC, but could confirm its protection against CIN. The MTD will be evaluated for efficacy in a future trial, specifically in pediatric populations.

D.3 – Methods

D.3.1 - Study protocol

This was a prospective, non-randomized, single center dose escalation trial of patients with stage 3 or worse chronic renal disease (glomerular filtration rate [GFR] < 60 mL/min/1.73 m^2) who underwent a digital subtraction angiography (DSA) and/or vascular intervention with an isotonic nonionic contrast material (Iodixanol) between the years 2012 and 2015. Indication for the procedures was established by a vascular team including vascular surgeons, interventional radiologists, and vascular physicians. Interventions were carried out according to international guidelines. Our primary objective was to establish the MTD of both IV and IA NAC. The secondary objective was to determine NAC pharmacology given IV or IA.

The study was approved by the Institutional Review Committee (12935-0/2011-EKL) and all subjects gave written informed consent.

D.3.2 - Eligibility requirements

Patients between 18 and 85 years of age at risk for CIN were eligible to participate if they had stage 3 or worse kidney impairment (renal failure staging was determined by the following formula: Modification of Diet in Renal Disease, GFR ([mL/min/1.73 m^2] = 175 × [Serum creatinine]$^{-1.154}$ × [Age]$^{-0.203}$ × [0.742 if the subject was female]) with a life expectancy of 4 weeks from the date of registration (*569*).

D.3.3 - Exclusion criteria

Subjects were excluded if they had acute kidney injury (e.g., significant change over 4 weeks), were on dialysis, had a systolic blood pressure of < 90 mmHg, had decompensated heart failure at the time of admission, had a history of severe reactive airway disease, were at high risk for general anesthesia, were pregnant, had a positive serum human chorionic gonadotropin or was lactating, or who had contraindications to NAC or the contrast agent.

D.3.4 - Treatment plan

D.3.4.1 - Dose escalation

A group of three subjects was aimed to be evaluated at each of the following fixed dose levels of NAC: dose level 1, 150 mg/kg/day; dose level 2, 300 mg/kg/day; dose level 3, 600 mg/kg/day; dose level 4, 900 mg/kg/day; and dose level 5, 1200 mg/kg/day. The first dose level was based on the standard of care treatment of acetaminophen overdose (*570*). The dose escalation was evaluated by the rate of grade 3 or 4 toxicities. In case of a severe toxicity reaction an additional dose level was added. Toxicity was graded according to National Cancer Institute Common Terminology Criteria for Adverse Events version 3.0. (*571*). The dosing algorithm can be seen in **Fig. D.1**. The NAC MTD was defined as one dose level below the dose that produced grade 3 or 4 toxicity.

D.3.4.2 - Assignment for IV versus IA NAC

Patients were assigned to IV or IA using the last digit of their hospital identification number. Those with even last digits received IV NAC and those with odd last digits received IA NAC. If the MTD was achieved for one group, all subsequent subjects were treated with the other regimen.

D.3.4.3 - Premedication

Since it has been previously shown that NAC has dose dependent anaphylactoid reactions in 23–48% of patients, all participants received premedication prior to NAC administration (*572*). Premedication regimen consisted of 100 mg IV methylprednisolone and 50 mg ranitidine 3 h prior to NAC, and 50 mg diphenhydramine 10 min prior to NAC. Additional doses of 25 mg diphenhydramine were given 10 min after the start of the NAC infusion and repeated as clinically indicated.

D.3.4.4 - Administration of the study drug

The study drug (Acetylcysteine [Fluimucil Antidote]) is available as a 20% solution in 25 mL (200 mg/mL) single dose glass vials. The NAC was diluted to 150, 300, 450, and 600 mg/kg in 250 mL of diluent (5% dextrose in water [Isodex]). The 900 and 1200 mg/kg doses were designed to be diluted in 500 mL of diluent. Each of the above dilutions were given either IV through a peripheral vein using an infusion pump (Alaris GH) or IA down the descending aorta through a fluid injection system (Medrad Avanta) over a period of 25–55 min. In the case of IV injection, the flow rate was 1000 mL/h. For IA administration a pigtail catheter was used (the tip of the catheter was positioned at the level of the renal arteries) and a pulsed infusion of 16.5 mL volume at 16.5 mL/sec was performed and repeated for a total of 15 injections. In the event of grade 1 or 2 toxicities the infusion rate was reduced.

D.3.5 - Subject monitoring

Vital signs (pulse and respiration rate), blood pressure, electrical activity of the heart, and oxygen saturation were recorded by a cardiologist at baseline, prior to NAC infusion, every 10 min during infusion, and for 30 min after completion of NAC infusion. The patient was closely monitored for anaphylactoid reaction throughout the endovascular procedure in the angiogram suite and in the recovery unit after the DSA and/or intervention. In the recovery unit, fluid intake and output were measured for 2–4 h until the subject was sent to the ward.

D.3.5.1 - Laboratory analysis of the blood samples

Blood samples were taken at baseline, prior to NAC, then 5 and 15 min after the NAC administration, as well as 24, 48, and 72 h following the radiologic procedure. Study drug and GSH levels were assessed prior to, then 5 and 15 min after the completion of the study drug infusion. Serum NAC and GSH analyses were done in our Research Laboratory using a high-performance liquid chromatography assay. Details of this procedure have been described previously (*566*).

D.3.5.2 - Statistical analysis

Statistical analysis was performed with SPSS 21.0 software (IBM Corp., Armonk, NY) and SAS 9.4 software (SAS Institute Inc., Cary, NC). Continuous variables were expressed as means and standard deviations and were compared between two groups using the Students' *t* test. A linear mixed-effects model was applied to evaluate dose response relationships and differences at various time points for pharmacological factors while accounting for correlations among the multiple observations within the same patient. All analyses were two-tailed, and values of $p \leq 0.05$ were considered statistically significant.

D.4 – Results

D.4.1 - Patient data

Twenty-eight subjects (13 women, 15 men; mean age: 72.2 ± 6.8 years) were enrolled. Fifteen subjects had DSA (lower or upper extremity angiography, N = 6; aortic arch and selective four-vessel cerebral angiography, N = 3; lower extremity plus aortic arch and selective four-vessel cerebral angiography, N = 3; renal angiography, N = 3) while 12 underwent percutaneous transluminal angioplasty with or without stent placement (internal carotid artery stenting, N = 4; renal artery stenting, N = 2; crural artery percutaneous transluminal angioplasty, N = 2; subclavian artery stenting, N = 1; common iliac artery stenting, N = 1; common iliac artery plus renal artery stenting, N = 1; superficial femoral artery stenting, N = 1). One patient (7_IV) did not have radiologic intervention due to NAC-related acute severe toxicity.

D.4.2 - *N*-Acetylcysteine toxicity

The administered NAC volume and NAC infusion time did not differ significantly between the corresponding IV and IA groups (**Table D.1**).

D.4.3 - Maximum tolerated IV dose

Thirteen participants received IV NAC. Three patients completed dose level 1 and three completed dose level 2 without having grade 3 or 4 toxicity. The first subject (7_IV) enrolled to dose level 3 developed rashes, flushing, pruritus, and an intense bronchospasm immediately after completion of the study drug administration which rapidly progressed to respiratory and cardiac arrest. Successful cardiorespiratory resuscitation was performed according to the 2010 American Heart Association guidelines at which point the participant was transported to the intensive care unit where he was monitored for 3 days (*573*). The patient left the hospital 6 days post NAC in good condition. Due to the serious toxicity in this subject, the protocol was modified and a new dose level of 450 mg/kg NAC was inserted between the 300 and 600 mg/kg doses.

Participants 8_IV, 9_IV, and 10_IV received 450 mg/kg dose of NAC. None had grade 3 or 4 toxicity, therefore 450 mg/kg was considered to be the MTD and three additional patients were treated with the same dose in order to gain more data on NAC toxicity and pharmacokinetics (**Fig. D.2**).

D.4.4 - Maximum tolerated IA dose

Fifteen subjects received IA NAC. The first participant (1_IA) enrolled to the group developed an anaphylactic reaction with life-threatening symptoms. She was treated according to the 2011 World Allergy Organization anaphylaxis guidelines in the angiogram suite and was transported to the intensive care unit where she was monitored for 3 days (*574*). The patient left the hospital 5 days post NAC infusion in good condition. The anaphylactic reaction occurred immediately after completion of the DSA. The time interval between the anaphylactic reaction and NAC infusion was 1 h. The case was discussed by a multidisciplinary team which considered the adverse reaction to be a consequence of the contrast agent rather than NAC based on the elapsed time from the study drug infusion to the time of the anaphylactic reaction. Also, the subject provided information after the adverse reaction that she developed hives on her chest 2 months previously after a cardiac catheterization. Furthermore, the cardiac catheterization was done in a different hospital, the hives were not mentioned in the final report, and the participant answered no for the question whether she had allergic reaction to anything in her life both prior to study enrollment and before the interventional procedure. Although two additional participants completed dose level 1 without having grade 3 or 4 toxicity, three more patients were treated with the same dose. Neither 300 nor 450 mg/kg dose produced severe toxicity. The 450 mg/kg dose was considered to be the MTD and three additional subjects received that dose (**Fig. D.2**).

D.4.5 - Minor toxicities

Grade 1 or 2 toxicities were seen in six participants (21.4%). Two-thirds of the minor toxicities occurred at a dose of 450 mg/kg NAC. All of them resolved either

spontaneously or by giving appropriate treatment over 30 min to 12 h following the toxicity (**Table D.2**).

D.4.6 - *N*-Acetylcysteine pharmacokinetics

Results of the high-performance liquid chromatography analysis are summarized in **Fig. D.3**.

D.4.7 - Serum NAC levels

At baseline, NAC and GSH were not detected in the serum samples. Blood levels of NAC showed a significant linear dose response both 5 min (slope, 1.07 mM increase for every 150 mg/kg rise in NAC dose; $p = 0.001$) and 15 min after IV administration (slope, 0.48 mM increase for every 150 mg/kg rise in NAC dose; $p = 0.002$). Similar significant linear dose responses were observed after IA injection with a slope of 1.22 mM for every 150 mg/kg increase in NAC dose at 5 min ($p < 0.001$) and with a slope of 0.58 mM for every 150 mg/kg increase in NAC dose at 15 min ($p = 0.005$). In each group, NAC levels were nearly halved from 5 to 15 min post infusion. In particular, the overall mean NAC level was 1.63 mM (SE: 0.23) and 0.81 mM (SE: 0.21), respectively, 5 and 15 min after IV administration; and 2.93 mM (SE: 0.22) and 1.42 mM (SE: 0.15), respectively, 5 and 15 min after IA injection. At 5 min post infusion, NAC concentrations were significantly higher in the IA groups compared to the corresponding IV groups ($p < 0.001$; $p = 0.023$, $p = 0.009$, respectively) (**Table D.1, Fig. D.3**).

D.4.8 - Serum GSH levels

A significant linear dose response relationship was noted for GSH concentrations in the IV group. Since the relationships were similar at 5 and 15 min, an overall dose response relationship was estimated to yield a 0.37 mM increase in GSH values for every 150 mg/kg rise in NAC dose ($p < 0.001$). In contrast to patients in the IV group, the overall dose response relationship was not significantly linear in the IA group ($p = 0.068$). The mean GSH concentrations were higher in the IA than in the IV group (**Table D.1**, **Fig. D.3**).

D.5 – Discussion

Our goal was to provide the MTD of NAC as a correct scientific basis for future efficacy trials, particularly in pediatric populations. Four hundred and fifty mg/kg NAC was found to be the MTD in this study, and we have shown that it can be given with an acceptable toxicity both IV and IA in adults with impaired kidney function undergoing DSA with or without intervention. By determining the MTD we potentially gain the maximum concentration of NAC in the brain and cochlea to diminish the toxicity of agents like cisplatin, although the entry of NAC may be limited by the BBB and blood-labyrinth barrier.

A key factor in previous failed trials with NAC is that oral NAC is known to have 5–10% bioavailability in humans due to extensive first pass metabolism to GSH (*575*). Oral NAC reaches a serum peak about an hour after ingestion and has an elimination half-life of 2.27 h (*576*). Furthermore, there is no clear evidence that NAC effects are mediated indirectly by its metabolites.

The potential of oral NAC to be oto- and nephroprotective was examined in several preclinical studies. Dickey et al. determined in rats, that a single IV administration of 1500 mg/kg NAC is non-toxic, and three IV injections of 1200 mg/kg NAC, 4 h apart, are safe and well-tolerated (*566*). In another study by Dickey et al. rats received NAC infusion at 100, 400 and 1200 mg/kg IV. Blood samples were taken 15 min post inoculation. Another group of rats was given NAC 1200 mg/kg orally, with blood samples collected after 15 and 60 min. Total NAC concentrations were analyzed and similarly to our findings, blood levels of NAC showed a rough linear dose response after IV administration of NAC. In contrast to the IV results, the group given NAC 1200 mg/kg by the oral route had very low levels of serum NAC (*566*). In their third study, rats were treated with cisplatin 10 mg/kg intraperitoneally 30 min after NAC 400 mg/kg given by intraperitoneal, oral, or IV routes, compared with cisplatin alone. NAC was chemoprotective against the cisplatin nephrotoxicity, depending on the route of administration. Rats receiving NAC IV had very low blood urea nitrogen levels 3 days post treatment. In the case of oral or intraperitoneal NAC administration, the blood urea nitrogen concentrations were as high as in the group of rats who did not get NAC (*566*).

In their fourth study, rats were treated with cisplatin 10 mg/kg intraperitoneally 30 min after NAC 50 mg/kg infused IV or IA. The blood urea nitrogen levels were significantly lower in the IA group—the blood urea nitrogen levels were similar to those when NAC was injected IV at high dose (400 mg/kg)—indicating a significantly reduced rate of nephrotoxicity for the IA delivery (*566*). Assuming that this rat chemoprotective model represents the effects of cisplatin as those of contrast agents in humans, these observations call into question if oral NAC or low dose IV NAC has any clinical impact on cisplatin induced oto- and nephrotoxicity.

Briguori et al. and Marenzi et al. were the only investigators who made dose comparisons in humans. Briguori et al. compared single dose NAC 600 mg orally twice a day for 48 h with double dose NAC 1200 mg (17.1 mg/kg for a 70 kg subject) orally twice a day for 48 h. Although these doses were not high and were given orally, the outcome was favorable for the double dose (*577*). Marenzi et al. compared two IV doses (600 and 1200 mg total dose per patient) prior to the angioplasty and two oral doses (600 and 1200 mg twice a day for 48 h) after the procedure with placebo. A greater increase in serum creatinine was observed in the placebo group compared to patients treated with NAC and the higher NAC IV dose was even better than the lower dose, which implies that NAC actions may be dose dependent (*578*). These observations are in line with the findings of the above-mentioned rat studies and demonstrate the importance of this phase I trial.

It is also worth considering that the route of NAC administration markedly affects its biodistribution. In an animal study performed by our group, we found that when radiolabeled NAC was administered IA into the right carotid artery of the rat, high levels of radiolabel were found throughout the right cerebral hemisphere, regardless of whether or not the BBB was opened. Delivery was 0.41% of the injected dose, comparable to the levels found in the liver (0.57%) and kidney (0.70%). In contrast, the aortic infusion above the renal arteries prevented the brain delivery and changed the biodistribution of NAC. The change in tissue delivery with different modes of administration is likely due to NAC being deacetylated and the amino acid cysteine is rapidly bound by tissues via the amino acid transporters (*562*).

The limitations of our study include the special subject population: all patients were older than 50 years, had impaired kidney function, and atherosclerotic disease. Although serum creatinine values were measured both before and after contrast agent administration additional trials should be performed to determine whether either IV or IA 450 mg/kg NAC is protective against CIN or chemoprotective against cisplatin in pediatric subjects.

D.6 – Conclusions

In conclusion, we found that NAC can be safely given both IV and IA at a dose of 450 mg/kg in adults with reduced renal function. Phase II and III studies are needed to determine whether high IV and IA doses can avoid oto- and nephrotoxicity of platinum-based chemotherapy, and if yes, whether a particular route of administration of NAC provides improved chemoprotection. A considerable hurdle with NAC is disentangling the mixed results from studies utilizing oral NAC administration; we advocate for careful analysis and comparison of oral route trials in humans with those of IV or IA. A phase I trial in children is currently underway with different doses of NAC after cisplatin to prevent ototoxicity (clinicaltrials.gov NCT02094625).

D.7 – Figures and Tables

Table D.1: NAC pharmacokinetic parameters.
N-Acetylcysteine and contrast agent volumes, *N*-acetylcysteine administration time, baseline serum creatinine levels, and 5-min *N*-acetylcysteine and glutathione concentrations

Parameter	**NAC dose (mg/kg)**	**IV group (Mean ± SD)**	**IA group (Mean ± SD)**	**p value**
NAC volume (mL)	150	63.25 ± 50.61	51.88 ± 6.6	0.31
	300	109.5 ± 6.89	132.5 ± 46.37	0.183
	600	294	NA	NA
	450	167.58 ± 44.63	166.13 ± 41.61	0.956
NAC administration time (min)	150	26.67 ± 2.89	31.67 ± 7.53	0.196
	300	31.67 ± 5.77	38.33 ± 2.89	0.173
	600	51	NA	NA

Parameter	**NAC dose (mg/kg)**	**IV group (Mean ± SD)**	**IA group (Mean ± SD)**	**p value**
	450	40 ± 6.32	42.5 ± 8.22	0.569
CA volume (mL)	150	94.33 ± 69.89	109.17 ± 56.16	0.768
	300	80 ± 39.69	86.67 ± 64.29	0.887
	600	0	NA	NA
	450	89.5 ± 15.86	88.5 ± 25.81	0.937
Baseline serum creatinine (μmol/L)	150	201 ± 11.97	118.17 ± 15.53	0.402
	300	123.67 ± 33.23	160 ± 24.76	0.343
	600	157	NA	NA
	450	209.33 ± 54.4	171.5 ± 52.89	0.486

Parameter	**NAC dose (mg/kg)**	**IV group (Mean ± SD)**	**IA group (Mean ± SD)**	**p value**
NAC concentration at 5 min (mM)	150	0.43 ± 0.1	1.66 ± 0.32	*< 0.001*
	300	1.04 ± 0.6	3.12 ± 0.77	*0.023*
	600	4.53	NA	NA
	450	2.03 ± 0.95	4.1 ± 1.22	*0.009*
GSH concentration at 5 min (mM)	150	0.13 ± 0.16	0.2 ± 0.04	0.514
	300	0.13 ± 0.03	0.96 ± 0.36	0.058
	600	0.21	NA	NA
	450	0.19 ± 0.04	0.89 ± 0.31	*0.003*

Italicized p-values indicate statistically significant values

IV intravenous, *IA* intra-arterial, *SD* standard deviation, *NAC N*-acetylcysteine, *NA* not applicable, *CA* contrast agent, *GSH* glutathione

Table 2: Toxicities attributed to *N*-acetylcysteine.

Group	**Patient number**	**Weight (kg)**	**NAC dose (mg/kg)**	**NAC volume (mL)**	**NAC toxicity**
IV	4_IV	84	300	126	Grade 1, facial erythema
	7_IV	98	600	294	Grade 4, respiratory and cardiac arrest
	10_IV	96	450	216	Grade 2, pruritus and rash
	11_IV	103	450	231.75	Grade 1, coughing
IA	1_IA	55	150	41.25	Grade 4[a], anaphylaxis
	8_IA	101	300	151.5	Grade 1, nausea
	10_IA	95	450	213.75	Grade 1, coughing
	11_IA	80	450	180	Grade 1, facial erythema

NAC N-acetylcysteine, *IV* intravenous, *IA* intra-arterial

[a]Adverse reaction to contrast agent rather than to NAC

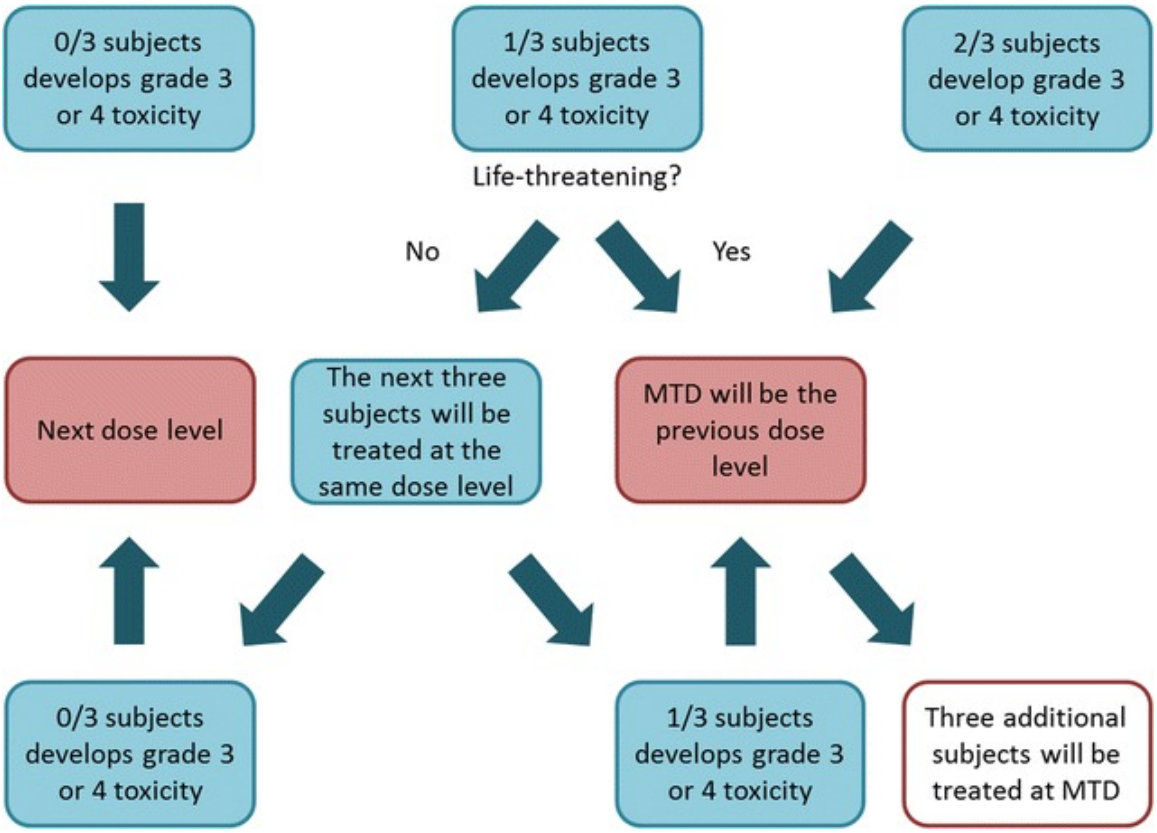

Fig. D.1: Dosing algorithm for *N*-acetylcysteine to determine the maximum tolerated dose in adults with chronic kidney disease.

The *N*-acetylcysteine maximum tolerated dose was defined as one dose level below the dose that produced grade 3 or 4 toxicity. *MTD* maximum tolerated dose

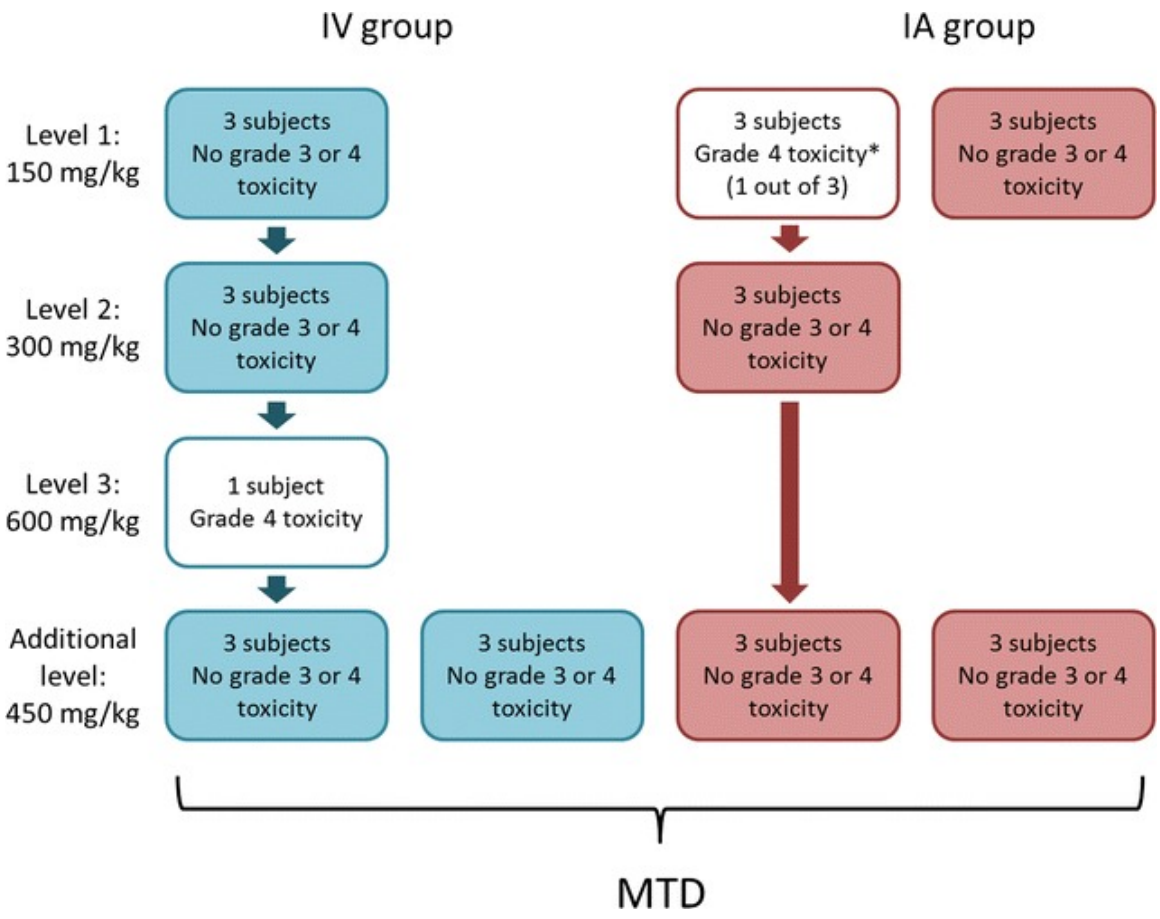

Flg. D.2: Establishment of the maximum tolerated dose for *N*-acetylcysteine in adults with chronic kidney disease.

Four hundred and fifty mg/kg *N*-acetylcysteine was found to be the maximum tolerated dose in both intravenous and intra-arterial groups. Asterisk: Adverse reaction to contrast agent rather than to *N*-acetylcysteine. *IV* intravenous, *IA* intra-arterial, *MTD* maximum tolerated dose.

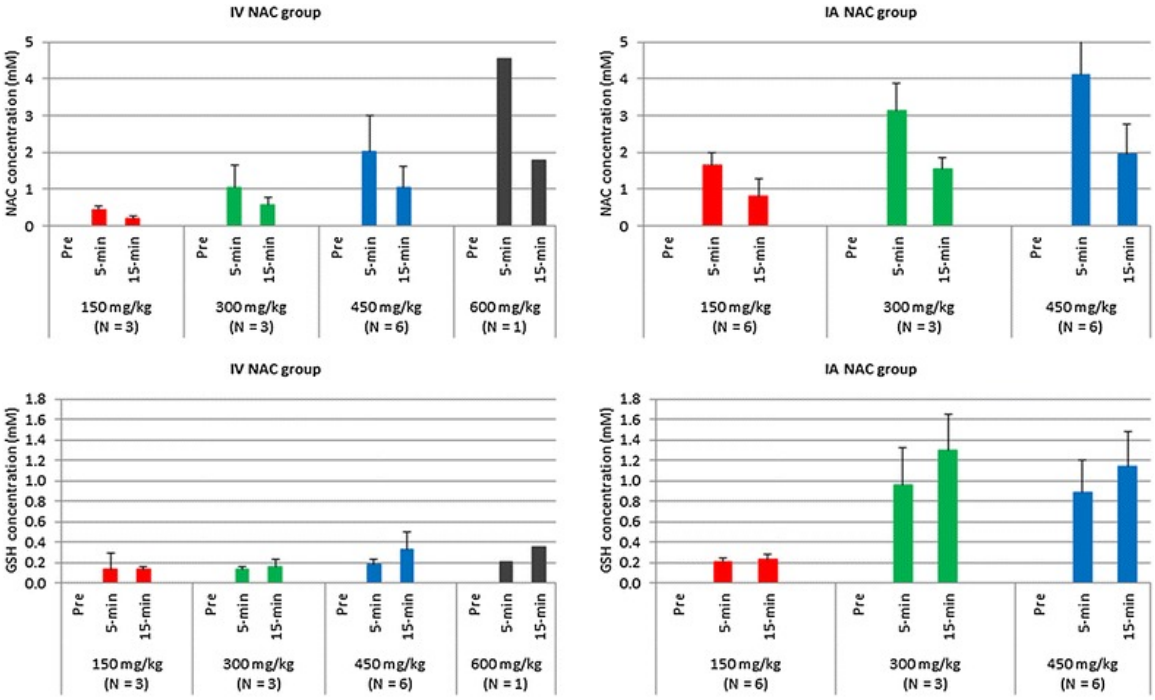

Fig. D.3: *N*-Acetylcysteine pharmacokinetics: serum concentrations of *N*-acetylcysteine and glutathione at different dose levels and time intervals.
Blood levels of *N*-acetylcysteine (upper row) showed a significant linear dose response, while gluthatione concentrations (lower row) were inconsistently elevated. *IV* intravenous, *IA* intra-arterial, *NAC N*-acetylcysteine, *GSH* glutathione.

Appendix E: Community Outreach

Evidence Supporting Free Head and Neck Cancer Screenings

Authors: Zachary Urdang BS[1], David Rosales[2], QiLiang Chen PhD[1], Ryan J. Li MD[3], Peter E. Andersen[3] MD, Neil D. Gross MD[4], Daniel R. Clayburgh MD PhD[3]

Author Affiliations:

1. MD/PhD Program, School of Medicine, Oregon Health and Science University, Portland, OR
2. Cancer CURE Program, Oregon Health and Science University, Portland OR
3. Department of Otolaryngology-Head and Neck Surgery, Oregon Health and Science University, Portland, OR
4. Department of Otolaryngology-Head and Neck Surgery, MD Anderson Cancer Center, Houston, TX

This work was presented at the 2017 American Academy of Otolaryngology-Head and Neck Surgery Annual Meeting, Chicago, IL and submitted to The Journal of Otolaryngology Head and Neck Surgery.

Contributions: Zachary conceptualized and wrote the IRB protocol, supervised data collection and analysis, analyzed the data, and wrote the manuscript.

E.1 - Abstract

Objectives:

1) Determine participant demographics, risk factors, and motivation in Head and Neck Cancer Awareness and Screening Program (HNCASP).

2) Examine follow up and outcomes of screening participants with positive findings in a HNCASP

Study Design: Retrospective review of prospectively collected surveys and cross-sectional phone interview.

Setting: Tertiary care academic medical center

Subjects and Methods: During the years 2012 to 2016, HNCASP participants filled out demographic and risk factor surveys followed by a HNC screening examination. Participants with suspicious findings were contacted by telephone to determine if follow up occurred, diagnosis, and treatment rendered.

Results: There were 929 participants with mean age 54±17 years (61% female). The predominant motivational factor for HNCASP participation was to learn more about HNC (41%). 156 positive screenings required further evaluation (16.8%) and 47 of these completed follow up interviews. Thirteen of 47 reported resolution of the issue; 27 saw a provider, and 10 intended to see a provider in the near future. The delay between screening and provider appointment was 2.1 months with 12 confirmed cancer cases (1.1% of all participants)—five basal cell carcinomas, three cutaneous squamous cell carcinomas, one melanoma, one lymphoma, and two mucosal squamous cell carcinoma.

Conclusions: A significant proportion of HNCASP participants benefited from this screening opportunity. Education regarding HNC is the primary benefit of HNCASP, although a significant subset of patients was identified that needed follow up, and several cancers were detected.

E.2 - Introduction

Cancer of the head and neck accounts for approximately 3% of all malignancies with about 53,000 cancers of the head and neck diagnosed in the U.S. annually (*579, 580*). Furthermore, the burden of head and neck cancer in the U.S. tends to weigh more heavily on those who face socio-economic adversity (*581*). Traditional risk factors for head and neck cancer include: male gender, age greater than 50, tobacco use, alcohol consumption, sun exposure and family history. Over the past 10-15 years the incidence of head and neck cancer in the age group younger than 50 years old has sharply increased. The rise in this cancer has been epidemiologically linked to human papilloma virus (HPV) infection of the oropharynx (*582-585*). Despite the availability of a HPV vaccine, the incidence of HPV-related oropharyngeal cancer continues to rise, and is now equal to or has surpassed the incidence of HPV-related cervical cancer (*586*). Despite these numbers, head and neck cancers generally do not receive the same level of public attention as other malignancies.

Cancer awareness and screening programs are a popular means of promoting cancer education and performing outreach to the community at large. Head and neck cancer does not always receive the same level of attention as other cancers in the lay press and popular consciousness; thus, head and neck cancer awareness and screening programs (HNCASP) have gained popularity as a relatively straightforward and low-cost means to educate the general population regarding this disease. Education is particularly important for HNC, given the prominent psychological and emotional aspects of this disease (*587-592*). Patients diagnosed with HNC tend to suffer substantially more psychiatric co-morbidity when compared to cancers of other body regions. This is generally believed to be a result of the potentially devastating consequences of HNC progression and treatment sequelae upon the patient's face and multiple bodily functions such as respiration, swallowing, and speech. Importantly, these psychological aspects can lead to the delay of diagnosis and treatment, subsequently lowering the chances of a favorable outcome (*593, 594*). Thus, it is important to understand the factors which motivate one to seek or delay care concerning potential HNC.

Several other institutions that have sponsored HNCASP events have retrospectively shared their experiences (*595-603*) screening the general public, underserved populations, and even participants of NASCAR sporting events. However, there is a significant gap in our knowledge regarding the utility of these programs in identifying pathology and the long-term follow up that participants may receive. Furthermore, psychological factors surrounding patient willingness to seek care have been characterized in the clinical setting, they have yet to be explored in the context of HNCASP events. With this in mind, we conducted a study of participants at our institutional HNCASP, that for nearly 10 years has focused on education, cancer awareness, and providing an entry point into the health care system for patients with head and neck concerns. Over the course of 5 years, surveys were collected from participants regarding demographics, cancer risk factors, concerning symptoms, and motivations for attending the HNCASP. As a follow up, phone interviews were conducted with participants with positive screening findings to determine the outcomes of the positive finding, if further medical evaluation had been performed, diagnosis, and treatment.

E.3 - Materials and Methods

A retrospective review of prospectively collected data was performed regarding the Oregon Health and Science University HNCASP. This HNCASP was initiated in 2008, and provided a free day of screening for head and neck cancer to the Portland community annually. Beginning in 2013, a standardized intake survey was given to all participants in the HNCASP, collecting demographic data, medical history and risk factor assessment, and motivation for seeking screening. These responses, along with screening results, were collated into a single database over the years 2013-2016. This study was approved by the OHSU Institutional Review Board.

Participants who received a positive screen for head and neck pathology and were instructed to follow up for further medical assessment were contacted by phone in late 2016. Participants were asked about their ability to seek care, diagnosis obtained, treatment received, and resolution of their concern. Participation in this telephone survey was entirely voluntary.

Data were analyzed using SPSS version 24. Descriptive statistics were performed for all variables.

E.4 - Results

E.4.1 - Demographics and risk factors of participants

929 participants attended HNCASP between 2013-2016. Demographic information for participants is shown in **Table E.1**. Significantly, a majority of patients were Caucasian, had a college education or greater, had medical insurance, and had a primary care physician.

Most participants reported significant sun exposure (**Table E.2**). The most common risk factor was regular alcohol use (2+ drinks/day, 58%), although current and former tobacco use was frequently reported. Self-reported radiation exposure (23%) was quite high; however, many of these responses included narratives such as "have received x-rays at the doctor's office". Notably, 15% of participants reported themselves or a current/recent partner being HPV-positive.

E.4.2 - Motivational factors for attendance

Five motivational factors and a free-response line for attendance of HNCASP were presented to participants at the end of the intake forms and participants could check as many options as they saw fit; these results are shown in **Table E.3**. Desire to learn more about HNC (46%) was the most popular reason for attending the event followed by symptoms related to the head and neck region (30%). Most participants did not utilize the free-response option.

E.4.3 - Participant outcomes

Overall, 17% of patients had a positive screening examination and were recommended to seek follow up care (**Fig. E.1**). 47 of these patients were able to be contacted by phone to assess long-term follow up. Of those that did not seek further care, a majority reported resolution of their symptoms as the reason for avoiding follow up; the remaining participants noted a variety of obstacles to seeking care that prevented follow up. The majority of patients referred for follow up did seek care with a specialist, and a

total of 12 cancer cases were identified, representing 26% of participants that were contacted regarding follow up, and 1.3% of all participants in the HNCASP. These cancers included 5 basal cell carcinomas, 3 cutaneous squamous cell carcinomas, 2 mucosal squamous cell carcinomas, 1 melanoma, and 1 lymphoma.

E.5 - Discussion

The debate over the efficacy of HNCASP's nationally and worldwide remains unresolved with no solid evidence that these events either improve or degrade health outcomes for HNCs. Indeed, earlier detection of cancers improves outcomes; however, screening the general population for low-incidence disease inevitably generates false-positive results, leading to excessive testing, increased medical costs, and undue stress for patients. Beyond the simple service of screening for cancers, HNCASPs also fulfill an educational and awareness role; thus, their impact likely extends beyond the basic numbers of patients screened or cancers identified. Previously, there has not been significant study of the motivations of participants to seek out screening or the long-term outcomes of those who receive a positive screening test at a HNCASP. In this study, we assessed the demographics, motivations, and outcomes for participants of a HNCASP over several years.

Analysis of the demographics of our HNCASP participants demonstrated that participants were generally female, caucasian, highly educated, and had health insurance and a primary care physician. While the racial mix of participants is likely most reflective of the demographics of Portland, OR, the remaining demographic profile of participants mirrors the findings of previous results of a HNCASP at another tertiary care academic institution (*604*). This likely due to the location of the HNCASP on the campus of an academic center. Many of the participants in the HNCASP were employees of the medical center, as the screening event was most convenient for them to attend. This finding was further borne out in the analysis of self-reported risk factors. A significant percentage of participants reported a history of sun exposure and alcohol use, while tobacco use was significantly lower than that typically seen in patients with head and neck cancer. Interestingly, 15% participants reported that either they or their partners were HPV+; knowledge of risk factor is likely not present in the general populations, but would not be unexpected in the relatively medically savvy employees of a medical center.

A significant gap in the literature remains regarding the long-term outcomes and follow up of participants in HNCASPs. While occasionally a diagnosis, or strongly suspected cancer, may be identified at a HNCASP; however, unless the participant

returns to the same institution for follow up and biopsy confirmation, it is quite difficult to determine the overall efficacy of a screening program. Thus, to our knowledge the telephone follow-up survey conducted in this project is the first data to assess the outcomes of positive screens at a HNCASP. As expected from a telephone follow up survey, a large number of participants could not be reached or declined to participate. 57% of those that responded followed up with a physician regarding the findings of their screening, and of these, 12 confirmed cancer were identified. Several other participants were still in the process of evaluation for their screening findings. Thus, the number of cancers identified (1.3% of participants) is likely a significant underestimate of the true number of cancers identified by screening. However, only a few patients with positive screening findings reported not seeking further care due to barriers to medical care access; if screening occurred in a population with different socioeconomic demographics, it is quite likely that far more participants would not receive follow up.

Even with these caveats, a 1.3% cancer detection rate is comparable to other widespread cancer detection strategies, which are often much more intensive and costly. Colon cancer screening is routinely performed using either colonoscopy or fecal immunochemical testing (FIT). Colorectal cancer detection rates for colonoscopy have been reported between 0.4-6.9% (*605-607*), while FIT cancer detection rates of 0.7-0.8% (*605, 606*) have been reported. Colon adenoma detection rates are somewhat higher for both tests, although colonoscopy appears superior for this. Similarly, mammography has been shown to have a 2.6-5.4% (*608, 609*) rate of breast cancer detection. For prostate cancer, the cumulative cancer detection rate over 4 years of prostate-specific antigen testing is 8.2% (*610*). Thus, the 1.3% cancer detection rate for HNCASP is in line with other cancer screening procedures, although is much less invasive or costly for participants.

It is important to recognize that there are other, less tangible benefits to a HNCASP. In this study, insurance or care-related concerns was relatively low, with 37.6% of patients noting this as a reason for screening. A far greater percentage of participants (91.1%) noted a desire to learn more about head and neck cancer as a motivating factor for HNCASP attendance. While these relative percentages may vary if the HNCASP were held among a different demographic of participants (for example, in a

rural setting or urban underserved area) they do highlight the important role that HNCASP may fill regarding education and improving awareness of head and neck cancer.

This study does have significant limitations that should be acknowledged. As a retrospective review, there is inherent potential for bias with any missing information. Furthermore, telephone surveys typically have low response rates, and a number of participants with positive screening results could not be contacted, which may further bias the results. Finally, the setting and nature of this HNCASP may limit its generalizability to other settings. As noted previously, this event was held on the campus of an academic medical center and served a demographic that trended towards more educated patients with less tobacco use and better access to medical care. Moving the HNCASP to a relatively underserved area would likely significant increase the cancer rate, but many more patients with significant barrier to care or inability to follow up may be expected.

Despite these limitations, this study does indicate the value of HNCASPs. The rate of cancer detection is comparable to other, more widespread cancer screening procedures, thus the (relatively small) costs of this and other HNCASP appear justified purely based on potential improvements in oncologic outcome based on earlier cancer detection. However, HNCASP also provide a valuable method for community outreach and education, and may have an impact beyond only the number of participants screened on any given day. Future research is needed to better understand the utility of HNCASP in early cancer detection and long-term oncologic outcomes, and to determine ways to maximize the educational and community-building aspects of these programs.

E.6 – Figures and Tables

Table E.1: Participant characteristics

Participants, n	929	**Insurance Type, n (%)**	
Findings, n (%)	156 (17)	Private	432 (47)
Age (mean ± SD; years)	54 ± 17	Medicare	257 (28)
Gender, n (%)		Medicaid	79 (9)
Female	552 (61)	Other	12 (1)
Male	349 (39)	No Response	76 (15)
Ethnicity, n (%)		**Primary Care Provider, n (%)**	
African American	31 (3)	Yes	633 (68)
Asian	75 (8)	No	283 (30)
Caucasian	707(76)	No Response	19 (2)
Hispanic	53 (6)	**How did you hear about the event, n (%)**	
Native American	18 (2)	Online outside of OHSU	146 (16)
Other	26 (3)	Poster at OHSU	155 (17)
No Response	23 (2)	News	44 (5)
Education, n (%)		OHSU Website	64 (7)
No High School	9 (1)	Poster/Flyer outside of OHSU	71 (8)
High School	226 (24)	My doctor/dentist	19 (2)
Undergraduate	341 (37)	Banner on busy Portland Road	26 (3)
Graduate/Professional	262 (28)	Radio	0 (0)
Other	91 (2)	Other	151 (16)
No Response	23 (2)	No Response	3 (0.3)

Insurance, n (%)			
Insured	780 (84)		
Uninsured	74 (8)		
No Response	73 (8)		

Table E.2: Participant reported risk factors

Risk Factors			
Sun Exposure, n (%)			
No	128 (13)		
Childhood Sunburns	383 (41)		
Childhood Sunny climate	292 (31)		
Sunbathing	221 (24)		
Tanning Booth	48 (5)		
Outdoor Work	193 (21)		
Behavioral and Medical Factors	**Yes**	**No**	**Quit**
Tobacco Smoking, n (%)	53 (6)	515 (55)	333 (36)
Alternative Tobacco Use, n (%)	42 (5)	887 (95)	
Cannabis Use, n (%)	56 (6)	652 (70)	171 (18)
Alcohol Use, n (%)	537 (58)	281 (30)	131 (14)
Skin Lesion History, n (%)	185 (20)	744 (80)	
Tongue or Throat Cancer, n (%)	75 (8)	854 (92)	
Patient or Partner HPV Positive, n (%)	142 (15)	787(85)	
Immunosuppression, n (%)	65 (7)	864 (93)	
Diabetes Mellitus, n (%)	61 (7)	868 (93)	
Organ Transplant, n (%)	5 (0.5)	924 (99.5)	
Radiation Exposure, n (%)	209 (22)	720 (88)	
Agent Orange Exposure, n (%)	17 (2)	712 (98)	

Table E.3: Motivational Factors for Attending HNCASP

Motivational Factor on Intake Form	**n**	**(%)**
Concerned about having head and neck cancer	450	48.4
Head and neck related symptoms	688	74.1
Interested in learning more	837	90.1
Insurance related concerns	349	37.6
Have you put off seeing a physician	430	46.3

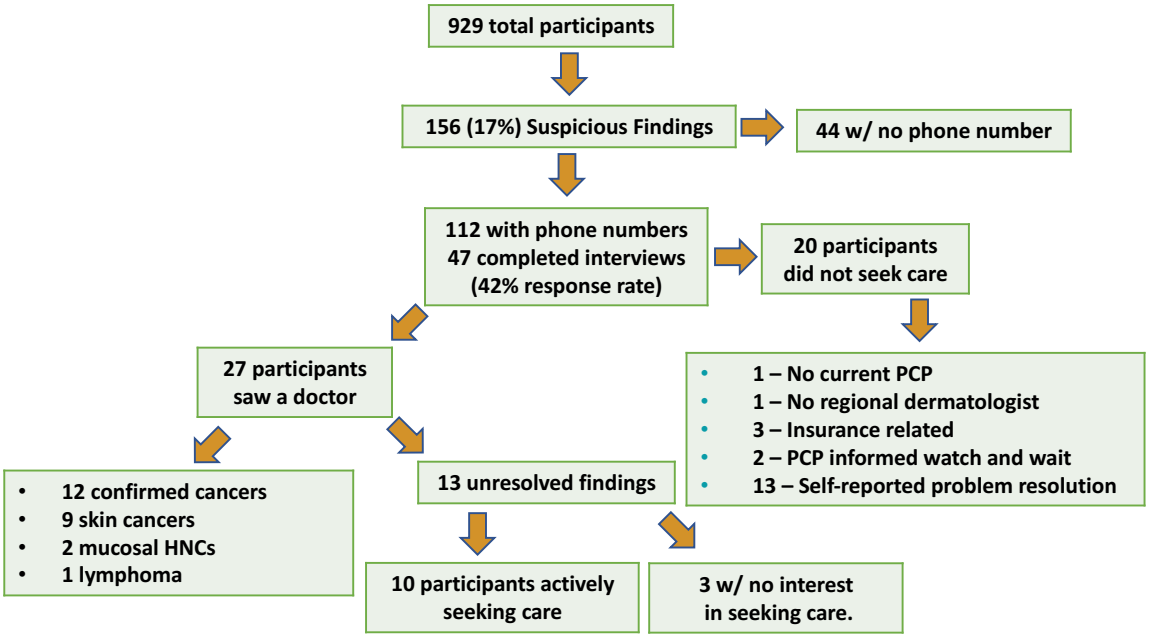

Figure E.1: Participant screening phone interview outcomes.

Bibliography

1. W. H. Organization. (2017).
2. D. Calvin, S. R. Watley, Diabetes and hearing loss among underserved populations. *Nursing Clinics of North America* **50**, 449-456 (2015).
3. A. Belachew, Y. Berhane, Noise-induced hearing loss among textile workers. *The Ethiopian Journal of Healh Development* **13**, (2017).
4. T. S. Wells, A. D. Seelig, M. A. Ryan, J. M. Jones, T. I. Hooper, I. G. Jacobson, E. J. Boyko, Hearing loss associated with US military combat deployment. *Noise Health* **17**, 34-42 (2015).
5. G. Pouryaghoub, R. Mehrdad, S. Pourhosein, Noise-Induced hearing loss among professional musicians. *Journal of Occupational Health* **59**, 33-37 (2017).
6. A. M. Goman, F. R. Lin, Prevalence of Hearing Loss by Severity in the United States. *Am J Public Health* **106**, 1820-1822 (2016).
7. S. D. Emmett, H. W. Francis, The socioeconomic impact of hearing loss in U.S. adults. *Otol Neurotol* **36**, 545-550 (2015).
8. J. A. Czechowicz, A. H. Messner, E. Alarcon-Matutti, J. Alarcon, G. Quinones-Calderon, S. Montano, J. R. Zunt, Hearing impairment and poverty: the epidemiology of ear disease in Peruvian schoolchildren. *Otolaryngology Head & Neck Surgery* **142**, 272-277 (2010).
9. A. M. H. Korver, R. J. H. Smith, G. Van Camp, M. R. Schleiss, M. A. K. Bitner-Glindzicz, L. R. Lustig, S.-i. Usami, A. N. Boudewyns, Congenital hearing loss. **3**, 16094 (2017).
10. C. H. Yang, T. Schrepfer, J. Schacht, Age-related hearing impairment and the triad of acquired hearing loss. *Front Cell Neurosci* **9**, 276 (2015).
11. F. H. Linthicum, Jr., J. Doherty, K. I. Berliner, Idiopathic sudden sensorineural hearing loss: vascular or viral? *Otolaryngol Head Neck Surg* **149**, 914-917 (2013).
12. A. Vambutas, S. Pathak, AAO: Autoimmune and Autoinflammatory (Disease) in Otology: What is New in Immune-Mediated Hearing Loss. *Laryngoscope Investig Otolaryngol* **1**, 110-115 (2016).
13. D. Weil, S. Blanchard, J. Kaplan, P. Guilford, F. Gibson, J. Walsh, P. Mburu, A. Varela, J. Levilliers, M. D. Weston, P. M. Kelley, W. J. Kimberling, M. Wagenaar, F. Levi-Acobas, D. Larget-Piet, A. Munnich, K. P. Steel, S. D. M. Brown, C. Petit, Defective myosin VIIA gene responsible for Usher syndrome type 1B. *Letters to Nature* **374**, 60-61 (1995).
14. Z. M. Ahmed, S. Riazuddin, S. L. Bernstein, Z. Ahmed, S. Khan, A. J. Griffith, R. J. Morell, T. B. Friedman, S. Riazuddin, E. R. Wilcox, Mutations of the protocadherin gene PCDH15 cause Usher syndrome type 1F. *American Journal of Human Genetics* **69**, 25-34 (2001).
15. H. Bolz, B. von Brederlow, A. Ramirez, E. C. Bryda, K. Kutsche, H. G. Nothwang, M. Seeliger, S.-C. M. D., M. C. Vila, O. P. Molina, A. Gal, C. Kubisch, Mutation of CDH23, encoding a new member of the cadherin gene family, causes Usher syndrome type 1D. *Nature Genetics* **27**, 108-112 (2001).

16. J. M. Bork, L. M. Peters, S. Riazuddin, S. L. Bernstein, Z. M. Ahmed, S. L. Ness, R. Polomeno, A. Ramesh, M. Schloss, C. R. Srisailpathy, S. Wayne, S. Bellman, D. Desmukh, Z. Ahmed, S. N. Khan, V. M. Kaloustian, X. C. Li, A. Lalwani, S. Riazuddin, M. Bitner-Glindzicz, W. E. Nance, X. Z. Liu, G. Wistow, R. J. Smith, A. J. Griffith, E. R. Wilcox, T. B. Friedman, R. J. Morell, Usher syndrome 1D and nonsyndromic autosomal recessive deafness DFNB12 are caused by allelic mutations of the novel cadherin-like gene CDH23. *American Journal of Human Genetics* **68**, 26-37 (2001).
17. D. F. Barker, S. L. Hostikka, J. Zhou, L. T. Chow, A. R. Oliphant, S. C. Gerken, M. C. Gregory, M. H. Skolnick, C. L. Atkin, K. Tryggvason, Identification of mutations in COL4A5 collagen gene in Alport syndrome. *Science* **248**, 1224-1227 (1990).
18. J. Zhou, D. F. Barker, S. L. Hostikka, M. C. Gregory, C. L. Atkin, K. Tryggvason, Single base mutation in alpha 5(IV) collagen chain gene converting a conserved cysteine to serine in Alport syndrome. *Genomics* **9**, 10-18 (1991).
19. S. A. Ross, Z. Novak, K. B. Fowler, N. Arora, W. J. Britt, S. B. Boppana, Cytomegalovirus blood viral load and hearing loss in young children with congenital infection. *Pediatr Infect Dis J* **28**, 588-592 (2009).
20. S. J. Schachtele, M. B. Mutnal, M. R. Schleiss, J. R. Lokensgard, Cytomegalovirus-induced sensorineural hearing loss with persistent cochlear inflammation in neonatal mice. *Journal of Neurovirology* **17**, 201-211 (2011).
21. R. J. Stokroos, F. W. Albers, J. Schirm, The etiology of idiopathic sudden sensorineural hearing loss. Experimental herpes simplex virus infection of the inner ear. *American Journal of Otology* **19**, 447-452 (1998).
22. B. E. Cohen, A. Durstenfeld, P. C. Roehm, Viral causes of hearing loss: a review for hearing health professionals. *Trends in Hearing* **18**, 1-17 (2014).
23. N. I. Girgis, Z. Farid, I. A. Mikhail, I. Farrag, Y. Sultan, M. E. Kilpatrick, Dexamethasone treatment for bacterial meningitis in children and adults. *The Pediatric Infectious Disease Journal* **8**, 848-851 (1989).
24. S. M. Bhatt, C. Cabellos, N. J. B., C. Halpin, A. Lauretano, W. Z. Xu, E. Tuomanen, The impact of dexamethasone on hearing loss in experimental pneumococcal meningitis. *The Pediatric Infectious Disease Journal* **11**, 93-96 (1995).
25. B. Fireman, S. B. Black, H. R. Shinefield, J. Lee, E. Lewis, P. Ray, Impact of the pneumococcal conjugate vaccine on otitis media. *Pediatric Infectious Disease Journal* **22**, 10-16 (2003).
26. J. A. Brody, T. Overfield, R. McAlister, Draining ears and deafness among alaskan eskimos. *JAMA Otolaryngology Head & Neck Surgery* **81**, 29-33 (1965).
27. A. Jacob, V. Rupa, A. Job, A. Joseph, Hearing impairment and otitis media in a rural primary school in South India. *International Journal of Pediatric Otorhinolaryngology* **39**, 133-138 (1997).
28. C. Tian, B. S. Harris, K. R. Johnson, Ectopic Mineralization and Conductive Hearing Loss in Enpp1asj Mutant Mice, a New Model for Otitis Media and Tympanosclerosis. *PLoS One* **11**, e0168159 (2016).
29. F. Suga, J. R. Lindsay, Labyrinthitis ossificans due to chronic otitis media. *Annals of Otology, Rhinology & Laryngology* **84**, 37-44 (1975).

30. Z. Papp, S. Rezes, I. Jokay, I. Sziklai, Sensorineural hearing loss in chronic otitis media. *Otology & Neurotology* **24**, 141-144 (2003).
31. M. C. Liberman, L. D. Liberman, S. F. Maison, Chronic Conductive Hearing Loss Leads to Cochlear Degeneration. *PLoS One* **10**, e0142341 (2015).
32. N. Watson, B. Ding, X. Zhu, R. D. Frisina, Chronic inflammation - inflammaging - in the ageing cochlea: A novel target for future presbycusis therapy. *Ageing Res Rev* **40**, 142-148 (2017).
33. Y. Dong, M. Li, P. Liu, H. Song, Y. Zhao, J. Shi, Genes involved in immunity and apoptosis are associated with human presbycusis based on microarray analysis. *Acta Otolaryngologica* **134**, 601-608 (2014).
34. C. Sanchez-Rodriguez, E. Martin-Sanz, E. Cuadrado, J. J. Granizo, R. Sanz-Fernandez, Protective effect of polyphenols on presbycusis via oxidative/nitrosative stress suppression in rats. *Experimental Gerontology* **83**, 31-36 (2016).
35. C. Hederstierna, U. Rosenhall, Age-related hearing decline in individuals with and without occupational noise exposure. *Noise Health* **18**, 21-25 (2016).
36. J. J. Miller, L. Beck, A. Davis, D. E. Jones, A. B. Thomas, Hearing loss in patients with diabetic retinopathy. *American Journal of Otolaryngology* **4**, 342-346 (1983).
37. T. L. Smith, E. Raynor, J. Prazma, J. E. Buenting, H. C. Pillsbury, Insulin-dependent diabetic microangiopathy in the inner ear. *The Laryngoscoope* **105**, 236-240 (1995).
38. S. Ulu, A. Bucak, M. S. Ulu, A. Ahsen, A. Duran, F. Yucedag, A. Aycicek, Neutrophil-lymphocyte rato as a new predictive and prognostic factor at the hearing loss of diabetic patients. *European Archives of Oto-Rhino-Laryngology* **271**, 2681-2686 (2014).
39. R. C. Bone, R. A. Balk, F. B. Cerra, R. P. Dellinger, A. M. Fein, W. A. Knaus, R. M. H. Schein, W. J. Sibbald, Definitions for sepsis and organ failure and guidelines for the use of innovative therapies in sepsis. *Chest* **101**, 1644-1655 (1992).
40. B. Goldstein, B. Giroir, A. Randolph, International pediatric sepsis consensus conference: definitions for sepsis and organ dysfunction in pediatrics. *Pediatric Critical Care Medicine* **6**, 2-8 (2005).
41. L. F. Gentile, L. L. Moldawer, DAMPs, PAMPs, and the origins of SIRS in bacterial sepsis. *Shock* **39**, 113-114 (2013).
42. P. Matzinger, The danger model: A renewed sense of self. *Science* **296**, 301-305 (2002).
43. M. J. Jimenez-Dalmaroni, M. E. Gerswhin, I. E. Adamopoulos, The critical role of toll-like receptors--From microbial recognition to autoimmunity: A comprehensive review. *Autoimmunity Reviews* **15**, 1-8 (2016).
44. B. McDonald, P. Kubes, Innate Immune Cell Trafficking and Function During Sterile Inflammation of the Liver. *Gastroenterology* **151**, 1087-1095 (2016).
45. A. Poltorak, X. He, I. Smirnova, M. Y. Liu, C. Van Huffel, X. Du, D. Birdwell, E. Alejos, M. Silva, C. Galanos, M. Freudenberg, P. Ricciardi-Castagnoli, B. Layton, B. Beutler, Defective LPS signaling in C3H/HeJ and C57BL/10ScCr mice: mutations in Tlr4 gene. *Science* **282**, 2085-2088 (1998).

46. C. C. Baker, I. H. Chaudry, H. O. Gaines, A. E. Baue, Evaluation of factors affecting mortality rate after sepsis in a murine cecal ligation and puncture model. *Surgery* **94**, 331-335 (1983).
47. D. G. Remick, D. E. Newcomb, G. L. Bolgos, D. R. Call, Comparison of the mortality and inflammatory response of two models of sepsis: lipopolysaccharide vs. cecal ligation and puncture. *Shock* **13**, 110-116 (2000).
48. J. A. Buras, B. Holzmann, M. Sitkovsky, Animal models of sepsis: setting the stage. *Nature Reviews in Drug Discovery* **4**, 854-865 (2005).
49. K. M. Druey, P. R. Greipp, Narrative Review: The Systemic Capillary Leak Syndrome. *Annals of Internal Medicine* **153**, 90-98 (2010).
50. G. Marx, B. Vangerow, C. Burczyk, K. F. Gratz, N. Maassen, M. Cobas Meyer, M. Leuwer, E. Kuse, H. Rueckoldt, Evaluation of noninvasive determinants for capillary leakage syndrome in septic shock patients. *Intensive Care Medicine* **26**, 1252-1258 (2014).
51. N. Burkard, M. Meir, S. Flemming, C. T. Germer, N. Schlegel, Endothelial barrier dysfunction, loss of microcirculatory flow and organ failure in sepsis: current clinical view of sepsis and links to basic research. *Medical Research Archives* **5**, 1-18 (2017).
52. L. Smart, S. P. J. Macdonald, S. Burrows, E. Bosio, G. Arendts, D. M. Fatovich, Endothelial glycocalyx biomarkers increase in patients with infection during Emergency Department treatment. *Journal of Critical Care* **42**, 304-309 (2017).
53. F. Dal-Pizzol, H. A. Rojas, E. M. dos Santos, F. Vuolo, L. Constantino, G. Feier, M. Pasquali, C. M. Comim, F. Petronilho, D. P. Gelain, J. Quevedo, J. C. Moreira, C. Ritter, Matrix metalloproteinase-2 and metalloproteinase-9 activities are associated with blood-brain barrier dysfunction in an animal model of severe sepsis. *Molecular neurobiology* **48**, 62-70 (2013).
54. W. M. Armstead, R. Mirro, O. P. Thelin, M. Shibata, S. L. Zuckerman, D. R. Shanklin, D. W. Vusija, C. W. Leffler, Polyethylene glycol superoxide dismutase and catalase attenuate increased blood-brain barrier permeability after ischemia in piglets. *Stroke* **23**, 755-762 (1992).
55. T. Barichello, J. C. Lemos, J. S. Generoso, A. L. Cipriano, G. L. Milioli, D. M. Marcelino, F. Vuolo, F. Petronilho, F. Dal-Pizzol, M. C. Vilela, A. L. Teixeira, Oxidative stress, cytokine/chemokine and disruption of blood-brain barrier in neonate rats after meningitis by Streptococcus agalactiae. *Neurochemical Research* **36**, 1922-1930 (2011).
56. C. C. Lee, Y. Sun, S. Qian, H. W. Huang, Transmembrane pores formed by human antimicrobial peptide LL-37. *Biophysical Journal* **100**, 1688-1696 (2011).
57. J. M. Harlan, Neutrophil mediated vascular injury. *Acta Medica Scandinavica* **221**, 123-129 (1987).
58. M. S. Blum, E. Toninelli, J. M. Anderson, M. S. Balda, J. Zhou, L. O'Donnell, R. Pardi, J. R. Bender, Cytoskeletal rearrangement mediates human microvascular endothelial tight junction modulation by cytokines. *American Journal of Physiology* **273**, H286-H294 (1997).
59. T. B. Rajavashisth, J. K. Liao, Z. S. Galis, S. Tripathi, U. Laufs, J. Tripathi, N. N. Chai, X. P. Xu, S. Jovinge, P. K. Shah, P. Libby, Inflammatory cytokines and oxidized low density lipoproteins increase endothelial cell expression of

membrane type 1-matric metalloproteinase. *Journal of Biological Chemistry* **274**, 11924-11929 (1999).
60. G. S. Herron, M. J. Banda, E. J. Clark, J. Gavrilovic, Z. Werb, Secrestion of metalloproteinases by stimulated capillary endothelial cells. *Journal of Biological Chemistry* **261**, 2814-2818 (1986).
61. R. Hanemaaijer, P. Kookwijk, L. L. Clercq, W. J. De Vree, V. W. van Hinsbergh, Regulation of matrix metalloproteinase expression in human vein and microvascular endothelial cells. Effects of tumour necrosis factor alpha, interleukin 1 and phorbol ester. *Biochemical Journal* **296**, 803-809 (1993).
62. R. A. Balk, Severe sepsis and septic schock: definitions, epidemiology, and clinical manifestations. *Critical Care Clinics* **16**, 179-192 (2000).
63. P. O. Nystrom, The systemic inflammatory response syndrome: definitions and aetiology. *Journal of Antimicrobial Chemotherapy* **41**, 1-7 (1998).
64. M. Singer, C. S. Deutschman, C. W. Seymour, M. Shankar-Hari, D. Annane, M. Bauer, R. Bellomo, G. R. Bernard, J. D. Chiche, C. M. Coopersmith, R. S. Hotchkiss, M. M. Levy, J. C. Marshall, G. S. Martin, S. M. Opal, G. D. Rubenfeld, T. van der Poll, J. L. Vincent, D. C. Angus, The Third International Consensus Definitions for Sepsis and Septic Shock (Sepsis-3). *JAMA* **315**, 801-810 (2016).
65. A. L. Beal, F. B. Cerra, Multiple organ failure syndrome in the 1990s systemic inflammatory response and organ dysfunction. *JAMA* **271**, 226-233 (1994).
66. R. C. Bone, Sir Issac Newton, spesis, SIRS, and CARS. *Critical Care Medicine* **24**, 1125-1128 (1996).
67. N. S. Ward, B. Casserly, A. Ayala, The compensatory anti-inflammatory response syndrome (CARS) in critically ill patients. *Clinical Chest Medicine* **29**, 617-625, viii (2008).
68. H. B. Sapan, I. Paturusi, A. A. Islam, I. Yusuf, I. Patellongi, M. N. Massi, A. D. Pusponegoro, S. K. Arief, I. Labeda, L. Rendy, M. Hatta, Impact of interleukin-6 and interleukin-10 serum levels and mRNA expression level on polytrauma patients. *Chinese Journal of Traumatology* **Ahead of Print**, 1-5 (2017).
69. H. G. Gomez, S. M. Gonzalez, J. M. Londono, N. A. Hoyos, C. D. Nino, A. L. Leon, P. A. Velilla, M. T. Rugeles, F. A. Jaimes, Immunological characterization of compensatory anti-inflammatory response syndrome in patients with severe sepsis: a longitudinal study*. *Critical Care Medicine* **42**, 771-780 (2014).
70. R. P. Dellinger, M. M. Levy, A. Rhodes, D. Annane, H. Gerlach, S. M. Opal, J. E. Sevransky, C. L. Sprung, I. S. Douglas, R. Jaeschke, T. M. Osborn, M. E. Nunnally, S. R. Townsend, K. Reinhart, R. M. Kleinpell, D. C. Angus, C. S. Deutschman, F. R. Machado, G. D. Rubenfeld, S. Webb, R. J. Beale, J. L. Vincent, R. Moreno, Surviving Sepsis Campaign: international guidelines for management of severe sepsis and septic shock, 2012. *Intensive Care Medicine* **39**, 165-228 (2013).
71. A. Kumar, D. Roberts, K. E. Wood, B. Light, J. E. Parrillo, S. Sharma, R. Suppes, D. Feinstein, S. Zanotti, L. Taiberg, D. Gurka, A. Kumar, M. Cheang, Duration of hypotension before initiation of effective antimicrobial therapy is the critical determinant of survival in human septic shock. *Critical Care Medicine* **34**, 1589-1596 (2006).

72. A. Kumar, R. Zarychanski, B. Light, J. Parrillo, D. Maki, D. Simon, D. Laporta, S. Lapinsky, P. Ellis, Y. Mirzanejad, G. Martinka, S. Keenan, G. Wood, Y. Arabi, D. Feinstein, A. Kumar, P. Dodek, L. Kravetsky, S. Doucette, G. Cooperative Antimicrobial Therapy of Septic Shock Database Research, Early combination antibiotic therapy yields improved survival compared with monotherapy in septic shock: a propensity-matched analysis. *Critical Care Medicine* **38**, 1773-1785 (2010).
73. C. W. Seymour, F. Gesten, H. C. Prescott, M. E. Friedrich, T. J. Iwashyna, G. S. Phillips, S. Lemeshow, T. Osborn, K. M. Terry, M. M. Levy, Time to treatment and mortality during mandated emergency care for sepsis. *New England Journal of Medicine* **376**, 2235-2244 (2017).
74. J. L. Houghton, K. D. Green, W. Chen, S. Garneau-Tsodikova, The future of aminoglycosides: the end or renaissance? *Chembiochem* **11**, 880-902 (2010).
75. B. D. Freeman, C. Natanson, Anti-inflammatory therapies in sepsis and septic shock. *Expert Opinion on Investigational Drugs* **9**, 1651-1663 (2000).
76. D. Gao, Z. yang, Q. Qi, Roles of PD-1, Tim-3 and CTLA-4 in immunoreguation in regulatory T cells among patients with sepsis. *INternational Journal of Experimental Medicine* **8**, 18998-19005 (2015).
77. J. T. Muenzer, C. G. Davis, K. Chang, R. E. Schmidt, W. M. Dunne, C. M. Coopersmith, R. S. Hotchkiss, Characterization and modulation of the immunosuppressive phase of sepsis. *Infection and Immunology* **78**, 1582-1592 (2010).
78. N. C. Arbour, E. Lorenz, B. C. Schutte, J. Zabner, J. N. Kline, M. Jones, K. Frees, J. L. Watt, D. A. Schwartz, TLR4 mutations are associated with endotoxin hyporesponsiveness in humans. *Nature Genetics* **25**, 187-191 (2000).
79. D. M. Agnese, J. E. Calvano, S. J. Hahm, S. M. Coyle, S. A. Corbett, S. E. Calvano, S. F. Lowry, Human toll-like receptor 4 mutations but not CD14 polymorphisms are associated with an increased risk of gram-negative infections. *Journal of Infectious Disease* **186**, 1522-1525 (2002).
80. A. Schatz, E. Bugie, S. A. Waksman, Streptomycin, a substance exhibiting antibiotic activity against gram-positive and gram-negative bacteria. *Proceedings of the Society for Experimental Biology and Medicine* **55**, 66-69 (1944).
81. P. Dozzo, H. E. Moser, New aminoglycoside antibiotics. *Expert Opinion on Therapeutic Patents* **20**, 1321-1341 (2010).
82. S. N. Hobbie, S. Akshay, S. K. Kalapala, C. M. Bruell, D. Shcherbakov, E. C. Bottger, Genetic analysis of interactions with eukaryotic rRNA identify the mitoribosome as target in aminoglycoside ototoxicity. *PNAS* **105**, 20888-20893 (2008).
83. K. Hamasaki, R. R. Rando, Specific Binding of Aminoglycosides to a Human rRNA Construct Based on a DNA Polymorphism Which Causes Aminoglycoside-Induced Deafness. *Biochemistry* **36**, 12323-12328 (1997).
84. Z. Gao, Y. Chen, M.-X. Guan, Mitochondrial DNA mutations associated with aminoglycoside induced ototoxicity. *Journal of Otology* **12**, 1-8 (2017).
85. B. M. Wang, N. D. Weiner, A. Takada, J. Schacht, Characterization of aminoglycoside-lipid interactions and development of a refined model for ototoxicity testing. *Biochemical Pharmacology* **33**, 3257-3262 (1984).

86. R. Brasseur, G. Laurent, J. M. Ruysschaert, P. Tulkens, Interactions of aminoglycoside antibiotics with negatively charged lipid bilayers: biochemical and conformational studies. *Biochemical Pharmacology* **33**, 629-637 (1984).
87. M. B. Carlier, G. Laurent, P. J. Claes, H. J. Vanderhaeghe, P. M. Tulkens, Inhibition of lysosomal phospholipases by aminoglycoside antibiotics: in vitro comparative studies. *Antimicrobial Agents and Chemotherapy* **23**, 440-449 (1983).
88. G. Laurent, M. B. Carlier, B. Rollman, F. Van Hoof, P. Tulkens, Mechanism of aminoglycoside-induced lysosomal phospholipidosis: in vitro and in vivo studies with gentamicin and amikacin. *Biochemical Pharmacology* **31**, 3861-3870 (1982).
89. F. Van Bambeke, M. P. Mingeot-Leclercq, A. Schanck, R. Brasseur, P. M. Tulkens, Alterations in membrane permeability induced by aminoglycoside antibiotics: studies on liposomes and cultured cells. *European Jourand of Pharmacology: Molecular Pharmacology* **247**, 155-168 (1993).
90. S. Bera, G. G. Zhanel, F. Schweizer, Antibacterial activities of aminoglycoside antibiotics-derived cationic amphiphiles. Polyol-modified neomycin B-, kanamycin A-, amikacin-, and neamine-based amphiphiles with potent broad spectrum antibacterial activity. *Journal of Medicinal Chemistry* **53**, 3626-3631 (2010).
91. B. Findlay, G. G. Zhanel, F. Schweizer, Cationic amphiphiles, a new generation of antimicrobials inspired by the natural antimicrobial peptide scaffold. *Antimicrobial Agents and Chemotherapy* **54**, 4049-4058 (2010).
92. N. P. Chongsiriwatana, J. S. Lin, R. Kapoor, M. Wetzler, J. A. C. Rea, M. K. Didwania, C. H. Contag, A. E. Barron, Intracellular biomass flocculation as a key mechanism of rapid bacterial killing by cationic, amphipathic antimicrobial peptides and peptoids. *Scientific Reports* **7**, 16718 (2017).
93. Y. Chen, W. G. Huang, D. J. Zha, J. H. Qiu, J. L. Wang, S. H. Sha, J. Schacht, Aspirin attenuates gentamicin ototoxicity: from the laboratory to the clinic. *Hearing Research* **226**, 178-182 (2007).
94. S. Sha, G. Zajic, C. J. Epstein, J. Schacht, Overexpression of copper/zinc-superoxide dismutase protects from kanamycin-induced hearing loss. *Audiology & Neurotology* **6**, 117-123 (2001).
95. T. Karasawa, Q. Wang, Y. Fu, D. M. Cohen, P. S. Steyger, TRPV4 enhances the cellular uptake of aminoglycoside antibiotics. *J ournal of Cell Science* **121**, 2871-2879 (2008).
96. R. S. Stepanyan, A. A. Indzhykulian, A. C. Velez-Ortega, E. T. Boger, P. S. Steyger, T. B. Friedman, G. I. Frolenkov, TRPA1-mediated accumulation of aminoglycosides in mouse cochlear outer hair cells. *Journal of The Association for Research in Otolaryngology* **12**, 729-740 (2011).
97. A. Alharazneh, L. Luk, M. Huth, A. Monfared, P. S. Steyger, A. G. Cheng, A. J. Ricci, Functional hair cell mechanotransducer channels are required for aminoglycoside ototoxicity. *PLoS One* **6**, e22347 (2011).
98. A. B. A. Kroese, A. Das, A. J. Hudspeth, Blockage of the transduction channels of hair cells in the bullfrog's sacculus by aminoglycoside antibiotics. *Hearing Research* **37**, 203-218 (1989).

99. H. Ohmori, Mechano-electrical transduction currents in isolated vestibular hair cells of the chick. *Journal of Physiology* **359**, 180-217 (1985).
100. L. F. Corns, S. L. Johnson, C. J. Kros, W. Marcotti, Tmc1 Point Mutation Affects Ca2+ Sensitivity and Block by Dihydrostreptomycin of the Mechanoelectrical Transducer Current of Mouse Outer Hair Cells. *Journal of Neuroscience* **36**, 336-349 (2016).
101. P. D. Holohan, P. P. Sokol, C. R. Ross, R. Coulson, M. E. Trimble, D. A. Laska, P. D. Williams, Gentamicin-induced increases in cytosolic calcium in pig kidney cells (LLC-PK1)1. *The Journal of Experimental Therapeutics* **247**, 349-354 (1988).
102. R. Esterberg, D. W. Hailey, A. B. Coffin, D. W. Raible, E. W. Rubel, Disruption of intracellular calcium regulation is integral to aminoglycoside-induced hair cell death. *Journal of Neuroscience* **33**, 7513-7525 (2013).
103. J. M. Weinberg, R. J. Simmons, H. D. Humes, Alterations of mitochondrial respiration induced by aminoglycoside antibiotics. *Research Communications in Chemical Pathology and Pharmacology* **27**, 521-531 (1980).
104. T. Kitahara, H. S. Li-Korotky, C. D. Balaban, Regulation of mitochondrial uncoupling proteins in mouse inner ear ganglion cells in response to systemic kanamycin challenge. *Neuroscience* **135**, 639-653 (2005).
105. R. Esterberg, T. Linbo, S. B. Pickett, P. Wu, H. C. Ou, E. W. Rubel, D. W. Raible, Mitochondrial calcium uptake underlies ROS generation during aminoglycoside-induced hair cell death. *Journal of Clinical Investigation* **126**, 3556-3566 (2016).
106. W. Liesniak, V. L. Pecoraro, J. Schacht, Ternary complexes of gentamicin with iron and lipid catalyze formation of reactive oxygen species. *Chemical Research in Toxicology* **18**, 357-364 (2005).
107. R. Allam, M. N. Darisipudi, K. V. Rupanagudi, J. Lichtnekert, J. Tschopp, H. J. Anders, Cutting edge: cyclic polypeptide and aminoglycoside antibiotics trigger IL-1beta secretion by activating the NLRP3 inflammasome. *Journal of Immunology* **186**, 2714-2718 (2011).
108. S. Sha, J. Schacht, Stimulation of free radical formation by aminoglycoside antibiotics. *Hearing Research* **128**, 112-118 (1999).
109. H. Jiang, S. H. Sha, J. Schacht, NF-kappaB pathway protects cochlear hair cells from aminoglycoside-induced ototoxicity. *J Neurosci Res* **79**, 644-651 (2005).
110. E. Ozbek, M. Cekmen, Y. O. Ilbey, A. Simsek, E. C. Polat, A. Somay, Atorvastatin prevents gentamicin-induced renal damage in rats through the inhibition of p38-MAPK and NF-kappaB pathways. *Renal failure* **31**, 382-392 (2009).
111. J. H. Lee, S. H. Oh, T. H. Kim, Y. Y. Go, J. J. Song, Anti-apoptotic effect of dexamethasone in an ototoxicity model. *Biomaterial Research* **21**, 4 (2017).
112. G. B. Kauffman, R. Pentimalli, S. Doldi, M. D. Hall, Michele Peyrone (1813-1883), Discoverer of Cisplatin. *Platinum Metals Review* **54**, 250-256 (2010).
113. B. Rosenberg, L. V. Camp, T. Krigas, Inhibition of cell division in *Escherichia coli* by electrolysis products from a platinum electrode. *Nature* **205**, 698-699 (1965).

114. B. Rosenberg, L. V. Camp, J. E. Trosko, V. H. Mansour, Platinum compounds: a new class of potent antitumour agents. *Nature* **222**, 385-386 (1969).
115. S. Dasari, P. B. Tchounwou, Cisplatin in cancer therapy: molecular mechanisms of action. *European Journal of Pharmacology* **740**, 364-378 (2014).
116. M. Rozencweig, D. D. Von Hoff, M. Slavik, F. M. Muggia, *Cis*-diamminedichloroplatinum (II): a new anticancer drug. *Annals of Internal Medicine* **86**, 803-812 (1977).
117. D. J. Beck, R. R. Brubaker, Effect of *cis*-platinum(II)diamminodichloride on wild type and deoxyribonucleic acid repair-deficient mutants of *Escherichia coli*. *Journal of Bacteriology* **116**, 1247-1252 (1973).
118. S. L. Gonias, A. C. Oakley, P. J. Walther, S. V. Pizzo, Effects of diethyldithiocarbamate and nine other nucleophiles on the intersubunit protein cross-linking and inactivation of purified human alpha2-macroglobulin by cisdiamminedichloroplatinum(II). *Cancer Research* **44**, 5764-5770 (1984).
119. A. Casini, C. Gabbiani, G. Mastrobuoni, L. Messori, G. Moneti, G. Pieraccini, Exploring metallodrug-protein interactions by ESI mass spectroscopy: the reaction of anticancer platinum drugs with horse heart cytochrome c. *ChemMedChem* **1**, 413-417 (2006).
120. S. Waissbluth, S. J. Daniel, Cisplatin-induced ototoxicity: transporters playing a role in cisplatin toxicity. *Hearing Research* **299**, 37-45 (2013).
121. S. Ishida, J. Lee, D. J. Thiele, I. Herskowitz, Uptake of the anticancer drug cisplatin mediated by the copper transporter Ctr1 in yeast and mammals. *PNAS* **99**, 14298-14302 (2002).
122. X. Yang, M. Page, P-glycoprotein expression in ovarian cancer cell line following treatment with cisplatin. *Oncology Research* **7**, 619-624 (1995).
123. N. Kitada, K. Takara, M. Tsujimoto, T. Sakaeda, N. Ohnishi, T. Yokoyama, Effects of platinum derivatives on the function and expression of p-glycoprotein/MDR1 in LLC-PK1 cells: in the cases of carboplatin and nedaplatin. *Journal of Cancer Molecules* **3**, 23-28 (2007).
124. K. K. Filipski, W. J. Loos, J. Verweij, A. Sparreboom, Interaction of Cisplatin with the human organic cation transporter 2. *Clinical Cancer Research* **14**, 3875-3880 (2008).
125. G. Ciarimboli, D. Deuster, A. Knief, M. Sperling, M. Holtkamp, B. Edemir, H. Pavenstadt, C. Lanvers-Kaminsky, A. am Zehnhoff-Dinnesen, A. H. Schinkel, H. Koepsell, H. Jurgens, E. Schlatter, Organic cation transporter 2 mediates cisplatin-induced oto- and nephrotoxicity and is a target for protective interventions. *American Journal of Pathology* **176**, 1169-1180 (2010).
126. D. Ding, J. He, B. L. Allman, D. Yu, H. Jiang, G. M. Seigel, R. J. Salvi, Cisplatin ototoxicity in rat cochlear organotypic cultures. *Hearing Research* **282**, 196-203 (2011).
127. B. Liedert, V. Materna, D. Schadendorf, J. Thomale, H. Lage, Overexpression of cMOAT (MRP2/ABCC2) is associated with decreased formation of platinum-DNA adducts and decreased G2-arrest in melanoma cells resistant to cisplatin. *Journal of Investigative Dermatology* **121**, 172-176 (2003).
128. V. Materna, B. Liedert, J. Thomale, H. Lage, Protection of platinum-DNA adduct formation and reversal of cisplatin resistance by anti-MRP2 hammerhead

ribozymes in human cancer cells. *International Journal of Cancer* **115**, 393-402 (2005).
129. T. Kimitsuki, T. Nakagawa, K. Hisashi, S. Komune, S. Komiyama, Cisplatin blocks mechano-electric transducer current in chick cochlear hair cells. *Hearing Research* **71**, 64-68 (1993).
130. A. J. Thomas, D. W. Hailey, T. M. Stawicki, P. Wu, A. B. Coffin, E. W. Rubel, D. W. Raible, J. A. Simon, H. C. Ou, Functional mechanotransduction is required for cisplatin-induced hair cell death in the zebrafish lateral line. *Journal of Neuroscience* **33**, 4405-4414 (2013).
131. N. Milosavljevic, C. Duranton, N. Djerbi, P. H. Puech, P. Gounon, D. Lagadic-Gossmann, M. T. Dimanche-Boitrel, C. Rauch, M. Tauc, L. Counillon, M. Poet, Nongenomic effects of cisplatin: acute inhibition of mechanosensitive transporters and channels without actin remodeling. *Cancer Research* **70**, 7514-7522 (2010).
132. Y. H. Chu, M. Sibrian-Vazquez, J. O. Escobedo, A. R. Phillips, D. T. Dickey, Q. Wang, M. Ralle, P. S. Steyger, R. M. Strongin, Systemic Delivery and Biodistribution of Cisplatin in Vivo. *Molecular Pharmaceutics* **13**, 2677-2682 (2016).
133. E. Norberg, V. Gogvadze, M. Ott, M. Horn, P. Uhlen, S. Orrenius, B. Zhivotovsky, An increase in intracellular Ca2+ is required for the activation of mitochondrial calpain to release AIF during cell death. *Cell Death Differ* **15**, 1857-1864 (2008).
134. R. A. Hromas, P. A. Andrews, M. P. Murphy, C. P. Burns, Glutathione depletion reverses cisplatin resistance in murine L1210 leukemia cells. *Cancer letters* **34**, 9-13 (1987).
135. P. A. Andrews, M. A. Schiefer, M. P. Murphy, S. B. Howell, Enhanced potentiation of cisplatin cytotoxicity in human ovarian carcinoma cells by prolonged glutathione depletion. *Chemico-Biological Interactions* **65**, 51-58 (1988).
136. S. Nakano, M. Gemba, Potentiation of cisplatin-induced lipid peroxidation in kidney cortical slices by glutathione depletion. *Japanese Journal of Pharmacology* **50**, 87-92 (1989).
137. W. Lieberthal, V. Triaca, J. Levine, Mechanisms of death induced by cisplatin in proximal tubular epithelial cells: apoptosis vs. necrosis. *American Journal of Physiology Renal Physiology* **270**, F700-F708 (1996).
138. T. Kaur, D. Mukherjea, K. Sheehan, S. Jajoo, L. P. Rybak, V. Ramkumar, Short interfering RNA against STAT1 attenuates cisplatin-induced ototoxicity in the rat by suppressing inflammation. *Cell Death and Disease* **2**, e180 (2011).
139. P. Ehrlich, Uber die Beziehungen von chemische constitution, vertheilung, und pharmakologischer wirkung. *Collected Studies in Immunity*, 567-595 (1906).
140. E. E. Goldmann, Die aussere und innere sekretion des genden und gekranken organismus im licht der vatalen farbung. *Beitr Klin Chir* **64**, (1909).
141. W. G. Mayhan, D. D. Heistad, Permeability of blood-brain barrier to various sized molecules. *American Journal of Physiology* **248**, H712-H718 (1985).
142. T. Nitta, M. Hata, S. Gotoh, Y. Seo, H. Sasaki, N. Hashimoto, M. Furuse, S. Tsukita, Size-selective loosening of the blood-brain barrier in claudin-5-deficient mice. *Journal of Cellular Biology* **161**, 653-660 (2003).

143. H. Van De Waterbeemd, G. Camenisch, G. Folkers, J. R. Chretien, O. A. Raevsky, Estimation of blood-brain barrier crossing of drugs using molecular size and shape, and H-bonding descriptors. *Journal of Drug Targeting* **6**, 151-165 (1998).
144. C. M. Van Itallie, J. M. Anderson, The role of claudins in determining paracellular charge selectivity. *Proceedings of the American Thoracic Society* **1**, 38-41 (2004).
145. E. Neuwelt, N. J. Abbott, L. Abrey, W. A. Banks, B. Blakley, T. P. Davis, B. Engelhardt, P. Grammas, M. Nedergaard, J. Nutt, W. Pardridge, G. A. Rosenberg, Q. Smith, L. R. Drewes, Strategies to advance translational research into brain barriers. *The Lancet Neurology* **7**, 84-96 (2008).
146. J. Millan, L. Hewlett, M. Glyn, D. Toomre, P. Clark, A. J. Ridley, Lymphocyte transcellular migration occurs through recruitment of endothelial ICAM-1 to caveola- and F-actin-rich domains. *Nature Cellular Biology* **8**, 113-123 (2006).
147. M. De Bock, V. Van Haver, R. E. Vandenbroucke, E. Decrock, N. Wang, L. Leybaert, Into rather unexplored terrain-transcellular transport across the blood-brain barrier. *Glia* **64**, 1097-1123 (2016).
148. D. Knowland, A. Arac, K. Sekiguchi, M. Hsu, S. Lutz, J. Perrino, G. Steinberg, B. Barres, A. Nimmerjahn, D. Agalliu, Stepwise recruitment of transcellular and paracellular pathways underlies blood-brain barrier breakdown in stroke. *Neuron* **82**, 603-617 (2014).
149. L. Claudio, Y. Kress, W. T. Norton, C. F. Brosnan, Increased vesicular transport and decreased mitochondrial content in blood-brain barrier endothelial cells during experimental autoimmune encephalomyelitis. *American Journal of Pathology* **135**, 1157-1168 (1989).
150. A. A. Vu, G. S. Nadaraja, M. E. Huth, L. Luk, J. Kim, R. Chai, A. J. Ricci, A. G. Cheng, Integrity and regeneration of mechanotransduction machinery regulate aminoglycoside entry and sensory cell death. *PLoS One* **8**, e54794 (2013).
151. Y. Kobayashi, N. Ohshiro, R. Sakai, M. Ohbayashi, N. Kohyama, T. Yamamoto, Transport mechanism and substrate specificity of human organic anion transporter 2 (hOat2 [SLC22A7]). *J Pharm Pharmacol* **57**, 573-578 (2005).
152. A. Axelsson, The vascular anatomy of the cochlea in the guinea pig and in man. *Acta Oto-Laryngologica* **S243**, 3+ (1968).
153. S. K. Juhn, L. P. Rybak, L. W. Fowlks, Transport chareacteristics of the blood-perilymph barrier. *American Journal of Otolaryngology* **3**, 392-396 (1982).
154. R. R. Ciuman, Communication routes between intracranial spaces and inner ear: function, pathophysiologic importance and relations with inner ear diseases. *American Journal of Otolaryngology* **30**, 193-202 (2009).
155. H. Rask-Andersen, A. Schrott-Fischer, K. Pfaller, R. Glueckert, Perilymph/modiolar communications routes in the human cochlea. *Ear & Hearing* **27**, 457-465 (2006).
156. O. Seterkers, E. Ferrary, C. Amiel, Production of Inner Ear Fluids. *Physiological Reviews* **68**, 1083-1128 (1988).
157. B. Kellerhals, Perilymph production and cochlear blood flow. *Acta Oto-Laryngologica* **87**, 370-374 (1979).
158. M. E. Glasscock, The stapes gusher. *Archives of otolaryngology* **98**, 82-91 (1973).

159. L. Neng, F. Zhang, A. Kachelmeier, X. Shi, Endothelial cell, pericyte, and perivascular resident macrophage-type melanocyte interactions regulate cochlear intrastrial fluid-blood barrier permeability. *Journal of the Association for Research in Otolaryngology* **14**, 175-185 (2013).
160. X. Shi, Pathophysiology of the cochlear intrastrial fluid-blood barrier (review). *Hearing Research* **338**, 52-63 (2016).
161. X. Shi, Resident macrophages in the cochlear blood-labyrinth barrier and their renewal via migration of bone-marrow-derived cells. *Cell Tissue Research* **342**, 21-30 (2010).
162. W. Zhang, M. Dai, A. Fridberger, A. Hassan, J. Degagne, L. Neng, F. Zhang, W. He, T. Ren, D. Trune, M. Auer, X. Shi, Perivascular-resident macrophage-like melanocytes in the inner ear are essential for the integrity of the intrastrial fluid-blood barrier. *PNAS* **109**, 10388-10393 (2012).
163. E. Zemel, A. Loewenstein, B. Lei, M. Lazar, I. Perlman, Ocular pigmentation protects the rabbit retina from gentamicin-induced toxicity. *Investigative Ophthalmology & Visual Science* **36**, 1875-1884 (1995).
164. B. Hirt, Z. H. Penkova, A. Eckhard, W. Liu, H. Rask-Andersen, M. Muller, H. Lowenheim, The subcellular distribution of aquaporin 5 in the cochlea reveals a water shunt at the perilymph-endolymph barrier. *Neuroscience* **168**, 957-970 (2010).
165. F. F. Offner, P. Dallos, M. A. Cheatham, Positive endocochlear potential: Mechanism of production by marginal cells of stria vascularis. *Hearing Research* **29**, 117-124 (1987).
166. Y. Yang, M. Dai, T. M. Wilson, I. Omelchenko, J. E. Klimek, P. A. Wilmarth, L. L. David, A. L. Nuttall, P. G. Gillespie, X. Shi, Na+/K+-ATPase alpha1 identified as an abundant protein in the blood-labyrinth barrier that plays an essential role in the barrier integrity. *PLoS One* **6**, e16547 (2011).
167. R. C. Cmejrek, C. A. Megerian, Obstructing lesions of the endolymphatic sac and duct mimicking Meniere's disease. *ENT-Ear, Nose & Throat Journal* **83**, 753-756 (2004).
168. A. M. Amlani, K. Chesk, A. Hersey, An acoustical assessment of the music memory in commercially available hearing aids. *Journal of Communication Disorders, Deaf Studies & Hearing Aids* **2**, 109 (2014).
169. J. Domenech, M. Carulla, J. Traserra, Sensorineural high-frequency hearing loss after drill-generated acoustic trauma in tympanoplasty. *Archives of Oto-Rhino-Laryngology* **246**, 280-282 (1989).
170. J. N. Fayad, A. O. Makarem, F. H. Linthicum, Jr., Histopathologic assessment of fibrosis and new bone formation in implanted human temporal bones using 3D reconstruction. *Otolaryngol Head Neck Surg* **141**, 247-252 (2009).
171. M. Seyyedi, J. B. Nadol, Jr., Intracochlear inflammatory response to cochlear implant electrodes in humans. *Otol Neurotol* **35**, 1545-1551 (2014).
172. F. Ghavi, H. Mirzadeh, M. Imani, C. Jolly, M. Farhadi, Corticosteroid-releasing cochlear implant: a novel hybrid of biomaterial and drug delivery system. *J Biomed Mater Res B Appl Biomater* **94**, 388-398 (2010).
173. A. Wrzeszcz, B. Dittrich, D. Haamann, P. Aliuos, D. Klee, I. Nolte, T. Lenarz, G. Reuter, Dexamethasone released from cochlear implant coatings combined with a

protein repellent hydrogel layer inhibits fibroblast proliferation. *J Biomed Mater Res A* **102**, 442-454 (2014).
174. L. Astolfi, E. Simoni, N. Giarbini, P. Giordano, M. Pannella, S. Hatzopoulos, A. Martini, Cochlear implant and inflammation reaction: Safety study of a new steroid-eluting electrode. *Hear Res* **336**, 44-52 (2016).
175. J. B. Nadol, Jr., Patterns of neural degeneration in the human cochlea and auditory nerve: Implications for cochlear implantation. *Otolaryngol Head Neck Surgery* **117**, 220-228 (1997).
176. P. A. Leake, O. Stakhovskaya, A. Hetherington, S. J. Rebscher, B. Bonham, Effects of brain-derived neurotrophic factor (BDNF) and electrical stimulation on survival and function of cochlear spiral ganglion neurons in deafened, developing cats. *J Assoc Res Otolaryngol* **14**, 187-211 (2013).
177. Q. Yu, Q. Chang, X. Liu, Y. Wang, H. Li, S. Gong, K. Ye, X. Lin, Protection of spiral ganglion neurons from degeneration using small-molecule TrkB receptor agonists. *J Neurosci* **33**, 13042-13052 (2013).
178. J. L. Pinyon, S. F. Tadros, K. E. Froud, A. C. Y. Wong, I. T. Tompson, E. N. Crawford, M. Ko, R. Morris, M. Klugmann, G. D. Housley, Close-Field electroporation gene delivery using the cochlear implant electrode array enhances the bionic ear. *Science Translational Medicine* **6**, 233ra254 (2014).
179. K. Oshima, K. Shin, M. Diensthuber, A. W. Peng, A. J. Ricci, S. Heller, Mechanosensitive hair cell-like cells from embryonic and induced pluripotent stem cells. *Cell* **141**, 704-716 (2010).
180. S. Goncalves, E. Bas, B. J. Goldstein, S. Angeli, Effects of Cell-Based Therapy for Treating Tympanic Membrane Perforations in Mice. *Otolaryngology Head Neck Surgery* **154**, 1106-1114 (2016).
181. B. El Baba, C. Barake, R. Moukarbel, R. Jurjus, S. Sertel, A. Jurjus, in *Neurological Regeneration*. (2017), chap. Chapter 11, pp. 181-194.
182. P. A. Santi, S. B. Johnson, Decellularized ear tissues as scaffolds for stem cell differentiation. *J Assoc Res Otolaryngol* **14**, 3-15 (2013).
183. H. J. Adler, Y. Raphael, New hair cells arise from supporting cell conversion in the acoustically damaged chick inner ear. *Neuroscience letters* **205**, 17-21 (1996).
184. P. M. White, A. Doetzlhofer, Y. S. Lee, A. K. Groves, N. Segil, Mammalian cochlear supporting cells can divide and trans-differentiate into hair cells. *Nature* **441**, 984-987 (2006).
185. K. Mizutari, M. Fujioka, M. Hosoya, N. Bramhall, H. J. Okano, H. Okano, A. S. Edge, Notch inhibition induces cochlear hair cell regeneration and recovery of hearing after acoustic trauma. *Neuron* **77**, 58-69 (2013).
186. M. Izumikawa, R. Minoda, K. Kawamoto, K. A. Abrashkin, D. L. Swiderski, D. F. Dolan, D. E. Brough, Y. Raphael, Auditory hair cell replacement and hearing improvement by Atoh1 gene therapy in deaf mammals. *Nature Medicine* **11**, 271-276 (2005).
187. K. Kawamoto, S. Ishimoto, R. Minoda, D. E. Brough, Y. Raphael, Math1 gene transfer generates new cochlear hair cells in mature guinea pigs in vivo. *The Journal of Neuroscience* **23**, 4395-4400 (2003).
188. J. S. Kang, M. H. Lee, Overview of therapeutic drug monitoring. *Korean J Intern Med* **24**, 1-10 (2009).

189. D. Mulherin, J. Fahy, W. Grant, M. Keogan, B. Kavanagh, M. FitzGerald, Aminoglycoside induced ototoxicity in patients with cystic fibrosis. *Irish Journal of Medical Science* **160**, 173-175 (1991).
190. R. M. Cardinall, J. C. M. J. de Groot, E. H. Huizing, J. E. Veldman, G. F. Smoorenburg, Dose-dependent effect of 8-day cisplatin administration upon the morphology of the albino guinea pig cochlea. *Hearing Research* **144**, 135-146 (2000).
191. R. D. Moore, P. S. Lietman, C. R. Smith, Clinical response to aminoglycoside therapy: Importance of the ratio of peak concentration to minimal inhibitory concentration. *The Journal of Infectious Diseases* **155**, 93-99 (1987).
192. M. L. Avent, B. A. Rogers, A. C. Cheng, D. L. Paterson, Current use of aminoglycosides: indications, pharmacokinetics and monitoring for toxicity. *Internal Medicine Journal* **41**, 441-449 (2011).
193. F. Follath, M. Wenk, S. Vozeh, Plasma concentration monitoring of aminoglycosides. *Journal of Antimicrobial Chemotherapy* **8**, 37-43 (1981).
194. C. Bartal, A. Danon, F. Schlaeffer, K. Reisenberg, M. Alkan, R. Smoliakov, A. Sidi, Y. Almog, Pharmacokinetic dosing of aminoglycosides: a controlled trial. *The American Journal of Medicine* **114**, 194-198 (2003).
195. R. D. Moore, C. R. Smith, P. S. Lietman, The association of aminoglycoside plasma levels with mortality in patients with gram-negative bacteremia. *The Journal of Infectious Diseases* **149**, 443-448 (1984).
196. R. J. V. van der Hulst, E. W. Boeschoten, F. W. Nielsen, D. G. Struijk, W. D. Dreschler, R. A. Tange, Ototoxicity monitoring with ultra-high frequency audiometry in peritoneal dialysis patients treated with vancomycin or gentamicin. *ORL: Oto-rhino-laryngologica* **53**, 19-22 (1991).
197. T. G. Christopher, D. Korn, A. D. Blair, A. W. Forrey, M. A. O'Neill, R. E. Cutler, Gentamicin pharmacokinetics during hemodialysis. *Kidney International* **6**, 38-44 (1974).
198. E. J. Begg, M. L. Barclay, S. B. Duffull, A suggested approach to once-daily aminoglycoside dosing. *British Journal of Clinical Pharmacology* **39**, 605-609 (1995).
199. M. J. Rybak, B. J. Abate, S. L. Kang, M. J. Ruffing, S. A. Lerner, G. L. Drusano, Prospcetive evaluation of the effect of an aminoglycoside dosing regimen on rates of observed nephrotoxicity and ototoxicity. *Antimicrobial Agents and Chemotherapy* **43**, 1549-1555 (1999).
200. C. D. Freeman, D. P. Nicolau, P. P. Belliveau, C. H. Nightingale, Once-daily dosing of aminoglycosides: review and recommendations for clinical practice. *Journal of Antimicrobial Chemotherapy* **39**, 677-686 (1997).
201. M. Barza, J. P. A. Ioannidis, J. C. Cappelleri, J. Lau, Single or multiple daily doses of aminoglycosides: a meta-analysis. *British Medical Journal* **312**, 338-344 (1996).
202. S. H. Powell, W. L. Thompson, M. A. Luthe, R. C. Stern, D. A. Grossniklaus, D. D. Bloxham, D. L. Goroden, M. R. Jacobs, A. O. DiScenna, H. A. Cash, J. D. Klinger, Once-daily vs. continuous aminoglycoside dosing: Efficacy and toxicity in animal and clinical studies of gentamicin, netilmicin, and tobramycin. *The Journal of Infectious Diseases* **147**, 918-932 (1983).

203. J. M. Prins, H. R. Buller, E. J. Kuijper, R. A. Tange, P. Speelman, Once versus thrice daily gentamicin in patients with serious infections. *The Lancet* **341**, 335-339 (1993).
204. W. Sneader, The dicovery of aspirin: a reappraisal. *British Medical Journal* **321**, 1591-1594 (2000).
205. A. C. Vlot, D. A. Dempsey, D. F. Klessig, Salicylic Acid, a multifaceted hormone to combat disease. *Annu Rev Phytopathol* **47**, 177-206 (2009).
206. J. R. Vane, R. M. Botting, *The history of aspirin. In Aspirin and other salicylates*. (Chapman & Hall, London, 1992), vol. 1.
207. E. N. Myers, J. M. Bernstein, Salicylate Ototoxicity. *Archeives of Otolaryngology* **82**, 483-493 (1965).
208. Wall Street Journal. **March 30**, (1964).
209. R. Marchese-Ragona, G. Marioni, P. Marson, A. Martini, A. Staffieri, The discovery of salicylate ototoxicity. *Audiology & neuro-otology* **13**, 34-36 (2008).
210. P. Tosco, L. Lazzarato, Mechanistic insights into cyclooxygenase irreversible inactivation by aspirin. *ChemMedChem* **4**, 939-945 (2009).
211. S. R. Clark, A. C. Ma, S. A. Tavener, B. McDonald, Z. Goodarzi, M. M. Kelly, K. D. Patel, S. Chakrabarti, E. McAvoy, G. D. Sinclair, E. M. Keys, E. Allen-Vercoe, R. Devinney, C. J. Doig, F. H. Green, P. Kubes, Platelet TLR4 activates neutrophil extracellular traps to ensnare bacteria in septic blood. *Nat Med* **13**, 463-469 (2007).
212. C. Bertagnini, Sulle alterazioni che alcuni acidi subiscono nell'organismo animale. *Nuovo Cimento* **1**, 363-372 (1855).
213. G. Muller, Beitrag zur wirkung des salicylsauren natrons beim diabetes mellitus. *Berl Klin Wochenschr* **14**, 66-75 (1877).
214. D. I. Macht, J. Greenberg, S. Isaacs, The effect of some antipyretics on the acuity of hearing. *Journal of Pharmacology and Experimental Therapeutics* **15**, 149-165 (1920).
215. J. Luc Puel, S. C. J. R. Bledsoe, R. P. Bobbin, G. Ceasar, M. Fallon, Comparative actions of salicylate on the amphibian lateral line and guinea pig cochlea. *Hearing Research* **9**, 295-316 (1983).
216. M. J. Guitton, J. Caston, J. Ruel, R. M. Johnson, R. Pujol, J. Puel, Salicylate Induces Tinnitus through Activation of Cochlear NMDA Receptors. *The Journal of Neuroscience* **23**, 3944-3952 (2003).
217. K. Ochi, J. J. Eggermont, Effects of salicylate on neural activity in cat primary auditory cortex. *Hearing Research* **95**, 63-76 (1996).
218. A. Didier, J. M. Miller, A. L. Nuttall, The vascular component of sodium salicylate ototoxicity in the guinea pig. *Hearing Research* **63**, 199-206 (1993).
219. M. A. Hyppolito, J. A. de Oliveira, M. Rossato, Cisplatin ototoxicity and otoprotection with sodium salicylate. *Eur Arch Otorhinolaryngol* **263**, 798-803 (2006).
220. G. Li, S. Sha, E. Zotova, J. Arezzo, T. Van De Water, J. Schacht, Salicylate Protects Hearing and Kidney Function from Cisplatin Toxicity without Compromising its Oncolytic Action. *Laboratory Investigation* **82**, 585-596 (2002).

221. D. McFadden, H. S. Plattsmier, Aspirin can potentiate the temporary hearing loss induced by intense sounds. *Hearing Research* **9**, 295-316 (1983).
222. S. Sha, J. Schacht, Salicylate attenuates gentamicin-induced ototoxicity. *Laboratory Investigation* **79**, 807-813 (1999).
223. S. S. Sha, J. H. Qiu, J. Schacht, Aspirin to prevent gentamicin-induced hearing loss. *New England Journal of Medicine* **354**, 1856-1857 (2006).
224. M. Grootveld, B. Halliwell, Aromatic hydroxylation as a potential measure of hydroxyl-radical formation in vivo. *Biochemical Journal* **237**, 499-504 (1986).
225. H. Raza, A. John, Implications of altered glutathione metabolism in aspirin-induced oxidative stress and mitochondrial dysfunction in HepG2 cells. *PLoS One* **7**, e36325 (2012).
226. A. Jain, J. Martensson, E. Stole, P. A. M. Auld, A. Meister, Glutathione deficiency leads to mitochondrial damage in brain. *PNAS* **88**, 1913-1917 (1991).
227. D. S. Whitlon, L. S. Wright, S. A. Nelson, R. Szakaly, F. L. Siegel, Maturation of cochlear glutathione-S-transferase correlates with the end of the sensitive period for ototoxicity. *Hearing Research* **137**, 43-50 (1999).
228. K. Aoyama, S. W. Suh, A. M. Hamby, J. Liu, W. Y. Chan, Y. Chen, R. A. Swanson, Neuronal glutathione deficiency and age-dependent neurodegeneration in the EAAC1 deficient mouse. *Nat Neurosci* **9**, 119-126 (2006).
229. T. L. Perry, D. V. Godin, S. Hansen, Parkinson's disease: a disorder due to nigral glutathione deficiency? *Neuroscience letters* **33**, 305-310 (1982).
230. A. M. Cantin, R. C. Hubbard, R. G. Crystal, Glutathione deficiency in the epithelial lining fluid of the lower respiratory tract in idiopathic pulmonary fibrosis. *American Review of Respiratory Disease* **139**, 370-372 (1989).
231. S. Leichtweis, L. L. Ji, Glutathione deficiency intensifies ischaemia-reperfusion induced cardiac dysfunction and oxidative stress. *Acta Physiologica* **172**, 1-10 (2001).
232. B. H. Lauterburg, M. E. Velez, Glutathione deficiency in alcoholics: risk factor for paracetamol hepatotoxicity. *Gut* **29**, 1153-1157 (1988).
233. L. A. Herzenberg, S. C. De Rosa, J. Gregson Dubs, M. Roederer, M. T. Anderson, S. W. Ela, S. C. Deresinski, L. A. Herzenberg, Glutathione deficiency is associated with impaired survival in HIV disease. *PNAS* **94**, 1967-1972 (1997).
234. R. Buhl, K. J. Holroyd, A. Mastrangeli, A. M. Cantin, H. A. Jaffe, F. B. Wells, C. Saltini, R. G. Crystal, Systemic glutathione deficiency in symptom-free HIV-seropositive individuals. *The Lancet* **2**, 1294-1298 (1989).
235. H. K. Prins, M. Oort, J. A. Loos, C. Zurcher, T. Beckers, Congenital nonspherocytic hemolytic anemia, associated with glutathione deficiency of the erythrocytes. *Blood* **27**, 145-166 (1966).
236. B. Sergi, A. R. Fetoni, A. Ferraresi, D. Troiani, G. B. Azzena, G. Paludetti, M. Maurizi, The role of antioxidants in protection from ototoxic drugs. *Acta Otolaryngologica* **124**, 42-45 (2004).
237. L. P. Rybak, C. Whitworth, S. Somani, Application of antioxidants and other agents to prevent cisplatin ototoxicity. *The Laryngoscope* **109**, 1740-1744 (1999).
238. S. L. McFadden, D. Ding, D. Salvemini, R. J. Salvi, M40403, a superoxide dismutase mimetic, protects cochlear hair cells from gentamicin, but not cisplatin toxicity. *Toxicology and Applied Pharmacology* **186**, 46-54 (2003).

239. J. G. Kalkanis, C. Whitworth, L. P. Rybak, Vitamin E reduces cisplatin ototoxicity. *The Laryngoscope* **114**, 538-542 (2004).
240. G. Lorito, S. Hatzopoulos, G. Laurell, K. C. M. Campbell, J. Petruccelli, P. Giordano, K. Kochanek, L. Sliwa, A. Martini, H. Skarzynski, Dose-dependent protection on cisplatin-induced ototoxicity- an electrophysiological study on the effect of three antioxidants in the Sprague-Dawley rat animal model. *Medical Science Monitoring* **17**, BR179-186 (2011).
241. C. Abbruzzese, P. Fornari, R. Massidda, F. Veglio, S. BUbaldini, Thiosulphate leaching for gold hydrometallurgy. *Hydrometallurgy* **39**, 265-276 (1995).
242. G. Hilson, A. J. Monhemius, Alternatives to cyanide in the gold mining industry: what prospects for the future? *Journal of Cleaner Production* **14**, 1158-1167 (2006).
243. G. Mannaioni, A. Vannacci, C. Marzocca, A. M. Zorn, S. Peruzzi, F. Moroni, Acute Cyanide Intoxication Treated with a Combination of Hydroxycobalamin, Sodium Nitrite, and Sodium Thiosulfate. *Journal of Toxicology: Clinical Toxicology* **40**, 181-183 (2002).
244. D. L. Schrijvers, Extravasation: a dreaded complication of chemotherapy. *Annals of Oncology* **14**, iii26-iii30 (2003).
245. T. V. Goolsby, F. A. Lombardo, Extravasation of chemotherapeutic agents: prevention and treatment. *Semin Oncol* **33**, 139-143 (2006).
246. R. Madasu, M. J. Ruckenstein, F. Leake, E. Steere, T. Robbins, Ototoxic effects of supradose cisplatin with sodium thiosulfate neutralization in patients with head and neck cancer. *Archieves of Otolaryngology Head and Neck Surgery* **123**, 978-981 (1997).
247. C. G. Musso, P. Enz, F. Vidal, R. Gelman, A. Lizarraga, L. D. Giuseppe, A. Kowalczuk, L. Garfi, R. Galimberti, L. Algranati, Use of sodium thiosulfate in the treatment of calciphylaxis. *Saudi Journal of Kidney Diseases and Transplantation* **20**, 1065-1068 (2009).
248. A. Pasch, T. Schaffner, U. Huynh-Do, B. M. Frey, F. J. Frey, S. Farese, Sodium thiosulfate prevents vascular calcifications in uremic rats. *Kidney International* **74**, 1444-1453 (2008).
249. W. C. Otto, R. D. Brown, L. Gage-White, S. Kupetz, M. Anniko, J. E. Penny, C. M. Henley, Effects of cisplatin and thiosulfate upon auditory brainstem responses of guinea pigs. *Hearing Research* **35**, 79-86 (1988).
250. E. A. Neuwelt, R. E. Brummett, L. G. Remsen, R. A. Kroll, M. A. Pagel, C. I. McCormick, S. Guitjens, L. L. Muldoon, *In vitro* and animal studies of sodium thiosulfate as a potential chemoprotectant against carboplatin-induced ototoxicity. *Cancer Research* **56**, 706-709 (1996).
251. T. Saito, J. Zhang, Y. Manabe, T. Ohtsubo, H. Saito, The effect of sodium thiosulfate on ototoxicity and pharmacokinetics after cisplatin treatment in guinea pigs. *European Archives of Oto-Rhino-Laryngology* **254**, 281-286 (1997).
252. D. T. Dickey, Y. J. Wu, L. L. Muldoon, E. A. Neuwelt, Protection against cisplatin-induced toxicities by N-acetylcysteine and sodium thiosulfate as assessed at the molecular, cellular, and in vivo levels. *Journal of Pharmacology and Experimental Therapeutics* **314**, 1052-1058 (2005).

253. D. R. Freyer, L. Chen, M. D. Krailo, K. Knight, D. Villaluna, B. Bliss, B. H. Pollock, J. Ramdas, B. Lange, D. Van Hoff, M. L. VanSoelen, J. Wiernikowski, E. A. Neuwelt, L. Sung, Effects of sodium thiosulfate versus observation on development of cisplatin-induced hearing loss in children with cancer (ACCL0431): a multicentre, randomised, controlled, open-label, phase 3 trial. *The Lancet Oncology* **18**, 63-74 (2017).
254. E. A. Neuwelt, K. Gilmer-Knight, C. Lacy, H. S. Nicholson, D. F. Kraemer, N. D. Doolittle, G. W. Hornig, L. L. Muldoon, Toxicity profile of delayed high dose sodium thiosulfate in children treated with carboplatin in conjunction with blood-brain-barrier disruption. *Pediatric Blood Cancer* **47**, 174-182 (2006).
255. E. A. Neuwelt, R. E. Brummett, N. D. Doolittle, L. L. Muldoon, R. A. Kroll, M. A. Pagel, R. Dojan, V. Church, L. G. Remsen, J. S. Bubalo, First evidence of otoprotection against carboplatin-induced hearing loss with a two-compartment system in patients with central nervous system malignancy using sodium thiosulfate. *The Journal of Pharmacology and Experimental Therapeutics* **286**, 77-84 (1998).
256. T. M. Harned, O. Kalous, A. Neuwelt, J. Loera, L. Ji, P. Iovine, R. Sposto, E. A. Neuwelt, C. P. Reynolds, Sodium thiosulfate administered six hours after cisplatin does not compromise antineuroblastoma activity. *Clinical Cancer Research* **14**, 533-540 (2008).
257. N. D. Doolittle, L. L. Muldoon, R. E. Brummett, R. M. Tyson, C. Lacy, J. S. Bubalo, D. F. Kraemer, M. C. Heinrich, J. A. Henry, E. A. Neuwelt, Delayed sodium thiosulfate as an otoprotectant against carboplatin-induced hearing loss in patients with malignant brain tumors. *Clinical Cancer Research* **7**, 493-500 (2001).
258. L. L. Muldoon, M. A. Pagel, R. A. Kroll, C. M. Brummett, N. D. Doolittle, E. G. Zuhowski, M. J. Egorin, E. A. Neuwelt, Delayed administration of sodium thiosulfate in animal models reduces platinum ototoxicity without reduction of antitumor activity. *Clinical Cancer Research* **6**, 309-315 (2000).
259. P. V. Pierre, C. Engmer, I. Wallin, G. Laurell, H. Ehrsson, High concentrations of thiosulfate in scala tympani perilymph after systemic administration in the guinea pig. *Acta Otolaryngology* **129**, 132-137 (2009).
260. J. Wang, R. V. Lloyd Faulconbridge, A. Fetoni, M. J. Guitton, R. Pujol, J. L. Puel, Local application of sodium thiosulfate prevents cisplatin-induced hearing loss in the guinea pig. *Neuropharmacology* **45**, 380-393 (2003).
261. C. E. Berglin, P. V. Pierre, T. Bramer, K. Edsman, H. Ehrsson, S. Eksborg, G. Laurell, Prevention of cisplatin-induced hearing loss by administration of a thiosulfate-containing gel to the middle ear in a guinea pig model. *Cancer Chemotherapy Pharmacology* **68**, 1547-1556 (2011).
262. J. Hochman, M. Wellman, L. Blakley, Prevention of aminoglycoside-induced sensorineural hearing loss. *Journal of Otolaryngology* **35**, 153-156 (2006).
263. G. Deng, B. Blakley, Reducing aminoglycoside ototoxicity. *University of Manitoba Thesis*, (2012).
264. L. L. Muldoon, Y. J. Wu, M. A. Pagel, E. A. Neuwelt, N-acetylcysteine chemoprotection without decreased cisplatin antitumor efficacy in pediatric tumor models. *Journal of Neurooncology* **121**, 433-440 (2015).

265. J. Yoo, S. J. Hamilton, D. Angel, K. Fung, J. Franklin, L. S. Parnes, D. Lewis, V. Venkatesan, E. Winquist, Cisplatin otoprotection using transtympanic L-N-acetylcysteine: a pilot randomized study in head and neck cancer patients. *Laryngoscope* **124**, E87-94 (2014).
266. A. R. Fetoni, M. Ralli, B. Sergi, C. Parrilla, D. Troiani, G. Paludetti, Protective effects of N-acetylcysteine on noise-induced hearing loss in guinea pigs. *Acta Otorhinolaryngologica Italica* **29**, 70-75 (2009).
267. D. T. Dickey, L. L. Muldoon, D. F. Kraemer, E. A. Neuwelt, Protection against cisplatin-induced ototoxicity by N-acetylcysteine in a rat model. *Hearing Research* **193**, 25-30 (2004).
268. L. Feldman, R. A. Sherman, J. Weissgarten, N-acetylcysteine use for amelioration of aminoglycoside-induced ototoxicity in dialysis patients. *Seminars Dialysis* **25**, 491-494 (2012).
269. L. Feldman, S. Efrati, E. Eviatar, R. Abramsohn, I. Yarovoy, E. Gersch, Z. Averbukh, J. Weissgarten, Gentamicin-induced ototoxicity in hemodialysis patients is ameliorated by N-acetylcysteine. *Kidney Int* **72**, 359-363 (2007).
270. B. Tokgoz, C. Ucar, I. Kocyigit, M. Somdas, A. Unal, A. Vural, M. Sipahioglu, O. Oymak, C. Utas, Protective effect of N-acetylcysteine from drug-induced ototoxicity in uraemic patients with CAPD peritonitis. *Nephrol Dial Transplant* **26**, 4073-4078 (2011).
271. M. A. Somdas, F. Korkmaz, S. G. Gurgen, M. Sagit, A. Akcadag, N-acetylcysteine Prevents Gentamicin Ototoxicity in a Rat Model. *J Int Adv Otol* **11**, 12-18 (2015).
272. R. D. Kopke, R. L. Jackson, J. K. Coleman, J. Liu, E. C. Bielefeld, B. J. Balough, NAC for noise: from the bench top to the clinic. *Hearing Research* **226**, 114-125 (2007).
273. D. T. Dickey, L. L. Muldoon, E. A. Neuwelt, paper presented at the 98th AACR Annual Meeting, Los Angeles, CA, April 14-18 2007.
274. M. G. Riga, L. Chelis, S. Kakolyris, S. Papadopoulos, S. Stathakidou, E. Chamalidou, N. Xenidis, K. Amarantidis, P. Dimopoulos, V. Danielides, Transtympanic injections of N-acetylcysteine for the prevention of cisplatin-induced ototoxicity: a feasible method with promising efficacy. *Am J Clin Oncol* **36**, 1-6 (2013).
275. L. L. Muldoon, J. Y. Wu, M. A. Pagel, K. A. Beeson, E. A. Neuwelt, paper presented at the Proceedings of the 105th Annual Meeting of the American Association for Cancer Research, San Diego, CA, 2014.
276. X. Liang, A. Kaya, Y. Zhang, D. T. Le, D. Hua, V. N. Gladyshev, Characterization of methionine oxidation and methionine sulfoxide reduction using methionine-rich cysteine-free proteins. *BMC Biochemistry* **13**, (2012).
277. J. Moskovitz, Methionine sulfoxide reductases: ubiquitous enzymes involved in antioxidant defense, protein regulation, and prevention of aging-associated diseases. *Biochimica et biophysica acta* **1703**, 213-219 (2005).
278. L. Bai, S. Sheeley, J. V. Sweedler, Analysis of Endogenous D-Amino Acid-Containing Peptides in Metazoa. *Bioanal Rev* **1**, 7-24 (2009).
279. P. C. Montecucchi, R. Decastiglione, S. Piani, L. Gozzini, V. Erspamer, Amino acid composition and sequence of dermorphin, a novel opiate-like peptide from

the skin of *Phyllomedusa sauvagei*. *International Journal of Peptide and Protein Research* **17**, 275-283 (1981).
280. L. Jervis, D. H. Smyth, The active transfer of D-methionine by the rat intestine *in vitro*. *Journal of Physiology* **150**, 51-58 (1960).
281. A. D'Aniello, G. D''Onofrio, M. Pischetola, G. D''Aniello, A. Veter, L. Petrucelli, G. H. Fisher, Biological role of D-amino acid oxidase and D-aspartate oxidase. *The Journal of biological chemistry* **268**, 26941-26949 (1993).
282. K. C. M. Campbell, L. P. Rybak, R. Meech, L. Hughes, D-Methionine provides excellent protection from cisplatin ototoxicity in the rat. *Hearing Research* **102**, 90-98 (1996).
283. K. Campbell, A. Claussen, R. Meech, S. Verhulst, D. Fox, L. Hughes, D-methionine (D-met) significantly rescues noise-induced hearing loss: timing studies. *Hearing Research* **282**, 138-144 (2011).
284. Z. Alagic, M. Goiny, B. Canlon, Protection against acoustic trauma by direct application of D-methionine to the inner ear. *Acta Otolaryngologica* **131**, 802-808 (2011).
285. D. J. Fox, M. D. Cooper, C. A. Speil, M. H. Roberts, S. C. Yanik, R. P. Meech, T. L. Hargrove, S. J. Verhulst, L. P. Rybak, K. C. Campbell, d-Methionine reduces tobramycin-induced ototoxicity without antimicrobial interference in animal models. *Journal of Cystic Fibrosis* **15**, 518-530 (2015).
286. S. H. Sha, J. Schacht, Antioxidants attenuate gentamicin-induced free radical formation in vitro and ototoxicity in vivo: D-methionine is a potential protectant. *Hearing Research* **142**, 34-40.
287. K. C. Campbell, S. M. Martin, R. P. Meech, T. L. Hargrove, S. J. Verhulst, D. J. Fox, D-methionine (D-met) significantly reduces kanamycin-induced ototoxicity in pigmented guinea pigs. *International Journal of Audiology* **55**, 273-278 (2016).
288. D. S. Lockwood, D. L. Ding, J. Wang, R. Salvi, D-methionine attenuates inner hair cell loss in carboplatin-treated chinchillas. *Audiology & Neurotology* **5**, 263-266 (2000).
289. A. Ekborn, G. Laurell, P. Johnstrom, I. Wallin, S. Eksborg, H. Ehrsson, D-methionine and cisplatin ototoxicity in the guinea pig: D-methionine influences cisplatin pharmacokinetics. *Hearing Research* **165**, 53-61 (2002).
290. K. D. Korver, L. P. Rybak, C. Whitworth, K. M. Campbell, Round window application of D-methionine provides complete cisplatin otoprotection. *Otolaryngology Head Neck Surgery* **126**, 683-689 (2002).
291. K. C. M. Campbell, R. P. Meech, L. P. Rybak, L. F. Hughes, D-Methionine protects against cisplatin damage to the stria vascularis. *Hearing Research* **138**, 13-28 (1999).
292. D. Reser, M. Rho, D. Dewan, L. Herbst, G. Li, H. Stupak, K. Zur, J. Romaine, D. Frenz, L. Goldbloom, R. Kopke, J. Arezzo, L- and D-methionine provide equivilent long term protection against CDDP-induced ototoxicity in vivo, with partial in vitro and in vivo retention of antineoplastic activity. *Neurotoxicology* **20**, 731-748 (1999).
293. G. Li, D. A. Frenz, S. Brahmblatt, J. G. Feghali, R. J. Ruben, D. Berggren, J. Arezzo, T. R. Van De Water, Round window membrane delivery of L-methionine

provides protection from cisplatin ototoxicity without compromising chemotherapeutic efficacy. *NeuroToxicology* **22**, 163-176 (2001).
294. K. C. M. Campbell, R. P. Meech, L. P. Rybak, L. F. Hughes, The effect of D-Methionine on cochlear oxidative state with and without cisplatin administration: mechanisms of otoprotection. *Journal of the American Academy of Audiology* **14**, 144-156 (2003).
295. R. J. M. Russell, J. B. Murray, G. Lentzen, J. Haddad, S. Mobashery, The complex of a designer antibiotic with a model aminoacyl site of the 30S ribosomal subunit revealed by x-ray crystallography. *Journal of the American Chemical Society* **125**, 3410-3411 (2003).
296. F. Franceschi, E. M. Duffy, Structure-based drug design meets the ribosome. *Biochemical Pharmacology* **71**, 1016-1025 (2006).
297. M. E. Huth, K. H. Han, K. Sotoudeh, Y. J. Hsieh, T. Effertz, A. A. Vu, S. Verhoeven, M. H. Hsieh, R. Greenhouse, A. G. Cheng, A. J. Ricci, Designer aminoglycosides prevent cochlear hair cell loss and hearing loss. *Journal of Clinical Investigation* **125**, 583-592 (2015).
298. E. Shulman, V. Belakhov, G. Wei, A. Kendall, E. G. Meyron-Holtz, D. Ben-Shachar, J. Schacht, T. Baasov, Designer aminoglycosides that selectively inhibit cytoplasmic rather than mitochondrial ribosomes show decreased ototoxicity: a strategy for the treatment of genetic diseases. *Journal of Biological Chemistry* **289**, 2318-2330 (2014).
299. D. W. Kimberlin, Meningitis in the Neonate. *Current treatment options in neurology* **4**, 239-248 (2002).
300. E. A. Radigan, N. A. Gilchrist, M. A. Miller, Management of aminoglycosides in the intensive care unit. *Journal of intensive care medicine* **25**, 327-342 (2010).
301. A. G. Cheng, P. R. Johnston, J. Luz, A. Uluer, B. Fligor, G. R. Licameli, M. A. Kenna, D. T. Jones, Sensorineural hearing loss in patients with cystic fibrosis. *Otolaryngol Head Neck Surg* **141**, 86-90 (2009).
302. D. M. Pillers, M. R. Schleiss, Gentamicin in the Clinical Setting. *The Volta Review* **105**, 205-210 (2005).
303. A. Erenberg, J. Lemons, C. Sia, D. Trunkel, P. Ziring, Newborn and infant hearing loss: detection and intervention.American Academy of Pediatrics. Task Force on Newborn and Infant Hearing, 1998- 1999. *Pediatrics* **103**, 527-530 (1999).
304. M. R. Jarvelin, E. Maki-Torkko, M. J. Sorri, P. T. Rantakallio, Effect of hearing impairment on educational outcomes and employment up to the age of 25 years in northern Finland. *British journal of audiology* **31**, 165-175 (1997).
305. C. R. Kennedy, D. C. McCann, M. J. Campbell, C. M. Law, M. Mullee, S. Petrou, P. Watkin, S. Worsfold, H. M. Yuen, J. Stevenson, Language ability after early detection of permanent childhood hearing impairment. *N Engl J Med* **354**, 2131-2141 (2006).
306. L. Schroeder, S. Petrou, C. Kennedy, D. McCann, C. Law, P. M. Watkin, S. Worsfold, H. M. Yuen, The economic costs of congenital bilateral permanent childhood hearing impairment. *Pediatrics* **117**, 1101-1112 (2006).

307. F. R. Lin, L. Ferrucci, E. J. Metter, Y. An, A. B. Zonderman, S. M. Resnick, Hearing loss and cognition in the Baltimore Longitudinal Study of Aging. *Neuropsychology* **25**, 763-770 (2011).
308. H. Li, P. S. Steyger, Systemic aminoglycosides are trafficked via endolymph into cochlear hair cells. *Sci Rep* **1**, 159 (2011).
309. W. Marcotti, S. M. van Netten, C. J. Kros, The aminoglycoside antibiotic dihydrostreptomycin rapidly enters mouse outer hair cells through the mechano-electrical transducer channels. *J Physiol* **567**, 505-521 (2005).
310. Q. Wang, P. S. Steyger, Trafficking of systemic fluorescent gentamicin into the cochlea and hair cells. *J Assoc Res Otolaryngol* **10**, 205-219 (2009).
311. A. M. Butt, Effect of inflammatory agents on electrical resistance across the blood-brain barrier in pial microvessels of anaesthetized rats. *Brain Res* **696**, 145-150 (1995).
312. N. J. Abbott, L. Ronnback, E. Hansson, Astrocyte-endothelial interactions at the blood-brain barrier. *Nature reviews. Neuroscience* **7**, 41-53 (2006).
313. N. Tsao, H. P. Hsu, C. M. Wu, C. C. Liu, H. Y. Lei, Tumour necrosis factor-alpha causes an increase in blood-brain barrier permeability during sepsis. *Journal of medical microbiology* **50**, 812-821 (2001).
314. J. W. Koo, Q. Wang, P. S. Steyger, Infection-mediated vasoactive peptides modulate cochlear uptake of fluorescent gentamicin. *Audiology & neuro-otology* **16**, 347-358 (2011).
315. K. Hirose, S. Z. Li, K. K. Ohlemiller, R. M. Ransohoff, Systemic lipopolysaccharide induces cochlear inflammation and exacerbates the synergistic ototoxicity of kanamycin and furosemide. *J Assoc Res Otolaryngol* **15**, 555-570 (2014).
316. D. G. Remick, D. E. Newcomb, G. L. Bolgos, D. R. Call, Comparison of the mortality and inflammatory response of two models of sepsis: lipopolysaccharide vs. cecal ligation and puncture. *Shock* **13**, 110-116 (2000).
317. H. Li, Q. Wang, P. S. Steyger, Acoustic trauma increases cochlear and hair cell uptake of gentamicin. *PLoS One* **6**, e19130 (2011).
318. C. F. Dai, D. Mangiardi, D. A. Cotanche, P. S. Steyger, Uptake of fluorescent gentamicin by vertebrate sensory cells in vivo. *Hear Res* **213**, 64-78 (2006).
319. C. F. Dai, P. S. Steyger, A systemic gentamicin pathway across the stria vascularis. *Hear Res* **235**, 114-124 (2008).
320. Q. Wang, A. Kachelmeier, P. S. Steyger, Competitive antagonism of fluorescent gentamicin uptake in the cochlea. *Hear Res* **268**, 250-259 (2010).
321. K. Balogh, Jr., F. Hiraide, D. Ishii, Distribution of radioactive dihydrostreptomycin in the cochlea. An autoradiographic study. *The Annals of otology, rhinology, and laryngology* **79**, 641-652 (1970).
322. S. Imamura, J. C. Adams, Distribution of gentamicin in the guinea pig inner ear after local or systemic application. *J Assoc Res Otolaryngol* **4**, 176-195 (2003).
323. G. P. Richardson, A. Forge, C. J. Kros, J. Fleming, S. D. Brown, K. P. Steel, Myosin VIIA is required for aminoglycoside accumulation in cochlear hair cells. *J Neurosci* **17**, 9506-9519 (1997).

324. W. J. Wu, S. H. Sha, J. D. McLaren, K. Kawamoto, Y. Raphael, J. Schacht, Aminoglycoside ototoxicity in adult CBA, C57BL and BALB mice and the Sprague-Dawley rat. *Hear Res* **158**, 165-178 (2001).
325. A. Forge, J. Schacht, Aminoglycoside antibiotics. *Audiology & neuro-otology* **5**, 3-22 (2000).
326. J. J. Boffa, W. J. Arendshorst, Maintenance of renal vascular reactivity contributes to acute renal failure during endotoxemic shock. *Journal of the American Society of Nephrology : JASN* **16**, 117-124 (2005).
327. I. Berczi, L. Bertok, T. Bereznai, Comparative studies on the toxicity of Escherichia coli lipopolysaccharide endotoxin in various animal species. *Can J Microbiol* **12**, 1070-1071 (1966).
328. M. S. Exton, Infection-induced anorexia: active host defence strategy. *Appetite* **29**, 369-383 (1997).
329. S. Studena, J. Martinkova, D. Slizova, O. Krs, M. Senkerik, D. Springer, J. Chladek, A rat model of early sepsis: relationships between gentamicin pharmacokinetics and systemic and renal effects of bacterial lipopolysaccharide combined with interleukin-2. *Biological & pharmaceutical bulletin* **35**, 1703-1710 (2012).
330. R. J. Lee, S. Wang, M. J. Turk, P. S. Low, The effects of pH and intraliposomal buffer strength on the rate of liposome content release and intracellular drug delivery. *Bioscience reports* **18**, 69-78 (1998).
331. T. Nakamoto, Y. Shiba, C. Hirono, M. Sugita, K. Takemoto, Y. Iwasa, Y. Akagawa, Carbachol-induced fluid movement through methazolamide-sensitive bicarbonate production in rat parotid intralobular ducts: quantitative analysis of fluorescence images using fluorescent dye sulforhodamine under a confocal laser scanning microscope. *European journal of cell biology* **81**, 497-504 (2002).
332. D. W. Lin, D. R. Trune, Breakdown of stria vascularis blood-labyrinth barrier in C3H/lpr autoimmune disease mice. *Otolaryngol Head Neck Surg* **117**, 530-534 (1997).
333. P. A. Stewart, E. M. Hayakawa, Interendothelial junctional changes underlie the developmental 'tightening' of the blood-brain barrier. *Brain Res* **429**, 271-281 (1987).
334. F. P. Miles, A. L. Nuttall, In vivo capillary diameters in the stria vascularis and spiral ligament of the guinea pig cochlea. *Hear Res* **33**, 191-200 (1988).
335. R. R. Taylor, G. Nevill, A. Forge, Rapid hair cell loss: a mouse model for cochlear lesions. *J Assoc Res Otolaryngol* **9**, 44-64 (2008).
336. J. R. Meyers, R. B. MacDonald, A. Duggan, D. Lenzi, D. G. Standaert, J. T. Corwin, D. P. Corey, Lighting up the senses: FM1-43 loading of sensory cells through nonselective ion channels. *J Neurosci* **23**, 4054-4065 (2003).
337. I. L. Calil, A. C. Zarpelon, A. T. Guerrero, J. C. Alves-Filho, S. H. Ferreira, F. Q. Cunha, T. M. Cunha, W. A. Verri, Jr., Lipopolysaccharide induces inflammatory hyperalgesia triggering a TLR4/MyD88-dependent cytokine cascade in the mice paw. *PLoS One* **9**, e90013 (2014).
338. J. E. Juskewitch, B. E. Knudsen, J. L. Platt, K. A. Nath, K. L. Knutson, G. J. Brunn, J. P. Grande, LPS-induced murine systemic inflammation is driven by

parenchymal cell activation and exclusively predicted by early MCP-1 plasma levels. *The American journal of pathology* **180**, 32-40 (2012).
339. M. Bosmann, N. F. Russkamp, P. A. Ward, Fingerprinting of the TLR4-induced acute inflammatory response. *Exp Mol Pathol* **93**, 319-323 (2012).
340. C. J. MacArthur, D. A. Pillers, J. Pang, J. B. Kempton, D. R. Trune, Altered expression of middle and inner ear cytokines in mouse otitis media. *Laryngoscope* **121**, 365-371 (2011).
341. D. R. Trune, B. E. Larrain, F. A. Hausman, J. B. Kempton, C. J. MacArthur, Simultaneous measurement of multiple ear proteins with multiplex ELISA assays. *Hear Res* **275**, 1-7 (2011).
342. S. Rivest, Regulation of innate immune responses in the brain. *Nature reviews. Immunology* **9**, 429-439 (2009).
343. J. J. Allensworth, S. R. Planck, J. T. Rosenbaum, H. L. Rosenzweig, Investigation of the differential potentials of TLR agonists to elicit uveitis in mice. *J Leukoc Biol* **90**, 1159-1166 (2011).
344. R. B. Yang, M. R. Mark, A. Gray, A. Huang, M. H. Xie, M. Zhang, A. Goddard, W. I. Wood, A. L. Gurney, P. J. Godowski, Toll-like receptor-2 mediates lipopolysaccharide-induced cellular signalling. *Nature* **395**, 284-288 (1998).
345. T. Matt, C. L. Ng, K. Lang, S. H. Sha, R. Akbergenov, D. Shcherbakov, M. Meyer, S. Duscha, J. Xie, S. R. Dubbaka, D. Perez-Fernandez, A. Vasella, V. Ramakrishnan, J. Schacht, E. C. Bottger, Dissociation of antibacterial activity and aminoglycoside ototoxicity in the 4-monosubstituted 2-deoxystreptamine apramycin. *Proc Natl Acad Sci U S A* **109**, 10984-10989 (2012).
346. S. Roy, M. M. Ryals, A. B. Van den Bruele, T. S. Fitzgerald, L. L. Cunningham, Sound preconditioning therapy inhibits ototoxic hearing loss in mice. *J Clin Invest* **123**, 4945-4949 (2013).
347. M. W. Yung, Intratympanic ototoxicity: influence of post-injection survival period. *The Journal of laryngology and otology* **101**, 1011-1019 (1987).
348. S. L. McFadden, D. Ding, R. Salvi, Anatomical, Metabolic and Genetic Aspects of Age-related Hearing Loss in Mice: Aspectos anatómicos, metabólicos y genéticos de la hipoacusia relacionada con la edad en ratones. *International Journal of Audiology* **40**, 313-321 (2001).
349. D. H. Darrow, E. M. Keithley, J. P. Harris, Effects of bacterial endotoxin applied to the guinea pig cochlea. *Laryngoscope* **102**, 683-688 (1992).
350. C. S. Kim, H. J. Kim, Auditory brain stem response changes after application of endotoxin to the round window membrane in experimental otitis media. *Otolaryngol Head Neck Surg* **112**, 557-565 (1995).
351. K. R. Henry, R. A. Chole, M. D. McGinn, D. P. Frush, Increased ototoxicity in both young and old mice. *Archives of otolaryngology* **107**, 92-95 (1981).
352. C. L. McClure, Common infections in the elderly. *Am Fam Physician* **45**, 2691-2698. (1992).
353. F. A. Manian, W. J. Stone, R. H. Alford, Adverse antibiotic effects associated with renal insufficiency. *Reviews of infectious diseases* **12**, 236-249 (1990).
354. R. H. Mathog, W. J. Klein, Jr., Ototoxicity of ethacrynic acid and aminoglycoside antibiotics in uremia. *N Engl J Med* **280**, 1223-1224 (1969).

355. N. Fischel-Ghodsian, Genetic factors in aminoglycoside toxicity. *Ann N Y Acad Sci* **884**, 99-109 (1999).
356. A. F. Ryan, R. C. Bone, Potentiation of kanamycin ototoxicity by a history of noise exposure. *Otolaryngology* **86**, ORL-125-128 (1978).
357. G. Kaplanski, B. Grane, G. T. Vaz, D. J. M., Jarisch-Herxheimer Reaction Complicating the Treatment of Chronic Q Fever Endocarditis: Elevated TNF and IL-6 Serum Levels. *Journal of Infection* **37**, 83-84 (1998).
358. J. L. Shenep, K. A. Mogan, Kinetics of Endotoxin Release during Antibiotic Therapy for Experimental Gram-Negative Bacterial Sepsis. *The Journal of Infectious Diseases* **150**, 380-388 (1984).
359. M. Fujioka, H. Okano, K. Ogawa, Inflammatory and immune responses in the cochlea: potential therapeutic targets for sensorineural hearing loss. *Frontiers in pharmacology* **5**, 287 (2014).
360. G. Laurell, A. Viberg, M. Teixeira, O. Sterkers, E. Ferrary, Blood-perilymph barrier and ototoxicity: an in vivo study in the rat. *Acta Otolaryngol* **120**, 796-803 (2000).
361. W. A. Banks, M. A. Erickson, The blood-brain barrier and immune function and dysfunction. *Neurobiology of disease* **37**, 26-32 (2010).
362. K. E. Driscoll, D. G. Hassenbein, B. W. Howard, R. J. Isfort, D. Cody, M. H. Tindal, M. Suchanek, J. M. Carter, Cloning, expression, and functional characterization of rat MIP-2: a neutrophil chemoattractant and epithelial cell mitogen. *J Leukoc Biol* **58**, 359-364 (1995).
363. A. Harada, N. Sekido, T. Akahoshi, T. Wada, N. Mukaida, K. Matsushima, Essential involvement of interleukin-8 (IL-8) in acute inflammation. *J Leukoc Biol* **56**, 559-564 (1994).
364. R. E. Vandenbroucke, E. Dejonckheere, P. Van Lint, D. Demeestere, E. Van Wonterghem, I. Vanlaere, L. Puimege, F. Van Hauwermeiren, R. De Rycke, C. Mc Guire, C. Campestre, C. Lopez-Otin, P. Matthys, G. Leclercq, C. Libert, Matrix metalloprotease 8-dependent extracellular matrix cleavage at the blood-CSF barrier contributes to lethality during systemic inflammatory diseases. *J Neurosci* **32**, 9805-9816 (2012).
365. I. Palmela, H. Sasaki, F. L. Cardoso, M. Moutinho, K. S. Kim, D. Brites, M. A. Brito, Time-dependent dual effects of high levels of unconjugated bilirubin on the human blood-brain barrier lining. *Front Cell Neurosci* **6**, 22 (2012).
366. R. Fian, E. Grasser, F. Treiber, R. Schmidt, P. Niederl, C. Rosker, The contribution of TRPV4-mediated calcium signaling to calcium homeostasis in endothelial cells. *Journal of receptor and signal transduction research* **27**, 113-124 (2007).
367. M. Jiang, Q. Wang, T. Karasawa, J. W. Koo, H. Li, S. P.S., Sodium-glucose transporter-2 (SGLT2; SLC5A2) enhances cellular uptake of aminoglycosides. *PLoS ONE* **9**, e108941 (2014).
368. W. Shi, N. Cui, Z. Wu, Y. Yang, S. Zhang, H. Gai, D. Zhu, C. Jiang, Lipopolysaccharides up-regulate Kir6.1/SUR2B channel expression and enhance vascular KATP channel activity via NF-kappaB-dependent signaling. *The Journal of biological chemistry* **285**, 3021-3029 (2010).

369. M. Sakagami, T. Harada, M. Sano, S. Sakai, T. Matsunaga, Quantitative evaluation of pinocytosis of capillaries of the stria vascularis under normal and experimental conditions. *Acta Otolaryngol* **103**, 189-197 (1987).
370. C. Tiruppathi, J. Shimizu, K. Miyawaki-Shimizu, S. M. Vogel, A. M. Bair, R. D. Minshall, D. Predescu, A. B. Malik, Role of NF-kappaB-dependent caveolin-1 expression in the mechanism of increased endothelial permeability induced by lipopolysaccharide. *The Journal of biological chemistry* **283**, 4210-4218 (2008).
371. J. Schacht, S. Lodhi, N. D. Weiner, Effects of neomycin on polyphosphoinositides in inner ear tissues and monomolecular films. *Advances in experimental medicine and biology* **84**, 191-208 (1977).
372. F. Van Bambeke, M. P. Mingeot-Leclercq, A. Schanck, R. Brasseur, P. M. Tulkens, Alterations in membrane permeability induced by aminoglycoside antibiotics: studies on liposomes and cultured cells. *Eur J Pharmacol* **247**, 155-168 (1993).
373. R. D. Moore, C. R. Smith, P. S. Lietman, Risk factors for the development of auditory toxicity in patients receiving aminoglycosides. *J Infect Dis* **149**, 23-30 (1984).
374. K. R. Henry, M. B. Guess, R. A. Chole, Hyperthermia increases aminoglycoside ototoxicity. *Acta Otolaryngol* **95**, 323-327. (1983).
375. R. A. Zager, Endotoxemia, renal hypoperfusion, and fever: interactive risk factors for aminoglycoside and sepsis-associated acute renal failure. *American journal of kidney diseases : the official journal of the National Kidney Foundation* **20**, 223-230 (1992).
376. G. S. Oh, H. J. Kim, J. H. Choi, A. Shen, C. H. Kim, S. J. Kim, S. R. Shin, S. H. Hong, Y. Kim, C. Park, S. J. Lee, S. Akira, R. Park, H. S. So, Activation of lipopolysaccharide-TLR4 signaling accelerates the ototoxic potential of cisplatin in mice. *J Immunol* **186**, 1140-1150 (2011).
377. K. M. Nicol, C. M. Hackney, E. F. Evans, S. R. Pratt, Behavioural evidence for recovery of auditory function in guinea pigs following kanamycin administration. *Hear Res* **61**, 117-131 (1992).
378. L. Chen, S. Xiong, Y. Liu, X. Shang, Effect of different gentamicin dose on the plasticity of the ribbon synapses in cochlear inner hair cells of C57BL/6J mice. *Molecular neurobiology* **46**, 487-494 (2012).
379. K. Liu, D. Chen, W. Guo, N. Yu, X. Wang, F. Ji, Z. Hou, W. Y. Yang, S. Yang, Spontaneous and Partial Repair of Ribbon Synapse in Cochlear Inner Hair Cells After Ototoxic Withdrawal. *Molecular neurobiology*, (2014).
380. E. C. Oesterle, Changes in the adult vertebrate auditory sensory epithelium after trauma. *Hear Res* **297**, 91-98 (2013).
381. K. C. Campbell, R. P. Meech, J. J. Klemens, M. T. Gerberi, S. S. Dyrstad, D. L. Larsen, D. L. Mitchell, M. El-Azizi, S. J. Verhulst, L. F. Hughes, Prevention of noise- and drug-induced hearing loss with D-methionine. *Hear Res* **226**, 92-103 (2007).
382. A. H. Sun, L. S. Parnes, D. J. Dreeman, Comparative perilymph permeability of cephalosporins and its significance in the treatment and prevention of suppurative labyrinthitis. *The Annals of Otology, Rhinology & Laryngology* **105**, 54-57 (1996).

383. C. Kilkenny, W. J. Browne, I. C. Cuthill, M. Emerson, D. G. Altman, Improving Bioscience Research Reporting: The ARRIVE Guidelines for Reporting Animal Research. *PLoS Biology* **8**, e1000412 (2010).
384. P. Skorup, L. Maudsdotter, M. Lipcsey, M. Castegren, A. Larsson, A. B. Jonsson, J. Sjolin, Beneficial antimicrobial effect of the addition of an aminoglycoside to a beta-lactam antibiotic in an E. coli porcine intensive care severe sepsis model. *PLoS One* **9**, e90441 (2014).
385. A. Fuchs, L. Zimmermann, M. Bickle Graz, J. Cherpillod, J. F. Tolsa, T. Buclin, E. Giannoni, Gentamicin exposure and sensorineural hearing loss in preterm infants. *PLoS One* **11**, e0158806 (2016).
386. R. van Altena, J. A. Dijkstra, M. E. van der Meer, J. F. Borjas Howard, J. G. Kosterink, D. van Soolingen, T. S. van der Werf, J. W. Alffenaar, Reduced chance of hearing loss associated with therapeutic drug monitoring of aminoglycosides in the treatment of multidrug-resistant tuberculosis. *Antimicrob Agents Chemother* **61**, (2017).
387. E. Pietersen, J. Peter, E. Streicher, F. Sirgel, N. Rockwood, B. Mastrapa, J. Te Riele, M. Davids, P. van Helden, R. Warren, K. Dheda, High frequency of resistance, lack of clinical benefit, and poor outcomes in capreomycin treated South African patients with extensively drug-resistant tuberculosis. *PLoS One* **10**, e0123655 (2015).
388. G. Al-Malky, S. J. Dawson, T. Sirimanna, E. Bagkeris, R. Suri, High-frequency audiometry reveals high prevalence of aminoglycoside ototoxicity in children with cystic fibrosis. *J Cyst Fibros* **14**, 248-254 (2015).
389. J. A. Handelsman, S. Z. Nasr, C. Pitts, W. M. King, Prevalence of hearing and vestibular loss in cystic fibrosis patients exposed to aminoglycosides. *Pediatr Pulmonol* **52**, 1157-1162 (2017).
390. J. B. Greene, R. Standring, F. Siddiqui, S. F. Ahsan, Incidence of cisplatin induced ototoxicity in adults with head and neck cancer. *Advances in Otolaryngology* **2015**, 1-4 (2015).
391. T. M. Brinkman, J. K. Bass, Z. Li, K. K. Ness, A. Gajjar, A. S. Pappo, G. T. Armstrong, T. E. Merchant, D. K. Srivastava, L. L. Robison, M. M. Hudson, J. G. Gurney, Treatment-induced hearing loss and adult social outcomes in survivors of childhood CNS and non-CNS solid tumors: Results from the St. Jude Lifetime Cohort Study. *Cancer* **121**, 4053-4061 (2015).
392. K. I. Kirk, R. T. Miyamoto, C. L. Lento, E. Ying, T. O''Neill, B. Fears, Effects of age at implantation in young children. *Annals of Otology, Rhinology & Laryngology* **111**, 69-73 (2002).
393. G. S. Oh, H. J. Kim, J. H. Choi, A. Shen, C. H. Kim, S. J. Kim, S. R. Shin, S. H. Hong, Y. Kim, C. Park, S. J. Lee, S. Akira, R. Park, H. S. So, Activation of lipopolysaccharide-TLR4 signaling accelerates the ototoxic potential of cisplatin in mice. *Journal of Immunology* **186**, 1140-1150 (2011).
394. J. W. Koo, L. Quintanilla-Dieck, M. Jiang, J. Liu, Z. D. Urdang, J. J. Allensworth, C. P. Cross, H. Li, P. S. Steyger, Endotoxemia-mediated inflammation potentiates aminoglycoside-induced ototoxicity. *Science Translational Medicine* **7**, 298ra118 (2015).

395. K. Hirose, S. Z. Li, K. K. Ohlemiller, R. M. Ransohoff, Systemic lipopolysaccharide induces cochlear inflammation and exacerbates the synergistic ototoxicity of kanamycin and furosemide. *Journal of the Association for Research in Otolaryngology* **15**, 555-570 (2014).
396. C. P. Cross, S. Liao, Z. D. Urdang, P. Srikanth, A. C. Garinis, P. S. Steyger, Effect of sepsis and systemic inflammatory response syndrome on neonatal hearing screening outcomes following gentamicin exposure. *International Journal of Pediatric Otorhinolaryngology* **79**, 1915-1919 (2015).
397. A. Poltorak, X. He, I. Smirnova, M. Y. Liu, C. Van Huffel, X. Du, D. Birdwell, E. Alejos, M. Silva, C. Galanos, M. Freudenberg, P. Ricciardi-Castagnoli, B. Layton, B. Beutler, Defective LPS signaling in C3H/HeJ and C57BL/10ScCr mice: mutations in TLR4 gene. *Science* **282**, 2085-2088 (1998).
398. J. M. Harlan, P. D. Killen, L. A. Harker, G. E. Striker, Neutrophil-mediated endothelial injury in vitro. *Journal of Clinical Inves* **68**, 1394-1403 (1981).
399. J. E. Meegan, X. Yang, D. C. Coleman, M. Jannaway, S. Y. Yuan, Neutrophil-mediated vascular barrier injury: Role of neutrophil extracellular traps. *Microcirculation* **24**, (2017).
400. K. Shim, Vibratome sectioning for enhanced preservation of the cytoarchitecture of the mammalian organ of Corti. *Journal of Visualized Experiments* **52**, e2793 (2011).
401. R. A. Musson, D. C. Morrison, R. J. Ulevitch, Distribution of endotoxin (lipopolysaccharide) in the tissues of lipopolysaccharide-responsive and -unresponsive mice. *Infection and Immunity* **21**, 448-457 (1978).
402. I. Berczi, L. Bertok, T. Bereznai, Comparative studies on the toxicity of escherichia coli lipopolysaccharide endotoxin in various animal models. *Canadian Journal of Microbiology* **12**, 1070-1071 (1966).
403. N. Kayagaki, M. T. Wong, I. B. Stowe, S. R. Ramani, L. C. Gonzalez, S. Akashi-Takamura, K. Miyake, J. Zhang, W. P. Lee, A. Muszyn´ ski, L. S. Forsberg, R. W. Carlson, V. M. Dixit, Noncanonical inflammasome activation by intracellular LPS independent of TLR4. *Science* **341**, 1246-1249 (2013).
404. L. Quintanilla-Dieck, B. Larrain, D. Trune, P. S. Steyger, Effect of systemic lipopolysaccharide-induced inflammation on cytokine levels in the murine cochlea: a pilot study. *Otolaryngol Head Neck Surg* **149**, 301-303 (2013).
405. M. K. Richards, F. Liu, H. Iwasaki, K. Akashi, D. C. Link, Pivotal role of granulocyte colony-stimulating factor in the development of progenitors in the common myeloid pathway. *Blood* **102**, 3562-3568 (2003).
406. W. A. Banks, A. M. Gray, M. A. Erickson, T. S. Salameh, M. Damodarasamy, N. Sheibani, J. S. Meabon, E. E. Wing, Y. Morofuji, D. G. Cook, M. J. Reed, Lipopolysaccharide-induced blood-brain barrier disruption: roles of cyclooxygenase, oxidative stress, neuroinflammation, and elements of the neurovascular unit. *J Neuroinflammation* **12**, 223 (2015).
407. J. Zhang, S. Chen, Z. Hou, J. Cai, M. Dong, X. Shi, Lipopolysaccharide-induced middle ear inflammation disrupts the cochlear intra-strial fluid-blood barrier through down-regulation of tight junction proteins. *PLoS One* **10**, e0122572 (2015).

408. R. Garraffo, C. Roptin, A. Boudjadja, Impact of neutropenia on tissue penetration of moxifloxacin and sparfloxacin in infected mice. *Drugs* **58**, 242-245 (1999).
409. C. J. Kirschning, H. Wesche, M. T. Ayres, M. Rothe, Human toll-like recepter 2 confers responsiveness to bacterial lipopolysaccharide. *Journal of Experimental Medicine* **188**, 2091-2097 (1998).
410. R. B. Yang, M. R. Mark, A. Gray, A. Huang, M. H. Xie, M. Zhang, A. Goddard, W. I. Wood, A. L. Gurney, P. J. Godowski, Toll-like receptor-2 mediates lipopolysaccharide-induced cellular signaling. *Nature* **395**, 284-288 (1998).
411. M. Hirschfeld, Y. Ma, J. H. Weis, S. N. Vogel, J. J. Weis, Cutting Edge: repurification of lipopolysaccharide eliminates signaling through both Human and murine toll-like receptor 2. *The Journal of Immunology* **165**, 618-622 (2000).
412. E. Siddall, M. Khatri, J. Radhakrishnan, Capillary leak syndrome: etiologies, pathophysiology, and management. *Kidney Int* **92**, 37-46 (2017).
413. S. J. van Deventer, H. R. Buller, J. W. ten Cate, L. A. Aarden, C. E. Hack, A. Sturk, Experimental endotoxemia in humans: analysis of cytokine release and coagulation, fibrinolytic, and compliment pathways. *Blood* **76**, 2520-2526 (1990).
414. E. S. Yi, T. R. Ulich, Endotoxin, interleukin-1 and tumor necrosis factor cause neutrophil-dependent microvascular leakage in postcapillary venules. *American Journal of Pathology* **140**, 650-663 (1992).
415. D. M. Guidot, M. J. Repine, B. M. Hybertson, J. E. Repine, Inhaled nitric oxide prevents neutrophil-mediated, oxygen radical-dependent leak in isolated rat lungs. *American Journal of Physiology - Lung Cellular and Molecular Physiology* **269**, L2-L5 (1995).
416. W. C. Conner, C. M. Gallagher, T. J. Miner, H. Tavaf-Motamen, K. M. Wolcott, T. Shea-Donohue, Neutrophil priming state predicts capillary leak after gut ischemia in rats. *Journal of Surgical Research* **84**, 24-30 (1999).
417. T. J. Standiford, S. L. Kunkel, N. W. Lukacs, M. J. Greenberger, J. M. Danforth, R. G. Kunkel, R. M. Strieter, Macrophage inflammatory protein-1 alpha mediates lunk leukocyte recruitment, lung capillary leak, and early mortality in murine endotoxemia. *The Journal of Immunology* **155**, 1515-1524 (1995).
418. R. S. Fishel, C. Are, A. Barbul, Vessel injury and capillary leak. *Crit Care Med* **31**, S502-511 (2003).
419. M. Jiang, Q. Wang, T. Karasawa, J. W. Koo, H. Li, P. S. Steyger, Sodium-glucose transporter-2 (SGLT2; SLC5A2) enhances cellular uptake of aminoglycosides. *PLoS One* **9**, e108941 (2014).
420. C. J. de Almeida, A. K. Witkiewicz, J. F. Jasmin, H. B. Tanowitz, F. Sotgia, P. G. Frank, M. P. Lisanti, Caveolin-2-deficient mice show increased sensitivity to endotoxemia. *Cell Cycle* **10**, 2151-2161 (2011).
421. S. Garrean, X. P. Gao, V. Brovkovych, J. Shimizu, Y. Y. Zhao, S. M. Vogel, A. B. Malik, Caveolin-1 regulates NF-kB activation and lung inflammatory response to sepsis induced by lipopolysaccharide. *The Journal of Immunology* **177**, 4853-4860 (2006).
422. B. Huang, Y. Ling, J. Lin, X. Du, Y. Fang, J. Wu, Force-dependent calcium signaling and its pathway of human neutrophils on P-selectin in flow. *Protein Cell* **8**, 103-113 (2017).

423. J. S. Gujral, J. Liu, A. Farhood, J. A. Hinson, H. Jaeschke, Functional importance of ICAM-1 in the mechanism of neutrophil-induced liver injury in bile duct-ligated mice. *American Journal of Physiology. Gastrointestinal and Liver Physiology* **286**, G499-G507 (2004).
424. S. I. Simon, Y. Hu, D. Vestweber, C. W. Smith, Neutrophil tethering on E-selectin activates integrin binding to ICAM-1 through a mitogen-activated protein kinase signal transduction pathway. *The Journal of Immunology* **164**, 4348-4358 (2000).
425. K. Hirose, J. J. Hartsock, S. Johnson, P. Santi, A. N. Salt, Systemic lipopolysaccharide compromises the blood-labyrinth barrier and increases entry of serum fluorescein into the perilymph. *J Assoc Res Otolaryngol* **15**, 707-719 (2014).
426. V. E. Henson, University of Washington St. Louis, (2013).
427. H. Li, P. S. Steyger, Systemic aminoglycosides are trafficked via endolymph into cochlear hair cells. *Scientific Reports* **1**, 159-164 (2011).
428. C. F. Dai, P. S. Steyger, A systemic gentamicin pathway across the stria vascularis. *Hearing Research* **235**, 114-124 (2008).
429. C. H. Choi, C. H. Jang, Y. B. Cho, S. Y. Jo, M. Y. Kim, B. Y. Park, Matrix metalloproteinase inhibitor attenuates cochlear lateral wall damage induced by intratympanic instillation of endotoxin. *Int J Pediatr Otorhinolaryngol* **76**, 544-548 (2012).
430. B. W. McColl, N. J. Rothwell, S. M. Allan, Systemic inflammation alters the kinetics of cerebrovascular tight junction disruption after experimental stroke in mice. *J Neurosci* **28**, 9451-9462 (2008).
431. C. Allen, P. Thornton, A. Denes, B. W. McColl, A. Pierozynski, M. Monestier, E. Pinteaux, N. J. Rothwell, S. M. Allan, Neutrophil cerebrovascular transmigration triggers rapid neurotoxicity through release of proteases associated with decondensed DNA. *J Immunol* **189**, 381-392 (2012).
432. F. Behnoud, K. Davoudpur, M. T. Goodarzi, Can aspirin protect or at least attenuate gentamicin ototoxicity in humans? *Saudi Medical Journal* **30**, 1165-1169 (2009).
433. S. H. Sha, J. H. Qiu, J. Schacht, Aspirin to prevent gentamicin-induced hearing loss. *New England Journal of Medicine* **354**, 1856-1857 (2006).
434. S. H. Sha, J. Schacht, Salicylate attenuates gentamicin-induced ototoxicity. *Laboratory Investigations* **79**, 807-813 (1999).
435. G. R. Bernard, W. D. Lucht, M. E. Niedermeyer, J. R. Snapper, M. L. Ogletree, K. L. Brigham, Effect of N-acetylcysteine on the pulmonary response to endotoxin in the awake sheep and upon in vitro granulocyte function. *Journal of Clinical Investigation* **73**, 1772-1784 (1984).
436. K. C. Campbell, R. P. Meech, L. P. Rybak, L. F. Hughes, D-Methionine protects against cisplatin damage to the stria vascularis. *Hearing Res* **138**, 13-28 (1999).
437. B. G. Hsu, R. P. Lee, F. L. Yang, H. J. Harn, H. I. Chen, Post-treatment with N-acetylcysteine ameliorates endotoxin shock-induced organ damage in conscious rats. *Life Sci* **79**, 2010-2016 (2006).
438. D. T. Dickey, Y. J. Wu, L. L. Muldoon, E. A. Neuwelt, Protection against cisplatin-induced toxicities by N-acetylcysteine and sodium thiosulfate as

assessed at the molecular, cellular, and in vivo levels. *J Pharmacol Exp Ther* **314**, 1052-1058 (2005).
439. N. D. Doolittle, L. L. Muldoon, R. E. Brummett, R. M. Tyson, C. A. Lacy, J. S. Bubalo, D. F. Kraemer, M. C. Heinrich, J. A. Henry, E. A. Neuwelt, Delayed sodium thiosulfate as an otoprotectant against carboplatin-induced hearing loss in patients with malignant brain tumors. *Clin Cancer Res* **7**, 493-500 (2001).
440. D. R. Freyer, The effects of sodium thiosulfate (STS) on cisplatin-induced hearing loss: A report from the Children's Oncology Group. *J Clin Oncol* **32:5s (suppl; abstr 10017)**, (2014).
441. L. L. Muldoon, M. A. Pagel, R. A. Kroll, R. E. Brummett, N. D. Doolittle, E. G. Zuhowski, M. J. Egorin, E. A. Neuwelt, Delayed administration of sodium thiosulfate in animal models reduces platinum ototoxicity without reduction of antitumor activity. *Clin Can Res* **6**, 309-315 (2000).
442. E. A. Neuwelt, R. E. Brummett, L. G. Remsen, R. A. Kroll, M. A. Pagel, C. A. McCormick, S. Goitjens, L. L. Muldoon, In vitro and animal studies of sodium thiosulfate as a potential chemoprotectant against carboplatin-induced ototoxicity. *Cancer Res* **56**, 706-709 (1996).
443. J. W. Griffith, C. L. Sokol, A. D. Luster, Chemokines and chemokine receptors: positioning cells for host defense and immunity. *Annu Rev Immunol* **32**, 659-702 (2014).
444. J. Etulain, K. Martinod, S. L. Wong, S. M. Cifuni, M. Schattner, D. D. Wagner, P-selectin promotes neutrophil extracellular trap formation in mice. *Blood* **126**, 242-246 (2015).
445. J. Schmutzhard, R. Glueckert, C. Pritz, M. J. Blumer, M. Bitsche, P. Lackner, M. Fille, H. Riechelmann, M. Harkamp, T. Sitthisak, A. Schrott-Fischer, Sepsis otopathy: experimental sepsis leads to significant hearing impairment due to apoptosis and glutamate excitotoxicity in murine cochlea. *Disease Models Mechanisms* **6**, 745-754 (2013).
446. N. Fischer, N. M. Mathonia, G. Hollerich, J. Veser, L. Pinggera, D. Dejaco, R. Glueckert, A. Schrott-Fischer, P. Lackner, H. Riechelmann, J. Schmutzhard, Surviving murine experimental sepsis affects the function and morphology of the inner ear. *Biology Open* **6**, 1401 (2017).
447. A. L. Smit, V. A. Lambermont, R. J. Stokroos, L. J. Anteunis, M. N. Chenault, S. M. Schaefer, L. W. Schoenmakers, B. Kremer, B. W. Kramer, Intrauterine Lipopolysaccharide-Induced Chorioamnionitis in a Sheep: Does It Affect the Auditory System? *Reproductive Sciences* **23**, 257-263 (2016).
448. J. Schmutzhard, C. H. Kositz, R. Glueckert, E. Schmutzhard, A. Schrott-Fischer, P. Lackner, Apoptosis of the fibrocytes type 1 in the spiral ligament and blood labyrinth barrier disturbance cause hearing impairment in murine cerebral malaria. *Malaria Journal* **11**, (2012).
449. M. B. Wood, J. Zuo, The Contribution of Immune Infiltrates to Ototoxicity and Cochlear Hair Cell Loss. *Front Cell Neurosci* **11**, 106 (2017).
450. J. W. Streilein, Immune Privilege as the result of local tissue barriers and immunosuppressive microenvironments. *Current Opinion in Immunology* **5**, 428-432 (1993).

451. A. P. Bautista, K. Meszaros, J. Bojta, J. J. Spitzer, Superoxide anion generation in the liver during the early stage of endotoxemia in rats. *Journal of Luekocyte Biology* **48**, 123-128 (1990).
452. F. Thiebaut, T. Tsuruo, H. Hamada, M. M. Gottesman, I. Pastan, M. C. Willingham, Cellular localization of the mutidrug-resistance gene product P-glycoprotein in normal human tissues. *PNAS* **84**, 7735-7738 (1987).
453. T. Gerloff, B. Stieger, B. Hagenbuch, J. Madon, L. Landmann, J. Roth, A. F. Hofmann, P. J. Meier, The sister of P-glycoprotein represents the canalicular bile salt export pump of mammalian liver. *The Journal of biological chemistry* **273**, 10046-10050 (1998).
454. T. Saito, Z. J. Zhang, H. Tsuzuki, T. Ohtsubo, T. Yamada, T. Yamamoto, H. Saito, Expression of p-glycoprotein in inner ear capillary endothelial cells of the guinea pig with special reference to blood-inner ear barrier. *Brain Reearch* **767**, 388-392 (1997).
455. X. Z., Z. Yaguang, Expression and significance of mdr_1mRNA in guinea pig cochlea lateral wall at different developmental stages. *Journal of Audiology and Speech Pathology* **1**, 013 (2005).
456. M. Suzuki, T. Yamasoba, K. Kaga, Development of the blood-labyrinth barrier in the rat. *Hearing Research* **116**, 107-112 (1998).
457. L. P. Rybak, C. Whitworth, V. Scott, Development of endocochlear potential and compound action potential in the rat. *Hearing Research* **59**, 189-194 (1992).
458. A. M. Hartz, B. Bauer, G. Fricker, D. S. Miller, Rapid modulation of P-glycoprotein-mediated transport at the blood-brain barrier by tumor necrosis factor-alpha and lipopolysaccharide. *Molecular Pharmacology* **69**, 462-470 (2006).
459. S. E. Lutz, J. R. Smith, D. H. Kim, C. V. L. Olson, K. Ellefsen, J. M. Bates, S. P. Gandhi, D. Agalliu, Caveolin1 Is Required for Th1 Cell Infiltration, but Not Tight Junction Remodeling, at the Blood-Brain Barrier in Autoimmune Neuroinflammation. *Cell Reports* **21**, 2104-2117 (2017).
460. T. Dileepan, E. D. Smith, D. Knowland, M. Hsu, M. Platt, P. Bittner-Eddy, B. Cohen, P. Southern, E. Latimer, E. Harley, D. Agalliu, P. P. Cleary, Group A Streptococcus intranasal infection promotes CNS infiltration by streptococcal-specific Th17 cells. *J Clin Invest* **126**, 303-317 (2016).
461. J. E. Lengfeld, S. E. Lutz, J. R. Smith, C. Diaconu, C. Scott, S. B. Kofman, C. Choi, C. M. Walsh, C. S. Raine, I. Agalliu, D. Agalliu, Endothelial Wnt/beta-catenin signaling reduces immune cell infiltration in multiple sclerosis. *Proc Natl Acad Sci U S A* **114**, E1168-E1177 (2017).
462. J. Mazzoni, J. R. Smith, S. Shahriar, T. Cutforth, B. Ceja, D. Agalliu, The Wnt Inhibitor Apcdd1 Coordinates Vascular Remodeling and Barrier Maturation of Retinal Blood Vessels. *Neuron* **96**, 1055-1069 e1056 (2017).
463. L. A. O'Neill, A. G. Bowie, The family of five: TIR-domain-containing adaptors in Toll-like receptor signalling. *Nature reviews. Immunology* **7**, 353-364 (2007).
464. S. J. De Cruz, N. J. Kenyon, C. E. Sandrock, Bench-to-bedside review: the role of nitric oxide in sepsis. *Expert Review in Respiratory Medicine* **3**, 511-521 (2009).

465. M. M. Bednar, R. S. McAuliffe, P. A. Lodge, C. E. Gross, The role of neutrophls and platelets in a rabbit model of thromboembolic stroke. *Stroke* **22**, 44-50 (1991).
466. D. E. Gladstone, K. W. Zamkoff, L. Krupp, R. Peyster, P. Sibony, C. Christodoulou, E. Locher, P. K. Coyle, High-dose cyclophosphamide for moderate to severe refractory multiple sclerosis. *Acrchieves of Neurology* **63**, 1388-1393 (2006).
467. C. T. Brandt, P. Caye-Thomasen, S. P. Lund, L. Worsoe, C. Ostergaard, N. Frimodt-Moller, F. Espersen, J. Thomsen, J. D. Lundgren, Hearing loss and cochlear damage in experimental pneumococcal meningitis, with special reference to the role of neutrophil granulocytes. *Neurobiology of disease* **23**, 300-311 (2006).
468. S. Kastenbauer, M. Klein, U. Koedel, H. W. Pfister, Reactive nitrogen species contribute to blood-labyrinth barrier disruption in suppurative labyrinthitis complicating experimental pneumococcal meningitis in the rat. *Brain Reearch* **904**, 208-217 (2001).
469. M. W. Uhl, K. V. Biagas, P. D. Grundl, M. A. Barmada, J. K. Schiding, E. M. Nemoto, P. M. Kochanek, Effects of neutropenia on edema, histology, and cerebral blood flow after traumatic brain injury in rats. *Journal of Neurotrauma* **11**, 303-315 (1994).
470. T. M. Carlos, R. S. B. Clark, D. Franicola-Higgins, J. K. Schiding, P. M. Kochanek, Expression of endothelial adhesion molecules and recruitment of neutrophils after traumatic brain injury in rats. *Journal of Leukocyte Biology* **61**, 279-285 (1997).
471. M. J. Whalen, T. M. Carlos, S. R. Wisniewski, R. S. B. Clark, J. A. Melick, D. W. Marion, P. M. Kochanek, Effect of neutropenia and granulocyte colony stimulating factor-inuced neutrophilia on blood-brain barrier permeability and brain edema after traumatic brain injury in rats. *Critical Care Medicine* **28**, 3710-3717 (2000).
472. E. Abraham, A. Carmody, R. Shenkar, J. Arcaroli, Neutrophils as early immunologic effectors in hemorrhage- or endotoxemia-induced acute lung injury. *American Journal of Physiology Lung Cellular Molecular Physiology* **279**, L1137-L1145 (2000).
473. K. Suda, H. Takeuchi, T. Hagiwara, T. Miyasho, M. Okamoto, K. Kawasako, S. Yamada, K. Suganuma, N. Wada, Y. Saikawa, K. Fukunaga, Y. Funakoshi, S. Hashimoto, H. Yokota, I. Maruyama, A. Ishizaka, Y. Kitagawa, Neutrophil elastase inhibitor improves survival of rats with clinically relevant sepsis. *Shock* **33**, 526-531 (2010).
474. R. R. Vethanayagam, W. Yang, Y. Dong, B. H. Hu, Toll-like receptor 4 modulates the cochlear immune response to acoustic injury. *Cell Death Dis* **7**, e2245 (2016).
475. M. Masuda, S. Kanzaki, S. B. Minami, J. Kikuchi, J. Kanzaki, H. Sato, K. Ogawa, Correlations of inflammatory biomarkers with the onset and prognosis of idiopathic sudden sensorineural hearing loss. *Otology & Neurotology* **33**, 1142-1150 (2012).

476. E. M. Keithley, X. Wang, G. C. Barkdull, Tumor necrosis factor alpha can induce recruitment of inflammatory cells to the cochlea. *Otology & Neurotology* **29**, 854-859 (2008).
477. R. Dagan, C. B. Hall, K. R. Powell, M. A. Menegus, Epidemiology and laboratory diagnosis of infection with viral and bacterial pathogens in infants hospitalized for suspected sepsis. *Journal of Pediatrics* **115**, 351-356 (1989).
478. P. J. Yoon, M. Price, K. Gallagher, B. E. Fleisher, A. H. Messner, The need for long-term audiologic follow-up of neonatal intensive care unit (NICU) graduates. *International Journal of Pediatric Otorhinolaryngology* **67**, 353-357 (2003).
479. N. Gurtler, N. Schmuziger, Y. Kim, A. N. Mhatre, M. Jungi, A. K. Lalwani, Audiologic testing and molecular analysis of 12S rRNA in patients receiving aminoglycosides. *Laryngoscope* **115**, 640-644 (2005).
480. M. de Hooga, G. A. van Zanten, L. J. Hoeve, A. M. Blom, J. N. van den Anker, A pilot case control follow-up study on hearing in children treated with tobramycin in the newborn period. *International Journal of Pediatric Otorhinolaryngology* **65**, 225-232 (2002).
481. J. Sokol, M. Hyde, Hearing Screenings. *Pediatrics in Review* **23**, 155-162 (2002).
482. R. D. Moore, C. R. Smith, P. S. Lietman, Association of aminoglycoside plasma levels with therapeutic outcome in gram-negative pneumonia. *The American Journal of Medicine* **77**, 657-662 (1984).
483. S. Liao, C. MacArthur, W. H. Martin, J. Mace, T. Lubianski, P. S. Steyger, Differences in DPOAE and AABR in Noise Exposed Infants in the Neonatal Intensive Care Unit. *Otolaryngology - Head and Neck Surgery* **149**, 244 (2013).
484. M. H. Baradarnfar, K. Karamifar, A. H. Mehrparvar, A. Mollasadeghi, M. Gharavi, G. Karimi, M. R. Vahidy, A. Baradarnfar, M. Mostaghaci, Amplitude changes in otoacoustic emissions after exposure to industrial noise. *Noise & Health* **14**, 28-31 (2012).
485. A. L. Berg, B. A. Prieve, Y. C. Serpanos, M. A. Wheaton, Hearing screening in a well-infant nursery: profile of automated ABR-fail/OAE-pass. *Pediatrics* **127**, 269-275 (2011).
486. K. Neumann, A. Indermark, Validation of a new TEOAE-AABR device for newborn hearing screening. *Int J Audiol* **51**, 570-575 (2012).
487. H. W. Helleman, E. J. Jansen, W. A. Dreschler, Otoacoustic emissions in a hearing conservation program: general applicability in longitudinal monitoring and the relation to changes in pure-tone thresholds. *Int J Audiol* **49**, 410-419 (2010).
488. D. Konrad-Martin, K. M. Reavis, G. McMillan, W. J. Helt, M. Dille, Proposed comprehensive ototoxicity monitoring program for VA healthcare (COMP-VA). *J Rehabil Res Dev* **51**, 81-100 (2014).
489. D. R. Myers, J. DeFehr, W. M. Bennett, G. A. Porter, G. D. Olsen, Gentamicin binding to serum and plasma proteins. *Clinical Pharmacology & Therapeutics* **23**, 356-360 (1978).
490. S. A. Fausti, J. A. Henry, H. I. Schaffer, D. J. Olson, R. H. Frey, W. J. McDonald, High-Frequeney Audiometric Monitoring for Early Detection of AminoglycosideOtotoxicity. *The Journal of Infectious Diseases* **165**, 1026-1032 (1992).

491. W. J. Wu, S. H. Sha, J. D. McLaren, K. Kawamoto, Y. Raphael, J. Schacht, Aminoglycoside ototoxicity in adult CBA, C57BL and BALB mice and the Sprague–Dawley rat
Author links open overlay panel. *Hearing Research* **158**, 165-178 (2001).
492. G. R. Bailie, D. Neal, Vancomycin Ototoxicity and Nephrotoxicity A Review. *Medical Toxicology* **3**, 376-386 (1988).
493. D. E. Bates, S. J. Beaumont, B. W. Baylis, Ototoxicity Induced by Gentamicin and Furosemide. *Annals of Pharmacotherapy* **36**, 446-451 (2002).
494. A. A. Chiodo, P. W. Alberti, Experimental, clinical and preventive aspects of ototoxicity. *European Archives of Oto-Rhino-Laryngology* **251**, 375-392 (1994).
495. P. Sinxadi, M. Blockman, Drug-induced Ototoxicity. *CME: Your SA Journal of CPD* **27**, 372-373 (2009).
496. D. J. Arnold, B. L. Lonsbury-Martin, G. K. Martin, High-frequency hearing influences lover-frequency distortion-product otoacoustic emissions. *Archieves of Otolaryngology Head and Neck Surgery* **125**, 215-222 (1999).
497. M. K. Md Daud, H. Mohamadi, A. Haron, N. A. Rahman, Ototoxicity screening of patients treated with streptomycin using distortion product otoacoustic emissions. *B-ENT* **10**, 53-58 (2014).
498. A. L. Berg, J. B. Spitzer, H. M. Towers, C. Bartosiewicz, B. E. Diamond, Newborn hearing screening in the NICU: profile of failed auditory brainstem response/passed otoacoustic emission. *Pediatrics* **116**, 933-938 (2005).
499. J. W. Hall, S. D. Smith, G. R. Popelka, Newborn Hearing Screening with Combined Otoacoustic Emissions and Auditory Brainstem Responses. *Journal of the American Academy of Audiology* **15**, 414-425 (2004).
500. Y. Shi, W. H. Martin, ABR and DPOAE Detection of Cochlear Damage by Gentamicin. *Journal of Basic and Clinical Physiology and Pharmacology* **8**, 141-155 (1997).
501. F. E. Musiek, J. A. Baran, Distortion Product Otoacoustic Emissions: Hit and False-Positive Rates in Normal-Hearing and Hearing-Impaired Subjects. *The American Journal of Otology* **18**, 454-461 (1997).
502. S. Hatzopoulos, J. Petruccelli, A. Ciorba, A. Martini, Optimizing otoacoustic emission protocols for a UNHS program. *Audiology and Neurotology* **14**, 7-16 (2009).
503. M. P. Gorga, S. T. Neely, B. Bergman, K. L. Beauchaine, J. R. Kaminski, J. Peters, W. Jesteadt, Otoacoustic emissions from normal-hearing and hearing-impaired subjects: Distortion product responses. *The Journal of the Acoustical Society of America* **93**, 2050-2060 (1993).
504. J. N. Brown, J. M. Miller, A. L. Nuttall, Age-related changes in cochlear vascular conductance in mice. *Hearing Research* **86**, 189-194 (1995).
505. M. A. Gratton, R. A. Schmiedt, B. A. Schulte, Age-related decreases in endocochlear potential are associated with vascular abnormalities in the stria vascularis. *Hearing Research* **102**, 181-190 (1996).
506. C. G. Le Prell, D. Yamashita, S. B. Minami, T. Yamasoba, J. M. Miller, Mechanisms of noise-induced hearing loss indicate multiple methods of prevention. *Hearing Research* **226**, 22-43 (2007).

507. J. M. Miller, T. Y. Ren, D. Golding-Wood, E. Laurikainen, A. L. Nuttall, Hydrops-Induced Changes in Cochlear Blood Flow. *Annals of Otology, Rhinology & Laryngology* **104**, 476-483 (1995).
508. T. Nakashima, S. Naganawa, M. Sone, M. Tominaga, H. Hayashi, H. Yamamoto, X. Liu, A. L. Nuttall, Disorders of cochlear blood flow. *Brain Research Reviews* **43**, 17-28 (2003).
509. A. L. Nuttall, Sound-induced cochlear ischemia/hypoxia as a mechanism of hearing loss. *Noise & Health* **2**, 17-32 (1999).
510. M. Dai, X. Shi, Fibro-vascular coupling in the control of cochlear blood flow. *PLoS One* **6**, e20652 (2011).
511. D. R. Trune, A. Nguyen-Huynh, Vascular Pathophysiology in Hearing Disorders. *Seminars in Hearing* **33**, 242-250 (2012).
512. P. Wangemann, Cochlear Blood Flow Regulation. *Advances in Oto-rhino-laryngology* **59**, 51-57 (2002).
513. C. Angelborg, M. Hillerdal, E. Hultcrantz, H. C. Larsen, The Microsphere Method for Studies of Inner Ear Blood Flow. *Journal of oto-rhino-larngology Head and Neck Surgery* **50**, 355-362 (1988).
514. N. Choudhury, F. Chen, X. Shi, A. L. Nuttall, R. K. Wang, Volumetric imaging of blood flow within cochlea in gerbil in vivo. *IEEE Journal of Selected Topics in Quantum Electronics* **16**, 524-529 (2010).
515. H. C. Larsen, C. Angelborg, E. Hultcrantz, The Effect of Glycerol on Cochlear Blood Flow. *ORL: Oto-rhino-laryngologica* **44**, 101-107 (1982).
516. J. L. Floc'h, W. Tan, R. S. Telang, S. M. Vlajkovic, A. Nuttall, W. D. Rooney, B. Pontre, P. R. Thorne, Markers of cochlear inflammation using MRI. *J Magn Reson Imaging* **39**, 150-161 (2014).
517. A. Monfared, N. H. Blevins, E. L. M. Cheung, J. C. Jung, G. Popelka, M. J. Schnitzer, In Vivo Imaging of Mammalian Cochlear Blood Flow Using Fluorescence Microendoscopy. *Otology & Neurotology* **27**, 144-152 (2006).
518. T. Nakashima, T. Hattori, E. Sato, M. Sone, M. Tominaga, Blood Flow Measurements in the Ears of Patients Receiving Cochlear Implants. *Annals of Otology, Rhinology & Laryngology* **111**, 998-1001 (2002).
519. R. Reif, J. Qin, L. Shi, S. Dziennis, Z. Zhi, A. L. Nuttall, R. K. Wang, Monitoring Hypoxia Induced Changes in Cochlear Blood Flow and Hemoglobin Concentration Using a Combined Dual-Wavelength Laser Speckle Contrast Imaging and Doppler Optical Microangiography System. *PloS One* **7**, e52041 (2012).
520. H. M. Subhash, V. Davila, H. Sun, A. T. Nguyen-Huynh, X. Shi, A. L. Nuttall, R. K. Wang, Volumetric in vivo imaging of microvascular perfusion within the intact cochlea in mice using ultra-high sensitive optical microangiography. *IEEE Trans Med Imaging* **30**, 224-230 (2011).
521. A. Axelsson, A. L. Nuttall, J. M. Miller, Observations of cochlear microcirculation using intravital microscopy. *Acta Oto-Laryngologica* **109**, 263-270 (1990).
522. A. L. Nuttall, Techniques for the observation and measurement of red blood cell velocity in vessels of the guinea pig cochlea. *Hearing Research* **27**, 111-119 (1987).

523. A. L. Nuttall, Cochlear blood flow: Measurement techniques. *American Journal of Otolaryngology* **9**, 291-301 (1988).
524. X. Shi, A. L. Nuttall, The demonstration of nitric oxide in cochlear blood vessels in vivo and in vitro: the role of endothelial nitric oxide in venular permeability. *Hearing Research* **172**, 73-80 (2002).
525. M. Dai, Y. Yang, I. Omelchenko, A. L. Nuttall, A. Kachelmeier, R. Xiu, X. Shi, Bone marrow cell recruitment mediated by inducible nitric oxide synthase/stromal cell-derived factor-1alpha signaling repairs the acoustically damaged cochlear blood-labyrinth barrier. *American Journal of Pathology* **177**, 3089-3099 (2010).
526. P. Wangemann, E. S. Cohn, D. D. Gruber, M. A. Gratton, Ca2+-dependence and nifedipine-sensitivity of vascular tone and contractility in the isolated superfused spiral modiolar artery in vitro. *Hearing Research* **118**, 90-100 (1998).
527. X. Shi, Cochlear pericyte responses to acoustic trauma and the involvement of hypoxia-inducible factor-1alpha and vascular endothelial growth factor. *American Journal of Pathology* **174**, 1692-1704 (2009).
528. F. Zhang, M. Dai, L. Neng, J. H. Zhang, Z. Zhi, A. Fridberger, X. Shi, Perivascular macrophage-like melanocyte responsiveness to acoustic trauma--a salient feature of strial barrier associated hearing loss. *FASEB J* **27**, 3730-3740 (2013).
529. X. Shi, W. Han, H. Yamamoto, W. Tang, X. Lin, R. Xiu, D. R. Trune, A. L. Nuttall, The cochlear pericytes. *Microcirculation* **15**, 515-529 (2008).
530. K. Hirose, C. M. Discolo, J. R. Keasler, R. Ransohoff, Mononuclear phagocytes migrate into the murine cochlea after acoustic trauma. *Journal of comparative neurology* **489**, 180-194 (2005).
531. H. Lang, Y. Ebihara, R. A. Schmiedt, H. Minamiguchi, D. Zhou, N. Smythe, L. Liu, M. Ogawa, B. A. Schulte, Contribution of bone marrow hematopoietic stem cells to adult mouse inner ear: mesenchymal cells and fibrocytes. *J Comp Neurol* **496**, 187-201 (2006).
532. H. C. Ou, G. W. Harding, B. A. Bohne, An anatomically based frequency-place map for the mouse cochlea. *Hearing Research* **145**, 123-129 (2000).
533. C. Aimoni, C. Bianchini, M. Borin, A. Ciorba, R. Fellin, A. Martini, G. Scanelli, S. Volpato, Diabetes, Cardiovascular Risk Factors and Idiopathic Sudden Sensorineural Hearing Loss: A Case-Control Study. *Audiology & Neurotology* **15**, 111-115 (2010).
534. M. A. Gratton, B. A. Schulte, N. M. Smythe, Quantification of the stria vascularis and strial capillary areas in quiet-reared young and aged gerbils. *Hearing Research* **114**, 1-9 (1997).
535. J. M. Miller, H. Dengerink, Control of inner ear blood flow. *American Journal of Otolaryngology* **9**, 302-316 (1988).
536. K. K. Ohlemiller, M. E. Rice, P. M. Gagnon, Strial microvascular pathology and age-associated endocochlear potential decline in NOD congenic mice. *Hearing Research* **244**, 85-97 (2008).
537. X. Shi, A. L. Nuttall, Expression of adhesion molecular proteins in the cochlear lateral wall of normal and PARP-1 mutant mice. *Hearing Research* **224**, 1-14 (2007).

538. M. Dai, A. Nuttall, Y. Yang, X. Shi, Visualization and contractile activity of cochlear pericytes in the capillaries of the spiral ligament. *Hearing Research* **254**, 100-107 (2009).
539. S. S. Spicer, B. A. Schulte, Spiral Ligament Pathology in Quiet-aged Gerbils. *Hearing Research* **172**, 172-185 (2002).
540. P. J. Drew, A. Y. Shih, J. D. Driscoll, P. M. Knutsen, P. Blinder, D. Davalos, K. Akassoglou, P. S. Tsai, D. Kleinfeld, Chronic optical access through a polished and reinforced thinned skull. *Nature Methods* **7**, 981-984 (2010).
541. H. M. Robinshaw, Early intervention for hearing impairment: differences in the timing of communicative and linguistic development. *British journal of audiology* **29**, 315-334 (1995).
542. C. Yoshinaga-Itano, A. L. Sedey, D. K. Coulter, A. L. Mehl, Language of early- and later-identified children with hearing loss. *Pediatrics* **102**, 1161-1171 (1998).
543. L. P. Rybak, C. A. Whitworth, D. Mukherjea, V. Ramkumar, Mechanisms of cisplatin-induced ototoxicity and prevention. *Hear Res* **226**, 157-167 (2007).
544. R. Assietti, J. J. Olson, Intra-arterial cisplatin in malignant brain tumors: incidence and severity of otic toxicity. *Journal of neuro-oncology* **27**, 251-258 (1996).
545. E. A. Neuwelt, R. E. Brummett, L. G. Remsen, R. A. Kroll, M. A. Pagel, C. I. McCormick, S. Guitjens, L. L. Muldoon, In vitro and animal studies of sodium thiosulfate as a potential chemoprotectant against carboplatin-induced ototoxicity. *Cancer Res* **56**, 706-709 (1996).
546. L. L. Muldoon, M. A. Pagel, R. A. Kroll, R. E. Brummett, N. D. Doolittle, E. G. Zuhowski, M. J. Egorin, E. A. Neuwelt, Delayed administration of sodium thiosulfate in animal models reduces platinum ototoxicity without reduction of antitumor activity. *Clin Cancer Res* **6**, 309-315 (2000).
547. M. Naziroglu, A. Karaoglu, A. O. Aksoy, Selenium and high dose vitamin E administration protects cisplatin-induced oxidative damage to renal, liver and lens tissues in rats. *Toxicology* **195**, 221-230 (2004).
548. A. Pace, A. Savarese, M. Picardo, V. Maresca, U. Pacetti, G. Del Monte, A. Biroccio, C. Leonetti, B. Jandolo, F. Cognetti, L. Bove, Neuroprotective effect of vitamin E supplementation in patients treated with cisplatin chemotherapy. *J Clin Oncol* **21**, 927-931 (2003).
549. G. Sener, H. Satiroglu, L. Kabasakal, S. Arbak, S. Oner, F. Ercan, M. Keyer-Uysa, The protective effect of melatonin on cisplatin nephrotoxicity. *Fundamental & clinical pharmacology* **14**, 553-560 (2000).
550. K. Tsuruya, M. Tokumoto, T. Ninomiya, M. Hirakawa, K. Masutani, M. Taniguchi, K. Fukuda, H. Kanai, H. Hirakata, M. Iida, Antioxidant ameliorates cisplatin-induced renal tubular cell death through inhibition of death receptor-mediated pathways. *American journal of physiology. Renal physiology* **285**, F208-218 (2003).
551. Y. J. Wu, L. L. Muldoon, E. A. Neuwelt, The chemoprotective agent N-acetylcysteine blocks cisplatin-induced apoptosis through caspase signaling pathway. *J Pharmacol Exp Ther* **312**, 424-431 (2005).
552. D. A. Stenstrom, L. L. Muldoon, H. Armijo-Medina, S. Watnick, N. D. Doolittle, J. A. Kaufman, D. R. Peterson, J. Bubalo, E. A. Neuwelt, N-acetylcysteine use to

prevent contrast medium-induced nephropathy: premature phase III trials. *Journal of vascular and interventional radiology : JVIR* **19**, 309-318 (2008).
553. S. Chu, L. Hu, X. Wang, S. Sun, T. Zhang, Z. Sun, L. Shen, S. Jin, B. He, Xuezhikang ameliorates contrast media-induced nephropathy in rats via suppression of oxidative stress, inflammatory responses and apoptosis. *Renal failure* **38**, 1717-1725 (2016).
554. L. Gao, W. F. Wu, L. Dong, G. L. Ren, H. D. Li, Q. Yang, X. F. Li, T. Xu, Z. Li, B. M. Wu, T. T. Ma, C. Huang, Y. Huang, L. Zhang, X. Lv, J. Li, X. M. Meng, Protocatechuic Aldehyde Attenuates Cisplatin-Induced Acute Kidney Injury by Suppressing Nox-Mediated Oxidative Stress and Renal Inflammation. *Frontiers in pharmacology* **7**, 479 (2016).
555. X. He, L. Li, H. Tan, J. Chen, Y. Zhou, Atorvastatin attenuates contrast-induced nephropathy by modulating inflammatory responses through the regulation of JNK/p38/Hsp27 expression. *Journal of pharmacological sciences* **131**, 18-27 (2016).
556. T. Kaur, V. Borse, S. Sheth, K. Sheehan, S. Ghosh, S. Tupal, S. Jajoo, D. Mukherjea, L. P. Rybak, V. Ramkumar, Adenosine A1 Receptor Protects Against Cisplatin Ototoxicity by Suppressing the NOX3/STAT1 Inflammatory Pathway in the Cochlea. *J Neurosci* **36**, 3962-3977 (2016).
557. C. Z. Li, H. H. Jin, H. X. Sun, Z. Z. Zhang, J. X. Zheng, S. H. Li, S. H. Han, Eriodictyol attenuates cisplatin-induced kidney injury by inhibiting oxidative stress and inflammation. *Eur J Pharmacol* **772**, 124-130 (2016).
558. D. Onk, O. A. Onk, K. Turkmen, H. S. Erol, T. A. Ayazoglu, O. N. Keles, M. Halici, E. Topal, Melatonin Attenuates Contrast-Induced Nephropathy in Diabetic Rats: The Role of Interleukin-33 and Oxidative Stress. *Mediators of inflammation* **2016**, 9050828 (2016).
559. L. Helboe, J. Egebjerg, M. Moller, C. Thomsen, Distribution and pharmacology of alanine–serine–cysteine transporter 1 (asc-1) in rodent brain. *European Journal of Neuroscience* **18**, 2227-2238 (2003).
560. M. A. Erickson, K. Hansen, W. A. Banks, Inflammation-induced dysfunction of the low-density lipoprotein receptor-related protein-1 at the blood-brain barrier: protection by the antioxidant N-acetylcysteine. *Brain, behavior, and immunity* **26**, 1085-1094 (2012).
561. S. A. Farr, H. F. Poon, D. Dogrukol-Ak, J. Drake, W. A. Banks, E. Eyerman, D. A. Butterfield, J. E. Morley, The antioxidants alpha-lipoic acid and N-acetylcysteine reverse memory impairment and brain oxidative stress in aged SAMP8 mice. *J Neurochem* **84**, 1173-1183 (2003).
562. E. A. Neuwelt, M. A. Pagel, B. P. Hasler, T. G. Deloughery, L. L. Muldoon, Therapeutic efficacy of aortic administration of N-acetylcysteine as a chemoprotectant against bone marrow toxicity after intracarotid administration of alkylators, with or without glutathione depletion in a rat model. *Cancer Res* **61**, 7868-7874 (2001).
563. S. D. Weisbord, M. Gallagher, J. Kaufman, A. Cass, C. R. Parikh, G. M. Chertow, K. A. Shunk, P. A. McCullough, M. J. Fine, M. K. Mor, R. A. Lew, G. D. Huang, T. A. Conner, M. T. Brophy, J. Lee, S. Soliva, P. M. Palevsky, Prevention of contrast-induced AKI: a review of published trials and the design of the

prevention of serious adverse events following angiography (PRESERVE) trial. *Clinical journal of the American Society of Nephrology : CJASN* **8**, 1618-1631 (2013).

564. M. Tepel, M. van der Giet, C. Schwarzfeld, U. Laufer, D. Liermann, W. Zidek, Prevention of radiographic-contrast-agent-induced reductions in renal function by acetylcysteine. *N Engl J Med* **343**, 180-184 (2000).
565. C. E. Berglin, P. V. Pierre, T. Bramer, K. Edsman, H. Ehrsson, S. Eksborg, G. Laurell, Prevention of cisplatin-induced hearing loss by administration of a thiosulfate-containing gel to the middle ear in a guinea pig model. *Cancer Chemotherapy Pharmacology* **68**, 1547-1556 (2011).
566. D. T. Dickey, L. L. Muldoon, N. D. Doolittle, D. R. Peterson, D. F. Kraemer, E. A. Neuwelt, Effect of N-acetylcysteine route of administration on chemoprotection against cisplatin-induced toxicity in rat models. *Cancer Chemother Pharmacol* **62**, 235-241 (2008).
567. G. Lorito, S. Hatzopoulos, G. Laurell, K. C. M. Campbell, J. Petruccelli, P. Giordano, K. Kochanek, L. Sliwa, A. Martini, H. Skarzynski, Dose-dependent protection on cisplatin-induced ototoxicity—an electrophysiological study on the effect of three antioxidants in the Sprague-Dawley rat animal model. *Medical Science Monitoring* **17**, BR179–BR186 (2011).
568. J. Yoo, S. J. Hamilton, D. Angel, K. Fung, J. Franklin, L. S. Parnes, D. Lewis, V. Venkatesan, E. Winquist, Cisplatin otoprotection using transtympanic l-N-acetylcysteine: a pilot randomized study in head and neck cancer patients. *Laryngoscope* **124**, E87-E94 (2014).
569. A. S. Levey, J. Coresh, T. Greene, L. A. Stevens, Y. L. Zhang, S. Hendriksen, J. W. Kusek, F. Van Lente, Using standardized serum creatinine values in the modification of diet in renal disease study equation for estimating glomerular filtration rate. *Ann Intern Med* **145**, 247-254 (2006).
570. K. Heard, Dart, R. (Wolters Kluwer, www.uptodate.com, 2016).
571. DCTD, NCI, NIH, DHHS, Common terminology criteria for adverse events, version 3.0. [http://ctep.cancer.gov].
572. E. A. Sandilands, D. N. Bateman, Adverse reactions associated with acetylcysteine. *Clinical toxicology (Philadelphia, Pa.)* **47**, 81-88 (2009).
573. A. H. Travers, T. D. Rea, B. J. Bobrow, D. P. Edelson, R. A. Berg, M. R. Sayre, M. D. Berg, L. Chameides, R. E. O'Connor, R. A. Swor, Part 4: CPR overview: 2010 American Heart Association Guidelines for Cardiopulmonary Resuscitation and Emergency Cardiovascular Care. *Circulation* **122**, S676-684 (2010).
574. F. E. Simons, L. R. Ardusso, M. B. Bilo, Y. M. El-Gamal, D. K. Ledford, J. Ring, M. Sanchez-Borges, G. E. Senna, A. Sheikh, B. Y. Thong, World allergy organization guidelines for the assessment and management of anaphylaxis. *The World Allergy Organization journal* **4**, 13-37 (2011).
575. S. Fishbane, J. H. Durham, K. Marzo, M. Rudnick, N-acetylcysteine in the prevention of radiocontrast-induced nephropathy. *Journal of the American Society of Nephrology : JASN* **15**, 251-260 (2004).
576. B. Hultberg, A. Andersson, P. Masson, M. Larson, A. Tunek, Plasma homocysteine and thiol compound fractions after oral administration of N-

acetylcysteine. *Scandinavian journal of clinical and laboratory investigation* **54**, 417-422 (1994).
577. C. Briguori, A. Colombo, A. Violante, P. Balestrieri, F. Manganelli, P. Paolo Elia, B. Golia, S. Lepore, G. Riviezzo, P. Scarpato, A. Focaccio, M. Librera, E. Bonizzoni, B. Ricciardelli, Standard vs double dose of N-acetylcysteine to prevent contrast agent associated nephrotoxicity. *European heart journal* **25**, 206-211 (2004).
578. G. Marenzi, E. Assanelli, I. Marana, G. Lauri, J. Campodonico, M. Grazi, M. De Metrio, S. Galli, F. Fabbiocchi, P. Montorsi, F. Veglia, A. L. Bartorelli, N-acetylcysteine and contrast-induced nephropathy in primary angioplasty. *N Engl J Med* **354**, 2773-2782 (2006).
579. R. Siegel, D. Naishadham, A. Jemal, Cancer statistics, 2013. *CA: A Cancer Journal for Clinicians* **63**, 11-30 (2013).
580. L. Dobrossy, Epidemiology of head and neck cancer: magnitude of the problem. *Cancer and Metastasis Reviews* **24**, 9-17 (2005).
581. J. Goodwin, G. Thomas, D. Parker, D. Joseph, S. Levis, E. Franzmann, C. Anello, J. Hu, Unequal burden of head and neck cancer in the United States. *Head and Neck* **30**, 358-371 (2008).
582. B. Paz, N. Cook, T. Odom-Maryon, Y. Xie, S. Wilczynski, Human papillomavirus (HPV) in head and neck cancer an association of HPV 16 with squamous cell carcinoma of Waldeyer's tonsillar ring. *Cancer* **79**, 595-604 (1997).
583. D. Clayburgh, D. Sauer, J. Schindler, Human papilloma virus in laryngeal squamous cell carcinoma. *Otolaryngology Head and Neck Surgery* **147**, P60 (2012).
584. S. Marur, G. D'Souza, W. Westra, A. Forastiere, HPV-associated head and neck cancer: a virus-related cancer epidemic. *Lancet Oncology* **11**, 781-789 (2010).
585. S. Syrjanen, Human papillomavirus (HPV) in head and neck cancer. *Journal of Clinical Virology* **32**, S59-S667 (2005).
586. A. K. Chaturvedi, E. A. Engels, R. M. Pfeiffer, B. Y. Hernandez, W. Xiao, E. Kim, B. Jiang, M. T. Goodman, M. Sibug-Saber, W. Cozen, L. Liu, C. F. Lynch, N. Wentzensen, R. C. Jordan, S. Altekruse, W. F. Anderson, P. S. Rosenberg, M. L. Gillison, Human papillomavirus and rising oropharyngeal cancer incidence in the United States. *J Clin Oncol* **29**, 4294-4301 (2011).
587. D. Kissane, S. Patel, R. Baser, R. Bell, M. Farberov, J. Ostroff, Y. Li, B. Singh, D. Kraus, J. Shah, Preliminary evaluation of the reliability and validity of the Shame and Stigma Scale in head and neck cancer. *Head and Neck* **35**, 172-183 (2013).
588. H. Bronheim, J. Strain, H. Biller, Psychiatric aspects of head and neck surgery part I: new surgical techniques and psychiatric consequences *General Hospital Psychiatry* **13**, 165-176 (1991).
589. E. Hammerlid, M. Ahlner-Elmqvist, K. Bjordal, A. Biörklund, J. Evensen, M. Boysen, M. Jannert, S. Kaasa, M. Sullivan, T. Westin, A prospective multicentre study in Sweden and Norway of mental distress and psychiatric morbidity in head and neck cancer patients. *British Journal of Cancer* **80**, 766-774 (1999).

590. A. Kugaya, T. Akechi, T. Okuyama, T. Nakano, I. Mikami, H. Okamura, Y. Uchitomi, Prevalence, predictive factors, and screening for psychologic distress in patients with newly diagnosed head and neck cancer. *Cancer* **88**, 2817-2823 (2000).
591. S. Singer, O. Krauß, J. Keszte, G. Siegl, K. Papsdorf, E. Severi, J. Hauss, S. Briest, A. Dietz, E. Brahler, R. Kortmann, Predictors of emotional distress in patients with head and neck cancer. *Head and Neck* **34**, 180-187 (2012).
592. J. Sykes, Managing the psychological aspects of plastic surgery patients. *Current Opinion in Otolaryngology & Head and Neck Surgery* **17**, 321-325 (2009).
593. O. Rozniatowski, M. Reich, Y. Mallet, N. Penel, C. Fournier, J. Lefebvre, Psychosocial factors involved in delayed consultation by patients with head and neck cancer. *Head and Neck* **27**, 274-280 (2005).
594. D. Tromp, X. Brouha, J. De Leeuw, G. Hordijk, J. Winnubst, Psychological factors and patient delay in patients with head and neck cancer. *European Journal of Cancer* **40**, 1509-1516 (2004).
595. C. Gourin, K. Kaboli, E. Blume, M. Nance, W. Koch, Characteristics of participants in a free oral, head and neck cancer screening program. *The Laryngoscope* **119**, 679-682 (2009).
596. E. Hapner, K. Bauer, J. Wise, The impact of a community-based oral, head and neck cancer screening for reducing tobacco consumption. *Otolaryngology Head and Neck Surgery* **145**, 7780782 (2011).
597. E. Hapner, J. Wise, Results of a large-scale head and neck cancer screening of an at-risk population. *Journal of Voice* **25**, 480-483 (2011).
598. E. Hapner, J. Wise, K. Bauer, J. Zhu, Head and neck surgery is education effective during head and neck cancer screenings? *Otolaryngology Head and Neck Surgery* **147**, P60-61 (2012).
599. C. Poh, G. Hislop, B. Currie, R. Lee, Oral cancer screening in a high-risk underserved community: Vancouver downtown eastside. *Journal of Health Care for the Poor and Underserved* **18**, 767-778 (2007).
600. M. Prout, J. Sidari, R. Witzburg, G. Grillone, C. Vaughan, Head and neck cancer screening among 4611 tobacco users older than forty years. *Otolaryngology Head and Neck Surgery* **116**, 201-208 (1997).
601. A. Shuman, P. Entezami, A. Chernin, N. Wallace, J. Taylor, N. Hogikyan, Demographics and efficacy of head and neck cancer screening. *Otolaryngology Head and Neck Surgery* **143**, 353-360 (2010).
602. L. White, A. Chin-Quee, C. Berg, J. Wise, E. Hapner, Differences in head and neck cancer risk perception between smoking and nonsmoking NASCAR attendees. *Otolaryngology Head and Neck Surgery* **147**, 63-68 (2012).
603. J. Wise, Results of a Community Based Head and Neck Cancer Screening. *Otolaryngology Head and Neck Surgery* **143**, P71 (2010).
604. C. G. Gourin, K. C. Kaboli, E. J. Blume, M. A. Nance, W. M. Koch, Characteristics of participants in a free oral, head and neck cancer screening program. *Laryngoscope* **119**, 679-682 (2009).
605. A. G. Singal, S. Gupta, C. S. Skinner, C. Ahn, N. O. Santini, D. Agrawal, C. A. Mayorga, C. Murphy, J. A. Tiro, K. McCallister, J. M. Sanders, W. P. Bishop, A. C. Loewen, E. A. Halm, Effect of Colonoscopy Outreach vs Fecal

Immunochemical Test Outreach on Colorectal Cancer Screening Completion: A Randomized Clinical Trial. *JAMA* **318**, 806-815 (2017).

606. S. Gupta, E. A. Halm, D. C. Rockey, M. Hammons, M. Koch, E. Carter, L. Valdez, L. Tong, C. Ahn, M. Kashner, K. Argenbright, J. Tiro, Z. Geng, S. Pruitt, C. S. Skinner, Comparative effectiveness of fecal immunochemical test outreach, colonoscopy outreach, and usual care for boosting colorectal cancer screening among the underserved: a randomized clinical trial. *JAMA Intern Med* **173**, 1725-1732 (2013).
607. L. Liu, K. Zhu, W. Yu, S. Zhang, G. Teng, J. Guo, Detection rate, anatomic stites, and pathologic types of colorectal cancer during colonoscopy procedures. *Surgical Laparoscopy Endoxcopy & Percutaneous Techniques* **27**, 394-399 (2017).
608. D. Gur, J. H. Sumkin, L. A. Hardesty, R. J. Clearfield, C. S. Cohen, M. A. Ganott, C. M. Hakim, K. M. Harris, W. R. Poller, R. Shah, L. P. Wallace, H. E. Rockette, Recall and detection rates in screening mammography. *Cancer* **100**, 1590-1594 (2004).
609. D. Gur, J. H. Sumkin, H. E. Rockette, M. Ganott, C. Hakim, L. Hardesty, W. R. Poller, R. Shah, L. Wallace, Changes in Breast Cancer Detection and Mammography Recall Rates After the Introduction of a Computer-Aided Detection System. *JNCI Journal of the National Cancer Institute* **96**, 185-190 (2004).
610. F. H. Schröder, J. Hugosson, M. J. Roobol, T. L. J. Tammela, S. Ciatto, V. Nelen, M. Kwiatkowski, M. Lujan, H. Lilja, M. Zappa, L. J. Denis, F. Recker, A. Berenguer, L. Määttänen, C. H. Bangma, G. Aus, A. Villers, X. Rebillard, T. van der Kwast, B. G. Blijenberg, S. M. Moss, H. J. de Koning, A. Auvinen, Screening and prostate-cancer mortality in a randomized european study. *The New England Journal of Medicine* **360**, 1320-1328 (2009).